Ocean and Atmosphere Pacific: OAP 95

SEA-LEVEL CHANGES AND THEIR EFFECTS

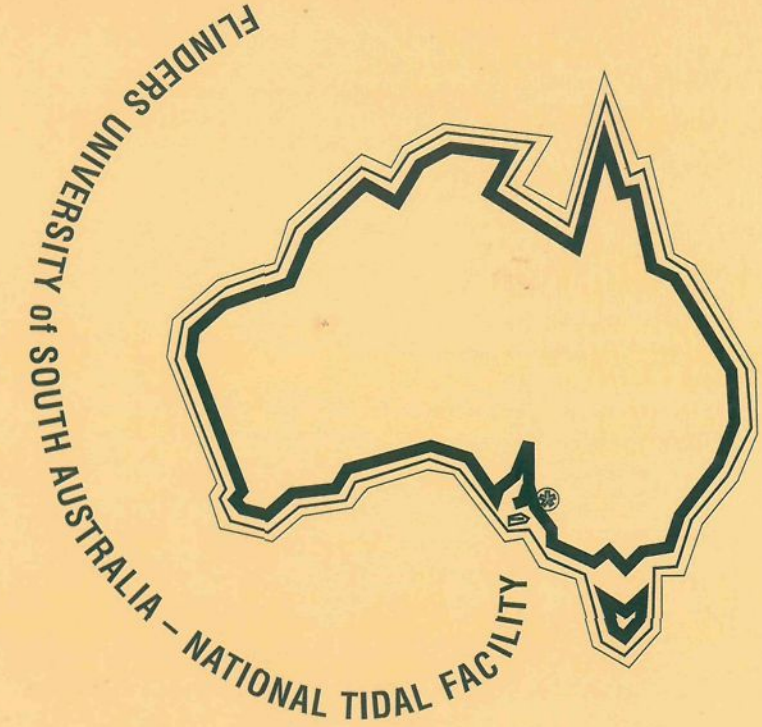

Editors

John Noye & Marcus Grzechnik

SEA-LEVEL CHANGES
AND
THEIR EFFECTS

Also published by World Scientific:

Computational Techniques and Applications: CTAC93
Proceedings of the Sixth Biennial Conference
Edited by David Stewart, Henry Gardner and David Singleton

Computational Techniques and Applications: CTAC95
Proceedings of the Seventh Biennial Conference
Edited by Robert L May and Alan K Easton

Computational Techniques and Applications: CTAC97
Proceedings of the Eighth Biennial Conference
Edited by John Noye, Michael Teubner and Andrew Gill

Modelling Coastal Sea Processes
Ocean and Atmosphere Pacific: OAP95
Edited by John Noye

Ocean and Atmosphere Pacific: OAP 95

SEA-LEVEL CHANGES AND THEIR EFFECTS

Editors

John Noye

Marcus Grzechnik

National Tidal Facility
The Flinders University of South Australia
Australia

World Scientific
Singapore • New Jersey • London • Hong Kong

Published by

World Scientific Publishing Co. Pte. Ltd.

P O Box 128, Farrer Road, Singapore 912805

USA office: Suite 1B, 1060 Main Street, River Edge, NJ 07661

UK office: 57 Shelton Street, Covent Garden, London WC2H 9HE

British Library Cataloguing-in-Publication Data
A catalogue record for this book is available from the British Library.

SEAL-LEVEL CHANGES AND THEIR EFFECTS
Ocean and Atmosphere Pacific: OAP95

ISBN 981-02-3618-2

Printed in Singapore by World Scientific Printers

Preface

This book is one of the outcomes of the international Ocean and Atmosphere, Pacific (OAP 95) conference held in Adelaide, South Australia on 23–27 October 1995. The conference was organised by the National Tidal Facility (NTF) of the Flinders University of South Australia, as part of the South Pacific Sea Level and Climate Monitoring Project, funded by AusAID. The aim of the conference was to enhance interaction between local scientists in the South Pacific region and to link regional understanding of climate variability and sea level change to global developments.

Two themes dominated the conference. Firstly, many presentations were concerned with the mathematical modelling of processes which occur in shallow coastal seas and secondly, many papers focused on changes in sea level and their associated effects. After the conference, so much interest was shown in these two areas, that the NTF canvassed delegates who had given outstanding papers, to determine whether they would be prepared to produce extended and updated versions of their presentations for publication in reviewed books, the cost to be borne by the NTF.

The first book to result from this NTF initiative, was published late last year with the title "Modelling Coastal Sea Processes". The present book, titled "Sea-Level Changes and Their Effects", is the second in this series. Articles included in this volume were selected on both their scientific merit and their usefulness to physical oceanographers, marine biologists and coastal developers. They cover a wide range of topics including the effects of long-term sea-level rise on flows in coral lagoons and its impact on mangroves, the determination of long-term sea-level change relative to vertical land movement, to the numerical modelling of short term sea-level changes due to tides and tsunamis and the relative effects of oceanic tides and meteorological events on sea-levels and currents in coastal waters.

The task of organising and editing this volume was carried out by Associate Professor John Noye, who was seconded part-time from the University of Adelaide to do this work. It included getting selected OAP 95 authors to agree

to participate in the project, organising additional authors where necessary to include important relevant topics which may otherwise have been omitted, arranging for at least two reviews to be received for each article submitted, and getting the authors to modify their articles in the light of the reviewers' reports.

Since his retirement from the University of Adelaide in late 1999, Dr Noye has continued working at the NTF augmenting the tidal modelling group which complements the NTF's expertise in deploying oceanographic instrumentation and archiving and analysing the data collected.

In Dr Noye's absence with illness, the project was taken over by Dr Marcus Grzechnik, an ex-student of Dr Noye's at the University of Adelaide. Marcus is currently employed as a part of the modelling research group at the NTF. His was a significant contribution to the successful completion of this manuscript, acknowledged by inclusion as co-editor.

Wolfgang Scherer
Director, NTF

Acknowledgements

We wish to thank Ms Di Paech, who typed the reams of correspondence involved in soliciting articles for this book and obtaining at least two reviews of each submitted manuscript. We are also grateful to James Chittleborough and Darrell Strauss for their help in preparing and modifying diagrams, and Kerry Spriggs for her thorough proof-reading and constructive comments. We must also thank the contributors to this book, all of whom spent a great deal of time preparing and modifying their manuscripts, and the 43 referees who assessed the merit of the articles submitted and wrote the associated reports.

John Noye
Marcus Grzechnik
Editors

This page is intentionally left blank

Contents

Sea-Level Changes and Their Effects
B.J. Noye & M.P. Grzechnik (Editors)

Sea-Level Change in the Pacific

P.D. Nunn
Geography Department, The University of the South Pacific, Suva, Fiji Islands

ABSTRACT: Long-term sea-level changes appear to be controlled largely by changes in the amounts of solar radiation received at the Earth's surface; cycles with periods of 41,000 years and 100,000 years have operated during the late Cenozoic (last 2.5 million years) and have been the major cause of the glacial-interglacial alternation within that time. Details of late Quaternary (last 300,000 years) sea-level changes have been gleaned from palaeotemperature analyses and dating of former shorelines on rapidly rising coasts such as the Huon Peninsula in Papua New Guinea. The latter suggests that Last Interglacial (130,000-120,000 years ago) sea level may have been 6 m higher than that during the present (Holocene) interglacial. During the intervening Last Glacial period (ice age), Pacific sea level reached 120 m below its present level some 17,000 years ago. Rapid postglacial sea-level rise culminated around 4000-3000 years in a sea level 1.5-2.0 m higher than the present in most parts of the region. Sea level reached its present level by about 1200 years ago. Minor fluctuations in the last millennium have brought about environmental changes and have affected human lifestyles. Since about AD 1800, sea level in the Pacific has been rising; in the last century this rise has been measured as about 15 cm. It is likely that this rise will accelerate at least twofold in the next century.

KEY WORDS: Pacific, sea-level change, Quaternary, Holocene, last millennium

CONTENTS

1. Introduction

A proper understanding of both recent and future sea-level change in the Pacific requires an appreciation of long-term changes. Throughout the late Cenozoic (last ~2.4 million years), the sea level in the Pacific, in common with the rest of the world, has fluctuated largely as a result of changes in the volume of land ice, mostly that in the northern hemisphere. These changes have been regular, controlled primarily by variations in solar radiation produced by cyclical changes in the orbit of the Earth around the Sun. Such changes are often called Milankovitch cycles and it was determined more than twenty years ago that they were the principal cause of late Cenozoic climate changes which, in turn, led to sea-level changes (Hays et al., 1976). Although recognised as the 'pacemaker of the ice ages', doubt has been expressed about whether variations in solar radiation alone can account for the temperature changes observed during the late Cenozoic. Other factors, including changes in greenhouse-gas and aerosol concentrations, are regarded as important (Manabe and Broccoli, 1985).

There are different Milankovitch cycles. The 41,000-year axial-tilt (obliquity) cycle dominated climate and sea-level change for most of the late Cenozoic up until around the end of the early Pleistocene (about 850,000 years ago). Thereafter the 100,000-year orbital-eccentricity cycle became the dominant control on climate and sea-level change. In other words, the early Pleistocene was dominated by cycles of sea-level change lasting approximately 41,000 years, of noticeably lower amplitude than those of the middle and late Pleistocene each of which lasted around 100,000 years. It is appropriate to note that shorter-term cycles have also been linked to sea-level change, ranging from the 23,000-year precessional cycle of the Earth's orbit to changes in sunspot activity within the past millennium (Nunn, 1999).

Sea-level changes of great antiquity are difficult to establish precisely using direct field mapping, for example, or other traditional techniques of palaeoenvironmental reconstruction. Some of the keenest insights have come about through proxy methods, particularly oxygen-isotope analyses of deep-ocean cores and ice sheets. A good discussion of such methods is given in Williams et al. (1993).

This article briefly discusses late Cenozoic sea-level changes and their value in understanding contemporary glacial-interglacial cycles before focusing on

the Holocene and, in particular, the time when a human presence was being felt across the entire Pacific Basin. A more detailed recent account was given by Nunn (1999).

2. The Late Cenozoic Context

Cyclic sea-level changes began shortly after the formation of northern hemisphere ice sheets on the land around 2.4 million years ago. By the start of the Quaternary Period (1.77 million years ago), several such changes had already occurred around the shores of the Pacific, marked for example by sedimentary evidence of periods of sea-level rise and fall in northern Alaska (Brigham-Grette and Carter, 1992).

Although oxygen-isotope data are available for much of the late Cenozoic, the record is least controversial for the late Pleistocene and Holocene. The oxygen-isotope ratio, expressed as $\delta^{18}O$, is an indication of palaeotemperature which, in turn, is thought to have been closely linked to sea level (Fig. 1).

Shorelines formed during high stands of early and middle Pleistocene sea level are commonly found along rapidly-rising coasts, such as occur at convergent plate boundaries around the periphery of the Pacific Basin. At such places, these shorelines have not been drowned or had their diagnostic sediment cover obscured by later reoccupation of the same level during a later sea-level high stand, for example. The classic site in the Pacific is the Huon Peninsula in Papua New Guinea from which shorelines dating back to at least 300,000 years ago are found (Chappell, 1974, 1983; Aharon and Chappell, 1986).

Each emerged shoreline on the Huon Peninsula was dated from the age of the associated coral reef. The actual height above sea level was compared to the calculated height given a constant rate of uplift. The difference between actual and calculated heights was assumed to be the difference between modern sea level and that at the time the shoreline was uplifted. Using this calculation for all the emerged shorelines, a picture of late Quaternary sea-level change was compiled (Fig. 1).

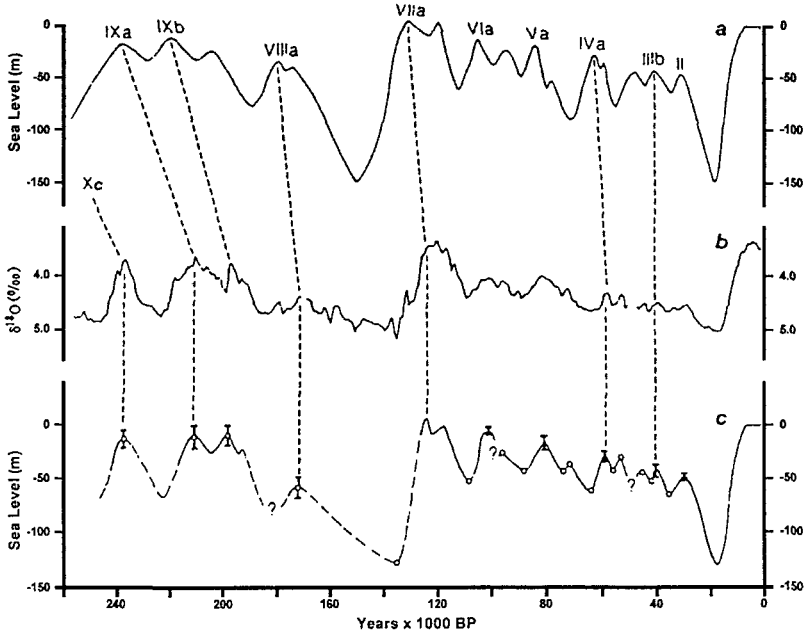

Figure 1. Correlations between late Pleistocene sea-level changes obtained from a study of emerged shorelines on the Huon Peninsula, Papua New Guinea (a), palaeotemperatures from oxygen-isotope analysis of deep-sea core V19-30 (b). The two curves have been reconciled to Milankovitch cycles and the bottom graph (c) for sea-level changes derived. This graph is considered the most accurate available representation of changing sea level during the late Quaternary (from Chappell and Shackleton, 1986).

The Huon Peninsula sea-level curve has been adopted as an informal global reference although difficulties with that view are known. A particular problem arises with the Last Interglacial sea-level maximum, which appears to have reached 6 m above its present level on the Huon Peninsula. Workers have assumed that Last Interglacial sea level was everywhere 6 m higher than present and have made assertions about both sea-level and tectonic histories elsewhere which are contradicted by other indicators; good examples are provided by Hawaii (Muhs and Szabo, 1994) and southern Tonga (Nunn, 1998a).

Similar studies to that on the Huon Peninsula have been carried out elsewhere in the Pacific but these have not generally yielded as much detail. Exceptions include the staircase of erosional terraces in South Taranaki, New Zealand, which date from at least 680,000 years ago (Pillans, 1983), and the reef terraces of the Ryukyu islands, Japan (Konishi et al., 1974; Ota and Omura, 1992). Ages and heights of the principal Pleistocene sea-level maxima recorded in the Pacific are given in Table 1.

Table 1. Ages (years Before Present) and heights (metres relative to present mean sea level) of late Pleistocene sea-level maxima and minima in the Pacific Basin (from the compilation in Nunn, 1994a).

Sea level	*Age (years BP)*	*Height (metres relative to present mean sea level)*
minimum	17,000	-130
maximum	29,000	- 46
maximum	40,000	- 41
maximum	59,000	- 28
maximum	81,000	- 19
maximum	106,000	- 19
maximum	118,000	0
maximum	124,000	+6
minimum	135,000	-130
maximum	175,000	- 24
maximum	215,000	- 6
maximum	240,000	- 30
maximum	325,000	0

The history of Pacific sea level during the Last Interglacial has been the subject of considerable discussion. This is not a wholly academic exercise, for the Last Interglacial is the period of climate most closely analogous to the one in which we are currently living (the Holocene Interglacial). An understanding of the heights Last Interglacial sea level attained and the rates and times at which it changed have the potential to illuminate our understanding of the Holocene and our long-term future. For example, a 6 m Last Interglacial sea-level maximum could be explained by the melting of the entire West Antarctic ice sheet (Mercer, 1968); the possibility that this might recur during the present interglacial is manifestly of interest.

Chappell (1974) first suggested that there may have been a double sea-level maximum during the Last Interglacial on the evidence of a disconformity between emerged reefs VIIb and VIIa on the Huon Peninsula. Work on emerged reefs elsewhere in the Pacific has supported this scenario; the debate in Hawaii has been particularly influential, Ku et al. (1974) and Sherman et al. (1993) both favouring the double maximum and Muhs and Szabo (1994) being against such an interpretation. A global compilation of dates from Last Interglacial emerged shorelines (Smart and Richards, 1994) favoured maxima 129,000 and 123,000 years ago.

The course of changing sea level during the Last Glacial (120,000-12,000 years ago) has been determined from a variety of sources, including oxygen-isotope and emerged-reef data (Fig. 1). The long fall of sea level between the start of the Last Glacial until its maximum, around 17,000 years ago, was not smooth and continuous but oscillatory; the overall cooling trend being broken by short-lived warm excursions termed interstadials during each of which sea level reached a maximum (Table 1).

Around the time of the Last Glacial maximum 17,000 years ago, Pacific sea level was around 120 m lower than today. The implications of this for climate and environment have hardly been looked at for most parts of the Pacific Basin. Pacific islands would have been larger and closer together; orographic effects in the trade-wind belt may have been more pronounced and many Pacific island grasslands date from a time of Last Glacial aridity (Nunn, 1994a). Continental shelves would have been exposed, a signal around the Antarctic periphery and elsewhere for ice sheets and valley glaciers to extend seaward.

3. Holocene Sea Levels

Postglacial flooding of continental shelves during deglaciation would have caused ice-sheet shrinkage, a process also associated with the accompanying warming. Elsewhere the displacement of coastal biotas, including people, would have caused immense disruption to ecosystems and may have been associated with biotic extinctions, although sea-level rise is also implicated in Holocene speciation (Nunn, 1994a).

Around Pacific islands, the rapidity of postglacial sea-level rise left many coral reefs struggling to maintain themselves within the photic zone near the sea surface. Some reefs gave up and were drowned, others caught up only later but a few, in places where oceanographic conditions were especially favourable to reef growth, managed to keep up with postglacial sea-level rise. Early Holocene rates of vertical reef accretion in the Pacific (Table 2) are minimum rates of contemporary sea-level rise.

Table 2. Rates of early Holocene vertical reef accretion from Pacific islands (after Nunn, 1994a).

Island	*Rate of reef accretion (mm/year)*	*Source of information*
Enewetak, Marshall	1.0-2.0	Tracey and Ladd, 1974
Mataiva, French Polynesia	0.2-2.5	Guilcher, 1988
Moruroa, French Polynesia	2.0-3.0	Labeyrie et al., 1969
New Caledonia	5.0 (maximum	Lecolle and Cabioch, 1988
Oahu, Hawaii	3.3 (average)	Easton and Olson, 1976
Tarawa, Kiribati	5.0-8.0	Marshall and Jacobson 1988

Although in a general sense, the rise of postglacial sea level was smooth (Fig. 1), there are clear indications from parts of the Pacific islands that there were still-stands of duration sufficient to cut broad shelves (e.g. Phipps and Preobrazhensky, 1977; Fletcher and Sherman, 1995); there has been no recent attempt to analyse these systematically for the Holocene within the Pacific region.

An issue which has inspired great controversy in the past few decades has been whether or not sea level in the Pacific (and elsewhere) exceeded its present level during the Holocene. For a long time, the debate was polarised between those who followed Fairbridge (1961) in showing a higher-than-present sea level and those who opposed this view, largely on account of the work of the 1967 CARMARSEL expedition (Curray et al., 1970), envisaging a continuous rise of sea level up to the present. Recent investigations, including some in the Caroline and Marshall Islands where CARMARSEL worked, has concluded that Holocene sea level throughout the Pacific exceeded its present level by 1.0-1.5 m (Nunn, 1995). Critical studies re-evaluating former work and its conclusions were made in Hawaii (Jones, 1992) and Micronesia (Kawana et al., 1995).

The Holocene sea-level maximum occurred at different times in different parts of the Pacific. To understand why, one must first appreciate that the sea-level maximum did not simply represent the time of maximum ocean-water volume, but also the effects of subsequent tectonic changes associated with deformation of the lithosphere caused by changing surface loads: principally ice on land shifting to the oceans as water (Lambeck and Nakada, 1985). No systematic analysis of the timing of the sea-level maximum has yet been made although in most places it occurred around 4000-3000 years ago.

The question of whether there has been just a single sea-level high stand during the Holocene in the Pacific has exercised many investigators. In a recent compilation from Fiji, Nunn (1995) showed how the data could either be interpreted as a single maximum or a series of six maxima, corresponding, remarkably, to those recognised by Fairbridge (1961) and Schofield (1980) at times when far fewer data were available (Fig. 2). Many of the dates from these maxima come from deposits which would be unlikely to survive a 100,000-year interglacial-glacial-interglacial cycle, so comparison with the Last Interglacial is inappropriate.

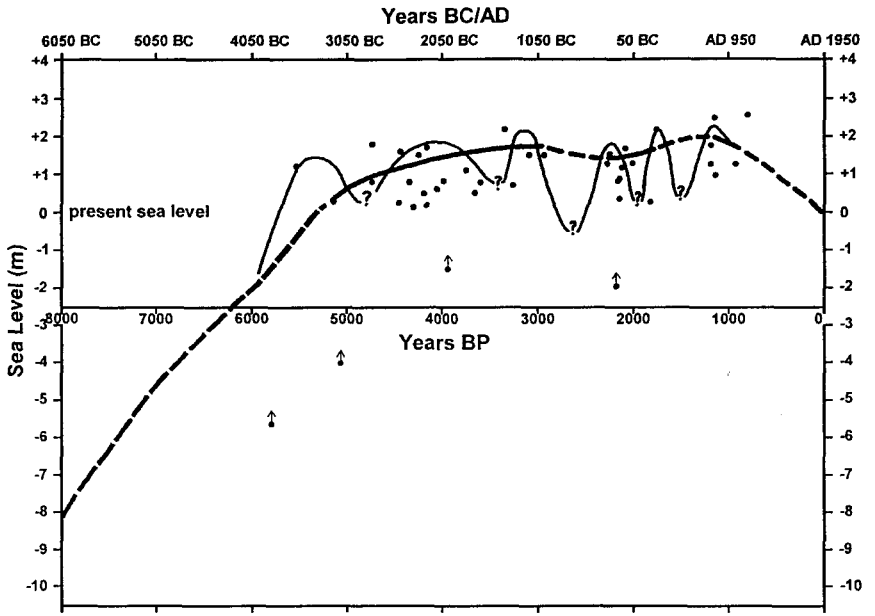

Figure 2. Holocene sea-level change in Fiji (after Nunn, 1995). The most likely curve is shown by the thick black line, an alternative with support from elsewhere by the thinner line. Up-arrows indicate that the site has subsided relative to sea level since its formation.

The 1.0-1.5 m fall of sea level during the late Holocene in the Pacific was probably accomplished largely by around 1200 years ago since which time coral reefs have concentrated on growing laterally rather than vertically. Humans had reached all parts of the Pacific Rim which they inhabit permanently today by the start of the Holocene. Colonisation of the islands took longer but all the main groups were occupied by the late Holocene. Many of these people depended greatly on coastal and nearshore resources, so made their homes close to the shoreline. The rise of sea level in the early Holocene displaced large numbers, forcing many to sail elsewhere; the initial colonisation of the island groups south, east and northeast of Solomon Islands may have been settled by people fleeing the effects of rising sea levels in southeast Asia.

The fall of sea level in the late Holocene transformed island environments in ways which made them far more attractive to potential settlers than they had been hitherto (Fig. 3; Plate 1). It is possible that this acted as a stimulus to people to settle them permanently, people who may have been reconnoitering them for several thousand years previously (Nunn, 1994b).

4. The Last Millennium

Sea-level fluctuations over the last millennium in the Pacific have been small yet highly significant to humans (Nunn, 1998b). Knowledge of the course of these sea-level changes is important to an understanding of why the sea level in the Pacific has changed in the last hundred years or so, and how it might change in the future. Examination of sea-level change over the last millennium also allows the physical fact of sea-level change to be linked more securely to its environmental consequences than it is possible to do for earlier times on account of the incompleteness of the evidence. An understanding of the environmental consequences of past sea-level changes is a valuable aid to understanding the likely impact of future sea-level changes on Pacific environments.

Sea-level changes over the past millennium were closely linked to contemporary temperature changes; in fact, one can be used as a rough proxy of the other. Yet there are considerable numbers of reliable data relating to sea level over the past millennium: reliable because the effects of tectonics in the places from which data are obtained can be considered

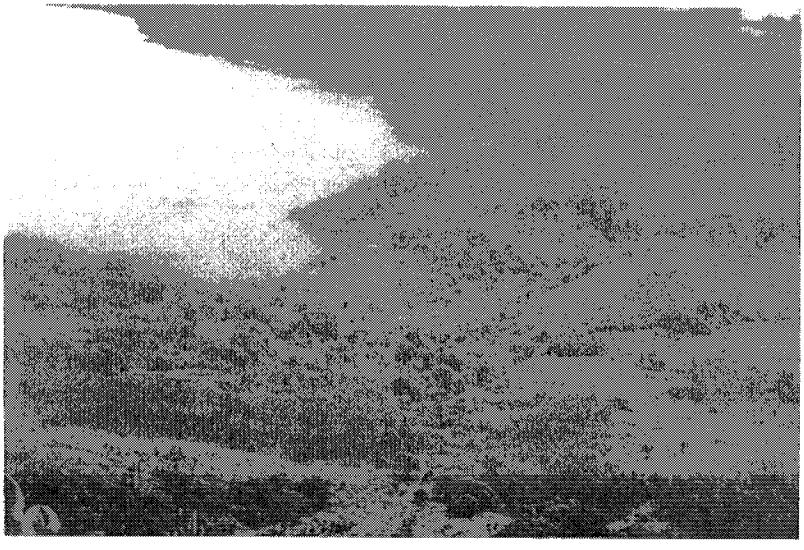

Plate 1. Coastal plain occupied by Tovu village, Totoya Island, southeast Fiji. Coastal plains such as this formed on shore platforms cut when sea level was at its Holocene maximum (see Fig. 3).

Figure 3. Relationship between sea level and an oceanic island to illustrate the effects of a common scenario of coastline and reef development during the middle to late Holocene (from Nunn, 1994a).

a. The time of the Holocene sea-level maximum. Sea level had been rising for the previous 11-13,000 years so little lateral erosion of the shoreline had been accomplished. Reefs struggled to catch up with rising sea level; until they did so, a high-energy window was open. Potential settlers would have found this island type unattractive.

b. Following a fall of sea level in the late Holocene, the shore platforms cut at the higher sea level would have emerged and become covered with terrigenous and marine detritus. Barrier reefs would have caught up with sea level, the high-energy window would have been closed so that shoreline erosion would have become relatively subdued. Fringing reefs would have developed and the lagoon become shallower. Potential settlers would have found this island type comparatively attractive.

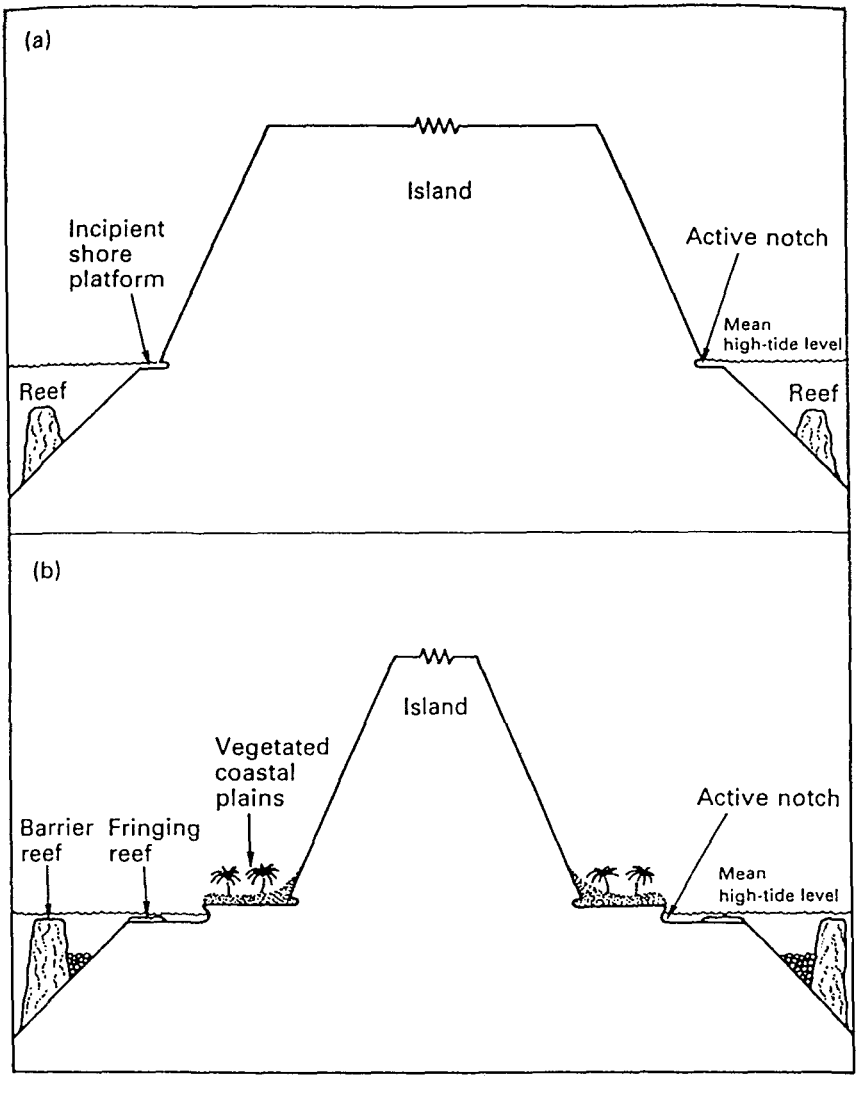
(a)
Island
Incipient shore platform
Active notch
Mean high-tide level
Reef
Reef
(b)
Island
Vegetated coastal plains
Barrier reef
Fringing reef
Active notch
Mean high-tide level

negligible over such a short time period. The following discussion uses data from New Zealand, Samoa and Fiji (Fig. 4).

Around 1200-1000 years ago, Pacific sea level is thought to have been close to its present level, having just completed its fall from a 1.0-1.5 m Holocene maximum 4000-3000 years ago. In the following 300-500 years, it rose again. It may have reached more than 1 m above its present level some 700 years ago. These changes occurred during the Little Climatic Optimum (LCO), a period during which temperatures rose and the climate of the Pacific islands became much drier than today (Nunn, 1992). The sea-level rise during the LCO is the most recent period which is analogous in rate to that in which we are presently living. It has been used to predict the 'background' sea-level change which may influence the IPCC estimates of future sea-level rise in the Pacific (Nunn et al., 1994).

The end of the LCO was marked by a rapid fall of sea level and temperature. A massive short-lived rise in precipitation in much of the Pacific devastated contemporary environments and caused widespread societal breakdown and intertribal warfare (Nunn, 1994c, 1999). No well-documented evidence of the human-environmental consequences of this sea-level fall (as opposed to the attendant climate changes) is known, although emerged reefs dating from the sea-level high at the end of the LCO have been identified (Plate 2).

Sea level during the Little Ice Age (LIA) was consistently lower than today, although there is some evidence for a marginally higher level around 500-300 years ago (Nunn, 1998b). When the LIA ended some 200-150 years ago, sea level was some 50-70 cm below its present level. Since this time it has risen. It is important to appreciate that this period of sea-level rise, coincident with the time of recent warming in Figure 4, began long before the influence of the human-enhanced greenhouse effect could have commenced. This period of sea-level rise is that which, in the Pacific region, has been monitored in the last hundred years or so.

For this reason, we know more about sea-level change in the last century although the importance of knowing the long-term context of this change is also manifest. Through monitoring of sea level over the past hundred years or so, we have also been able to understand attendant environmental changes. In most parts of the Pacific, one effect of rising sea level has been drowning of low-lying coastal areas. The responses by humans to this drowning have varied, ranging from migration inland (Plate 3) to building of

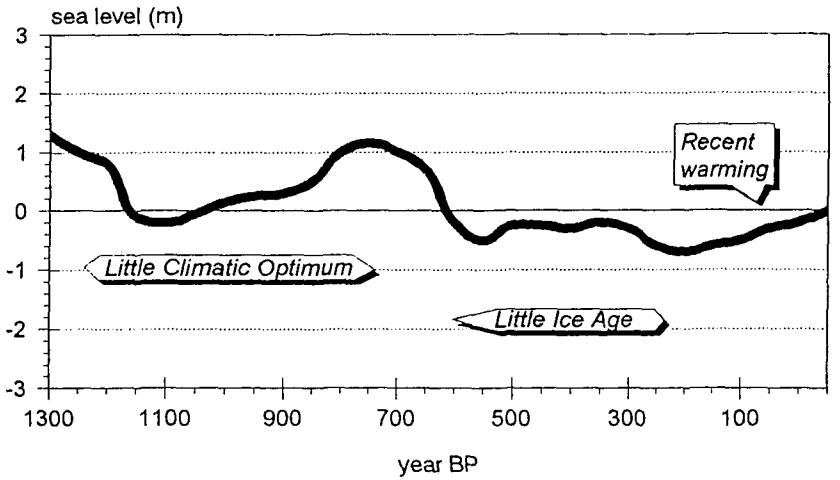

Figure 4. Pacific sea-level over the last thousand years showing the three main divisions. Although short-lived, the transition period between the Little Climatic Optimum and Little Ice Age was also notable on account of the comparative rapidity of the sea-level change and temperature fall which had major impacts on many Pacific environments and their inhabitants.

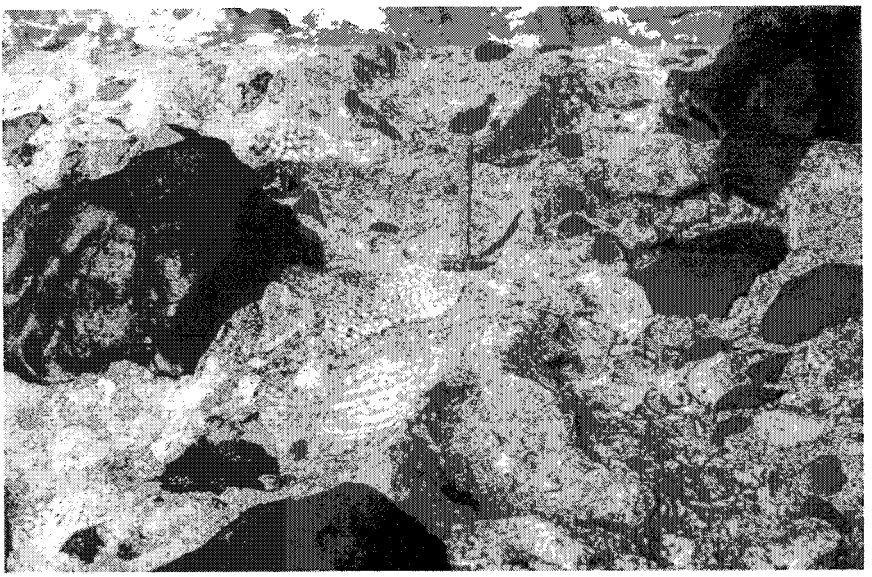

Plate 2. Emerged reef at Poloa, Tutuila island, American Samoa, dates from the sea-level high at the end of the Little Climatic Optimum.

Plate 3. The response to sea-level rise and overcrowding of the coastal zone today near Port Moresby, Papua New Guinea, has caused some people to build houses on stilts. The response to sea-level rise around the mid-Holocene was similar.

artificial structures to prevent further drowning (Plates 4 and 5). Many artificial structures have exacerbated problems associated with sea-level rise, as indeed have other environmental changes, both of human and non-human causation (Nunn, 1992).

5. The Future

Sea level will almost certainly continue to rise over the next hundred years or more, perhaps largely as a result of the human-enhanced greenhouse effect. The most recent report of the Intergovernmental Panel on Climate Change (IPCC) estimates that in response to rising temperatures (1.0°-3.5°C higher than 1990 levels in 2100), sea level will have risen by around 15-95 cm by the year 2100. At least, this represents nearly a twofold increase over the rate of sea-level rise monitored in the Pacific during the last century (see Fig. 4) and will produce problems of comparably greater magnitude. Along many Pacific coasts, increased inundation (flooding), saltwater intrusion of freshwater aquifers, and overrunning of coral reefs by large waves are among the many likely effects of this. The magnitude of the impact of such effects on human lifestyles depends largely on the degree of preparation of the Pacific nations in question. Many continental nations have already set up climate change task forces to produce multidisciplinary solutions to the anticipated problems, and legislation promoting those solutions is well advanced. Other governments are proving more complacent (Nunn et al., 1999).

Acknowledgements

The author is grateful to an anonymous reviewer for insightful comments.

References

Aharon, P. and Chappell, J. 1986. Oxygen isotopes, sea level changes and the temperature history of a coral reef environment in New Guinea over the last 10^5 years. *Palaeogeography, Palaeoclimatology, Palaeoecology*, 56, 337-379.

Plate 4. Coastal protection at Kumi Village, Vitilevu Island, Fiji consists of a line of oil drums filled with rocks and cemented together. The drums rust and fall apart after a while. The sea washes over the seawall and contributes to its undermining.

Plate 5. Seawall along the front of a south-coast tourist resort, Vitilevu Island, Fiji. Although effective in preventing shoreline erosion at this particular spot, the building of the seawall has caused a lot of scour of beach sand resulting in the exposure of beach rock at several points.

Brigham-Grette, J. and Carter, L.D. 1992. Pliocene marine transgressions of northern Alaska: circumarctic correlations and paleoclimatic interpretations. *Arctic*, 45, 74-89.

Chappell, J. 1974. Geology of coral terraces, Huon Peninsula, New Guinea: a study of Quaternary tectonic movements and sea level changes. *Geological Society of America, Bulletin*, 85, 553-70.

Chappell, J. 1983. A revised sea-level record for the last 300,000 years from Papua New Guinea. *Search*, 14, 99-101.

Chappell, J. and Shackleton, N.J. 1986. Oxygen isotopes and sea level. *Nature*, 324, 137-40.

Curray, J.R., Shepard, F.P. and Veeh, H.H. 1970. Late Quaternary sea-level studies in Micronesia: CARMARSEL expedition. *Geological Society of America, Bulletin*, 81, 1865-80.

Easton, W.H. and Olson, E.A. 1976. Radiocarbon profile of Hanauma Reef, Oahu, Hawaii. *Geological Society of America, Bulletin*, 87, 711-19.

Fairbridge, R.W. 1961. Eustatic changes in sea level. *Physics and Chemistry of the Earth*, 4, 99-185.

Fletcher, C.H. and Sherman, C.E. 1995. Submerged shorelines on O'ahu, Hawai'i: archive of episodic transgression during the deglaciation? *Journal of Coastal Research, Special Issue* 17, 141-152.

Guilcher, A. 1988. *Coral Reef Geomorphology*. New York: Wiley.

Hays, J.D., Imbrie, J. and Shackleton, N.J. 1976. Variations in the earth's orbit: pacemaker of the ice ages. *Science*, 194, 1121-1132.

Jones, A.T. 1992. Holocene coral reef on Kauai, Hawaii: evidence for a sea-level highstand in the central Pacific. *Society for Sedimentary Geology, Special Publication* 48, 267-271.

Kawana, T., Miyagi, T., Fujimoto, K. and Kikuchi, T. 1995. Late Holocene sea-level changes and mangrove development in Kosrae Island, the Carolines, Micronesia. In: Kikuchi, T. (editor). *Rapid Sea Level Rise and Mangrove Habitat.* Gifu University, Japan: Institute for Basin Ecosystem Studies, 1-7.

Konishi, K., Omura, A. and Nakamichi, O. 1974. Radiometric coral ages and sea level records from the late Quaternary reef complexes of the Ryukyu Islands. *Proceedings of the 2nd International Coral Reef Symposium*, 2, 595-613.

Ku, T.-L., Kimmel, M.A., Easton, W.H. and O'Neill, T.J. 1974. Eustatic sea level 120,000 years ago on Oahu, Hawaii. *Science*, 183, 959-62.

Labeyrie, J., Lalou, C. and Delibrias, G. 1969. Etude des transgressions marines sur l'atoll de Mururoa par la datation des differents niveaux de corail. *Cahiers du Pacifique*, 3, 59-68.

Lambeck, K. and Nakada, M. 1985. Holocene fluctuations in sea-level: constraints on mantle viscosity and melt-water sources. *Proceedings of the 5th International Coral Reef Congress*, 3, 79-84.

Lecolle, J.F. and Cabioch, G. 1988. La limite Holocène-Pléistocène dans le récif frangeant Ricaudy (Nouvelle-Calédonie): géochronologie, faciès et diagénèse. Implications eustatiques et néotectoniques. *Marine Geology*, 81, 241-60.

Manabe, S. and Broccoli, A.J. 1985. The influence of continental ice sheets on the climate of an ice age. Journal of Geophysical Research, 90, 2167-2190.

Marshall, J.F. and Jacobson, G. 1985. Holocene growth of a mid-Pacific atoll: Tarawa, Kiribati. *Coral Reefs*, 4, 11-17.

Mercer, J.H. 1968. Antarctic ice and Sangamon sea level. *International Association of Scientific Hydrology, Publication* 79, 217-225.

Muhs, D.R. and Szabo, B.J. 1994. New uranium-series ages of the Waimanalo limestone, Oahu, Hawaii: implications for sea level during the last interglacial period. *Marine Geology*, 118, 315-326.

Nunn, P.D. 1992. *Keimami sa vakila na liga ni Kalou (Feeling the hand of God): human and nonhuman impacts on Pacific island environments.* East-West Center, Occasional Paper (2nd revised edition), **13**, 69 pp.

Nunn, P.D. 1994a. *Oceanic Islands*. Oxford: Blackwell, 413 p.

Nunn, P.D. 1994b. Environmental change and the early settlement of Pacific Islands. East-West Center, Hawaii, Working Papers, Environmental Series 39. 31 p.

Nunn, P.D. 1994c. Beyond the naive lands: human history and environmental change in the Pacific Basin. In Waddell, E. and Nunn, P.D. (eds.). *The Margin Fades: Geographical Itineraries in a World of Islands*. Suva, Fiji: Institute of Pacific Studies, The University of the South Pacific, 5-27.

Nunn, P.D. 1995. Holocene sea-level changes in the south and west Pacific. *Journal of Coastal Research*, Special Issue 17, 311-319.

Nunn, P.D. 1998a. *Pacific Island Landscapes.* Suva: Institute of Pacific Studies, The University of the South Pacific, 332 p.

Nunn, P.D. 1998b. Sea-level changes over the past 1000 years in the Pacific. *Journal of Coastal Research*, 14, 23-30.

Nunn, P.D. 1999. *Environmental Change in the Pacific Basin: chronologies, causes, consequences*. London: Wiley, 357 pp.

Nunn, P.D., Veitayaki, J., Ram-Bidesi, V. and Vunisea, A. 1999. Coastal issues for oceanic islands: implications for human futures. *Natural Resources Forum*, 23, in press.

Nunn, P.D., Ravuvu, A.D., Aalbersberg, W., Mimura, N. and Yamada, K. 1994. *Assessment of Coastal Vulnerability and Resilience to Sea-Level Rise and Climate Change. Case Study: Yasawa Islands, Fiji. Phase 2: Development of Methodology.* Apia, Western Samoa: South Pacific Regional Environment Programme, 118 pp.

Ota, Y. and Omura, A. 1992. Contrasting styles and rates of tectonic uplift of coral reef terraces in the Ryukyu and Daito Islands, southwestern Japan. *Quaternary International*, 15/16, 17-29.

Phipps, C.V.G. and Preobrazhensky, B.V. 1977. Morphology, development and general coral distribution of some reefs of the Lau Islands, Fiji. *Bureau des Recherches de Géologiques et Minieres, Memoire*, 89, 440-455.

Pillans, B. 1983. Upper Quaternary marine terrace chronology and deformation, South Taranaki, New Zealand. *Geology*, 11, 292-297.

Schofield, J.C. 1980. Postglacial transgressive maxima and second-order transgressions of the southwest Pacific Ocean. In: Mörner, N.-A. (editor). *Earth Rheology, Isostasy and Eustasy.* New York: Wiley, 517-521.

Sherman, C.E., Glenn, C.R., Jones, A.T., Burnett, W.C. and Schwarcz, H.P. 1993. New evidence for two highstands of the sea during the last interglacial, oxygen isotope stage 5e. *Geology*, 21, 1079-1082.

Smart, P.L. and Richards, D.A. 1992. Age estimates for the late Quaternary high sea-stands. *Quaternary Science Reviews*, 11, 687-696.

Tracey, J.I. and Ladd, H.S. 1974. Quaternary history of Eniwetok and Bikini atolls, Marshall Islands. *Proceedings of the 2nd International Coral Reef Symposium*, 2, 537-50.

Williams, M.A.J., Dunkerley, D.L., De Deckker, P., Kershaw, A.P. and Stokes, T. 1993. *Quaternary Environments*. London: Edward Arnold.

This page is intentionally left blank

Sea-Level Changes and Their Effects
B.J. Noye & M.P. Grzechnik (Editors)

Effects of Sea-Level Rise on the Hydrodynamics of a Coral Reef Lagoon: Kaneohe Bay, Hawaii

Clifford J. Hearn[1] and Marlin J. Atkinson[2]

1. Oceanography, University College, University of New South Wales, Australian Defence Force Academy, Canberra, ACT 2600, Australia

2. Hawaii Institute of Marine Biology, University of Hawaii, PO Box 1346, Kaneohe, Hawaii, 96744, USA

ABSTRACT: This chapter considers the effect of a local relative sea-level rise on the flushing of Kaneohe Bay which is a coral reef lagoon on the windward shore of the island of Oahu in Hawaii. Kaneohe Bay has an unusually wide reef (from front to back) which is also comparatively deep. Its lagoon is forced by wave-driven currents across the reef, plus tides, wind, and buoyancy from mountain streams (entering the Bay after winter storms). The chapter presents a numerical model of Kaneohe Bay which is used to investigate the sensitivity of the various forcing mechanisms to a sea-level rise of 0.6 m; equivalent to about 10% of the present mean depth of Kaneohe Bay. An appreciable effect is only found for currents due to wave-breaking. The chapter proceeds to analyse the effect of sea-level rise on surface set-up due to breaking waves, friction on the reef flat, and the circulation of wave-forced currents in coral reef lagoons. It concludes that sea-level rise generally increases flow over the reef and consequently improves lagoonal flushing.

KEY WORDS: coral reefs, wave-driven flow, hydrodynamic-numeric, sea-level rise, friction.

CONTENTS

1. Introduction

This chapter considers the effect of sea-level rise (*slr*) on the hydrodynamics of a coral reef and its associated lagoon. It considers the effect of *slr* independently of changes which might result from coral reef growth and sediment movement. The coral reef system chosen for this study is Kaneohe Bay in Oahu which is one of the Hawaiian chain of islands shown in Figure 1. Kaneohe Bay is especially suitable because of the existence of a large data set (Bathen, 1968) and a three-dimensional baroclinic numerical model (Hearn, 1996). The model includes forcing of the Bay by waves breaking on the reef and so allows an investigation of the effect of sea-level rise on the process which is usually of greatest importance to water circulation in coral reef lagoons. Such lagoons are very variable in regard to freshwater input and Kaneohe Bay has the advantage of considerable streamflow so that the study is able to assess the influence of the *slr* on forcing of the Bay by coastal sources of positive buoyancy. The surface buoyancy flux is also important in summer and consists of a positive term due to net heating and a negative term arising from evaporation. A positive *slr* of 0.6m is chosen which is 10% of the existing mean depth of the lagoon and a significant fraction of the mean water depth over the reef. The numerical model is used to estimate the effect of this *slr* on the major hydrodynamic processes in the lagoon. An analytical model is also introduced which considers the effect of *slr* on wave forced currents, and their circulation in coral reef lagoons, and is used to interpret the results of the three-dimensional model of Kaneohe Bay.

2. Kaneohe Bay

Kaneohe Bay is a coral lagoon of the Central Pacific islands situated at 21° 30' N (Figure 1) and its bathymetry is shown in Figure 2. The Bay is some 15 km long and 6 km wide. The reef has two major openings to the ocean with a partially dredged channel running behind the reef, parallel to the shore where the maximum depth in the Bay of 16 m is encountered. The Bay is the site of an original volcanic crater which has sunken below sea-level. Its topography has produced a reef flat which is especially wide and extends over a distance of some 1000 to 1500 m (from front to back of the reef flat). This makes it particularly valuable for studies of the hydrodynamics and nutrient cycling of coral reefs. Much of the reef is close to mean lowest low water and mean sea level is about 1.0 m above

the top of the reef. Other variations, such as oceanic waves and barometric effects, may expose significant parts of the reef.

Bathen (1968) made the first study of the Bay which was followed by extensive field measurements and two-dimensional modelling (McAnally et al, 1974) . These were performed as part of studies of the environmental stress exerted on Kaneohe Bay (Smith et al, 1981) by sewerage discharge (which is now diverted to the open ocean). Kaneohe Bay lies on the eastern side of the island of Oahu which is part of the Hawaiian Island chain of volcanic islands (Figure 1) and is backed by very steep mountain slopes rising to a height of 1000m within a distance of 3 km from the shore. The Bay is on the windward side of Oahu with annual rainfall from the North East Trades rising from 2000 mm at the coast to 6000 mm at the mountain tops. Consequently, there is considerable positive buoyancy input into the Bay. This flow is very variable with storm peaks of a few days exceeding mean flows fivefold. Salinities close to the major creeks

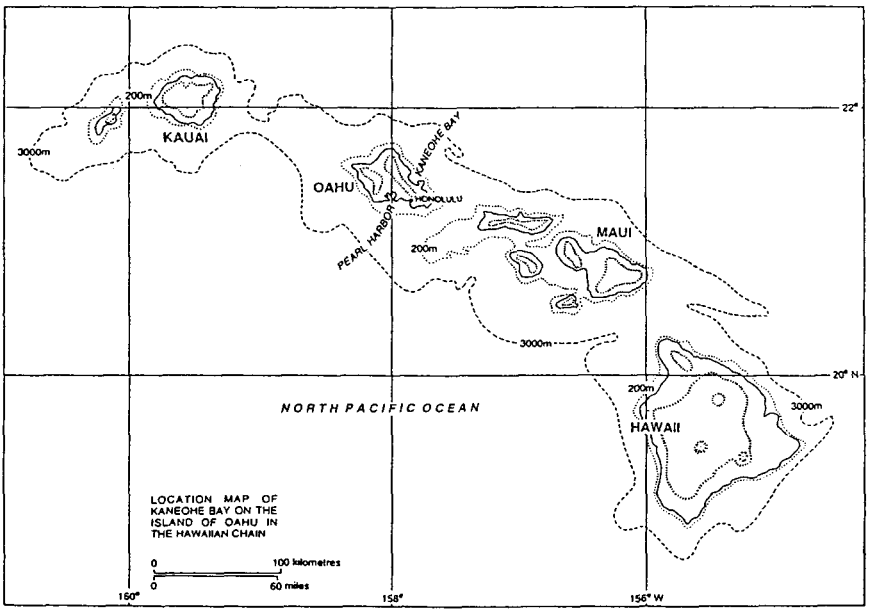

FIGURE 1. The Hawaiian Islands and location of Kaneohe Bay on the windward (eastern) side of Oahu.

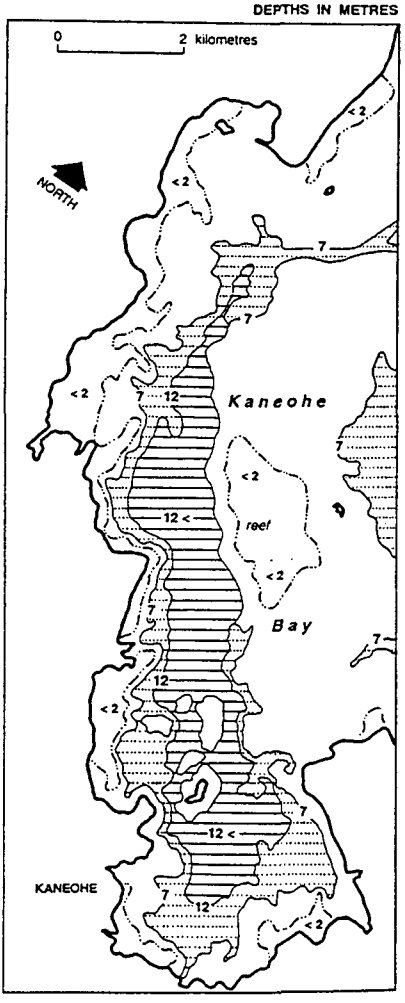

FIGURE 2. Bathymetry of Kaneohe Bay showing the main coral reef and the deep channel running behind the reef with depths in excess of 10m; the channel has a major exit to the ocean at the northern end of the Bay.

may be depressed by several parts per thousand. Stormwater plumes extend well offshore and subject the main reef to environmental stress from surface salinity depressions (in spite of wave induced inward flow across the reef). The Bay is therefore somewhat like a weak estuary in winter (Figure 3) and buoyancy forcing seems to play a major role in its winter dynamics. During the prevailing onshore Trade Winds, the freshwater plumes from creeks may be coastally trapped and flow northward

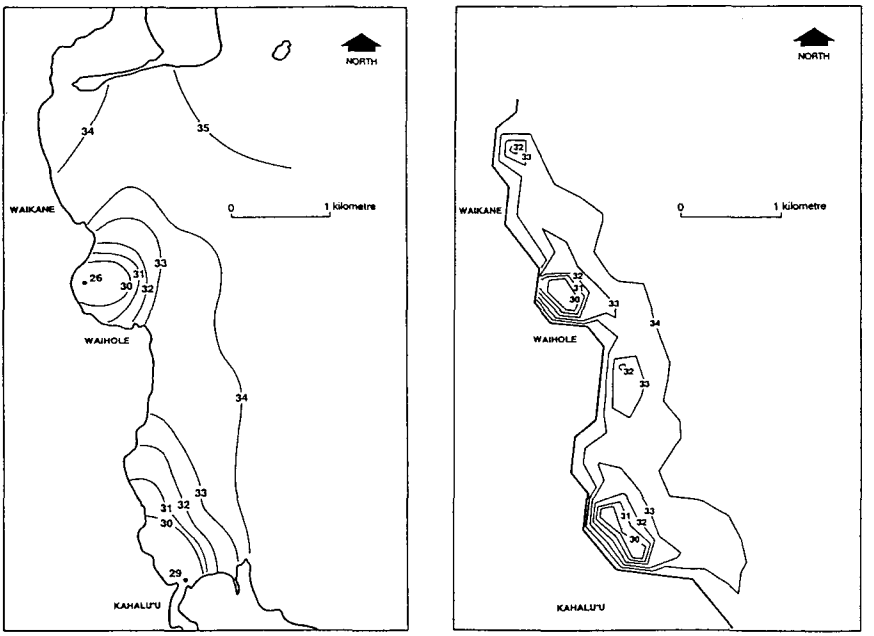

FIGURE 3. Left panel shows the observed surface salinity in northern part of Kaneohe Bay following a major storm. The right panel shows the SPECIES prediction of surface salinity on the same day using a coarse spatial grid of 300m.

producing a brackish alongshore coastal salinity front (Smith et al., 1981). Circulation in coral reef lagoons is governed by tides, wind, wave breaking and buoyancy input from the shore (eg, Andrews and Pickard, 1990). As with most nearshore lagoons, Kaneohe Bay has a deep channel behind the reef which carries the majority of the across-reef flow through the lagoon (Marsh et al., 1981; Hearn et al., 1986; Hearn and Parker, 1988). The channel has exits at either end of the lagoon through which water returns to the ocean; this topography is partly a result of the persistent scouring action of this current. The strength of across-reef flow is dependent on the strength of wave forcing and the tidal conditions. When wave conditions are calm the water may flow outward across the reef on a strong ebb tide. Winds are dominantly due to the North East Trades and blow consistently onshore with a speed of about 5 ms^{-1}.The Bay tends to divide hydrodynamically into a northern, central and southern basin (Figure 2). The northern and central areas of the Bay are apparently well mixed with flushing times of up to 10 days (depending on weather conditions). The southern basin is more isolated, and whilst there is efficient mixing within the basin, water exchange with the central area is slow and the basin receives little of the ocean water which flows inward across the reef.

3. Numerical Model of Kaneohe Bay

A three-dimensional baroclinic model called SPECIES is implemented for Kaneohe Bay (Hearn, 1996). The model itself is an extension of an earlier suite of barotropic models (Hearn and Hunter, 1987; Hearn et al., 1987) with the inclusion of density forcing. It has been recently applied to Tomales Bay in California (Hearn and Largier, 1997). The model includes the generation of currents by waves breaking on the reef. This involves the inclusion of a radiation stress (Longuett-Higgins, 1964) based on the wave height being a maximum fraction of water depth; this algorithm has been verified against field data (Symonds et al., 1995) from John Brewer Reef off the coast of Queensland in Australia. The frictional bottom stress over the reef is determined from the eddy viscosity (based on a turbulent kinetic energy calculation which includes the effect of wave motion) and a bottom friction coefficient taken from the work of Nelson (1996), Thomas and Atkinson (1997), Kraines et al. (1998), and Lugo-Fernandez et al. (1998) of $C_r = 0.1$. Most runs of the model are made with square cells of size 30m. The left panel of Figure 4 shows the model circulation due to breaking waves only. Notice the flow of water across the main reef and outward through the channel with some eddy formation at the ends of the

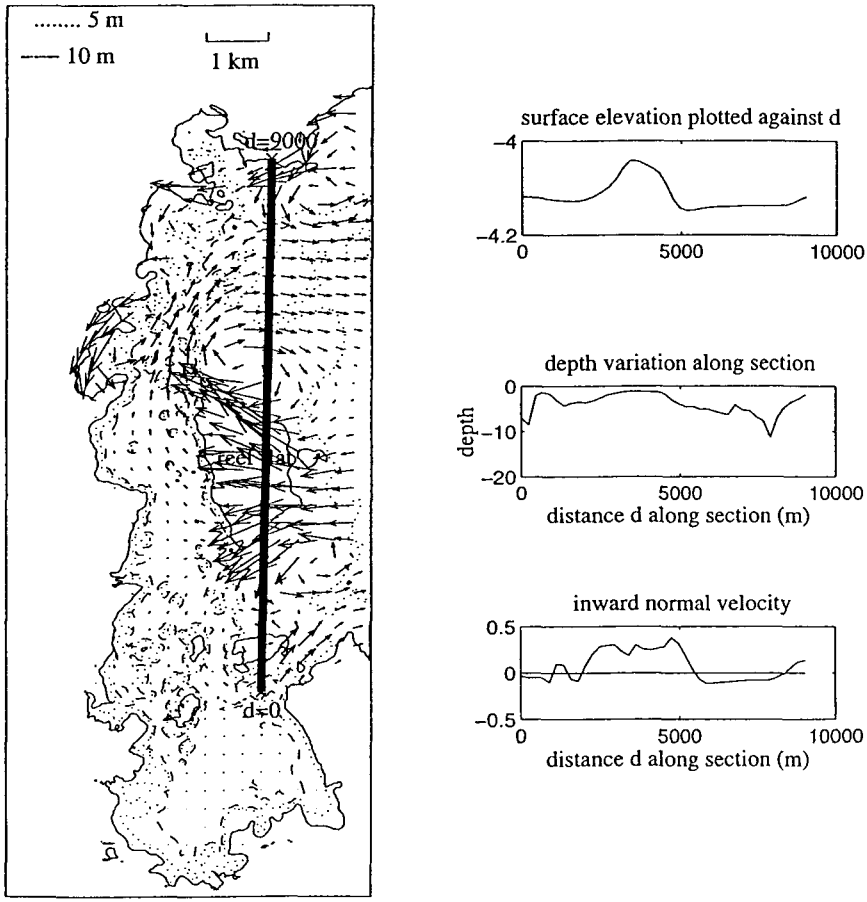

FIGURE 4. The left panel shows arrows corresponding to the currents driven by wave breaking on the main reef. The thick line is a section across the entrance to the Bay with distance d measured along the section from d = 0 to 9000 m. The right panels show the variation along the section of surface elevation, depth and inward normal velocity.

main reef. The thick line in the panel is a section across the boundary of the Bay with the distance d along the section extending from $d = 0$ in the south to $d = 9000$ at the northern end. The bottom panel on the right of Figure 4 shows the speed of flow normally to the section whilst the panel above it shows the depth variation along the section. Together these two panels illustrate the inward flow across the shallow reef and outward flow through the deep channel. The uppermost panel shows the wave set-up on the main reef which is discussed later.

Figure 3 shows a plot of model, and observed, surface salinities after a storm when flows had been steady for at least 5 days. The model used a standard forcing scenario consisting of onshore Trade Winds of speed 5 ms^{-1}, incoming swell waves of height of 3 m, and semidiurnal tides of amplitude corresponding to the annual mean of 0.37 m. Model flushing times are calculated for the entire Bay by comparing the mean salinity depression of the Bay with the rate of inflow of freshwater from streams after the model has reached a steady state. This gives the flushing time for land-based pollutants, and of all possible flushing times that could be defined, has greatest sensitivity to buoyancy forcing from streams. For the

forcing	flushing time of Bay (days)	volume flux over reef per unit width $m^2\ s^{-1}$	fractional increase in flushing rate divided by *slr*, $\bar{c}_L^{(0.6)}$ (m^{-1})
wave & tide	14 (11)	.24 (.30)	0.45 [0.33]
winter buoyancy & tide	9 (9)	.02 (.02)	0
summer buoyancy & tide	103 (85)	.00 (.00)	0
wind & tide	18(17)	.06 (.06)	0.1

Table 1. Model lagoonal flushing times for Kaneohe Bay and corresponding values after a *slr* of 0.6 m (values in round parenthesis). The table also shows the model current-depth coefficient $\bar{c}_L^{(0.6)}$ defined as the fractional change in lagoonal velocity, ie flushing rate, per *slr*. For wave and tide forcing (only) the value in square parenthesis is obtained from the one-dimensional analytical model.

cases in which this buoyancy forcing is turned-off, the associated salinity is still used as a tracer but with the dependence of density on salinity ignored in the model. Table 1 shows flushing times determined from model salinities in the Bay calculated with the three forcing mechanisms, ie wave breaking, wind stress, and buoyancy. The latter is based on either winter (positive buoyancy) conditions with long-term mean stream flows, or (for one model run) summer heating and evaporation using similar algorithms to Hearn and Largier (1997). Tidal variations are included in all runs. The table also shows, in round brackets, the flushing time after a sea-level rise (*slr*) of 0.6 m. The fourth column shows the fractional change in flushing rate divided by the *slr* of 0.6 m which is denoted by $\bar{c}_L^{(0.6)}$. The third column shows the volume flux across the reef for model cells that have depths between 1.0 and 1.1 m below present mean sea-level. It is to be emphasised that these model calculations assume that the bathymetry remains unchanged after the sea-level rise.

The results in Table 1 show that winter buoyancy and wave forcing are the dominant mechanisms for flushing the Bay. In comparing these two processes, it should be noted that their strengths depend, respectively, on stream flows, and the height of incoming swell waves, both of which are variable on time scales ranging from the seasonal down to the weather band of about 10 days. Flushing times of the Bay (due to the mean stream flows and 3 m swell waves assumed in the table) are typically about 10 days. Wind (and tidal) flushing alone are much weaker (by a factor of about 2) and summer buoyancy forcing is negligible. The only significant effect of *slr* is on wave forcing across the reef. For wind and buoyancy, the residual fluxes across the reef are both very small and essentially unchanged. The residual flux over the reef due to breaking swell waves increases by 27% which has a proportional effect on the total flushing time of the Bay. Note that this flux increase is fractionally less than the fractional increase in the height of the water column so that the velocity over the reef has decreased.

4. Nature of the Wave Driven Flow Over Coral Reefs

The classic papers on the breaking of waves on coral reefs are those of Munk and Sargent (1948), and von Arx (1948); for a recent general review see Andrews and Pickard (1990). Generally, the front of a reef consists of a steeply sloping region, called the fore-reef, at the back of which is the

reef-flat (comprising a fairly flat shallow region) and behind this comes the lagoon. This topography is shown in the second panel from the top on the right of Figure 4. The distance d is measured along a section represented by the heavy line in the left panel with $d = 0$ at the nearshore end of that section. The fore-reef terminates at about $d = 3000$ m and the reef flat extends from there to approximately 1800 m. The lagoon is evident as deeper water from $d = 0$ to 1800 m. The fore-reef extends down the steeply sloping side of the island into deep water. Waves break on the fore-reef, and on the front of the reef flat, to form the surf zone which is visually evident at the front of a reef. This reduces the wave height H of incoming waves and produces a radiation stress R,

$$R = -\frac{3g}{16}\frac{\partial H^2}{\partial x} \tag{1}$$

where x is distance measured along the direction in which the wave are propagating, ie $R > 0$ since H decreases with x. The origin of x is naturally chosen as the front of the reef flat. The distance d shown in Figure 5 is generally used to denote distance along a section (and different sections are shown in Figures 4 and 6) but for Figure 5 (only),

$$d = 3000 - x \qquad (metres) \tag{2}$$

Notice that R does not depend, per se, on the water depth and has the dimensions of a velocity squared; it is analogous to a wind stress.

A useful model for the variation of wave height assumes that H cannot exceed a known fraction γ of the total depth of the water $h+\eta$ where h is the depth below the height datum and η is the elevation of the surface above that datum, ie for breaking waves,

$$H = \gamma\left(h + \eta\right) \tag{3}$$

where γ is called the wave breaking ratio. Symonds (1994), and Symonds et al. (1995) use a value of $\gamma = 0.8$ to describe the breaking of waves across the fore-reef. However γ is known to varying with the slope σ of the bottom (Tait, 1972),

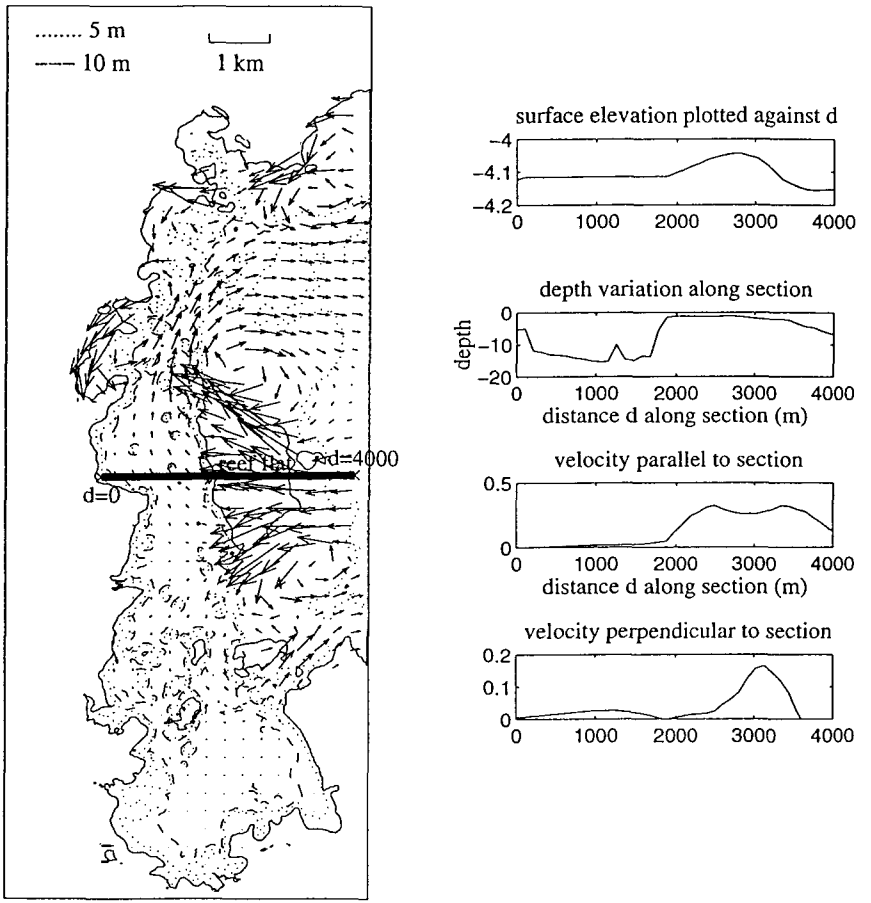

FIGURE 5. The left panel shows arrows corresponding to the currents driven by wave breaking on the main reef. The thick line is a section through the channel, and outward across the main reef, with distance d measured along the section from $d = 0$ to 4000 m. The right panels show the variation along the section of the surface elevation, depth and velocity parallel and perpendicular to the section.

$$\sigma \equiv -\frac{dh}{dx} \tag{4}$$

A value of about $\gamma = 0.8$ is satisfactory for the start of breaking of monochromatic waves. Nelson (1994) reports on laboratory experiments for wave-breaking over horizontal bottoms in which γ is reduced to less than 0.55, while Hardy et al. (1991) show that γ is reduced to 0.4 over a coral reef flat. Dally (1992) uses a value of $\gamma = 0.5$ to mark the conclusion of breaking for random waves on a beach while Hardy and Young (1991) calculated the energy remaining in the wave field at the end of breaking on a coral reef based on $\gamma = 0.5$.

The major effect of applying a surface stress to a coastal basin is to increase surface elevation until the resultant pressure gradient becomes essentially equal to the radiation stress, ie

$$\left(h+\eta\right)\frac{d\eta}{dx} = -\frac{3}{16}\frac{d\gamma^2\left(h+\eta\right)^2}{dx} \tag{5}$$

which means that at the back of the surf zone the surface is elevated above the surface of the open ocean. This is shown by the upper panel on the right of Figure 5 which gives the variation of the elevation in moving from beyond the start of the surf zone (at about d = 3600 m) to the front of the reef flat (at about d = 3000 m) and then across the reef flat to the start of the lagoon (at d = 1800 m). In Figure 5 the height datum, ie zero of elevation, is that used by the SPECIES model which is the highest sealevel expected in the most extreme circumstance, so that all elevations are negative. A more useful datum for the one-dimensional model is the open ocean water level corresponding to the SPECIES elevation of - 4.15 m in Figure 5. The one-dimensional model ignores all variability perpendicular to the direction of the incoming waves including all effects associated with the component of the radiation stress acting parallel to the reef. It also avoids any consideration of the effect of varying depth along the reef which tends to drive strong along-reef current as evident in the lowest panel on the right of Figure 5. A solution of (5) is possible if the wave breaking fraction γ is assumed constant but otherwise information is

required on the variation of bottom slope σ with x. For constant γ, (5) can be reduced to

$$\frac{d\eta}{dx} = -\frac{3}{8}\gamma\frac{d\gamma\left(h+\eta\right)}{dx} \tag{6}$$

without approximation. Integrating (6) gives the elevation at the back of the surf zone as $\Delta\eta$,

$$\Delta\eta = \Gamma\left[h_b - h_r\right] \tag{7}$$

$$\Gamma \equiv 1\Big/\left(1+\frac{8}{3\gamma^2}\right) \tag{8}$$

where h_r is the water depth over the reef flat and h_b is the depth at which the incoming waves (of incident height H_0) break on the fore-reef,

$$h_b \equiv H_0/\gamma \tag{9}$$

A *slr* increases h_r which according to (7) reduces the wave set-up by Γ * *slr*. The upper panel on the right of Figure 5, indicates a value of $\Delta\eta$ = 0.1 m for present sea-level.

It is evident from the upper panel on the right of Figure 5, that surface elevation decreases in moving from the front to back of the reef flat and the resultant pressure gradient drives a current over the reef flat. The primary force balance on the reef flat is between this pressure gradient and bottom friction. This assumes that the radiation stress, which was dominant on the fore-reef, has become secondary as wave breaking has essentially ceased. This is almost true, but not quite, because some breaking does occur due to the reduction in surface elevation as waves move across the reef flat; for the section shown in Figure 5 the wave height will reduce by $\Delta\eta/\gamma \sim 0.12$ m. The other dynamic process which could be important on the reef flat is advection but this can be shown to have a minor influence because the Froude number is small (except when the reef

flat is almost dry). With these provisos, the current at the front of the reef, denoted by u_r, is

$$u_r^2 = \frac{g h_r}{C_r} \frac{\Delta\eta}{a} f_2(r) \tag{10}$$

$$r \equiv \Delta\eta / h_r ; \quad f_2(r) \equiv \left(1 + \frac{3}{2} r + r^2 + \frac{1}{4} r^3 \right) \Big/ (1 + r)^2 \tag{11}$$

where C_r is the frictional drag coefficient on the reef flat and a is the distance from front to back of the reef flat (~ 1500 m). Provided that $r << 1$, ie the wave set-up is small compared to the water depth over the reef, the function f_2 reduces to unity in (10). This means that the square of u_r increases linearly with h_r simply due to the increase in total force exerted by the pressure gradient (whilst friction is independent of h_r). In practice, this small r limit is applicable unless the water depth over the reef is very small. Equation (10) has assumed that the wave set-up at the back of the reef flat, or the edge of the lagoon, $\Delta\eta_L$ is zero; strictly, $\Delta\eta$ in (10) should be replaced by $\Delta\eta - \Delta\eta_L$. The magnitude of $\Delta\eta_L$ can be estimated by assuming a frictional balance through the lagoon,

$$\frac{\Delta\eta_L}{\Delta\eta - \Delta\eta_L} \approx \frac{a_L C_L u_L^2}{h_L} \Big/ \frac{a C_r u_r^2}{h_r} \tag{12}$$

where h_L is the depth, a_L the path length, u_L the speed, and C_L the friction drag coefficient through the lagoon. For Kaneohe Bay, the reef flat has a ~ 1500 m, h_r ~ 1 m, whilst in the lagoon, a_L ~ 10 km, h_L ~ 10 m (in the main channel). As mentioned previously, a suitable value for C_r on the reef is 0.1 which is much higher than the value for the typical sandy bottom of the lagoon C_L ~ 0.0025. Hence assuming currents in the channel and on the reef flat are of the same order, the ratio in (12) is of order 10^{-2} which justifies the neglect of $\Delta\eta_L$ in (10).

In Figure 5, the elevation of the water surface at the back of the reef flat is - 4.12 m compared with an ocean level of - 4.15 m. So that although $\Delta\eta_L$ is smaller than $\Delta\eta$, it is not entirely negligible. SPECIES uses a submodel that recognises the type of coral or algae forming the bottom in each cell of

the model and assigns an appropriate bottom friction coefficient based on values measured in a flume by Thomas and Atkinson (1997). This means that parts of the Bay, other than the reef flat, have a higher bottom coefficient than sand and this increases the wave set-up at the back of the reef flat.

Substituting (7) into (10), now gives the relation of prime importance to this chapter which is the explicit dependence of the current at the front of the reef on the water depth over the reef, ie,

$$u_r^2 = u_0^2 F\left(h_r/h_b\right) f_2\left(r\right) \tag{13}$$

$$F\left(h_r/h_b\right) \equiv 4\left(h_r/h_b\right)\left(1 - h_r/h_b\right) \tag{14}$$

$$u_0^2 \equiv \frac{g\Gamma h_b^2}{4C_r a} \tag{15}$$

The depth dependence of u_r is contained in the function F which increases with h_r at small depths, reaches a maximum at $h_r = h_b/2$ and then decreases to zero at $h_r = h_b$. The decrease in u_r at larger h_r is due to the reduction in wave breaking. Note that h_b depends on wave height H_0.

5 Lagoonal Current

The volume flux density of the across-reef wave-driven current q is

$$q = \left[h_r + \Gamma\left(h_b - h_r\right)\right] u_r \tag{16}$$

As shown by Figures 4 and 5, most of this flux flows into the deep channel running along the back of the reef flat and is then carried back to the open ocean through the two gaps in the reef (at the northern and southern end of the Bay). Figure 6 shows the results of running SPECIES with wave-forcing only but using three layers z layers each 6.46 m thick (the upper layer is only partially filled with fluid). The left panel in Figure 6 shows flow in the bottom layer which only contains fluid in the deep channel (it is dry elsewhere). The velocity in the channel becomes large as it is

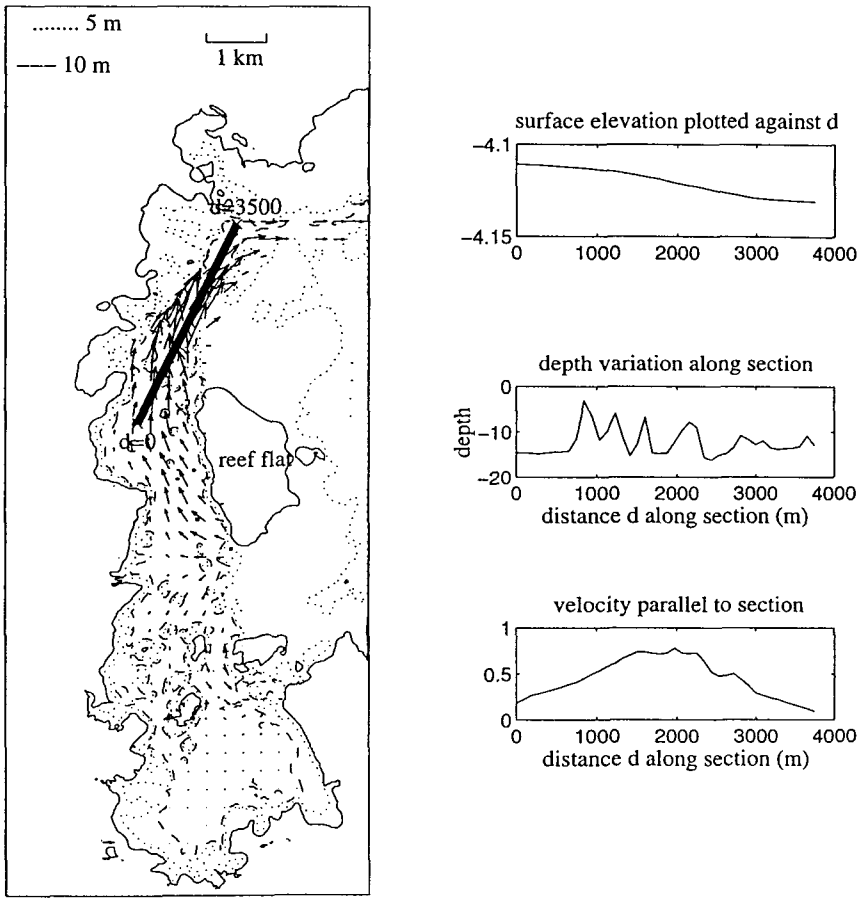

FIGURE 6. The left panel shows arrows corresponding to the currents at the bottom of the deep channel driven by wave breaking on the main reef. The thick line is a section taken along the channel just prior to the current exiting to the ocean with distance (d) measured along the section from d = 0 to 3500 m. The right panels show the variation along the section of surface elevation, depth and velocity parallel to the section.

constrained to flow through the gap in the reef. The top panel on the right of Figure 6 shows that an elevation change of 0.02 m is required to push the bottom water over the length of the section shown by the heavy line in the left panel; this is balanced by friction in the channel.

The cross-sectional area of the channel varies as sea-level changes but it can reasonably be assumed that this variation is fractionally very small compared to the fractional dependence of the volume flux q on h_r so that the lagoonal current u_L is proportional to q.

6. Current-Depth Coefficients

The dependencies of u_r and u_L on water depth over the reef are conveniently represented by the reef and lagoon current-depth coefficients,

$$c_r^{(0)} \equiv \frac{1}{u_r}\frac{du_r}{dh_r} \qquad c_L^{(0)} \equiv \frac{1}{u_L}\frac{du_L}{dh_r} \tag{17}$$

which have the dimensions of inverse heights. The advantage of defining the coefficients as the fractional rate of change of current with h_r is that they are independent of several physical parameters and in particular the lagoonal coefficient is independent of any geometric parameters relating u_L to q. There is a simple relation between the reef and lagoon current-depth coefficients defined in (17) which is a consequence of the fractional change in lagoonal current being the same as the fraction change in the across-reef flux q.

Hence using (16),

$$c_L^{(0)} = c_r^{(0)} + \left(h_r + \frac{h_b \Gamma}{1-\Gamma} \right)^{-1} \tag{18}$$

The second term on the right hand side of (18) represents the increase in lagoonal current which would occur even if the velocity across the reef were unchanged; it is simply due to the increase in volume flux over the reef arising from the increased height of the water column and contains a contribution due purely to the increase in ocean level and another due to the reduction in wave set-up.

A correction term should be added to (18) arising from changes with sea-level of the lateral variation of current across the channel. The most likely force balance in the channel is pressure gradient (due to $\Delta\eta_L$) and bottom friction. The current along the channel is driven by a gradient of $\Delta\eta_L$ in that direction which (as previously mentioned) has only a small effect on the flow over the reef. Denoting the direction along the channel by y, the force balance for the depth averaged current becomes,

$$gh_L \frac{\partial \Delta\eta_L}{\partial y} = C_d u_L^2 \tag{19}$$

and it is assumed that the current is parallel to the channel so that the elevation gradient with respect to y is independent of position across the channel whilst h_L, and hence u_L, do vary across the channel. The balance (19) is well illustrated by the panels in Figure 6 which show the change in elevation and current with distance d along a section through the channel (d represents y for that section). Hence u_L is inversely proportional to the square root of depth. The magnitude of the resultant correction term for (18) depends on the cross-sectional variation of depth in the channel. If the channel has a flat bottom the correction is zero. For other bathymetries, the current is affected but the fractional change is of the same order as the fractional change in depth. This means that the correction can be neglected provided that the lagoonal current is measured in the deeper parts of the channel.

7. Tidal Influences

Astronomical tides produce a true tidal current which flows over the reef, and through gaps in the reef, and is driven by a (small) difference in elevation between the ocean and lagoon. For most coral reef lagoons there is very little attenuation of the tidal amplitude between the ocean and lagoon and almost no difference of phase. Consequently, this true tidal current is almost exactly 90^o out of phase with the elevation. The magnitude of this current depends on the size and geometry of the lagoon and reef but it is not discussed further here.

The current flowing over the reef due to wave-breaking is affected by the variation of ocean tidal level. This is simply calculated by taking (13),

and applying a tidal variation to h_r; this assumes that the tidal variation of u_r is adequately described by these equilibrium relations. The across-reef current develops an oscillatory (but not sinusoidal) component which is here called the tidally modulated wave current; for a single tidal constituent this has the same period as the elevation. Because the current is a non-linear function of depth, h_r, the tidally averaged mean wave-driven current (which controls the wave flushing of the lagoon) differs from the across-reef current at the mean water depth. This effect on the mean current is significant because the mean water depth over a coral reef is often of similar magnitude to the mean tidal amplitude (so that the reef may be exposed at low water near spring tides). The tidally modulated wave current has components at both the tidal frequency and higher harmonics, ie sub-tidal frequencies (Symonds, 1994), both in-phase with the tidal elevation and 90° out of phase. The latter is not of interest here because it only supplements the normal tidal component whilst the in-phase component at the tidal frequency is a valuable measure of the dependence of the wave-driven current on ocean level.

The numerical model of Kaneohe Bay measures the change in tidal residues produced by a finite steady state change in water depth δh_r applied to tidal residues,

$$\overline{c}_r^{\left(\delta h_r\right)} \equiv \frac{1}{\overline{u}_r}\frac{\delta \overline{u}_r}{\delta h_r} \quad ; \quad \overline{c}_L^{\left(\delta h_r\right)} \equiv \frac{1}{\overline{u}_L}\frac{\delta \overline{u}_L}{\delta h_r} \tag{20}$$

which are a finite difference version of (17). Table 1 shows the value of the finite amplitude tidally averaged lagoonal coefficient, as obtained from the one-dimensional analysis, to be in reasonable agreement with the three-dimensional model.

8. Discussion and Conclusion

Some three-dimensional baroclinic model (SPECIES) simulations are reported for the effect of a sea-level rise (*slr*) on the flushing of Kaneohe Bay which include tidal, wind, buoyancy, and wave breaking processes. SPECIES shows that only wave breaking processes are significantly affected by *slr* which is a natural consequence of the large fractional change in the height of water above the reef. The model shows an increase of lagoonal current, and hence flushing rate, as sea-level rises. This

increase in flushing rate is based on the dispersion of a tracer released from a coastal site and is therefore representative of wave driven currents across the whole of the reef.

A simple analytical model has been presented of steady state wave forced currents across a reef which is applied to Kaneohe Bay, Hawaii. The model is intended to provide an understanding of the physics of the change in reef current with *slr*. The current on the reef is controlled by a balance between the pressure gradient due to the surface set-up (produced by waves breaking in the surf zone), and friction over the reef flat. Friction involves a coefficient C_f which can either be measured in a flume under low flow conditions (Thomas and Atkinson, 1997) or implied from wave dynamics (Nelson, 1996; Lugo-Fernadez, 1998). The model shows that the current across the reef increases to a maximum when the height reaches $h_b/2$ where h_b is the height at which wave breaking would cease. This is due to the increase of pressure gradient relative to bottom stress. As the depth over the reef increases beyond this point, the dominant change is due to the reduction of wave breaking and the current decreases to become zero when the height reaches h_b. For typical 1.5 m waves this height at which the current is maximal ($h_b/2$) is 0.9 m and so deeper reefs would show such a decrease with water height. The inclusion of tidal variations further reduces this maximum. The current in the lagoon behind the reef continues to increase even after the reef current has started to decrease. This is due to a continued increase in volume flux over the reef associated with the extra height of the water column. These predictions of the one-dimensional model are in agreement with the SPECIES model in which the current across the reef is found to decrease with *slr* (at a site with depth 1 m) whilst the volume flux over the reef, and the flushing rate of the lagoon, increase with *slr*. The variation of the reef and lagoonal currents with *slr* are represented by current-depth coefficients which are defined to be independent of the two most important physical parameters, ie C_f (friction coefficient on the reef), and geometric factors relating lagoonal current to reef current. The coefficients depend quite critically on the depth of the reef and as such their measurement provides considerable insight into the hydrodynamics of wave-driven flow. Further comparisons with field data are in progress at Kaneohe Bay.

References

Andrews, J. C. and Pickard G. L. (1990). The physical oceanography of coral-reef systems, in *Coral Reefs* edited by Z. Dubinsky, pp 11-48, Elsevier, Amsterdam.

Bathen, K. H. (1968). A Descriptive Study of the Physical Oceanography of Kaneohe Bay, Oahu, Hawaii, Hawaii Institute of Marine Biology, University of Hawaii, Technical Report, No. 14, 353pp.

Dally, W. R. (1992). Random breaking waves: a field verification of a wave-by-wave algorithm for engineering application, *Coastal Eng., 16*, 369-397.

Hardy, T. A., Young I. R, Nelson R. C., and Gourlay, M. R. (1991). Wave attenuation over a coral reef flat, *Proc. 22nd Intern. Conf. on Coastal Eng.*, Inst. of Engineers, Australia, 345-350.

Hardy, T. A. and Young I. R. (1991). Modeling spectral wave transformation on a coral reef flat, *Proc 10th Australian Conf. on Coastal and Ocean Eng.*, Inst. of Engineers Australia, 345-350.

Hearn, C. J. (1996). Application of the Model SPECIES to Kaneohe Bay, Oahu, Hawaii, *Proc 4th Int, Conf. on Estuarine and Coastal Modeling* (Ed. M L Spaulding and R T Cheng) ASCE, New York, pp 355-366.

Hearn, C. J., Hatcher, B. G., Masini, R. J., McComb, A. J. and Simpson, C. J. (1986). Oceanographic processes on the Ningaloo Coral Reef, Western Australia, *Environ. Dyn. Rep. ED-86-171*, 82 pp., The University of Western Australia, Perth, Australia.

Hearn, C. J. and Hunter, J. R. (1987). Modelling Wind-driven Flow in Shallow Systems on the Southwest Australian Coast, pp. 47-58. In: *Numerical Modelling: Applications to Marine Systems.* (Ed. J. Noye). Elsevier/North Holland, Amsterdam.

Hearn, C. J., Hunter, J. R. and Heron, M. L. (1987). The Effects of a Deep Channel on the Flushing of a Shallow Bay or Harbor, *J. Geophys. Res.*, 92: 3913-3924.

Hearn, C. J. and Largier, J. L. (1997). The summer buoyancy dynamics of a shallow mediterranean estuary and some effects of changing bathymetry; Tomales Bay, California. *Estuarine, Coastal and Shelf Science* 45: 497-506.

Hearn, C. J. and Parker, I. N. (1988). Hydrodynamic Processes on the Ningaloo Coral Reef, Western Australia. *Proc 6th International Coral Reef Symposium* 2: 497-502.

Kraines, S. B., Yanagi, T., Isobe M. and Komiyama, H. (1998). Wind-wave driven circulation on the coral reef at Bora Bay, Miyako Island *Coral Reefs,* 17: 133-143.

Longuett-Higgins, M. S. and Stewart, R. W. (1964). Radiation stress in water waves: a physical discussion with applications *Deep Sea Research* 11: 529-562.

Lugo-Fernadez, A., Roberts, H. H., Wiseman, W. J. and Carter, B. L. (1998). Water level and currents of tidal and infragravity periods at Tague Reef, St Croix (USVI), *Coral Reefs,* 17: 343-349.

Marsh, J. A. Jr., Ross, M. R. and Zolan, W. J. (1981). Water circulation on two Guam reef flats, *Proc. 4th Intern. Coral Reef Symp.*: 355-360.

McAnally, W. H. Jr., Lunz, J. D., Raney, D. C., Hudson, R. Y. and Letter J. V. Jr. (1974). Problem Definition and Modeling Techniques for the Study of Kaneohe Bay, Oahu, Hawaii, Hydraulics Laboratory, US Army Engineer Waterways Experimental Station, Vicksburg, Report Number H-74-2.

Munk, W. H. and Sargent, M. C. (1948). Adjustment of Bikini Atoll to ocean waves, *Trans. American Geophys. Union,* 29: 855-860, 1948.

Nelson, R. C. (1994). Depth limited design wave height in very flat regions, *Coastal Eng.,* 23: 43-59.

Nelson, R. C. (1996). Hydraulic roughness of coral reef platforms, *Applied Ocean Research* 18: 265-274.

Smith, S. V., Kimmerer, W. J., Laws, E. A., Brock, R. E., Walsh, T. W. (1981). Kaneohe Bay sewerage Diversion Experiment: Perspectives on Ecosystem Responses to Nutrient Perturbation, *Pacific Science*, 35, The University of Hawaii Press, Honolulu.

Symonds G. (1994). Theory and Observations of Currents and Setup over a Shallow Reef, *Proc. COASTAL DYNAMICS '94, Waterway, Port Coastal and ocean Division/ASCE*, Barcelona, Spain.

Symonds. G., Black. K. P., and Young, I. R. (1995). Wave-Driven Flow over Shallow Reefs, *J. Geophys. Res.*, 100: 2639-2648.

Tait, R. J. (1972). Wave set-up on coral reefs, *J. Geophys. Res..*, 77: 2207-2211.

Thomas, F. I. M. and Atkinson, M. J. (1997). Ammonia uptake by coral reefs; effects of water velocity and surface roughness on mass transfer. *Limnology and Oceanography*, 42: 81-88.

von Arx, W. S. (1948). The circulation systems of Bikini and Rongelap lagoons, *Trans. American Geophys. Union,* 29: 861-870.

This page is intentionally left blank

Sea-Level Changes and Their Effects
B.J. Noye & M.P. Grzechnik (Editors)

Possible Impacts of Predicted Sea-Level Rise on South Pacific Mangroves

Joanna Ellison
School of Applied Science, University of Tasmania, P. O. Box 1214, Launceston, Tasmania 7250, Australia.

ABSTRACT: In the Pacific islands the total mangrove area is about 343,735 ha, with largest areas in Papua New Guinea, Solomon Islands, Fiji and New Caledonia. A total of 34 species of mangroves occur, and 3 hybrids. These are of the Indo-Malayan assemblage, and decline in diversity from west to east across the Pacific, reaching a limit at American Samoa. Mangrove resources are traditionally exploited in the Pacific islands, for construction and fuel wood, medicines, and food supplies.

There are two main environmental settings for mangroves of the Pacific, deltaic and estuarine mangroves of high islands, and embayment, lagoon and reef flat mangroves of low islands. Past analogues indicate that the intertidal habitat of mangroves makes them sensitive to sea-level rise. Pacific island stratigraphic records and paleoecological reconstruction of mangrove response to Holocene sea-level rise has shown that low island mangroves could keep up with a sea-level rise of up to 12 cm/100 years. High island mangroves can keep up with sea-level rates of up to 45 cm/100 years, according to the supply of fluvial allochthonous sediment input.

A present analogue to sea-level rise impacts on Pacific island mangroves is provided by Bermuda, where tide gauge records since 1932 show sea-level rise at a rate of 28 cm/ 100 years. The largest mangrove area at Hungry Bay has problems with recent retreat of the seaward edge, and mangroves showing stress symptoms.

With ecological change likely in Pacific mangroves with sea-level rise, a regional monitoring system is needed. This has been the intention of a number of programs, but none is yet implemented.

Key words: mangroves, sea-level rise, Pacific, Tonga, American Samoa

CONTENTS

1. Introduction

Mangrove forests occur on low energy, sedimentary shorelines of the tropics, generally between mean tide and high tide elevations. Mangrove trees have special physiological and morphological adaptations to the environmental stresses of their intertidal habitat, of high salinity, low oxygen, poor nutrient availability and substrate mobility. Mangrove ecosystems have high faunal diversity of microbes (bacteria, Protozoa, fungi), invertebrate infauna (i.e. crabs), fish and birds.

In the Pacific islands there is a total area of mangroves of about 343,735 ha, the largest areas occurring in Papua New Guinea, Solomon Islands, Fiji and New Caledonia (Table 1). The world mangrove area is estimated at 14,197,635 ha (Lacerda et al., 1993), hence the Pacific islands has 2.42% of the worlds mangroves. The mangrove area of the Pacific islands is small in global terms, but each island group has a unique community structure, and the mangrove forests provide significant uses for human populations.

2. Mangroves of the Pacific Islands

Mangrove species distributions in the Pacific islands are shown in Figure 1, which is developed from the records of Ellison (1995).

The greatest diversity of mangroves in the world is southern Papua New Guinea owing to its location at the centre of the Indo-Malayan mangrove center of diversity, with 33 species and 2 hybrids (Ellison, 1995). Mangrove species diversity declines from Papua New Guinea east across the Pacific Islands; the Solomon Islands have 22 species. Four species do not extend beyond the Solomon Islands to the rest of the Pacific islands, *Aegiceras corniculatum*, *Avicennia alba*, *Osbornia octodonta* and *Sonneratia x gulngai*. The last is a putative hybrid between *S. alba* and *S. caseolaris* (Duke and Jackes, 1987), which could also occur in Vanuatu, where both the parents occur, provided these grow in close proximity (N.C. Duke, pers. comm.), but no records exist.

Two species extend beyond the Solomons only to Vanuatu, *Bruguiera parviflora* and *Sonneratia caseolaris*. Three species extend beyond the Solomons only to New Caledonia, *Bruguiera sexangula*, *Scyphiphora hydrophyllaceae* and *Rhizophora x lamarckii*. The limited range of these nine species defines the south west Pacific core of mangrove diversity in the Solomon Islands, Vanuatu and New Caledonia.

Table 1. Mangrove areas and species diversity in the Pacific islands.

Island Group	Mangrove[1] species	Mangrove Area (ha)	Source
Papua New Guinea	33 (2)	200,000	Scott, 1993
Palau	13	4,708	Cole et al., 1987
Northern Mariana Islands	5		Raulerson & Rinehart 1991
Guam	11	70	Scott, 1993
Fed. States Micronesia	14	8,564	Scott, 1993
Marshall Islands	5		
Nauru	2	1	Scott, 1993
Solomon Islands	20 (2)	64,200	Hansell & Wall, 1976
Vanuatu	14	2,750?	Scott, 1993
New Caledonia	14 (2)	20,250	Thollot, 1992
Kiribati	4		
Tuvalu	2	40	Scott, 1993
Fiji	8 (1)	41,000	Watling, 1985
Tonga	8	1,000	Saenger et al., 1983
Western Samoa	3	700	Pearsall & Whistler, 1991
American Samoa	3	52	Whistler, 1976
Niue	1		
French Polynesia	1		
Hawaii	2		
TOTAL	34 (3)	343,735	

([1] For number of species sources, see Ellison, 1995. Hybrids are in parentheses)

Six other species have similar eastern limits in the Solomon Islands, Vanuatu and New Caledonia but also occur to the north in Micronesia. *Ceriops tagal* occurs in Palau and Yap, and *Avicennia marina* extends to Guam and the Ryukyus. *Nypa fruticans* and *Rhizophora apiculata* extend to Pohnpei, and *Sonneratia alba* and *Rhizophora mucronata* extend to the Gilbert Islands in Kiribati (Fosberg and Sachet, 1987).

Some Pacific Islands may have reduced numbers of species owing to lack of suitable intertidal habitat. In the Northern Mariana Islands limited areas of mangrove exist on Saipan, with only one species, *Bruguiera gymnorhiza* (Scott, 1993). Nauru has a small area of mangroves on the NE coast (Fosberg, 1960; Fosberg 1975), with only *Bruguiera gymnorhiza.* In the Northern Marshalls, small areas of mangrove

(*Bruguiera gymnorhiza*) occur on Rongelap and Bikini atolls (Taylor, 1950). In Wallis and Futuna no mangroves occur (Scott 1993).

Seven species extend from the Indo-Malayan group towards its eastern limit in Polynesia, to characterise the low diversity mangroves of Fiji, Tonga and Samoa. The largest range is *Bruguiera gymnorhiza*, occurring in all Pacific island mangrove communities except for the northern Ryukyus and the southern limit of New Zealand. *Lumnitzera littorea* has the second largest range, not occurring in the Samoa group, or the southern Gilbert Islands of Kiribati (Fosberg, 1975). According to Fosberg (1975), *Rhizophora stylosa* does not occur in Micronesia with the exception of Guam, though Stemmerman (1981) notes that the separation from *Rhizophora mucronata* is not clear. *Rhizophora stylosa* extends south of the equator to Tuvalu and Tonga but not Samoa.

At the eastern limit of mangroves in Polynesia, low diversity of mangroves gives changes in community structure and microhabitat. In the absence of landward zone species, such as *Ceriops*, *Excoecaria agallocha* becomes more common in mangrove communities of Polynesia, forming extensive monospecific stands. In Tonga, *Excoecaria* forest dominates the mangrove area. In Samoa, *Bruguiera* occupies most of the mangrove area as no landward mangrove species are present, also possibly allowing the existence of coastal marshes described by Whistler (1976).

In New Caledonia, Fiji, Tonga and Samoa *Rhizophora mangle* (*R. samoensis*) occurs, disjunct from its extensive ranges in America. This is the only mangrove species present in both the Indo-Malayan and American mangrove assemblages (Chapman 1975; Tomlinson, 1986). It has been argued that this is indigenous (Ellison, 1991). In Fiji and New Caledonia *Rhizophora x selala* occurs, a hybrid between *R. mangle* and *R. stylosa* (Tomlinson, 1978).

Mangroves have been introduced in several Pacific islands to the east and north of the present limit. *Rhizophora mangle* from South America was introduced to Enewetak in 1954 (St. John, 1960). In Hawaii, *Rhizophora mangle* from Florida was introduced in 1902 to Molokai and Oahu, and *Bruguiera gymnorhiza* from the Philippines was introduced in 1922 to Oahu. Both species are well established today (Wester, 1982). In French Polynesia, there are small areas of *Rhizophora stylosa* on Moorea and Bora Bora. It is not certain whether this was introduced in the middle of this century (Fosberg, 1992), introduced earlier by Polynesians, or whether it is native (Taylor, 1979).

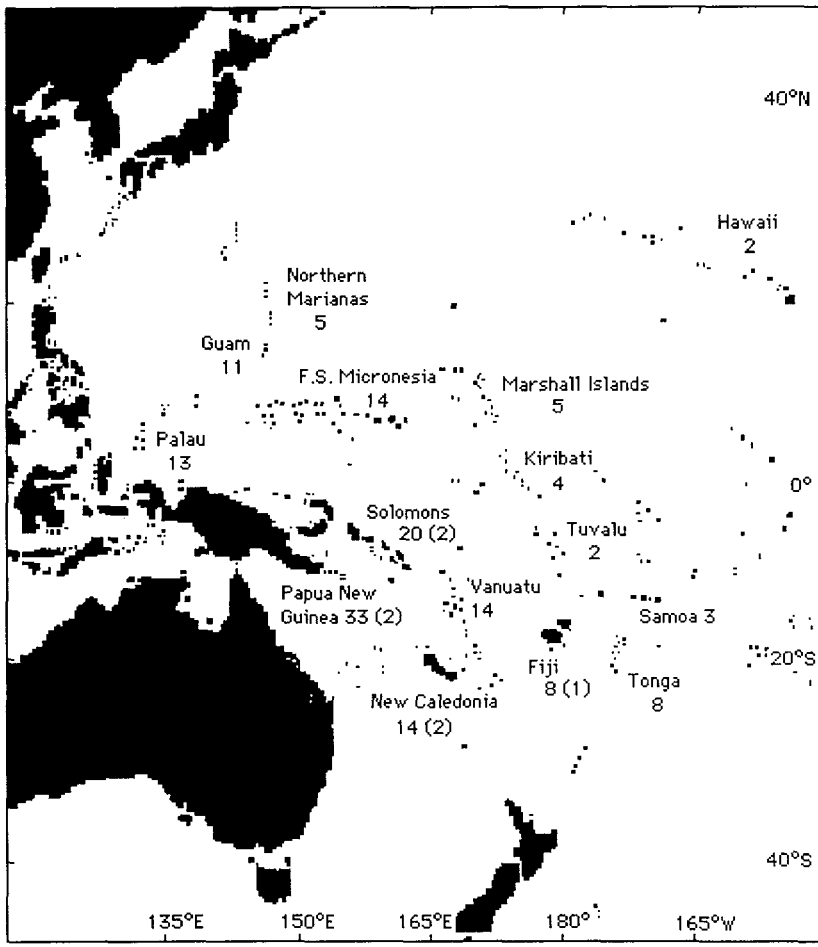

FIGURE 1. Mangrove species distributions in the Pacific Islands (Hybrids are in perentheses).

2.1 Mangrove Uses in the Pacific Islands

The importance of mangrove ecosystems is well established, as sediment traps promoting aggradation and maintaining the quality of coastal waters, natural breakwaters protecting coastlines from erosion during storms, a natural resource base for silviculture and a large range of economic products, habitats for rare fauna, and nurseries for commercially valuable fish and crustacean species, as well as for educational and tourism uses.

Mangrove areas in the Pacific islands are traditionally used for fishing, gathering of clams and crabs, wood for construction and handicrafts, and fuel wood gathering (Percival and Womersley, 1975; Pillai, 1985; Eley, 1988; Devoe, 1992; Unua, 1992). Tannins from the Rhizophoraceae are also used for protection of nets and fish traps owing to their fungicidal properties. The prop roots of *Rhizophora* are frequently used for the construction of fish traps, fuelwood, or light construction. A brown dye is obtained from the bark. The timber of *Lumnitzera littorea* is a good building material, being hard and durable, and resistant to marine borers. The showy red flowers are frequently used for leis.

There are more specialised uses developed in parts of the region. In Melanesia, sugar and vinegar can be made from the sap of *Nypa* (Percival and Womersley, 1975). Bark of the mangrove tree *Bruguiera gymnorhiza* is used in Polynesia to make a decorative dye for tapa (Fifita, 1992), the ceremonial bark cloth made from the paper Mulberry tree *Broussonetia papyrifera*. There are a range of traditional medicines derived from mangroves. The milky latex of *Excoecaria agallocha* can be used in traditional medicines (Pillai, 1985). Bark from *Xylocarpus* species are used by Tongans for treatment of internal bleeding and injuries (Whistler, 1992). *Avicennia* leaves are used for boils and contraceptives in P.N.G., and *Bruguiera* fruits are used for diarrhoea and malaria (Percival and Womersley, 1975).

A study of mangrove area conservation values was carried out by Prescott (1989), from interviews with villagers in Tonga. She showed that 83% of people interviewed used the mangroves in some way, primarily for tapa dye, fishing gear or medicines. There was concern with the over-exploitation of mangroves, and suggestion that there should be public awareness education and increased protection. There was also high awareness of the ecological function of mangroves, 64% knowing that mangroves sustained a food chain that benefitted fish, prawns and crabs,

and 90% recognised that mangroves had a protective function as a buffer zone.

3. Mangroves and Sea-Level Rise

Large mangrove ecosystems develop on sedimentary shorelines of gentle gradient, between mean sea level (MSL) and the level of mean high water spring tides. Growing in the upper half of the tidal range, their close relationship with sea-level position renders mangrove swamps particularly vulnerable to disruption by sea-level rise. With most Pacific islands having a tidal range of less than 1 m, mangrove ecosystems will be disrupted by a sea-level rise of 0.3 m, and will retreat landwards with a sea-level rise of 1 m. However, factors such as physiographic location, tidal range, species assemblage and sediment supply contribute to heterogeneity in mangrove response to rising sea-level, investigated below.

Research to investigate sea-level rise impacts on mangroves falls into two areas. First, sea-level effects on an ecosystem can be reconstructed from the past, from analysis of stratigraphy, provided the evidence is available from proxy indicators. This technique has the advantage of indicating long-term complex system response, though detail of short-term individual responses of species can usually only be speculated. Second, present day case studies can be examined, such as areas of the world where sea-level rise is occurring, or areas where flooding of mangroves has been carried out for mosquito control. From these approaches, monitoring programmes can be developed for identification of changes in the mangrove ecosystem resulting from climate change and sea-level rise.

3.1 Past Records of Mangrove Response to Sea-Level Rise

Within the intertidal habitat of mangroves, species have different preferences of elevation, salinity and frequency of inundation, resulting in species zones. Substrate elevation can be increased under mangroves, by accumulation of vegetative detritus to form a mangrove peat or mud, which may also contain matter brought in by the tides and by rivers. If the sedimentation rate keeps pace with rising sea-level, then the salinity and frequency of inundation preferences of mangrove species zones will

remain largely unaffected. If the rate of sea-level rise exceeds the rate of sedimentation, then mangrove species zones will migrate inland to their preferred elevation, and seaward margins will die back. As the accumulation of sediment under mangroves gives some ability to keep up with rising sea-level, the rate of sedimentation must be established to assess vulnerability, from studies of Holocene stratigraphy.

Stratigraphy of Pacific island mangroves indicates that mangroves have only become established in expansive swamps since the middle of the Holocene, about 6500 years before present (Ellison and Stoddart, 1991). Before this time they were limited by the interactive factors of rapid sea-level rise and lack of sedimentary shorelines. Mangroves probably survived this period as individual trees, as seen today on shorelines with too steep a gradient or that are too exposed for expansive swamp development.

There are two major environmental settings for mangroves of the Pacific, deltaic and estuarine mangroves of high islands, and embayment, lagoon and reef flat mangroves of low islands. These are assessed below for relative vulnerability to sea-level rise.

Deltaic and Estuarine Mangroves of High Islands

Deltaic and estuarine mangroves occur on islands sufficiently high to develop a river system and so deliver significant quantities of sediment to the coastal zone. These areas are the most extensive mangroves of the Pacific islands, for example the Rewa delta, Viti Levu, the Dumbéa delta, New Caledonia, and the estuaries of Palau and Ponape. The mangrove areas receive terrigenous sediment from the island, and also accumulate vegetative debris to form a mud.

These environments are demonstrated by mangroves of Tutuila, American Samoa (Figure 2). Tutuila is 32 km in length, 2-9 km wide, with steep and rugged terrain descending from a largely continuous central ridge of over 300 m, with maximum elevation of 524 m. Samoa marks the eastern boundary of mangroves in the Pacific, with two common species, *Rhizophora mangle*, which forms the seaward zone just above mean sea-level, and *Bruguiera gymnorhiza*, which forms the landward zone that approaches high tide mark. The total area of such habitats in American Samoa is relatively small (Whistler, 1976), but they consistently occur at the base of each river valley.

The mangrove swamps all have a stratigraphy of shallow mangrove mud, a mixture of peat and basaltic or calcareous sand, with 10-30% organic matter. Radiocarbon dates on organic mud samples indicate the mean rates of sedimentation (Table 2), ranging from 14.5 cm/ 100 years at Nu'uli (Pala Lagoon) to 45.2 cm/ 100 years at Masefau. The high rates on Tutuila probably reflect the steep gradients of this relatively young volcanic island, with resultant high rates of slope-wash. This is shown by the low organic matter of mangrove muds, of 10-30% organic content.

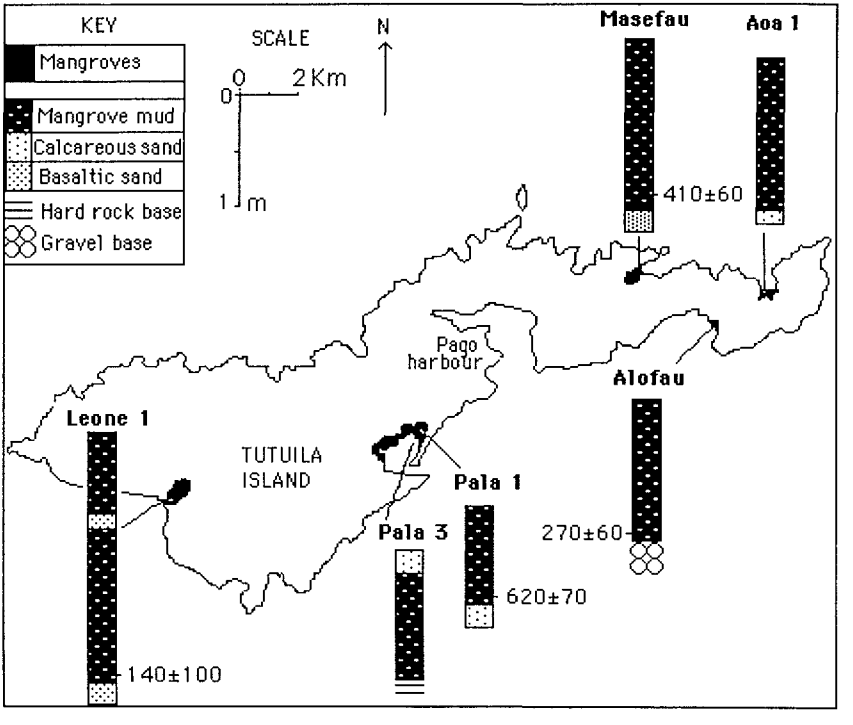

Figure 2. Coastal stratigraphy of Tutuila, American Samoa. Core depths indicate rapid sedimentation rates on this high island.

Table 2: C^{14} dates from mangrove stratigraphy, American Samoa.

Sample number	Beta lab. number	Depth (cm)	Depth rel. to MSL (cm)	C^{14} age yr BP	Sedimentation rate (cm/100 yr)
AN1-1	54276	355-370	272	3080±70	11.8
MA1-2	54278	135-150	118±25	410±60	34.6
AF1-1	54271	115-130	98±25	270±60	45.2
NU6-1	54280	80-100	65±25	620±70	14.5
LE1-1	54277	220-230	200±25	1140±100	19.7

Embayment, Harbour and Lagoon Mangroves of Low Islands

Embayment, harbour and lagoon mangroves can be extensive where fine sediment accumulates to form a broad intertidal slope. Low island mangroves do not have an external supply of sediment, and build up their substrate by accumulation of vegetative detritus to form a highly organic peat. Such locations are exemplified by Tongatapu (Figure 3).

In Tonga, Tongatapu has an area of 245 km^2, formed of limestone and lacking rivers, the highest point in the south- east is 65 m. Mangroves occur on the sheltered, leeward northern coast, and around the central Fanga 'Uta lagoon. Stratigraphy of these mangrove areas showed sediment depths of 1-4 m (Figure 3). At Folaha, the largest mangrove area in the western arm of the Fanga 'Uta lagoon, a mangrove peat occurs between depths of 1.3-2.3 m below present MSL (Ellison 1989, Ellison 1991). This peat unit underlies all of a 1 km transect across the modern swamp, and continues at lower levels beneath the lagoon. The peat in Folaha core 1 formed between 6870±90 and 5650±80 years BP, giving a rate of peat accumulation in this period of 7.7 cm /100 years. Mangrove assemblages contributing to formation of peat at the levels dated were identified by pollen analysis, and the present elevation of these assemblages has been used to determine past MSL. This shows that MSL was 3.2 m below present at 6870±90 BP, and 1.7 m below present MSL

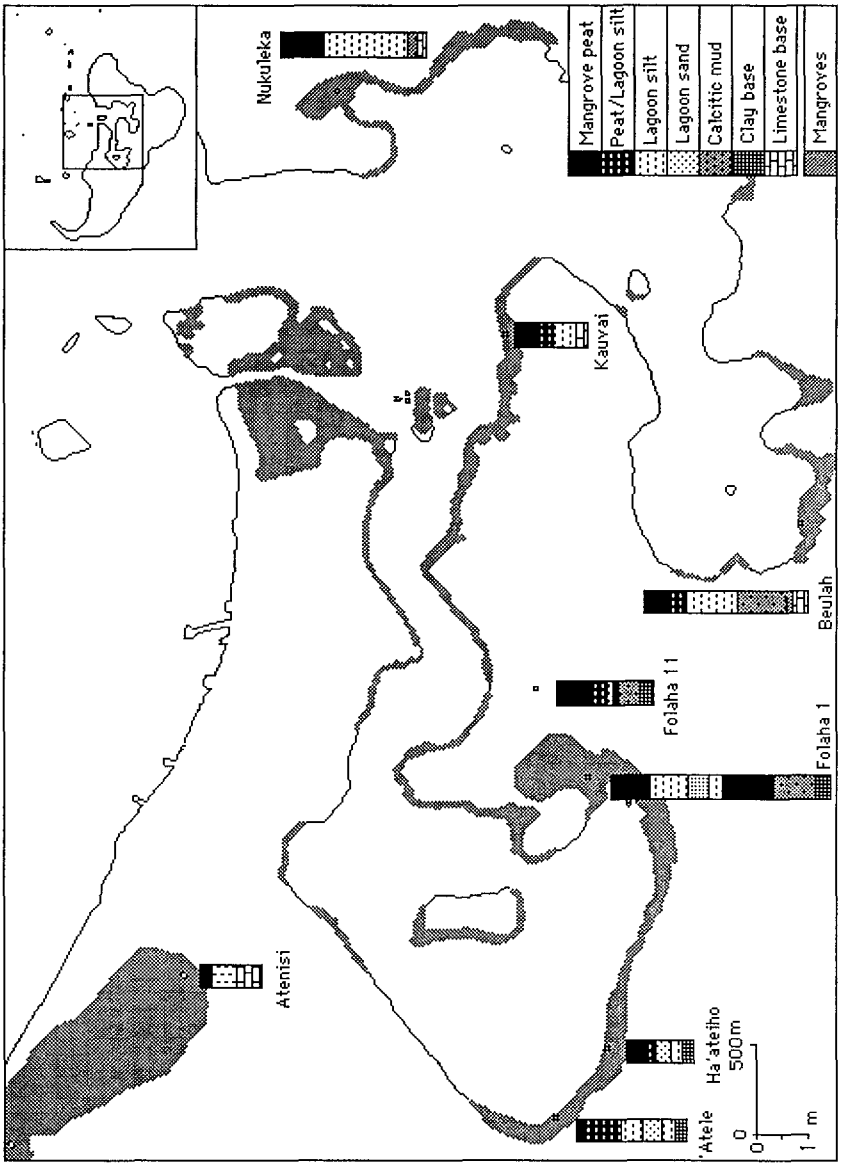

Figure 3. Coastal stratigraphy of central Tongatapu, Tonga. Core depths indicate low sedimentation rates on this low island.

5650±80 years BP (Ellison 1989). The rate of sea-level rise through the lower peat unit was 12.2 cm /100 years.

During this period of slowly rising sea-level, the mangrove ecosystem was able to persist by raising substrate levels at a roughly equivalent rate by peat formation. It was drowned out by more rapid sea-level rise, shown stratigraphically by transition from mangrove peat to overlying lagoonal sediment. This is the earliest Holocene peat building mangrove ecosystem in the Pacific, developing before other locations owing to the protected location of this part of the lagoon.

Mangrove stratigraphy from low island mangrove ecosystems indicates rates of accumulation of up to 12 cm/ 100 years. The rate from Tongatapu is similar to rates of peat accumulation from other low islands, Grand Cayman (Woodroffe 1981) and Bermuda (Ellison, 1993). This reflects the rate of authochthonous production by the mangrove trees, there being few sources of inorganic sediment in these environments.

Analysis

Comparison of mangrove stratigraphy from Samoa and Tonga shows that low island mangroves are more susceptible to disruption by rising sea-level owing to relatively low rates of sediment accretion. Stratigraphy from high islands and continental coastlines, that have more sediment coming off the land into intertidal areas from rivers and longshore drift, indicates that mangrove ecosystems will be better able to keep pace with sea-level rise. Low island mangroves could keep up with sea-level rise of up to 12 cm/ 100 years. High island mangroves could keep up with rates of 45 cm/ 100 years, provided the sediment supply is not restricted by construction such as dams on rivers leading to mangrove deltas. These differences are clearly illustrated by Figures 2 and 3, with deeper mangrove sediments on Tutuila relative to Tongatapu.

There is evidence from low island mangroves in carbonate settings in Florida may be able to keep up with sea-level rise of higher rates than oceanic islands, with accretion rates of up to 23 cm/ 100 years reported from the Florida Keys, and up to 27 cm/ 100 years reported from southwestern Florida (Snedaker et al., 1994).

While the consequences of greenhouse-induced climate change are probably not as dramatic as feared in the late 1980's, sea-level rise remains an issue for coastal ecosystems such as mangroves. Rates that can be expected to occur are the findings of the WMO /UNEP Inter

Governmental Panel on Climate Change (Warick et al., 1996). In summary, in the last 100 years there has been a rise of 10-25 cm in eustatic sea-level; the IPCC working group predicted a future sea-level rise of 15-95 cm by 2100, (mid range 50 cm). This would imply mean rates of rise of between 5 cm/ decade over the next century. Comparison with the rates of mangrove accretion indicates that island mangroves could experience serious problems with rising sea-level in the next 50 years, and oceanic low island mangroves could already be under stress.

3.2 Mangrove Problems with Sea Level Rise

The reasons for this inability of mangroves to keep up with higher rates of sea-level rise is not apparent from these past analogues. Some problems are demonstrated by mangrove dieback in Bermuda, a low island with a long tide gauge record of relatively rapid sea-level rise (Ellison, 1993). There are also other studies which indicate the problems which may develop in mangroves during rapid sea-level rise.

Erosion

Bermuda is a low limestone island without rivers, and the most northerly location for mangroves. Tide gauge records since 1932 show sea-level rise at a rate of 28±18 cm/100 years (Pirazzoli, 1986). The largest mangrove area (6.26 acres) at Hungry Bay has for the last 2000 years been building peat at a rate of 8.5 to 10.6 cm/ 100 years (Ellison, 1993). The rate of sea-level rise has exceeded the rate of sediment accretion, leading to retreat of the seaward margin accompanied by erosion. The substrate elevation of the seaward margin of mangroves is below mean sea-level, the normal lower limit for mangroves. Retreat of the seaward edge has caused loss of 2.24 acres of mangroves, commencing in the last few hundred years, with a second dieback between 1900 and 1947, and a third dieback in the last decade. Stratigraphy shows that before 4000 BP sea-level rose at a rate of 25 cm/ 100 years, from 4000 to 1000 years BP the rate of sea-level rise declined to 6 cm/ 100 years during which time mangroves established, and in the last 1000 years there was an increase to 14.3 cm/ 100 years, during which time the mangroves died back.

It is shown from Bermuda that mangrove sediment is subject to erosion with rising sea-level, with removal of mangrove substrate (above

MSL) and with some deposition subtidally offshore of the mangroves (Ellison, 1993). This corresponds with the Bruun Rule of beach erosion with sea-level rise (Bruun, 1962; Schwartz, 1967). Sheet erosion occurs at the peat surface, indicated by a 20 to 25 cm difference between the peat level above a small cliff, and the former peat surface as indicated by exposed horizontal roots of *Avicennia*. Then as trees recede and loosen the sediment, more rapid erosion occurs to form a 40-50 cm small cliff. Such erosion enhances the existing problem, for as the mangrove substrate surface is lowered and creeks widen, the problem of the differential between elevation and MSL increases.

Similar erosion patterns have been described by Semeniuk (1980) in N.W. Australia, identifying reversed succession as elevation declines. The effect of sheet erosion on mangrove zonation was migration of pioneer / seaward mangroves into more landward zones. The effect of cliffing on mangrove zonation was loss of the seaward zone, leading to truncated zonation and narrow fringes. The effect of tidal creek erosion was slumping of banks and loss of trees.

Erosion of mangrove substrate would seem to be a major problem in conditions of sea level rise. It is indicated that the Bruun Rule of beach erosion with sea-level rise is also appropriate for mangrove swamps, and may occur earlier owing to the finer texture of the sediment.

Increased Salinity

Increase in salinity in mangroves leading to salt stress can result from a number of factors as well as sea-level rise, such as groundwater depletion owing to reduced freshwater flux, groundwater extraction, and reduced rainfall. Two major physiological adaptations enable mangrove survival in saline ocean water (Scholander, *et al.*, 1962), salt exclusion in species of *Rhizophora* and *Laguncularia*, and salt excretion in species of *Aegialitis* and *Aegiceras*. Salt excluders not only operate ultrafiltration, but also cease or diminish transpiration and photosynthesis when exposed to saline water. Salt secretors can continue photosynthesis utilizing ocean water in transpiration, owing to salt glands in the leaves.

Stern and Voight (1959) grew 200 seedlings of *Rhizophora mangle* under different salinities, finding that seedling survival and growth increase by dry weight and seedling height were all inversely related to salt concentrations of the growing solutions. Ball and Farquhar (1984a) studied gas exchange characteristics in *Aegiceras corniculatum* and

Avicennia marina under different salinity and humidity conditions. They showed decreased photosynthetic capacity with increase of salinity, with *Aegiceras* being the more sensitive. Ball and Farquhar (1984b) studied the gas exchange characteristics of *Avicennia marina* with increasing salinity, finding that CO_2 assimilation rate, stomatal conductance, intercellular CO_2 concentration and evaporation rate all decreased. Increased salinity has the effect of decreasing net primary productivity to result in reduced growth, with a differential effect on species, indicating stress and changing competition between mangrove species during the climate change consequences of reduced precipitation and sea level rise.

The shallow water table of S. Florida is susceptible to saline intrusion from sea-level rise and groundwater extraction owing to low topography and porous rock. Alexander (1974) and Alexander and Crook (1974) from evidence of pine stumps in a salt water mangrove areas of Key Largo described landward encroachment of mangroves into grasslands and cypress swamps. Sternberg and Swart (1987) used isotopic measurements of plant stem water to determine relative ocean water and fresh water utilization in plants, and showed that mangroves can range from utilization of fresh to ocean water, indicating plasticity in the salt-tolerant physiological system. This would indicate that mangroves gain a competitive edge over faster growing glycophylic plants in conditions of increasing salinity.

In the Northern Territory, Woodroffe and Mulrennan (1993) document dramatic recent changes to the Lower Mary River floodplain, with saltwater intrusion and upstream expansion of the tidal creek network. This has caused death of freshwater wetland communities with loss of 60 km^2 of *Melaleuca* forest, and upstream invasion of mangroves. There are a number of possible reasons for these events, including relative sea-level rise (Woodroffe, 1995). Similar, though less spectacular extension of creeks has occurred on other river systems, such as the Alligator rivers (Woodroffe, 1995). Loss of freshwater wetlands with saline intrusion is documented in the Florida Keys (Ross, et al., 1994), where better tide records can attribute the cause to be to relative sea-level rise.

Inundation

Impoundment of mangroves for mosquito control provides an analogy to the effects of increased inundation with sea-level rise. Harrington and Harrington (1982) recorded extensive death of *Avicennia germinans* and

Rhizophora mangle at India River, E. Florida following 4 months of 30-45 cm depth of flooding of an impoundment. Flooding was sudden inundation, then sustained over the period. The natural tidal range in this area is 10-20 cm (Lahmann, 1988).

Naidoo (1983) found that prolonged flooding resulted in lower leaf water potentials; an increase in stomatal closing; and, degeneration of chloroplasts in *Bruguiera gymnorhiza*, leading to reduced rates of photosynthesis. When lenticels of aerial roots become inundated, oxygen concentrations in the plant fall dramatically (Scholander, 1955). If inundation is sustained, anoxic conditions and mortalities follow. This is thought to have been the cause of widespread mortality of *Avicennia germinans* stands in Puerto Rico recorded by Jimenez *et al.* (1985), following permanent flooding as a consequence of adjacent dredging.

Lahmann (1988) found that rates of litterfall in an impounded mangrove forest in Florida were reduced relative to natural fringe forest during flooded months. This indicates that the above ground net productivity of *Rhizophora mangle* is reduced by flooding, though phenology was not changed. Over several years of flooding survival of *Avicennia germinans* and *Laguncularia racemosa* seedlings was prevented by flooding, and *Rhizophora mangle* became more common, despite poor seedling establishment of *R. mangle* during flooded periods. The depth of flooding is was not indicated in this study.

4. Conclusion

Mangrove ecosystems are expected to show a sensitive response to predicted climate change and sea-level rise. The nature of this response is complex, and subject to factors of environmental setting. Sea-level position is central to the functional ecology of a mangrove swamp, and rise in sea-level will perturb every aspect of the ecosystem. This combined with effects of climate change, and stresses from storms and human disturbances will cause mangroves to experience disruption and area losses in the next few decades.

Certain identification of climate change and sea-level rise effects on mangroves requires long term monitoring of biological and physical parameters at a network of locations using standard techniques. This would allow comparison of data in order to distinguish a regional trend in change from that resultant from local effects. Though aimed at distinguishing climate change effects, the monitoring system would

therefore also show local effects and disturbances, which would provide environmental managers with ecological data to allow for informed management of mangrove ecosystems.

Several expert groups have identified the need for a global monitoring system of mangrove response to climate change (UNEP-IOC-WMO-IUCN, 1991; UNEP 1994), but none to date has been implemented. This is the intention of the UNEP-IOC-WMO-IUCN Long-Term Global Monitoring System of Coastal and Near Shore Phenomena Related to Climate Change (UNEP-IOC-WMO-IUCN, 1991), to be established as part of the Global Ocean Observing System. In the South Pacific region, SPREP recently developed a Regional Wetland Action Plan, in which actions 3.3.1 and 3.3.5 are development of a regional monitoring system for mangrove ecosystem health (Idechong et al., 1995). Such a regional monitoring networks would assist informed management with respect to climate change effects on mangroves.

Acknowledgement

This contribution was written while the author had tenure of an Australian Postdoctoral Research Fellowship for research into sea-level rise effects on mangroves.

References

Alexander, T. R. and Crook, A. G. (1974). Recent vegetational changes in southern Florida. In Gleason, P. J., ed., *Environments of South Florida: Present and Past*, pp. 61-72. Miami Geological Society, Miami.

Alexander, T. R. (1974). Evidence of recent sea-level rise derived from ecological studies on Key Largo, Florida. In Gleason, P. J., ed., *Environments of South Florida: Present and Past*, pp. 219-222. Miami Geological Society, Miami.

Ball, M. C. and Farquhar, G. D. (1984a). Photosynthetic and stomatal responses of two mangrove species, *Aegiceras corniculatum* and *Avicennia marina*, to long term salinity and humidity conditions. *Plant Physiology,* 74:1-6.

Ball, M. C. and Farquhar, G. D. (1984b). Photosynthetic and stomatal responses of grey mangrove, *Avicennia marina*, to transient salinity conditions. *Plant Physiology*, 74:7-11.

Bruun, P. (1962). Sea level rise as a cause of shore erosion. *Journal of the Waterways and Harbours Division, Proceedings of the American Society of Civil Engineers*, 88:117-130.

Chapman, V. J. (1975). Mangrove biogeography. In Walsh, G. E., Snedaker, S. C. and Teas, H. J.. eds., *Proceedings of the International Symposium on Biology and Management of Mangroves* 1: 3-21. University of Florida, Gainesville.

Cole, G. C., Falanruw, C. F., McLean, C. D., Whitesell, C. D. and Ambacher, A. H. (1987). *Vegetation survey of the Republic of Palau.* Forest Service Resource Bulletin PSW-22, U. S. Department of Agriculture.

Devoe, N. N. (1992). Country Report on Mangrove Forests in the Federated States of Micronesia. In T. Nakamura, ed., *Proceedings seminar and Workshop on integrated research on mangrove ecosystems in Pacific Islands Region,* pp. 62-78. Japan International Association for Mangroves, Tokyo.

Duke, N. C. and Jackes, B. R. (1987). A systematic revision of the mangrove genus *Sonneratia* (Sonneratiaceae) in Australasia. *Blumea* 32:277-302.

Eley, T. J. (1988). *Hunters of the reefs: The marine geography of the Kiwai, Papua New Guinea.* Ph.D. dissertation, University of California, Berkeley.

Ellison, J. C. (1989). Pollen analysis of mangrove sediments as a sea level indicator: Assessment from Tongatapu, Tonga. *Palaeogeography, Palaeoclimatology, Palaeoecology,* 74:327-341.

Ellison, J. C. (1991). The Pacific palaeogeography of *Rhizophora mangle* L. (Rhizophoraceae). *Botanical Journal of the Linnean Society* 105:271-284.

Ellison, J. C. (1993). Mangrove retreat with rising sea-level, Bermuda. *Estuarine Coastal and Shelf Science* 37:75-87.

Ellison, J. C. (1995). Systematics and distributions of Pacific Island mangroves. In Maragos, J. E., Peterson, M. N. A., Eldredge, L. G., Bardach, J. E. and Takeuchi, H. F. eds., *Marine and Coastal Biodiversity in the Tropical Island Pacific Region: Volume I. Species Systematics and Information Management Priorities*, pp. 59-74. East West Center, Honolulu.

Ellison, J. C. and Stoddart, D. R. (1991). Mangrove ecosystem collapse during predicted sea-level rise: Holocene analogues and implications. *Journal of Coastal Research* 7:151-165.

Fifita, N. P. (1992). Tonga Country Report. In T. Nakamura, ed., *Proceedings seminar and Workshop on integrated research on mangrove ecosystems in Pacific Islands Region,* pp. 79-89. Japan International Association for Mangroves, Tokyo.

Fosberg, F. R. (1960). The vegetation of Micronesia. *Bulletin of the American Museum of Natural History* 119:1-75.

Fosberg, F. R. (1975). Phytogeography of Micronesian mangroves. In Walsh, G. E., Snedaker, S. C. and Teas, H. J.. eds., *Proceedings of the International Symposium on Biology and Management of Mangroves* 1: 23-42. University of Florida, Gainesville.

Fosberg, F. R. (1992). Vegetation of the Society Islands. *Pacific Science* 46:232-250.

Fosberg, F. R. and Sachet, M. -H. (1987). Flora of the Gilbert Islands, Checklist. *Atoll Research Bulletin* 295:1-33.

Hansell, J. R. F. and Wall, J. R. D. (1976). *Land resources of the Solomon Islands. Volume 1: Introduction and Recommendations.* Land Resources Study 18, Land Resources Division. Ministry of Overseas Development,London.

Harrington, R. W. and Harrington, E. S. (1982). Effects on fishes and their forage organisms of impounding a Florida salt marsh to prevent

breeding by salt marsh mosquitos. *Bulletin of Marine Science* 32:523-531.

Idechong, N., Ellison, J. and Jaensch, R. (1995). A Draft Regional Wetlands Action Plan for the Pacific Islands. In *International Coral Reef Initiative Pacific Regional Workshop Report* (Suva, Fiji, 27 Nov-1 Dec 1995), pp.116-134. South Pacific Regional Environment Programme, Apia.

Jaensch, R. P., ed. (1994). *An Action Plan for Wetland Conservation in the South Pacific*. Asian Wetland Bureau, Darwin.

Jimenez, J.A., Martinez, R. and Encarnacion, L., (1985). Massive tree mortality in a Puerto Rican mangrove forest. *Caribbean Journal of Science*, 21: 75-78.

Lacerda, L. D., Conde, J. E., Alarcon, C., Alvarez-Leon, R., Bacon, P. R., D'Croz, L., Kjerfve, B., Polaina, J. and Vannucci, M. (1993). Mangrove ecosystems of Latin America and the Caribbean: a summary. In Lacerda, L. D., ed., *Conservation and Sustainable Utilization of Mangrove Forests in Latin America and Africa Regions*, pp. 1-42. International Tropical Timber Organization and International Society for Mangrove Ecosystems, Okinawa.

Lahmann, E. J. (1988). *Effects of different hydrological regimes on the productivity of Rhizophora mangle L. A case study of mosquito control impoundments at Hutchinson Island, Saint Lucie County, Florida.* Ph.D. dissertation, University of Miami.

Marshall, A. G. and Medway, L. (1976). A mangrove community in the New Hebrides, south-west Pacific. *Biological Journal of the Linnean Society* 8:319-336.

Naidoo, G. (1983). Effects of flooding on leaf water potential and stomatal resistance in Bruguiera gymnorrhiza. *New Phytologist*, 93:369-373.

Pearsall, S. H. and Whistler, W. A. (1991). *Terrestrial ecosystem mapping for Western Samoa.* Report for the Government of Western

Samoa. South Pacific Regional Environment Programme, Noumea, and East-West Centre, Honolulu.

Percival, M. and Womersley J. S. (1975). *Floristics and ecology of the mangrove vegetation of Papua New Guinea.* Papua New Guinea National Herbarium Botany Bulletin 8, Lae.

Pillai, G. (1985). Mangrove of Fiji their uses and management. In Field C. D., and Dartnall, A. J., eds., *Mangrove Ecosystems of Asia and the Pacific*, pp. 150-160. Australian Institute of Marine Science, Townsville.

Prescott, F. (1989). *The management of mangrove resources in Tonga.* M.Sc. Thesis, University of Sydney.

Raulerson, L. and Rinehart, A. (1991). *Trees and shrubs of the Northern Mariana Islands.* Office of the Governor, Saipan.

Ross, M. S., O Brien J. J. and Sternberg, L. D. (1994). Sea level rise and the reduction of pine forests in the Florida keys. *Ecological Applications,* 4:144.

Saenger, P., Hegerl, E.J. and Davie, J.D.S., 1983. *Global status of mangrove ecosystems.* IUCN Commission on Ecology Papers No. 3, Gland.

Scholander, P. F., Hammel, H. T., Hemmingsen, E. and Garey, W. (1962). Salt balance in mangroves. *Plant Physiology,* 37:722-729.

Scholander, P. F. L., Van Dam, L., and Scholander, S. I. (1955). Gas exchange in roots of mangroves. *American Journal of Botany,* 42:92-98.

Schwartz, M. L. (1967). The Bruun theory of sea level rise as a cause of shore erosion. *Journal of Geology,* 75:76-92.

Scott, D. A. (1993). *A Directory of Wetlands in Oceania.* International Waterfowl and Wetlands Research Bureau, Slimbridge, and Asian Wetland Bureau, Kuala Lumpar.

Semeniuk, V. (1980). Mangrove zonation along an eroding coastline in King Sound, North-Western Australia. *Journal of Ecology,* 68:789-812.

Snedaker, S. C., Meeder, J. F., Ross, M. S., and Ford, R. G. (1994). Discussion of Ellison, Joanna C. and Stoddart, David R., 1991. Mangrove ecosystem collapse during predicted sea-level rise: Holocene analogues and implications. *Journal of Coastal Research* 10:497-498.

St John, H. (1960). Flora of Eniwetok Atoll. *Pacific Science* 14:313-336.

Stern, W.L. and Voight, G.K. (1959). Effect of salt concentration on growth of red mangrove in culture. *Botanical Gazette,* 131:36-39.

Sternberg, L. da S. L. and Swart, P. K. (1987). Utilization of freshwater and ocean water by coastal plants of southern Florida. *Ecology,* 68:1898-1905.

Taylor, F. J. (1979). *Rhizophora* in the Society Islands. *Pacific Science* 33:173-176.

Taylor, W. R. (1950). *Plants of Bikini and other Northern Marshall Islands*. University of Michigan Press, Ann Arbor.

Thaman, R. R. (1992). Vegetation of Nauru and the Gilbert Islands: Case studies of poverty, degradation, disturbance and displacement. *Pacific Science* 46:128-158.

Thollot, P. (1992). Importance des mangroves pour la faune ichtyologique des recif corallins de Nouvelle- Caledonie. *Cybium* 16:331-344.

Tomlinson, P. B. (1978). *Rhizophora* in Australasia- some clarification of taxonomy and distribution. *Journal of the Arnold Arboretum* 59:156-169.

Tomlinson, P. B. (1986). *The Botany of Mangroves*. Cambridge University Press, Cambridge.

UNEP-IOC-WMO-IUCN (1991). Meeting of Experts on a Long-Term Global Monitoring System of Coastal and Nearshore phenomena, Pilot projects on mangroves and coral reefs. *Intergovernmental Oceanographic Commission Report of Meetings of Experts and Equivalent Bodies* 69.

UNEP (1994). *Assessment and Monitoring of Climatic Change Impacts on Mangrove Ecosystems.* UNEP Regional Seas Reports and Studies No 154.

Unua, W. B. O. (1992). Country report on the mangrove ecosystems of Papua New Guinea. In T. Nakamura, ed., *Proceedings seminar and Workshop on integrated research on mangrove ecosystems in Pacific Islands Region,* pp. 34-45. Japan International Association for Mangroves, Tokyo.

Warrick, R. A., Le Provost, C., Meier, M. F., Oerlemans, J. and Woodworth, P. L. (1996). Changes in sea level. In Intergovernmental Panel on Climate Change- Second Assessment Report, Working Group 1 *Climate Change 1995: The Science of Climate Change*, pp. 363-405. Cambridge University Press, Cambridge.

Watling, D., (1985). *A mangrove management plan for Fiji.* Government Press, Suva.

Wester, L. (1982). Introduction and spread of mangroves in the Hawaiian Islands. *Association of Pacific Coast Geographers Yearbook* , 43: 125-137.

Whistler, W. A. (1976). *Inventory and Mapping of Wetland Vegetation in the Territory of American Samoa.* Report for the U.S. Army Corps. of Engineers.

Whistler, W. A. (1992). *Flowers of the Pacific Island Seashore.* Isle Botanica, Hawaii.

Woodroffe, C.D. (1981). Mangrove swamp stratigraphy and Holocene transgression, Grand Cayman Island, West Indies. *Marine Geology,* 41:271-294.

Woodroffe, C. D. (1995). Response of tide dominated mangrove shorelines in Northern Australia to anticipated sea-level rise. *Earth Surface Processes and Landforms*, 20:65-85.

Woodroffe, C. D. and Mulrennan, M. E. (1993). *Geomorphology of the Lower Mary River Plains, Northern Territory.* North Australia Research Unit, Darwin.

Sea-Level Changes and Their Effects
B.J. Noye & M.P. Grzechnik (Editors)

Monitoring Sea Level: Who's Monitoring the Land?

S.M. Turner
National Tidal Facility, GPO Box 2100, Adelaide, Australia, 5001.
G.M. Homes
Australian Hydrographic Office, Locked Bag 8801, South Coast Mail Centre, New South Wales, Australia 2521

ABSTRACT: Concerns of Pacific island nations regarding the widely publicised issue of sea level rise associated with global warming are being addressed through a monitoring array of high resolution sea level stations established in eleven countries of the South Pacific Forum. While these stations accurately measure sea level, it is vital that the stability of the adjacent land mass be monitored to the same degree of accuracy.

To this end the stations are supported by networks of deep bench marks established at coastal and inland sites where possible. Repeat high precision levelling and Global Positioning System (GPS) connections are undertaken to monitor the stability of the sea level sensor. Surveyors use techniques capable of matching the size of the expected sea level rise in the order of 1.5mm/year.

Currently the geodetic monitoring program enables sea level change to be determined relative to the adjacent land. While this is of prime importance to the communities, the program needs to be enhanced to enable the monitoring of absolute sea level rise by separating eustatic sea level change from tectonic movement of the islands.

This paper describes the rationale behind the Pacific program, the essential geodetic survey support, technology transfer in high precision measurement and results of the monitoring to date.

A similar array of sea level stations has been established around Australia and in the Cocos (Keeling) Islands in the Indian Ocean. Geodetic survey support is provided by the Australian Commonwealth and State surveying agencies, coordinated through the Intergovernmental Committee on Surveying and Mapping. Although the Australian mainland is theoretically more stable than the Pacific islands, the same level of geodetic control is required to monitor the stability of the monitoring stations themselves.

KEY WORDS: surveying, Global Positioning System (GPS), geodesy, training, information.

CONTENTS

1. Introduction

Our planet is a natural place of change. The Earth's climate system has varied substantially in the past with severe impacts upon humankind. Recent droughts in Australia, floods in Europe and China, and the increasing prevalence of cyclones and hurricanes are examples of decadal climate change. Century-long climate changes are exemplified by phenomena such as the Little Ice Age.

Human activities are now causing additional changes, with equally large impacts. Atmospheric pollution hangs over many areas of the Northern Hemisphere while closer to Australia the hole in the ozone layer is getting larger over Antarctica. The greenhouse gases being added to the atmosphere will reside there for decades to centuries. These gases are predicted to increase average global surface temperatures by several degrees Celsius. Such warming is likely to raise sea level by expanding ocean water and melting glaciers and portions of the Greenland Ice sheet.

Sea level rise will increase the effect of tropical cyclones and other phenomena that propel storm surges. The effects on small low lying island nations such as Tuvalu, Kiribati and the Marshall Islands, where the bulk of the population lives along the coastal fringe, will be disastrous.

A prime need facing governments of the world, particularly those low-lying coral atoll nations of the South Pacific, is the ability to predict the possible environmental changes of the coming decades with the highest credibility.

Being able to better foresee these environmental perturbations will enable governments to make sound choices as to how they can adapt industry, trade and lifestyles to a future environment over which they have little influence.

The South Pacific Sea Level and Climate Monitoring Project, funded by the Australian Agency for International Development (AusAID), provides quality sea level and meteorological data through an array of the latest generation climate monitoring stations. These stations, backed by a rigorous geodetic survey, produce data, research and results upon which the nations of the South Pacific can make future developmental and societal decisions.

2. Community Concerns

The Earth's average surface temperature has risen approximately 0.7°C in the last century and the seven warmest years on record have occurred since 1990 with 1998 being the warmest. Climate modelling studies generally estimate that global temperatures will rise a few degrees in the next century. In the early 1980's, high-range estimates of 345cm and mid-range estimates of 180cm rise in sea level by the year 2100 were being predicted (Hoffman et al., 1983). More refined projections based on improved models now predict that global warming is most likely to raise sea level by 45 cm by the year 2100, with a one percent chance of a 112 cm rise (Titus and Narayan, 1995). This figure will change on a local scale due to factors such as compaction and subsidence of land, groundwater depletion and natural climate variations.

Against this background at the 1988 South Pacific Forum, the Prime Minister of Australia announced an initiative to undertake a feasibility study into the establishment of a network of stations to monitor climatic change in the Pacific. This initiative was made in response to concerns expressed by heads of governments over the impacts of the enhanced Greenhouse Effect on the region, particularly the effect of sea level rise on the low-lying coral atolls.

As a result of this study it was announced in 1989 that Australia would fund a project to generate an accurate record of the variance in long-term sea level for the South Pacific and establish methods to make this data readily available to and usable by the Pacific Island Countries (PIC's).

3. The Pacific Project

The Project aims to help the PIC's and their governments understand the scale and implications of changing sea levels and climate. In the Pacific, the task is difficult since climate is only one part of the problem of changing sea levels. Others include the movement of the earth's crust due to movements of continental plates, active volcanoes and earthquakes that occur throughout the region. A major component of the Project is a geodetic survey that aims to isolate these movements from the eustatic sea level changes.

The geodetic survey component of the South Pacific Sea Level and Climate Monitoring Project was established to:

- Set up high resolution monitoring stations in the region to measure the relative motions of land and sea at each station (Fig 1).

- Carry out geodetic observations to measure movements of the crust at other strategic sites in each country with respect to the reference station. In this way, these measurements can be used to identify localised problems from changes to sea level and movements of the earth.

- Help identify changes to sea levels with reference to a similar network of stations in Australia and elsewhere in the world, whether these changes are due to thermal expansion of the ocean, contributions from land ice, or changing properties of water from different ocean zones.

- Collaborate with ongoing international geodetic programs, which may be incorporating satellite altimetry, radio astronomy and gravity techniques, to provide a measure of regional vertical control, and exchange information and data with national, regional and international Climate Change centres.

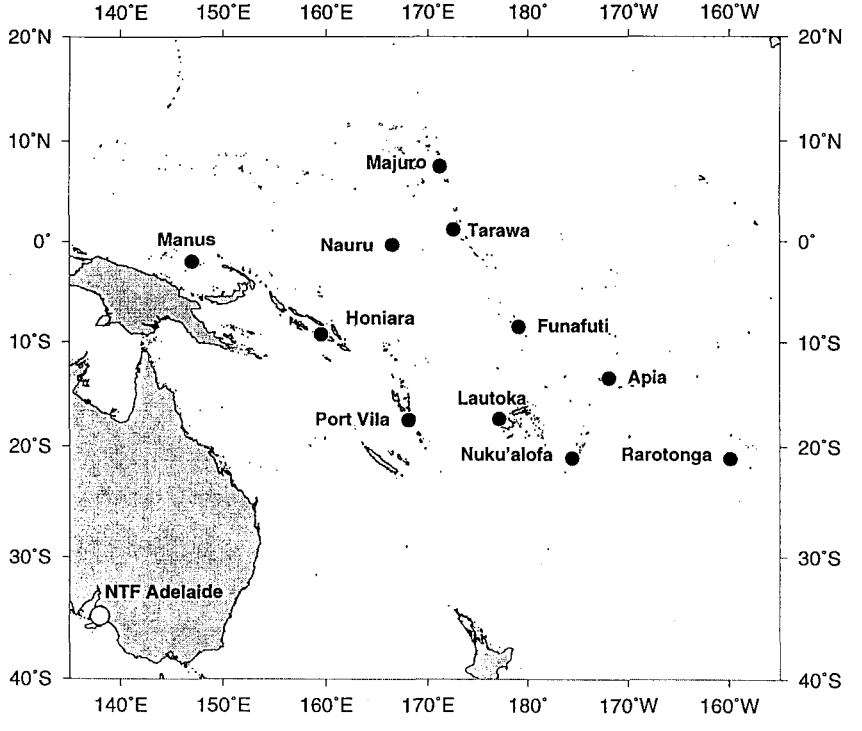

Figure 1.
South Pacific Sea Level and Climate Monitoring Project Sites

The Sea Level and Climate Monitoring Station

To improve the accuracy in measuring sea level changes, tide gauges must use "state of the art" technology, improved sensors, digital recording, and additional meteorological inputs. The aim is to monitor ocean levels with an accuracy of better than ±1mm, as the present estimate of global sea level rise is 1.5 ± 0.5mm per year.

The development of the Sea Level Fine Resolution Acoustic Measuring Equipment (SEAFRAME) station (Fig 2) has improved on the capability of conventional tide gauges (Homes, 1992). Eleven of these stations were commissioned in the Project area over a two-year period, commencing in October 1992. These stations are similar to the 14 stations operating around the Australian coastline.

The equipment has built-in sensors that measure:

1. Water level, using a very sensitive acoustic sensor, and a pressure sensor as a backup;
2. Wind speed and direction, and maximum wind gust;
3. Air and water temperatures; and
4. Atmospheric pressure.

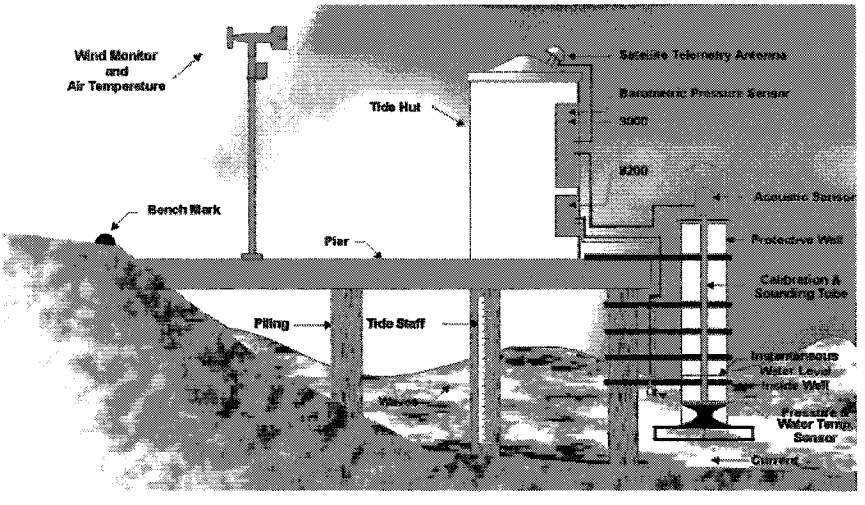

Figure 2.
Typical SEAFRAME Installation

The equipment has the capability to measure sea level changes within a one millimetre resolution, every six minutes. Other measurements are recorded once every hour. Data are recorded in a data logger and then automatically transmitted hourly via the Japanese Geostationary Meteorological Satellite to the Bureau of Meteorology in Melbourne. The data is then sent to the National Tidal Facility (NTF) in Adelaide by Internet.

At the NTF, data are stored on a long-term strategic data bank for later analysis, refined for use by governments, and made available on request from the general public.

The stations have been designed to operate in harsh environments with on-site maintenance required only once every 12 to 18 months. Out of necessity, all eleven stations have been established on manmade structures within port and harbour facilities. It is only in these facilities that there is a guarantee of the water depth and reliable power and telecommunications required by the equipment. Security of the equipment is of vital concern. Siting the equipment within port and harbour environs offers some measure of protection from theft and vandalism, although there is the risk of accidental damage arising from normal day to day working within such busy and confined areas.

4. Geodetic Survey

Although the precision required to determine the Greenhouse Effect trend is very close to the threshold that is physically possible, the SEAFRAME equipment used in this Project has been specifically designed with the special and rare quality of datum stability. This datum can be monitored with respect to a Tide Gauge Bench Mark (TGBM).

However, problems arise in that the Greenhouse resolution demands that the vertical stability of the TGBM itself should be monitored. It is important to note that up to the present time all mean sea level time series are relative mean sea levels. There is an ambiguity in that it is impossible to separate the vertical crustal movement at the TGBM from the real (eustatic) sea level rise, without further information (Liren, 1995).

The SEAFRAME sites satisfy the oceanographic and operating requirements of the equipment. However, they are not ideal from a geodetic perspective. Many of the port and harbour facilities in the Pacific region are established on reclaimed land or on unconsolidated soils. Consequently, any manmade structure is likely to settle over a period of time. During the installation phase every endeavour was made to ensure that the supporting structure for the SEAFRAME installation was embedded into bedrock but this was not always possible.

Of critical importance is a rigorous survey to measure the settlement of the installation.

In early 1992, a four-phase, 20-year, Geodetic Survey Plan (NTF, 1992a) was prepared for the geodetic monitoring of the stability of the stations. The plan was prepared based on recommendations from a committee of experts set up by the International Association for the Physical Sciences of the Ocean (IAPSO) which met in 1988 at Woods Hole, USA, to investigate the geodetic fixing of tide gauge bench marks (Carter et al., 1989). The principal recommendations of this committee were that:

- All gauges to be used to monitor sea level must have a local network of several (6 to 10) bench marks resurveyed by spirit levelling or GPS at least once a year.

- Tide gauges should be organised into regional networks and the relative positions of the gauges within each network should be determined by frequent, preferably at least once per year, GPS surveys designed to achieve sub-centimetre accuracy.

- The regional sea level networks should be organised around the primary stations of the International Earth Rotation Service (IERS) Terrestrial Reference Frame (ITRF).

- Absolute gravity measurements should be made at all of the IERS primary stations, near as many individual tide gauges as possible (with highest priority being given to island tide gauges), and in regions of glacial rebound and tectonic activity.

Phase 1

While the tide gauge exhibits a high degree of datum stability, it is essential that the datum stability be checked periodically by precise levelling to an array of deep-seated bench marks located close to the tide gauge.

Every precaution is taken to ensure the safety of the tide gauges but the gauge datum may be affected by natural phenomena such as cyclones and storm surges (Fig 3), by movement of the gauge due to settlement or port operations and from unauthorised activities.

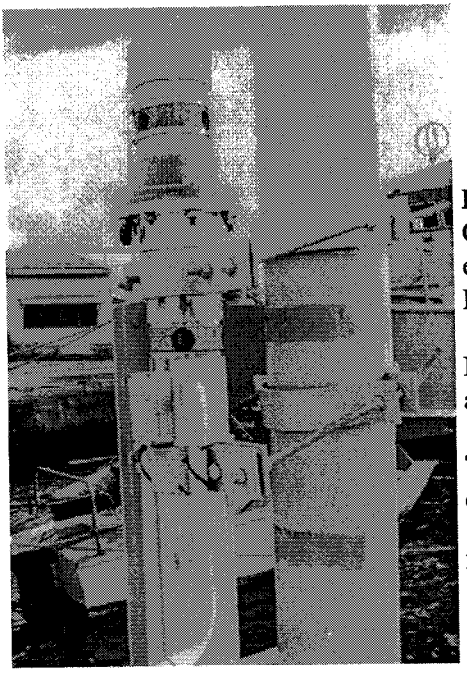

Figure 3.
Cook Islands support pile and environmental tube after Cyclone Pam, December 1997

Note the damaged threaded rods and displaced brackets.

The paint marks indicate the original position of the brackets.

Photo: A. Suskin, NTF

Bench marks, consisting of marine grade stainless steel, and conforming to the Project specifications (NTF, 1992b) have been established with at least one at each site satisfying the requirements for a GPS site. A regular program of precise differential levelling using a digital level and a pair of 2 metre bar-coded invar staves is undertaken between these bench marks and the tide gauge. To help maintain a uniformity of datums, bench marks used by local authorities for the monitoring of other, less accurate, tide gauges in the area are also levelled wherever possible.

Phase 2

The precise differential levelling in Phase 1 monitors the stability of the tide gauge in relation to the TGBM in the coastal zone of the island. However, it does not determine whether the coastal zone is moving in relation to the main body of the island.

Wherever possible, a second array of 3-4 bench marks has been established approximately 10 kilometres inland from the tide gauge in either stable ground or, more preferably, bedrock.

Precise differential levelling of the inland array of bench marks is done in conjunction with the survey of the coastal bench mark array. These surveys monitor the relative stability of the two arrays in isolation.

GPS observations and / or precise differential levelling are carried out between the arrays in conjunction with the levelling of the coastal and inland arrays. The GPS observations are done simultaneously with the levelling. Local survey personnel actively participate in the field surveys and are being progressively trained in both precise levelling and GPS observations.

Phase 3

Phases 1 and 2 help to establish the relative difference between sea level and tectonic motions at one point on the main island in each country (except in Papua New Guinea where the station is situated in the Admiralty Island group). The magnitude of tectonic movements in the Pacific can vary over small distances between islands within a PIC whereas sea level signals over similar distances are assumed to be the same. Of specific importance to the

people of other islands in each nation group are the movements of sea level relative to their island.

It is proposed to install a bench mark in other major islands and then make regular GPS connections to the main island. From these observations relative movement between the main island and the outer islands can be deduced. Similarly, trends in sea level can also be deduced for these outer islands. This data will be of vital importance to the PIC's for future use in climate impact evaluation.

Phase 4

The sea level movements this Project is aiming to detect are small and require the use of the latest geodetic techniques. Of importance in understanding the variance of sea level in a regional sense is the detection of small vertical movement over large distances.

Space geodetic techniques and absolute gravity measurements offer the possibility of directly measuring, over long distances, the vertical movement of bench marks. However, it is currently not feasible to use transportable VLBI and SLR nor absolute gravity in the Pacific region on a regular basis. The equipment needed for these techniques is expensive, large and requires considerable logistical support.

The remaining alternative able to resolve vertical movement over long distances is GPS. It is proposed to carry out inter nation GPS observations between each SEAFRAME tide gauge. Furthermore, it is proposed that this network be tied to core GPS stations established by the IGS (International GPS Geodynamics Service) under the auspices of the International Union of Geodesy and Geophysics.

There are two advantages to tying the network to the core stations. Firstly, the network will be surrounded by a series of stations with highly accurate geocentric coordinates. These stations can be used in an adjustment to produce the best possible results for all GPS-observed stations within the Project area. Secondly, this will relate the tectonically active South Pacific area to Australia, which is more tectonically stable and where sea level is also being monitored by a complimentary project.

5. Results

To date, regular Phase 1 and Phase 2 surveys have been carried out by NTF staff in association with staff from the in-country national survey organisations. In comparison to Phases 1 and 2, Phases 3 and 4 are very expensive and a watching brief is being kept on international developments in GPS before proceeding with this part of the survey. Also, other similar

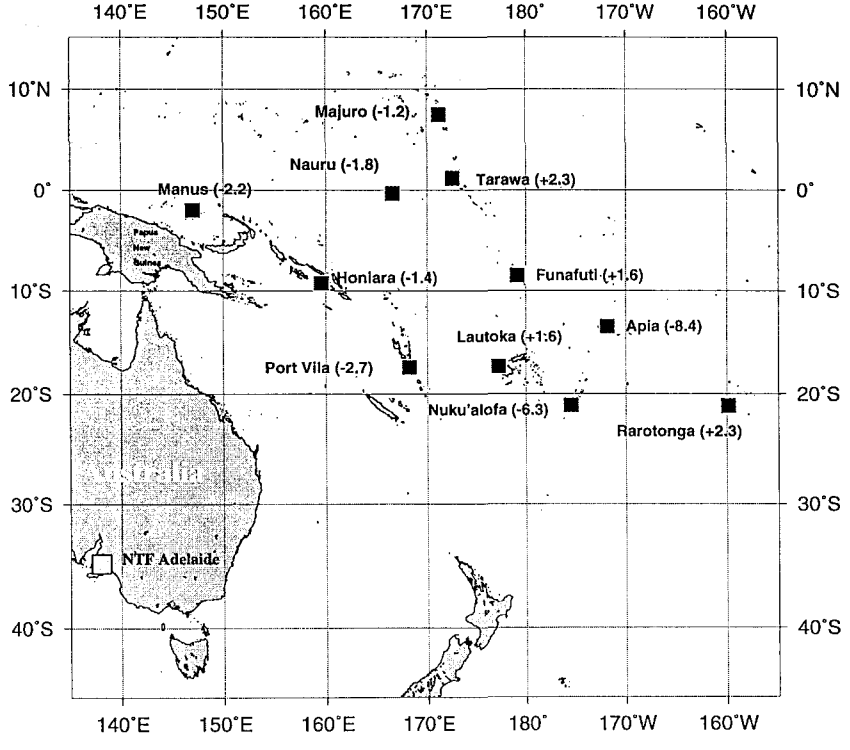

Figure 4.
Relative movement (mm) between SEAFRAME Sensor Bench Mark and nearest deep bench mark 1992 - 1998

international projects are being identified in the area with the aim of sharing resources.

The rigorous survey techniques followed in the field enable the Project's levelling specifications (NTF, 1992c) to be satisfied. In these specifications, the allowable misclosure between the forward and backward levelling runs was set at ± 2mm√K where K is the distance of the forward run, measured in kilometres. Internal consistencies of better than 1mm√K are regularly achieved while the specification is easily attained.

This Project, by the very nature of the signal it is endeavouring to measure, is planned to extend more than 20 years. Therefore it will be some time before any real trends become apparent from the data.

However, even at this early stage, with up to four surveys at some sites, movement greater than 2mm√K between the TGBM and the SEAFRAME Sensor Bench Mark has been detected at every site (Fig 4), although some of the distances levelled are very small. The larger relative movement at Apia is due to the settling of the installation while at Nuku'alofa the installation was knocked by a ferry.

In Tuvalu, over four levelling epochs from 1993 to 1997, we have noticed a progressive tilt of the land between the SEAFRAME station and the conventional tide gauge operated on the same island as part of the Tropical Ocean Global Atmosphere program by the University of Hawaii (Fig 5). A relative movement of more than 12mm between the two tide gauges, 3.1km apart, has been observed.

Two geodetic GPS receivers with geodetic L1/L2 antennas are also used on the Project. GPS heights of specific coastal and inland bench marks at each location have been determined once. Only recently has the second epoch of GPS measurements been made between the coastal and inland bench mark arrays. At the time of writing, the results are not yet available.

Continued regular surveys are required before any further comment can be made about the relative stability of the SEAFRAME stations.

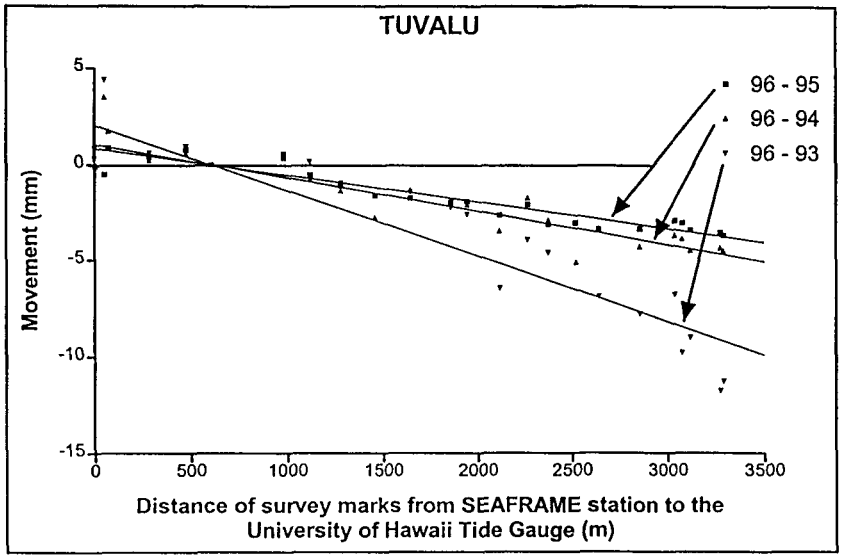

Figure 5.
Bench Mark Levelling, Fongafale, Funafuti atoll, Tuvalu

To date, obvious and sudden datum shifts have occurred at several sites due to both natural phenomena and human interference. In these cases an adjustment is made to the sea level record after survey measurement to ensure that all results relate to a common datum. More survey observations are required at those sites where the datum movement is gradual and is generally of a much smaller magnitude.

6. Information and Training

Training - Surveys

Training is an important aspect of this Project. Currently the PIC's do not have the capacity to carry out differential levelling or GPS surveys to the standards required by this Project. Visiting survey teams are endeavouring to progressively train their PIC counterparts in all field aspects of precise differential levelling and GPS surveys.

PIC input was low initially but is slowly increasing with the involvement of counterparts in all aspects of field work. Over time this increased involvement of local personnel in the survey program will contribute to the overall efficiency of the Project.

The aim of the training program is to train PIC personnel to the level where they will be able to undertake all field observations themselves using the appropriate equipment and techniques and adopting the necessary standards. It is then anticipated that the Project will need only to provide general oversight and supervision to ensure the successful completion of field surveys.

In addition, this technology transfer will provide the expertise to undertake other high precision surveys in-country as required and will lead to an improvement in the quality of the national levelling networks.

Training - Workshops

In the first phase of the Project, four "rounds" of training workshops were conducted, three in the region and the fourth at the NTF in Adelaide. In each of the first three rounds, the then thirteen island member countries of the Forum were divided into three regional groups and their representatives attended workshops in a regional centre. The training team moved between regional centres to deliver the workshops. The fourteenth country, Palau, joined the Forum after the completion of these workshops.

The first round of workshops was aimed at raising public awareness and educating the educators and media on climate and sea level change issues. The unique mix of technical specialists, educators and journalists made for some lively debate.

The second and third rounds were progressively more technical, covering the reasons for and methods of monitoring the ocean and atmosphere, and data interpretation and its applications. The concepts of the geodetic survey control were introduced at this stage.

The final two-week hands-on workshop was more intensive, utilising the full resources of the NTF, its staff and associates. The workshop was attended by

two representatives from each country, selected from among those who had attended previous workshops.

Training – Short-term Attachments

Following on from the training workshops, a program of short-term attachments of island government specialists to the NTF, and other Australian institutions where appropriate has been initiated. Selected, previously trained, specialists have undertaken specific courses including "Precise Vertical Survey Control". Other courses have been provided in data management and sea level research. This involvement in course work will lead to individuals undertaking further formal education and training and playing an active part in capacity building within their own governments.

Information

The importance placed on the information and training needs of the region in relation to sea level and climate change is reflected in the funding, under the Project, of a Climate Change Officer attached to the South Pacific Regional Environment Programme (SPREP), based in Apia, Samoa. This Officer is responsible for the coordination of training activities with the NTF and the dissemination of data and information from the Project and other sources to the governments of the region.

Currently there are two information "products" emanating from the Project. The first is a Monthly Data Report that portrays the data from the stations in graphical form with minimal interpretation. The second is a quarterly report prepared, from material supplied by the NTF and other sources, published and distributed by SPREP. This latter report is aimed at providing information of use to the technical specialist, to the policy advisers, to the media, to the educators, and ultimately to the general public of the island nations.

One of the spinoffs from the data obtained from the stations in the Pacific, is the availability of very significantly improved tidal predictions for the eleven ports concerned. The benefits to shipping in the region will be recognised as this information becomes widely available and used in conjunction with the real-time data display systems being installed in the port offices.

The Project has also assisting in the development of curriculum material for teaching the future island leaders (the children of today) on environmental issues. This material has been published in two volumes.

7. The Australian Scene

At the same time as the feasibility study for the Pacific Project was being undertaken, the Permanent Committee on Tides and Mean Sea Level in Australia was successfully campaigning for the establishment of a similar array of stations around the country at strategic locations. This array was to be established for the promotion of research into sea level trends in response to climate change. The resultant Australian Baseline Sea Level Monitoring Project was funded under the Greenhouse Climate Change Core Research Program, administered by the Department of Environment, Sport and Territories. Under this project and through co-operation with the National Ocean Service of the U.S. National Oceanic and Atmospheric Administration and several local port authorities an array of stations has been installed commencing in May 1991 (Fig 6).

The ultimate aim of this initiative is clear, that in an extended period of twenty or more years it is required that the secular change of sea levels in the Australian Region must be determined in its own right, and as ground truth support for other research into matters of climate change.

Funding for the Australian array did not match that of the Pacific array, based partly on the expectation that the various State Surveying and Mapping agencies would be prepared to provide the essential geodetic survey support. As agencies found it harder to meet this expectation, the Geodesy Group of the Intergovernmental Committee on Surveying and Mapping (ICSM) was called in to coordinate activities and to fight for external support. The NTF is a member of this Geodesy Group.

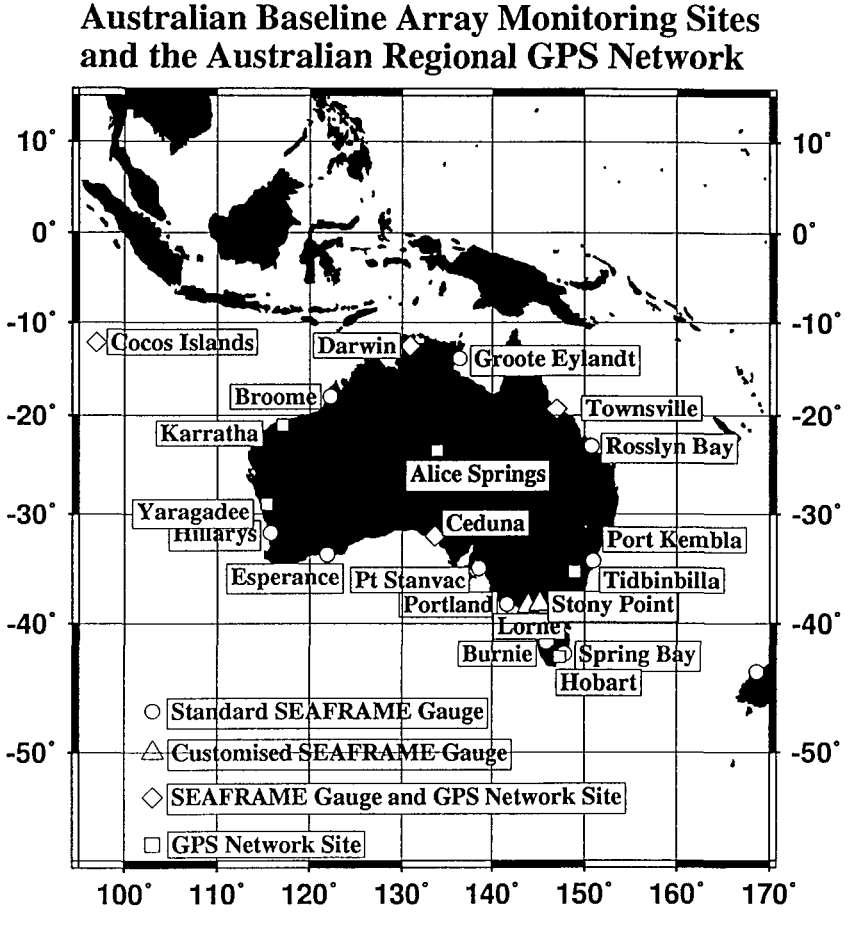

Figure 6.
The Australian Baseline Array Monitoring Sites and the Australian Regional GPS Network

8. Future Directions

The Geodesy Group of ICSM is maintaining a watching brief on developments in space-based geodetic techniques. Since the Woods Hole workshop, GPS geodetic precision has improved substantially, especially over the long distances expected to be measured in the Pacific Project. Due to improvements in i) the GPS satellite constellation, ii) tracking networks on the ground, and iii) analysis techniques and software, continuously operated GPS stations can monitor the horizontal and vertical velocities of points anywhere on Earth, separated by thousands of kilometres, with day to day repeatability of a centimetre or better (Blewitt, 1994).

Since the original 1989 meeting the same group of experts has met twice to further discuss advances in geodetic techniques for monitoring tide gauges. In 1993 the group (Carter, 1994) recommended that:

- GPS receivers should be placed permanently at selected tide gauge stations and operated continuously. This approach will allow tide gauges in remote locations, including isolated islands, to be monitored.

- The IGS should be asked to organise and manage a sea level monitoring GPS network in the same way that they are currently managing the satellite orbit - earth orientation network. One major advantage foreseen is that the sea level monitoring network would automatically be tied directly to the ITRF. In fact, it is possible that many of the tide gauge stations could be directly incorporated into the ITRF as primary stations.

Following on from the 1993 meeting, the group again met in 1997 to review the status of measuring changes in sea level over the previous ten years (Neilan et al., 1998).

A recommendation from this meeting that is of vital geodetic importance for the monitoring of tide gauges is the setting up of a Technical Working Group. This group has been set up to recommend standards and specifications for operating GPS at tide gauge sites.

The Working Group is to consider, document and make recommendations on:

- making measurements for precise ties (e.g., between the GPS, the tide gauge, the tide gauge bench marks, the local reference networks, etc.)
- data handling of the survey information
- site stability aspects
- monumentation techniques
- collocation philosophy and observing methods (continuous measurement rationale)
- absolute gravity measurements for complimentary information on vertical crustal movements and mass redistribution
- environmental parameters, meteorological sensors, ancilliary equipment, etc.

Clearly the recommendations of this working group will have major implications for the geodetic monitoring of all tide gauges. While little can be done about the site selection of the existing gauges there may be major changes in carrying out the geodetic monitoring of these gauges.

The installation of permanent GPS receivers at the SEAFRAME stations, while being expensive in the short term, has the possibility of saving money in the long term. Developments in this field are eagerly awaited and are being closely monitored.

While the eleven SEAFRAME stations cover a large portion of the Pacific there are still some large areas of ocean without monitoring stations. Additional stations in the northern Cook Islands, eastern Kiribati, the Federated States of Micronesia and Palau, would significantly add to the data coverage for the region. The governments of the region are actively pursuing avenues of support to enable the establishment of these further stations.

9. Conclusion

The Pacific Ocean plays an important part in the world's weather patterns. In turn the world is having an impact upon the weather in the Pacific and its effects upon those who live in the region. Through its network of climate monitoring stations, this Project, with its intensive and long-term study, will

benefit Pacific islanders by providing data on changes to sea level and climate in their own region.

The Project is providing training to islanders in high precision geodetic survey techniques, sea level and climate data analysis and interpretation techniques. As surveys are repeated, researchers will be able to separate the land movement from the relative sea level change data and provide more accurate information.

With the information, products and training activities, staff within the various national governments will be able to provide sound technical advice to their policy makers for the development of appropriate national and regional policies on the environment, climate change and response strategies.

The Pacific region is tectonically unstable. All the SEAFRAME stations have been installed on man made structures within port and harbour areas. Most of these sites are on unstable or reclaimed land and therefore the stations are prone to movement. Results to date show that not all the sites are stable. Only a geodetic survey can monitor the stability of the SEAFRAME stations. Regular geodetic surveys are essential to the determination of changes in absolute sea the level in the region.

This paper is an extended and updated version of a paper presented to the 37th Australian Surveyors Congress, 13-19 April 1996, Perth, Western Australia.

References

Blewitt, G., (1994). Technology Status Report, The Global Positioning System. *Report of the Surrey Workshop of the IAPSO Tide Gauge Bench Mark Fixing Committee*, NOAA Technical Report, NOSOES0006, Silver Spring, MD 20910, USA

Carter, W.E., D.G. Aubry, T. Baker, C. Boucher, K.O. Emery, C. LeProvost, D. Pugh, W.R. Peltier, M. Zumberge, R.H. Rapp, and R.E. Schutz, (1989). *Geodetic Fixing of Tide Gauge Bench Marks*, Woods Hole Oceanographic Institute Report, WHOI-89-31/CRC-89-5, Woods Hole, MA 02543, USA.

Carter, W.E.(Ed.), (1994). *Report of the Surrey Workshop of the IAPSO Tide Gauge Bench Mark Fixing Committee*, NOAA Technical Report, NOSOES0006, Silver Spring, MD 20910, USA

Hoffman, J.S., D. Keyes and J.G. Titus, (1983). *Projecting Future Sea Level Rise, Methodology Estimates to the Year 2100 and Research Needs*. U.S. Environmental Protection Agency, Washington DC

Homes, G.M., (1992). Changing Technology - Monitoring Sea Level Change. *The Australian Surveyor*, 37(1):13–22.

Liren, H. (1995). Isostatic Datum for Studying Sea Level Change along the Coast of China. *Mar.Geod.* 18:333–339.

Neilan, R., P.A. Van Scoy and P.L. Woodworth (eds), *Proceedings of the Workshop on Methods for Monitoring Sea Level: GPS and Tide Gauge Benchmark Monitoring, GPS Altimeter Calibration,* Workshop organised by the IGS and PCTMSL, Jet Propulsion Laboratory, Pasadena, CA, 17-18 March 1997, 1998.

NTF (1992,a). *Geodetic Survey Plan*, National Tidal Facility, The Flinders University of South Australia, SA, July, 1992.

NTF (1992,b). *Specifications for the Establishment of Bench Marks for Differential Levelling and GPS Surveys*, National Tidal Facility, The Flinders University of South Australia, SA, April, 1992.

NTF (1992,c). *Standards for the Conduct of Precise Differential Levelling*, National Tidal Facility, The Flinders University of South Australia, SA, October, 1992.

Titus, J.G. and V.K. Narayan, (1995). *The Probability of Sea Level Rise*, U.S. Environmental Protection Agency, Washington DC

Sea-Level Changes and Their Effects
B.J. Noye & M.P. Grzechnik (Editors)

Relative Sea-Level Change and Geologic Corrections to South Australian Tide Gauge Records

Elizabeth J. Barnett and Nick Harvey
Mawson Graduate Centre for Environmental Studies, University of Adelaide, Adelaide, 5005

ABSTRACT: Estimates of sea-level change from tide-gauge data require a correction for vertical land movement. For Australia, much of the change in land level during the Holocene is due to hydroisostacy, but other processes such as tectonism or groundwater extraction are also in effect in some areas. There have been several geological studies of sea-level change around Australia, although few have been carried out close to tide gauges. Exceptions to this are in South Australia at Port Adelaide, Port Pirie and Thevenard where long-term tidal data exist. Present sea-level trends at these localities have been corrected to account for vertical land movements. The adjusted trends indicate secular sea-level rises between 0.24 to 0.40 mm/year, which are significantly lower than the IPCC estimates. Essentially, the South Australian trends define eustatic sea-level rise in the region influenced by ENSO or other climatic phenomena.

In addition to historical tide gauges, a number of SEAFRAME stations have been positioned around Australia to enable zero-order levelling for vertical movements. Several decades of data are first needed before reliable sea-level estimates can be obtained. This is also the case for global sea-level change derived from satellite altimetry. Even then, sea-level estimates from tidal records will continue to be important, particularly in regard to local coastal management strategies.

KEY WORDS: sea-level change, Holocene, hydroisostacy, vertical land movements, tidal data.

CONTENTS

1. Introduction

Present global sea-level rise estimates are based on tide-gauge records, many of which are situated in coastal regions and have not been adequately corrected for local relative land/sea level movements. The Intergovernmental Panel for Climate Change Second Scientific Assessment for Climate Change (Warrick et al., 1996) provided a range of best estimates of sea-level rise between 1 and 2.5 mm/year. These estimates include only the longest available tidal records in the data set and utilise geodynamic models to filter out long-term vertical movements. While there is no apparent acceleration of global sea-level rise, the average rise during the present century is significantly higher than the average rate for the last several thousand years.

The range of relative sea-level change estimated from tide-gauge data throughout the world varies as much as ±10 mm/year, depending on whether regions are undergoing subsidence or uplift (e.g. Gornitz and Seeber, 1990; Peltier and Tushingham, 1991). Several researchers have accounted for land/sea level changes by excluding known areas of relative movement, using tide-gauge records of more than 20 or 30 years, or clustering data into geographic regions of similar vertical motion (Gornitz et al., 1982; Aubrey and Emery, 1983; Barnett, 1984; Gornitz and Lebedeff, 1987; Flemming, 1992). While these approaches best approximate global eustatic sea-level change, on a regional or local scale, the actual geologic processes affecting each tide gauge are often not investigated.

Sea-level change results from numerous factors, and separating these factors over different spatial and temporal scales for their contribution to relative sea level is a complex proposition. While hourly observed sea level can be compared to the predicted astronomical tide for sea-level residuals (Mitchell, 1991), phenomena such as El Niño Southern Oscillation (ENSO) are generally complicated to compute due to a time-lag component influencing different tide gauges. In addition, several geologic and anthropogenic processes affect relative land/sea levels at tide gauge locations. In particular, the isostatic response of continental margins, tectonic activity and human activities can influence local sea level. These must be taken into account before tidal records can yield realistic sea-level trends for use in global sea-level estimates. Vertical crustal movements together with related changes in the geoid are major factors masking global sea-level change (Zerbini et al., 1996). It has been suggested that secular tide-gauge data are dominated by neotectonic and anthropogenic effects resulting in an over-estimation of global sea-level

rise by two to three times when these factors are ignored (Pirazzoli, 1989).

It is the variations in vertical movements and their effects on relative land/sea levels that will be the focus of this paper. Within the Australian context, vertical movements at the coast result largely from isostatic adjustment of the earth's crust, although in different regions the extent of this adjustment varies considerably (Lambeck and Nakada, 1990). There have been numerous studies of Holocene sea levels carried out around Australia, however, few exist in close proximity to tide gauges that have been operating over several decades. Only by removing the component of long-term relative land/sea levels from tidal data can present sea-level trends be adequately assessed. This type of approach has been tested in South Australia where several tide-gauge stations operate in the vicinity of tidally dominated sediments deposited over the past 7,000 years BP. The effects of isostatic adjustment or anthropogenic activities on relative land/sea levels can be deduced from the sediments and then applied to the tide-gauge data. Geologically uncorrected sea-level trends for South Australia are quite anomalous, even though previously, trends from Inner and Outer Harbors, Port Adelaide, have been used in studies of regional and global sea-level change (Barnett, 1984; Aubrey and Emery, 1986; Gornitz and Lebedeff, 1987). By considering the geophysical and geologic processes acting at tide-gauge localities and correcting for them, better estimates of secular sea-level changes can be obtained.

2. Holocene Sea Level Variation

Holocene sea-level variations have essentially been caused by a combination of eustatic, glacio-hydroisostatic, tectonic and sedimentary processes. Eustatic sea-level change results from changes in ocean volume caused by glacial melting or freezing and thermal expansion or contraction of water (Wigley and Raper, 1987), whereas isostatic sea-level change is brought about by geoidal undulations of the Earth and its response to surface loading by ice or meltwater during glacial and interglacial cycles (Peltier, 1980). Tectonic events including earthquakes can increase relative sea level changes significantly due to a reduction in ocean basin capacity (Bilham and Barrientos, 1991; Stiros et al., 1994). In large-scale deltaic regions, sediment loading, subsidence and compaction substantially affect relative sea level. Anthropogenic activities such as groundwater extraction can also influence sea level (Belperio, 1993; Sahagian et al., 1994). Overviews of the causes of relative sea-level changes including geologic processes, climatic and

oceanographic effects are given by Emery and Aubrey (1991) and Pirazzoli (1993).

2.1 Geophysical Modelling of Eustatic and Isostatic Adjustment for the Australian Margin

Modelling of the relatively tectonically stable Australian coast has been carried out by Lambeck and Nakada (1990) for eustasy and isostasy, as well as in other areas of greater tectonic activity such as Greece and south-western Turkey (Lambeck, 1995). Their model is based on eustatic, isostatic and tectonic parameters such that relative sea-level change, $\Delta\xi(\varphi, t)$ at location φ and time t, can be schematically written as:

$$\Delta\xi(\varphi, t) = \Delta\xi_e(t) + \Delta\xi_I(\varphi, t) + \Delta\xi_T(\varphi, t),$$

where $\Delta\xi_e(t)$ is the eustatic sea level, $\Delta\xi_I(\varphi, t)$ is the isostatic correction and $\Delta\xi_T(\varphi, t)$ is the tectonic contribution. For Australia, the variability of late Holocene highstands is generally attributed to hydroisostasy. Lambeck and Nakada (1990) developed a high spatial resolution glacio-hydro-isostaic sea-level model where the tectonic component is considered to be small. They expressed the change in the sea level measured relative to the present sea level as the sum of four terms:

$$\Delta\xi(\varphi, \lambda: t) = \Delta\xi_e + \Delta\xi_r + \Delta\xi_i + \Delta\xi_w,$$

where ξ_e is the volume of meltwater divided by the surface area of the oceans ($\Delta\xi_e$ is the equivalent sea-level term); and the corrective terms are ξ_r for the rigid Earth, ξ_i for the ice load and ξ_w for the melt-water load. Each contribution of $\Delta\xi$ is expressed relative to its value at the present time t_p. The solution to this equation requires an Earth model E, an ice model I, and ocean basin model O, as has been used by Farrell and Clarke (1976) and others to estimate sea-level change at different locations. At sites far from the former Pleistocene ice sheets, the dominant corrective term becomes the water load ξ_w, and the ocean basin function O, in particular, must be of very high resolution (Nakada and Lambeck, 1987). For Australia, ξ_i and $\Delta\xi_r$ are nearly constant and largely reflect the global change in gravitational potential due to changing mass distributions.

Lambeck and Nakada (1990) defined several Earth models for sea-level change in which high viscosity lithospheric thickness and upper and lower mantle viscosity are the parameters. As an example, their model E14 has an upper mantle viscosity of 2×10^{20} Pa s and a lower mantle viscosity of

10^{22} Pa s. Lithospheric thicknesses of 50 or 150 km are defined by E14(50) and E14(150), respectively. During the Holocene postglacial marine transgression, sea-level change is largely independent of the choice of Earth model, and the dominant contribution in the far field, applicable to Australia at some distance from the former ice sheet, is the equivalent sea-level term $\Delta\xi_e$. A comparison of E14(50) with sites of the eastern Australian margin revealed little spatial variation. However, variation between different longitudinal regions from the present shore was predicted due to the tilting effect of the water term $\Delta\xi_w$, with the sea-level curve offshore lagging behind coastal curves by about 1,000 years. The far-field data were thus considered to be sensitive indicators of the timing and rates of meltwater addition to the oceans.

Lambeck and Nakada (1990) predicted sea level for Australia to have reached its present position around 6,000 years BP, although the timing t* does vary. This appears to be mostly due to regional responses in the water load term $\Delta\xi_w$. After rapid sea-level rise along the continental margin, the water load is transmitted via the lithosphere to the mantle inducing flow away from the sub-ocean mantle to beneath the unloaded continent. The consequence of this process is that a coastal highstand is formed, the amplitude of which depends on the Earth model used and the coastal geometry (Figure 1a and b). In regions such as a narrow gulf far from the continental margin, a more elevated highstand would be formed. For Spencer Gulf, South Australia, t* is predicted to increase progressively from the entrance of the gulf to the northern end by about 500 to 1,000 years. When a continued minor contribution of Antarctic meltwater from 6,000 yr BP onward is considered, the variation in t* with distance up the gulf becomes more marked (Figure 1c). Sea-level at Port Pirie in the northern Spencer Gulf would have first reached its present level about 6,700 years BP, followed by a highstand shortly thereafter. This compares with less than 6,000 years BP for Cape Spencer near the entrance to the gulf. If glacial melting did continue at a slow rate to present, the effect would be to raise the equivalent sea level by 1 m from 6,000 years BP which would lower the highstand by about 1 m.

Lambeck and Nakada (1990) examined much of the geological evidence around Australia for late Holocene sea-level change. Through an iterative approach, they were able to determine that the average lithospheric thickness for coastal and offshore regions is about 70-80 km, upper mantle viscosity is about 2 x 10^{20} Pa s, lower mantle viscosity is about (5-10)10^{21} Pa s, and that there is some lateral variation in the upper mantle. They also concluded that meltwater to the oceans has continued after 6,000 years BP and that the most likely source is the Antarctic and

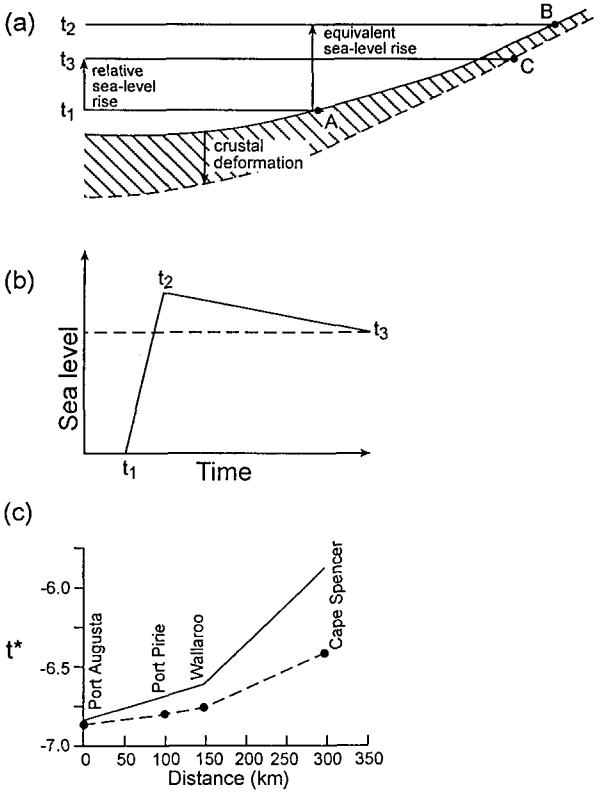

Figure 1. a) Illustration of Holocene sea-level change along a continental margin distal to the former Pleistocene ice sheets. Sea level rises rapidly from time t_1 to t_2 and the shoreline transgresses from position A to B. After melt water addition to the oceans ceases, sea level ameliorates as a consequence of crustal hydroisostatic deformation, and at time t_3 the shoreline regresses to position C. b) The sea-level curve has maximum highstand at time t_2. The amplitude of the highstand varies depending on proximity to the continental margin and former ice sheets. c) The time t* at which sea-level first reached its present level along Spencer Gulf from Port Augusta in the north to Cape Spencer in the south (Figure 2) based on model E14(50). The solid line indicates minor Antarctic melting continuing from 6,000 years BP to present and the dashed line represents ice model ARC3+ANT3 in which melting ceased at 6000 years BP (modified from Lambeck and Nakada, 1990).

mountain glaciers. Their predictions for Holocene sea levels for regions around Australia showed considerable geographical variation, although in general, there was a progression in highstands from south to north reflecting the Antarctic ice-load contribution.

The effects of an Antarctic meltwater contribution on relative sea level from 6,000 years to present requires further investigation. Has meltwater addition from the Antarctic to the oceans continued into the late Holocene, and if so, has the rate varied? The altitudes and ages of raised beaches from the Ross embayment, Antarctica, were investigated (Colhoun et al., 1992) and it was found that the ice margin during the last glacial maximum at 20,000 years BP was thinner and less extensive than previously thought, such that its contribution to the drop in sea level was only 0.5 to 2.5 m. In the region, deglaciation was well advanced by 10,000 years BP and was complete by 6,000 years BP. These finding imply that either sea level fell less during the last glacial maximum or that there was a much greater ice volume in the Northern Hemisphere. Evidence from the northern Windmill Islands, Antarctica, also suggests deglaciation had occurred by 5,500 corrected years BP, and that isostatic uplift rates were 0.5 to 0.6 m/100 years (Goodwin, 1993).

Geophysical models such as those devised by Lambeck and Nakada (1990) can be corroborated or contrasted with others from different regions of the Earth (e.g. Davis and Mitrovica, 1996), as well as with empirical studies of Holocene sea level. All of the models developed by Lambeck and Nakada (1990), Lambeck et al. (1990) and Lambeck (1993a,b; 1995) have relied on geological and geomorphological studies to help define the model parameters. While geophysical models provide regional interpretations of relative land/sea levels, geological and geomorphological observations enable estimates of sea-level change at the local level.

2.2 Empirical Studies of Late Holocene Sea Level

Several regional studies of Holocene sea-level change have been presented in the global context (Pirazzoli, 1991; Emery and Aubrey, 1991). Around Australia, sea levels over the past 15,000 years BP have been reviewed by Hopley (1983), with several sea-level studies having since been carried out (e.g. Belperio et al., 1984a and b; Gostin et al., 1984, 1988; Cann and Gostin, 1985; Semeniuk, 1985; Thom and Roy, 1985; Woodroffe et al., 1985; Semeniuk and Searle, 1986; Bryant et al., 1992; Belperio, 1993; Carter et al., 1993; Collins et al., 1993; Beaman et al.,

1994; Gagan et al., 1994; Larcombe et al., 1995; Woodroffe, 1995; Harvey et al., 1999, in press). There is extensive geomorphological and geological evidence for variations in Holocene sea levels around Australia's margin, although the imprecise nature of many sea-level indicators often restricts the interpretation of Holocene sea-level behaviour. Problems associated with the interpretation of sea-level indicators include: i) the need to establish the relationship of each indicator to sea level at the time of its formation, ii) the relation of the submerged or elevated shoreline indicator to present sea-level datum, and iii) dating errors.

Much of the Holocene sea-level highstand research for Australia has been based on geomorphic or sedimentological evidence (Figure 2). Smart (1976), Rhodes (1982) and Chappell et al. (1982) documented chenier ridges along the shore of the Gulf of Carpentaria that indicated Holocene highstands in excess of 2 m had developed by about 6,000 years BP. Chappell et al. (1983) examined microatolls on offshore reefs islands and reefs of north eastern Queensland. These indicated a highstand of 1 to 1.5 m around 5,500 to 6,000 years BP. A highstand of 1.65 m is indicated by encrustations of the oyster *Saccostrea cucculata*, Magnetic Island, Townsville, which remained at that level until 3,590 years BP (Beaman et al., 1994). Along the northern New South Wales coast, Flood and Frankel (1989) found intertidal calcareous worm tube indicating a Holocene highstand of at least 1 m as recently as 3,420 years BP, but in central and southern New South Wales, Thom and Roy (1983, 1985) provided evidence from *in situ* tree stumps near present mean sea level and high water mark indicating that little if any highstand occurred. Shell bed evidence from eastern Victoria (Gill and Lang, 1982) and Warrnambool in the west (Gill, 1983) indicates highstands of 2 m about 6,000 years BP. In Tasmania, no Holocene highstand has been identified (Bowden and Colhoun, 1984). Considerable evidence can be found in South Australia for variable Holocene sea-level highstands (Burne, 1982; Belperio et al., 1983, 1984b; Hails et al., 1983; Belperio, 1993, 1995; Barnett et al., 1996). The highest magnitudes between 3 and 5 m above present sea level occur in the upper reaches of the Spencer Gulf and Gulf of St Vincent, and then decrease toward the continental shelf. The evidence from Western Australia is varied, with Holocene emergence of 0.5 m indicated in the Swan Estuary in Perth (Kendrick, 1977), compared to 2.5 m some 20 km away at Rottnest Island (Playford, 1983) and 2 to 3 m to the north and south of Perth (Woods and Searle, 1983; Searle and Woods, 1986). This suggests that local tectonic activity occurred in this area during the late Holocene. Semeniuk and Searle (1986) found evidence for local tectonism within the Perth Basin, although a highstand

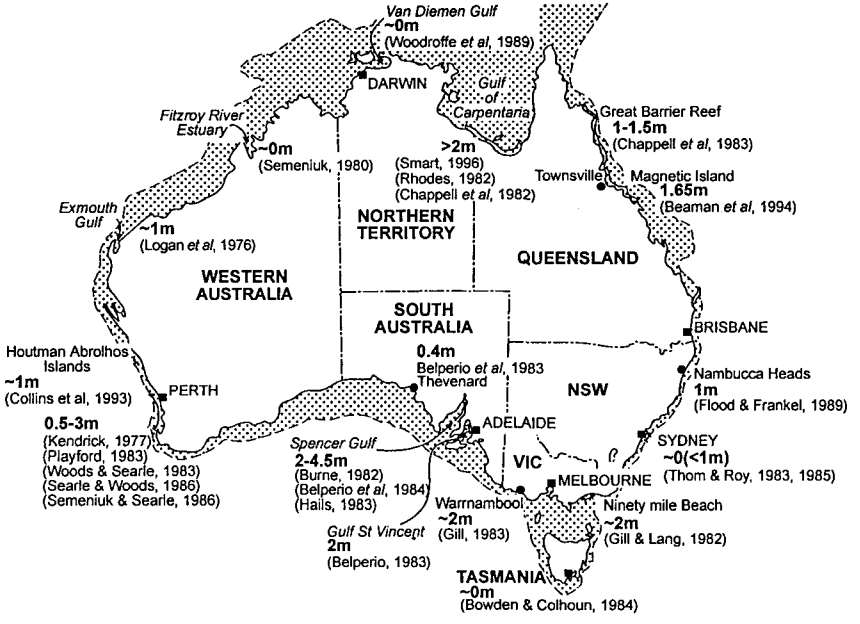

Figure 2. Location of Holocene sea-level studies cited in the text and heights of sea-level highstands (modified after Lambeck and Nakada, 1990).

of 2.5 m at Rockingham Plain within the basin was the most consistent with eustatic-hydroisostatic interpretations. Along the central West Australian coast, evidence from coral reefs of the Houtman Abrolhos Islands (Collins et al., 1993) and tidal flats in southern Exmouth Gulf (Logan et al., 1976) infers a sea-level high of about 1 m until at least 4,000 years BP. For northern Australia, there is little detectable sea-level change for the Fitzroy River Estuary region (Semeniuk, 1980), and van Diemen Gulf region, east of Darwin (Woodroffe et al., 1989).

While many of these studies provide empirical data to support variations in Holocene sea levels around Australia, few can be correlated with present sea-level variations estimated from tidal data since few were conducted in close proximity to tide-gauge stations. Exceptions to this are studies carried out nearby the Port Adelaide, Port Pirie and Thevenard tide gauges in South Australia (Belperio et al., 1983; Belperio, 1993; Barnett et al., 1996; Harvey et al., 1999) where several of the longest tidal

records exist. In these studies, detailed below, isostatic and anthropogenic contributions to vertical land movements were deduced from evidence within the tidal sediments deposited nearby the tide-gauge stations.

2.2.1 South Australian Holocene Tidal Successions

In Gulf St Vincent, the Spencer Gulf and sheltered bays along the Great Australian Bight, much of the coast consists of low gradient subtidal, intertidal and supratidal zones with specific vegetation growth related to the level of tidal inundation. The subtidal zone, at and below mean low water spring (MLWS) tide level contains abundant growth of subtidal *Posidonia australis* seagrass. The intertidal zone, between MLWS and mean high water spring (MHWS) tide levels, consists of *Zostera* sp. seagrass or bare sandy tidal flats. These are replaced by mangrove woodland and samphire communities higher in the tidal spectrum. Above MHWS tide level is the supratidal zone. In this zone, inundation is less frequent and vegetation growth is restricted to occasional samphires and saltbushes between bare expanses of evaporative flats (Gostin et al., 1984; Cann and Gostin, 1986; Barnett et al., 1996).

Within the subsurface, vertical sediment accumulation mimics the lateral zonation of facies, with subtidal *Posidonia* seagrass facies overlain by intertidal sandflat facies and subsequently mangrove and samphire facies. By association to present coastal zonation, these subsurface facies can be used to indicate Holocene paleosea-levels relative to the tidal datum and Australian Height Datum. In particular, the boundary between intertidal sandflat and mangrove or samphire facies represents the paleo-shoreline and has been used as a suitable paleosea-level indicator in these regions.

Successive samples from this boundary and the top of the seagrass facies at South Australian tide-gauge localities have been radiocarbon dated and the results plotted on an age-depth curve to obtain the heights of the Holocene highstand and determine rates of sea-level fall (Figure 3). For Port Pirie, the Holocene highstand is estimated at 2.2 m AHD, with sea-level falling from around 6,600 years BP to present level (Barnett et al., 1996; Harvey et al., 1999). The data indicated a regressive trend for sea-level fall of 0.33 mm/year. A lower than expected Holocene highstand is evident for Port Adelaide, with subsidence from human activities the main cause (Belperio, 1993). When data from the intertidal sandflat/mangrove boundary were plotted, the sea-level curve was 1 m lower than the sea-level curve for Port Gawler, just 18 km to the north of Port Adelaide. This was attributed to sediment compaction arising from wetland

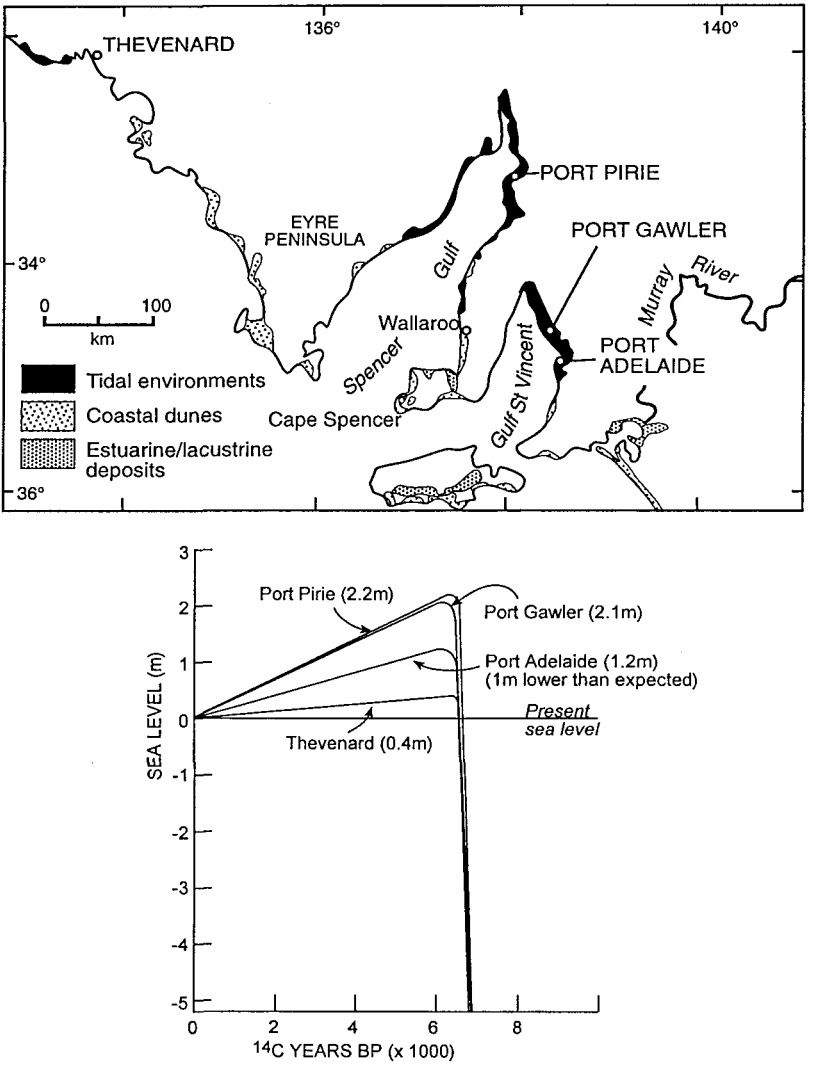

Figure 3. a) Extent of Holocene sedimentation in South Australian regions mentioned in text; b) Holocene sea-level curves. Variations in the height and timing of the highstands are considered mainly due to hydroisostatic effects, apart from Port Adelaide where anthropogenic activities have caused relative sea-level rise.

reclamation and groundwater withdrawal over the last 50 to 100 years. The effects of wetland reclamation were most pronounced where mangrove areas were drained. Groundwater extraction covered a wider region although generally had a more subtle subsidence effect. The long-term rate of sea-level fall for Port Adelaide is estimated to be 0.32 mm/year, while relative sea-level rise due to anthropogenic subsidence over the last 50 years, estimated from geodetic relevelling, is 1.8 and 2.2 mm/year for Inner and Outer Harbors, respectively (Culver, 1970). The net effect has been an overall relative sea-level rise in the Port Adelaide region. Similar investigations at Tourville Bay, about 20 km east of the Thevenard tide-gauge station, reveal a highstand around 0.4 m (Belperio et al., 1983, 1988). This infers a long-term sea-level fall of 0.06 mm/year. The importance of the South Australian studies is that the sea-level change rates apply directly to tide-gauge localities, and can therefore be used in conjunction with present rates of sea-level change estimated from tidal data.

3. Present Sea-Level Trends

The study of global sea levels for the past century has involved analysis of tidal data from numerous gauges around the world. Many of the trends in sea level derived from these data are highly variable due to eustatic, isostatic, tectonic, sedimentary, oceanographic and atmospheric processes operating at each tide-gauge location. As a result, any regional averaging of tide gauge data to obtain global sea-level trends without considering local effects can be highly erroneous. Tide-gauge data from numerous locations such as Japan (e.g. Aubrey and Emery, 1986), Europe (e.g. Emery and Aubrey, 1985, Emery et al., 1988) and North America (e.g. Gornitz and Lebedeff, 1987) are each contaminated to varying degree by tectonic activity, effects of subsidence due to sediment loading and glacio-hydro-isostatic adjustment, thereby masking the global eustatic component of sea level. Although Australia is a relatively tectonically stable continent, hydroisostatic adjustment and anthropogenic activities must also be taken into consideration to effectively determine regional sea-level trends from tide-gauge data.

3.1 Australian Sea-Level Trends

Tidal records from Australian tide-gauge stations that contained over 10 years of record were reviewed by Aubrey and Emery (1986). Each record was corrected to a local datum and represented mean annual sea

levels, computed from averaged hourly readings for each year of record. Only eight had greater than 20 years of record and least squares regression confidence levels calculated from t-tests higher than 0.98. Since the lunar tide period is 18.6 years, records less than 20 years are mostly inappropriate for sea-level analysis. Longer term tide-gauge records have subsequently been processed and analysed using least squares regression by the National Tidal Facility (B. Mitchell, pers. comm.) (Figure 4).

Aubrey and Emery (1986) noted that the change in coastal elevation from their eight stations ranged from +0.1 to -4.7 mm/year. The average was -2.2 mm/year, with negative values indicating submergence of the land. This approach has several difficulties as it compares widely separated tide gauges with no correction for isostasy or local neotectonic factors, and tidal data was expressed in terms of relative vertical movement rather than relative sea-level variation. Other contributions to tide-gauge data such as atmospheric variations and steric effects were not duly considered. Bryant et al. (1988) provided a useful example of meteorological and oceanographic factors along the Sydney coast and sea-level measurements at Fort Denison between 1943 and 1980. Their results suggested that the climate regime was influenced more by Hadley cell position, sea surface temperature and regional rainfall than by sea level, storm waves and the Southern Oscillation index, and that lower sea levels were associated with the blocking of aseasonal high pressure cells over the Tasman Sea. They also noted that for Australia generally, subtle changes in climate variability have occurred and that these have not been spatially constant.

Aubrey and Emery (1986) applied eigenanalysis to Australian tidal data to account for periodic coherent variations in sea level caused by currents or oceanic surges. Through a modification of the method they were able to include records that had long gaps (given sufficient overlap of records from different stations), and eliminate records that were vastly different from other stations owing to measurement errors or different processes. Sea-level trends deduced from eigenanalysis were compared to those from regression analysis, and it was found that the synthetic eigenanalysis estimates approximated local regression trends. However, a comparison of the then Port Adelaide Inner and Outer Harbor trends reveals that while the Outer Harbor trends are similar (3.2 mm/year from eigenanalysis and 3.0 mm/year from regression analysis), the trends for Inner Harbor vary considerably (1.2 and 2.5 mm/year, respectively). Anthropogenically induced subsidence was not taken into account. This is despite the fact that most of the tide gauges that were analysed are located in major cities and ports of Australia. Instead, their discussion of low-frequency relative sea-level fluctuations was based on submergence or emergence associated

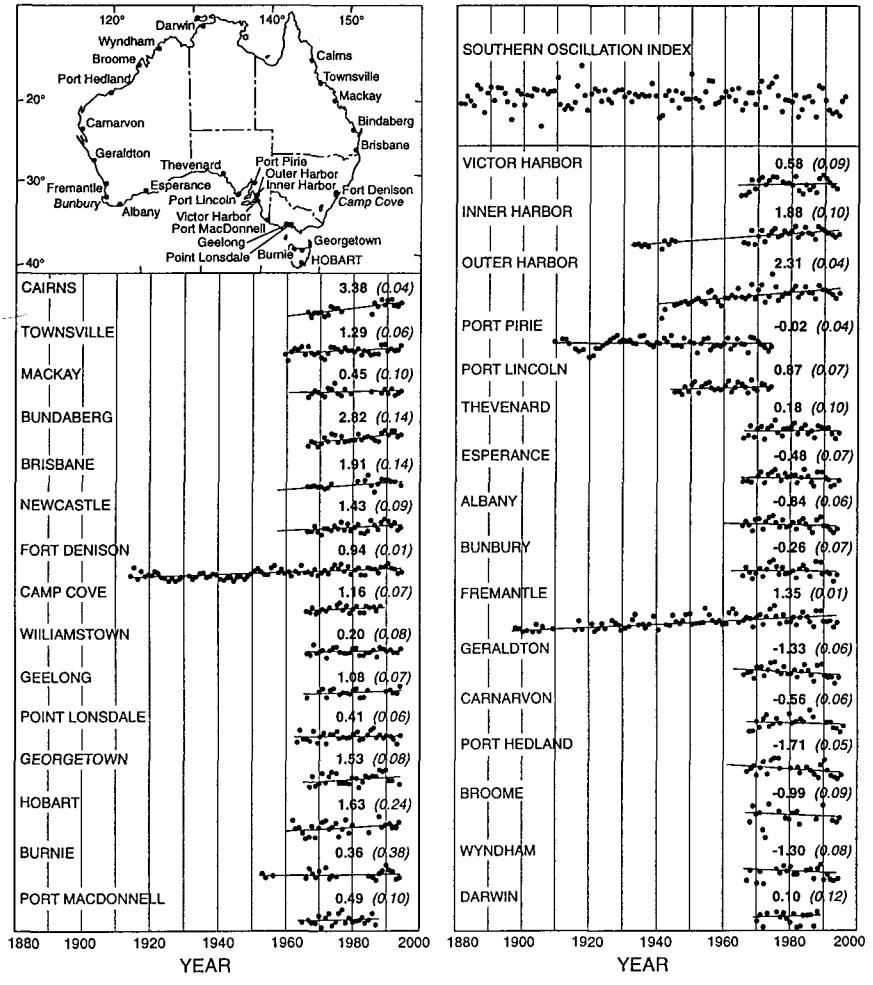

Figure 4. Tide gauges in Australia having at least 20 years data and sea-level trends in mm/year (2x standard deviation in parentheses). A weighted monthly mean is calculated depending on the reliability and continuity of the data and an equation for nodal corrections is applied to derive the sea-level trends; also included is the Southern Oscillation Index (National Tidal Facility).

with sedimentary basin distribution and convergent or divergent tectonic history. The effects of isostasy were discussed only briefly, but as shown by Chappell (1983) and Lambeck and Nakada (1990), hydroisostatic adjustment in the absence of anthropogenic effects can explain many regional variations in sea-level trends.

3.2 South Australian Sea-Level Trends

The opportunity exists in South Australia to correct several tide-gauge records geologically for vertical movements since research has been carried out in regions where there are both tidal records and Holocene tidal sequences (Table 1). The South Australian neotectonically adjusted trends are all lower than 1 to 2.5 mm/year as determined by Warrick et al. (1996) for present global sea-level rise. However, several qualifications are necessary for Table 1. The sea-level trends calculated from tide-gauge data vary with the addition of new tidal data and are dependent on the length of the record. While local atmospheric factors at each tide gauge are removed from the tidal data, interdecadal influences such as ENSO are more complex and as such, their component or influence remains in the record (B. Mitchell, pers. comm.). In general, Australian sea-level data from 1991 to 1993 exhibit sea-level decreases, a trend which is reflected by a negative Southern Oscillation Index. ENSO conditions were in effect for that period (Figure 4), but as pointed out by Bryant et al. (1988), blocking of high pressure cells over southern Australia can also lower sea levels. Neotectonic corrections to tide-gauge sea-level trends must be viewed with some caution, particularly considering the difference between long-term geological processes over the millennium scale and tidal records over the decadal scale. In addition, for anthropogenic processes, the rate of general subsidence caused by wetland reclamation or groundwater extraction can really only be approximated for each tide-gauge location.

Given these constraints, the adjusted Port Pirie and Thevenard tide-gauge sea-level trends are considered to provide more reliable estimates. Over 50 years of tidal data exist for Port Pirie and a detailed geological investigation of the area revealed no anthropogenically induced vertical movement, but rather slow hydroisostatic uplift over the past 6,600 years BP. Less hydroisostatic effect is apparent for Thevenard such that only minor geologic correction to the tide-gauge data is necessary. The secular adjusted sea-level trends provide a more regional perspective of sea-level variations, without the localised effects of vertical movements. Providing the geologic corrections for eustatic-isostatic and anthropogenic processes

are of appropriate magnitude, the adjusted rates give an estimate of eustatic sea-level rise influenced by ENSO and other climatic phenomena.

Tide Gauge	Years of Record	Sea-Level Trend (mm/year)	Isostatic Response (mm/year)	Anthropogenic Effects (mm/year)	Adjusted Trend (mm/year)
Thevenard	27.8	0.18	0.06	N/E	0.24
Port Pirie	58.3	-0.02	0.33	N/E	0.31
Outer Harbor	52.1	2.31	0.32[1]	-2.2[2] subsidence	0.43
Inner Harbor	39.1	1.88	0.32[1]	-1.8[2] "	0.40

Table 1. Sea-level trends for selected South Australian tide gauges, 1994 data inclusive. Notes: N/E: not evident; [1] the isostatic response for Port Adelaide is based on the Port Gawler sea-level curve; [2] the rates of subsidence at Outer and Inner Harbors were derived from geodetic relevelling (Culver, 1970; Belperio, 1993).

3.3 Australian Baseline Sea Level Monitoring Stations

Apart from measurement of sea-level trends using historical tide-gauge data, sea-level monitoring is carried out by the National Tidal Facility using an array of SEAFRAME (Sea-Level Fine Resolution Acoustic Measuring Equipment) stations that have been zero-order levelled using the Global Positioning System (GPS). Most tide gauges are surveyed to local reference datums and thereby measure relative sea-level variations between the position of the land and ocean surfaces. Through the use of GPS and space geodesy techniques, vertical movements at selected tide gauges can be measured independently of mean sea level. Fourteen SEAFRAME stations contribute to the Australian Baseline Sea Level Monitoring project which was initially established in the early 1990s through the Greenhouse Climate Change Core Research Program in the Department of Environment, Sport and Territories. Each gauge in this array has been installed with the Next Generation Water Level Measurement System (NGWLMS) developed by the National Ocean Service of NOAA (NOS, 1986). This system links an air-acoustic sea-level sensor with a microprocessor-controlled data acquisition and telemetry system, and is self calibrating. Primary and secondary sensors that record water level provide values every second, and ancillary sensors record wind speed and direction, air temperature, water temperature and barometric pressure on an hourly basis.

3.3.1 Geodetic Levelling

Levelling commenced in Australia in 1945 in order to link geodetic datums around the continent, although the levelling was generally of third-order accuracy (Leppert, 1970). In the 1970s, relevelling took place in parts of the established network using first-order techniques. An overall sea-level fall of 50 cm was found between Coffs Harbor and Cairns in northern Queensland. This discrepancy inferred that, at least in these regions, variations in regional relative sea level were mostly due to levelling instrument error rather than tectonic or eustatic processes (Aubrey and Emery, 1986).

Since the 1980s, there has been greater effort to bring about zero-order geodetic and absolute gravity measurements (Homes, 1992). High-precision levelling has been carried out on the SEAFRAME tide gauges of the Australian Baseline Sea-Level Monitoring Array. Routine high-precision levelling between the sensor head and the tide gauge bench mark detects any movement of the sensor relative to the bench mark. First order-levelling provides $4\sqrt{k}$ mm precision, where k is the distance between bench marks in kilometres. The stability of tide-gauge bench marks is affected by the marine tide on the deflection of the vertical in the vicinity of the coast and by deformation of the Earth's crust due to tidal loading (Homes, 1992). These effects can be removed at around 10 km since beyond this distance, errors in high-precision levelling outweigh loading effects. To determine whether the land itself is moving, geodetic fixing of tide-gauge bench marks with particular reference to space geodetic techniques and absolute gravity measurements is required. The International Association for the Physical Science of the Ocean (IAPSO) Commission on Mean Sea Level and Tides Geodetic Committee in 1989 concluded amongst other recommendations that tide gauges used to monitor sea level must have a local network of up to 10 bench marks that are resurveyed using spirit levelling or Global Positioning System (GPS) at least once a year, and that regional sea-level networks should be organised around primary stations of the International Earth Rotation Service Terrestrial Reference Frame (Carter et al., 1989). Primary stations are those that utilise very long baseline interferometry (e.g. Tidbinbilla in ACT and Mount Pleasant in Tasmania) and satellite laser ranging techniques (e.g. Yaragadee in WA and Orraral in ACT). With highest level dual-frequency differential GPS measurements between tide-gauge bench marks and these stations, a vertical accuracy of close to 1 cm is achievable over these distances (Homes, 1989). Absolute gravity measurements although expensive are further required to verify vertical movements, as well as tidal gravity measurements to correct for the

effects of the marine tide in coastal environments (Lennon, 1990).

3.4 Satellite Altimetry

Satellite altimetry measures ocean currents and sea-surface topography and is being utilised to estimate global sea-level change. While previous methods to monitor present sea level have mostly been confined to tide gauges at coastal localities, altimetric observations of ocean circulation have the potential to cover wide regions on a continuous global basis (Wunsch, 1991). Although satellite altimetry has the potential for global distribution, existing altimeter data is thus far limited to only several years. Wagner and Cheney (1992) concluded that altimeters and the orbit model which provides a geocentric reference for the ocean surface require careful calibration with absolute standards before global mean sea-level change can be effectively monitored. Topex/Poseidon data indicate that mean sea level has risen at a rate of a few mm/year, the same order of magnitude as estimated from tidal records (Minster et al., 1995). Estimates of sea-level based on December 1992 to April 1996 data from altimeters aboard the Topex/Poseidon satellite have been reduced from 3 to 5 mm/year to 1 to 3 mm/year due to an algorithm error in the computer program (Kopytoff, 1996). Until such time that satellite altimetry can provide accurate data on ocean dynamics, analysis of long-term tide-gauge records remains the most feasible method to determine sea-level trends, particularly at the regional or local scale.

4. Discussion and Conclusions

At different tide gauges, any number of oceanic, atmospheric, geologic and anthropogenic processes are in effect and their relative contributions to the tidal record are not easily assessed. Previous estimates of Australian sea-level trends calculated from tidal data have not duly considered vertical movements caused by isostasy, tectonism or anthropogenic influences. The South Australian studies have been conducted in areas where both Holocene peritidal deposition and tide gauges exist so that geologic processes can be related directly to the tidal records and removed from present sea-level trends.

An assumption in this work is that long-term Holocene vertical movements can be directly removed from tide-gauge sea-level trends. Within this assumption, the rate of vertical movement is considered constant over thousands of years, although researchers such as Allen (1995) suggest that, at least for the Northern Hemisphere, Flandrian (Holocene) sea-level rise has been oscillatory with fluctuations on the

scale of decimetres to metres over hundreds of years. Additionally, while no acceleration of sea-level can be deduced from tidal data over the last century, Gornitz and Lebedeff (1987) found that the global rate of corrected sea-level rise increased by 0.6 mm/year between 1932-1982 relative to 1880-1931, although substantially different rates occurred between regions. Gornitz and Lebedeff (1987) were concerned about the subtraction of long-term trends from individual tide gauges and tested this assumption on the relatively quiescent United States east coast. They found that only three out of 36 stations had residual errors outside of the 95 % confidence limit of combined tide-gauge and long-term trends, and that the data showed a uniform difference between short- and long-term records. Plots of the United States east coast tide-gauge and long-term data also showed similar spatial variations. However, averaged geological trends can superimpose or induce underestimates of the effects of short-term nonlinear vertical movements (Zerbini et al., 1996).

Interannual to multidecadal sea-level variations can produce trends up to ±10 mm/year. Trends estimated from records of no greater than 20 years tend to reflect decadal fluctuations more than long-term vertical movements. Zerbini et al. (1996) suggested that a scatter in trend estimates was not necessarily due to crustal movements but rather to the effect of variable record lengths, and that required record lengths depend on the local magnitude of decadal sea-level variability. Although decadal to multidecadal sea-level variations may dominate sea-level trends, vertical movements are often of the same order of magnitude as the long-term trends, and must therefore be identified and monitored to separate the geological processes at tide gauges from the oceanographic-atmospheric contributions.

The detailed geologic investigations conducted adjacent to tide gauges in South Australia have identified vertical movement within the tidal record and used indicators of Holocene sea level relative to tidal datum to construct late Holocene sea-level curves which establish the heights of highstands for different regions. This approach provides an average, underlying rate of vertical land movement over the past 7,000 years BP, although episodic variations in isostatic or anthropogenic adjustment, as also any tectonic activity if present, affect relative land/sea-level changes over the short term. Further vertical movement studies utilising Holocene sea-level indicators and long-term tidal data from other regions of Australia would improve regional sea-level trend analyses.

Geophysical modelling of eustatic, isostatic, and tectonic parameters can be used to corroborate local geological studies of Holocene relative sea-

level change and short-term changes due to human activities. When geologic studies are carried out nearby tide-gauge localities, neotectonic and anthropogenic corrections can be applied to tidal data. With the introduction of SEAFRAME stations around the Australian coast, high-resolution data will be available from participating gauges, although several decades of data will be required before sea-level trends can be established. The SEAFRAME stations have been positioned for an evenly spaced distribution around the Australia coast. While data from these stations will be useful for global sea-level trends, the data may be less applicable to the management of several major urban and regional coastal centres in Australia at some distance from the SEAFRAME stations. Tide gauges in populated areas contain many of the longest records and, ideally, these should also be networked to zero-order bench marks. Tide-gauge records corrected for vertical movements will continue to be important even after a consistent tide-gauge reference system using space techniques is established, since these data are necessary as a baseline for the detection of any acceleration in sea-level change.

In addition to GPS space geodesy to fix tide-gauge benchmarks, Satellite Laser Ranging (SLR) and Very Long Baseline Interferometry (VLBI) measurements provide constraints for the Earth models used to derive sea-level change (Carter, 1994; Zerbini et al., 1996), and absolute gravity measurements at tide-gauge benchmarks constitute an independent check on vertical crustal velocities (Lambeck, 1994). Satellite altimetry provides another perspective on global sea-level change, although more altimetry data are required at greater resolution before any eustatic sea-level rise can be firmly established.

Several methods for estimating sea-level change need to be considered before reliable rates of change can be obtained. Although these methods involve separate techniques to investigate oceanographic-atmospheric, geophysical and geologic components of sea-level variability, each deals with complex processes over different spatial and temporal scales. Several difficulties arise as a result of the interplay of these processes, not least of which are the problems of determining global sea-level change from local data, or only several years of altimetric data.

In coastal regions, estimates of secular sea-level trends can be applied to planning and management of the coastal zone. The eustatic component of sea-level variability and vertical movements apparent at the local or regional level need to be incorporated into coastal management strategies. This aside, the uncertainty of the frequency and severity of storm surges at the coast is less easily accommodated within coastal planning. The

combination of sea-level and climate processes ultimately determines the vulnerability of coastal areas, particularly for low-lying regions. This can only be reduced through a consideration of all elements that contribute to relative sea-level change both in the present and for future scenarios.

Acknowledgments

We are indebted to Mr W. Mitchell at the National Tidal Facility for analysis of Australian tide-gauge data and Dr A.P. Belperio from Mines and Energy, South Australia, for geological data. Comments on the manuscript by Dr A.P. Belperio and Professor R. Bourman were much appreciated. The work was supported in part by a National Greenhouse Advisory Committee Grant, Department of Environment, Sport and Territories.

References

Allen, J.R.L. (1995). Salt-marsh growth and fluctuating sea level: implications of a simulation model for Flandrian coastal stratigraphy and peat-based sea-level curves. *Sedimentary Geology,* 100: 21-45.

Aubrey, D.G. and Emery, K.O. (1983). Eigenanalysis of recent United States sea levels. *Cont. Shelf Res.,* 2: 21-33.

Aubrey, D.G. and Emery, K.O. (1986). Australia - an unstable platform for tide-gauge measurements of changing sea levels. *Journal of Geology,* 94: 699-712.

Barnett, T.P. (1984). The estimation of "global" sea level change - A problem of uniqueness. *Journal of Geophysical Research,* 89: 7980-7988.

Barnett, E.J., Harvey, N., Bourman, R.P., Belperio, A.P. and Mitchell, W. (1996). Relative land/sea level changes to long term tidal records in South Australia. In Aung, T.H., ed., *Proceedings of the Ocean and Atmospheric Pacific International Conference*, pp. 10-11. National Tidal Facility, Flinders University of South Australia, Adelaide.

Beaman, R., Larcombe, P. and Carter, R.M. (1994). New Evidence for the Holocene sea-level high from the inner shelf, central Great Barrier Reef, Australia. *Journal of Sedimentary Research A,* 64: 881-885.

Belperio, A.P. (1993). Land subsidence and sea level rise in the Port Adelaide estuary: implications for monitoring the greenhouse effect. *Australian Journal of Earth Sciences*, 40: 359-368.

Belperio, A.P. (1995). Quaternary. In Drexel, J.F. and Preiss, W.V., eds., *The Geology of South Australia*, Vol. 2, Chapter 11, Geological Survey of South Australia Bulletin, 54, pp. 219-280. Department of Mines and Energy, South Australia.

Belperio, A.P., Hails, J.R. and Gostin, V.A. (1983). A review of Holocene sea levels in South Australia. In Hopley, D., ed., *Australian Sea Levels in the Last 15,000 Years, a Review,* Department of Geography, James Cook University of North Queensland Monograph Series, Occasional Paper 3, pp. 37-47. Department of Geography, James Cook University of North Queensland, Townsville, Qld.

Belperio, A.P., Smith, B.W., Pollach, H.A., Nittrouer, C.A., DeMaster, D.J., Prescott, J.R., Hails, J.R. and Gostin, V.A. (1984a). Chronological studies of the Quaternary marine sediments of northern Spencer Gulf, South Australia. *Marine Geology,* 61: 265-296.

Belperio, A.P., Hails, J. R., Gostin, V.A., and Polach, H.A. (1984b). The stratigraphy of coastal carbonate banks and Holocene sea levels of northern Spencer Gulf, South Australia. *Marine Geology,* 61: 297-313

Belperio, A.P., Gostin, V.A., Cann, J.H. and Murray-Wallace, C.V. (1988). Sediment-organism zonation and the evolution of Holocene tidal sequences in South Australia. In de Boer, P.L., van Gelder, A. and Nio, S.D., eds., *Tide-Influenced Sedimentary Environments and Facies,* pp. 475-497. D. Reidel Publishing Company, Dordrecht, Holland.

Bilham, R. and Barrientos, S. (1991). Sea-level rise and earthquakes. *Nature,* 350: 386.

Bowden, A.R. and Colhoun, E.A. (1994). Quaternary emergent shorelines of Tasmania. In Thom, B.F., ed., *Coastal Geomorphology in Australia,* pp. 313-341. Academic Press, Sydney.

Bryant, E., Roy, P.S. and Thom, B.G. (1988). Australia - an unstable platform for tide-gauge measurements of changing sea levels: a discussion. *Journal of Geology,* 96: 635-640.

Bryant, E.A., Young, R.W. Price, D.M. and Short, S.A. (1992).

Evidence for Pleistocene and Holocene raised marine deposits, Sandon Point, New South Wales. *Australian Journal of Earth Sciences,* 39: 481-493.

Burne, R.V. (1982). Relative fall of Holocene sea level and coastal progradation, northeastern Spencer Gulf, South Australia. *BMR Journal of Australian Geology and Geophysics,* 7: 35-45.

Cann, J.H. and Gostin, V.A. (1985). Coastal sedimentary facies and foraminiferal biofacies of the St Kilda Formation at Port Gawler, South Australia. *Transactions of the Royal Society of South Australia,* 109: 121-42.

Carter, R.M., Johnson, D.J. and Hooper, K.G. (1993). Episodic post-glacial sea-level rise and the sedimentary evolution of a tropical embayment (Cleveland Bay, Great Barrier Reef shelf, Australia). *Australian Journal of Earth Science,* 40: 229-255.

Carter, W.E., ed., (1994). *Report of the Surrey Workshop of the IAPSO Tide Gauge Bench Mark Fixing Committee.* Deacon Laboratory, Godalming, Surrey, United Kingdom, December 13-15, 1993. NOAA Tech. Rep., NOSOES0006.

Carter, W.E., Aubrey, D.G., Baker, T., Boucher, C., Le Provost, C., Peltier, W.R., Zumberge, M., Rapp, R.H., Schutz, R.E. and Emery, K.O. (1989). *Geodetic Fixing of Tide Gauge Bench Marks.* Woods Hole Oceanographic Institute Report WHOI-89-31/CRC-89-5. Woods Hole, MA 02543, USA.

Chappell, J. (1983). Evidence for smoothly falling sea level relative to north Queensland, Australia, during the last 6,000 yr. *Nature,* 302: 406-408.

Chappell, J., Rhodes, E.G., Thom, B.G. and Wallensky, E. (1982). Hydro-isostasy and the sea-level isobase of 5,500 B.P. in north Queensland, Australia. *Marine Geology,* 49: 81-90.

Chappell, J., Chivas, A., Wallensky, E., Pollach, H.A. and Aharon, P. (1983). Holocene palaeoenvironmental changes, central to north Great Barrier Reef inner zone. *Bureau of Mineral Resources Journal of Australian Geology and Geophysics,* 8: 223-235.

Colhoun, E.A., Mabin, M.C.G., Adamson, D.A. and Kirk, R.M. (1992).

Antarctic ice volume and contribution to sea-level fall at 20,000 yr BP from raised beaches. *Nature,* 358: 316-319.

Collins, L.B., Zui, Z.R., Wyrwoll, K.-H., Hatcher, B.G., Playford, P.E., Eisenhauser, A., Chen, J.H., Wasserburg, G.J. and Bonani, G. (1993). Holocene growth history of a reef complex on a cool-water carbonate margin: Easter Group of the Houtman Abrolhos, Eastern Indian Ocean. *Marine Geology,* 115: 29-46.

Culver, R. (1970). *Beach erosion assessment study.* University of Adelaide, Department of Civil Engineering, Adelaide.

Davis, J.L. and Mitrovica, J.X. (1996). Glacial isostatic adjustment and the anomalous tide gauge record of eastern North America. *Nature,* 379: 331-333.

Emery, K.O. and Aubrey, D.G. (1985). Glacial rebound and relative sea levels in Europe from tide-gauge records. *Tectonophysics,* 120: 239-255.

Emery, K.O. and Aubrey, D.G. (1991). *Sea Levels, Land Levels, and Tide Gauges.* Springer Verlag, New York.

Emery, K.O., Aubrey, D.G. and Goldsmith, V. (1988). Coastal neotectonics of the Mediterranean from tide-gauge records. *Marine Geology,* 81: 41-52.

Farrell, W.E. and Clark, J. A. (1976). On postglacial sea-level. *Geophysics J. R. Astron. Soc.*, 46: 647-667.

Flemming, N.C. (1992). Predictions of relative coastal sea-level change in the Mediterranean based on archaeological, historical and tide-gauge data. In Jeftic, L., Keckes, S. and Pernetta, J.C., eds., *Climate Change and the Mediterranean*, pp. 247-281. Edward Arnold, London.

Flood, P.G. and Frankel, E. (1989). Late Holocene higher sea level indicators from eastern Australia. *Marine Geology,* 90: 193-195.

Gagan, M.K., Johnson, D.P. and Crowely, G.M. (1994). Sea level control of stacked late Quaternary coastal sequences, central Great Barrier Reef. *Sedimentology,* 41: 329-51.

Gill, E.D. and Lang, J.G. (1982). The peak of the Flandrian Transgression in Victoria, S.E. Australia - faunas and sea level changes.

Proceedings of the Royal Society of Victoria, 94: 23-34.

Gill, E.D. (1983). Australian sea levels in the last 15,000 years - Victoria, S.E. Australia. In Hopley, D., ed., *Australian Sea Levels in the Last 15,000 Years, a Review,* Department of Geography, James Cook University of North Queensland Monograph Series, Occasional Paper 3, pp. 59-63. Department of Geography, James Cook University of North Queensland, Townsville, Qld.

Goodwin, I.D. (1993). Holocene deglaciation, sea-level change, and the emergence of the Windmill Islands, Budd coast, Antarctica. *Quaternary Research,* 40: 70-80.

Gornitz, V. and Lebedeff, S. (1987). Global sea-level changes during the past century. In Nummedal, D., Pilkey, O.H. and Howard, J.D., eds., *Sea Level Fluctuation and Coastal Evolution*, pp. 3-16. Society for Economic Paleonologists and Mineralogists, SEPM Special Publication 41.

Gornitz, V. and Seeber, L. (1990). Vertical crustal movements along the East Coast, North America from historic and late Holocene sea level data. *Tectonophysics,* 178: 127-150.

Gornitz, V., Lebedeff, S. and Hansen, J. (1982). Global sea level trend in the past century. *Science*, 215: 1611-1614.

Gostin, V.A., Hails, J.R. and Belperio, A.P. (1984). The sedimentary framework of northern Spencer Gulf, South Australia. *Marine Geology*, 61: 111-38.

Gostin, V.A., Belperio, A.P. and Cann, J.H. (1988). The Holocene non-tropical coastal and shelf carbonate province of southern Australia. *Sedimentary Geology*, 60: 51-70.

Hails, J.R., Belperio, A.P. and Gostin, V.A. (1983). Holocene sea levels of upper Spencer Gulf, South Australia. In Hopley, D., ed., *Australian Sea Levels in the Last 15,000 Years, a Review,* Department of Geography, James Cook University of North Queensland Monograph Series, Occasional Paper 3, pp. 48-53. Department of Geography, James Cook University of North Queensland, Townsville, Qld.

Harvey, N. and Belperio, A. (1994). Implications of climate change for the South Australian Coastline. *Transactions of the Royal Society of South Australia*, 118: 45-52.

Harvey, N., Barnett, E., Bourman, R.P. and Belperio, A.P. (1999). Holocene sea-level change at Port Pirie. South Australia: Implications for global sea-level rise estimates. Journal of Coastal Research, 15. In press.

Homes, G.M. (1989). Global climate change and the role of the Permanent Committee on Tides and Mean Sea Level. In *9th Australian Conference on Coastal and Ocean Engineering*, pp. 280-286. The Institution of Engineers, Australia.

Homes, G.M. (1992). Changing technology - monitoring sea level change. *The Australian Surveyor,* 37: 13-22.

Hopley, D., ed., (1983). *Australian Sea Levels in the Last 15,000 Years: A Review.* Department of Geography, James Cook University of North Queensland Monograph Series, Occasional Paper 3. Department of Geography, James Cook University of North Queensland, Townsville, Qld., 104 pp.

Kendrick, G.W. (1977). Middle Holocene marine molluscs from near Guilford, Western Australia, and evidence for climatic change. *Journal of the Royal Society, Western Australia*, 50: 97-104.

Kopytoff, V.G. (1996). Error inflated estimate of rising sea levels, researchers report. *The New York Times* ('Science Times' section), Tuesday July 30, page C4.

Lambeck, K. (1993a). Glacial rebound of the British Isles-I. Preliminary model results. *Geophysics Journal International,* 115: 941-959.

Lambeck, K. (1993b). Glacial rebound of the British Isles-II. A high-resolution, high-precision model. *Geophysics Journal International,* 115: 960-990.

Lambeck, K. (1994). Constraints of the late Weichselian ice sheet over the Barents Sea from observations of raised shorelines. *Eos, Transactions, American Geophysical Union*, 75, 44, Suppl., 221 pp.

Lambeck, K. (1995). Late Pleistocene and Holocene sea-level change in Greece and south-western Turkey: a separation of eustatic, isostatic and tectonic contributions. *Geophysics Journal International,* 122: 1022-1044.

Lambeck, K. and Nakada, M. (1990). Late Pleistocene and Holocene sea-

level change along the Australian coast. *Palaeogeography, Palaeoclimatology, Palaeoecology (Global and Planetary Change Section),* 89: 143-176

Lambeck, K., Johnson, P. and Nakada, M. (1990). Glacial rebound and sea-level change in northwestern Europe. *Geophysics Journal International,* 103: 451-468.

Larcombe, P. Carter, R.M., Dye, J. Gagan, M.K. and Johnson, D.P. (1995). New evidence for episodic post-glacial sea-level rise, central Great Barrier Reef, Australia. *Marine Geology,* 127: 1-44.

Lennon, G.W. (1990). The Australian programme for sea level and its links with climate. *Towards an Integrated System for Measuring Long Term Changes in Global Sea Level.* Report of a workshop held at Woods Hole Oceanographic Institute, May 1990.

Leppert, K. (1970). The Australian levelling adjustment, progress to April 1970. In Report of the symposium on coastal geodesy, 20-24 July, Munich. *International Union Geodesy Geophysics*, 223-231.

Logan, B.W., Brown, R.G. and Quilty, P.G. (1976). Carbonate Sediments of the West Coast of Western Australia. 25th International Geological Congress, Excursion Guide No. 37A.

Minster, J.F., Brossier, C. and Rogel, P. (1995). Variation of the mean sea level from Topex/Poseidon data. *Journal of Geophysical Research,* 100: 25,153-25,161.

Mitchell, W. (1991). Sea level and climate change. *The Second Australasian Hydrographical Symposium*, University of NSW, 9-12 December 1991, 353-360.

Nakada, M. and Lambeck, K. (1987). Glacial rebound and relative sea-level variations: a new appraisal. *Geophysical Journal of the Royal Astronomical Society,* 90: 171-224.

NOS (1986). *Specification for Next Generation Water Level Measurement System (NGWLMS) Field Unit.* National Ocean Service, National Oceanic and Atmospheric Administration, Rockville, Maryland, USA, 31 October 1986.

Peltier, W.R. (1980). Ice sheets, oceans, and the earth's shape. In Mörner,

N.A., ed., *Earth Rheology, Isostasy and Eustasy,* pp. 45-63. John Wiley and Sons, New York.

Peltier, W.R. and Tushingham, A.M. (1991). The influence of glacial isostatic adjustment on tide gauge measurements of secular sea level change. *Journal of Geophysical Research,* 96: 6,779-6,796

Pirazzoli, P.A. (1989). Present and near-future global sea-level changes. *Palaeogeography, Palaeoclimatology, Palaeoecology (Global and Planetary Change Section)*, 75: 241-258.

Pirazzoli, P.A. (1991). World altas of Holocene sea-level changes (book review). *Science*, 256: 1225.

Pirazzoli, P.A. (1993). Global sea-level changes and their measurement. *Global and Planetary Change,* 8: 135-148.

Playford, P.E. (1983). Geological research on Rottnest Island. *Journal of the Royal Society of Western Australia*, 66: 10-15.

Rhodes, E.G. (1982). Depositional model for a chenier plain, Gulf of Carpentaria, Australia. *Sedimentology,* 29: 201-221.

Sahagian, D.L., Schwartz, F.W. and Jacobs, D.K. (1994). Direct anthropogenic contributions to sea level rise in the twentieth century. *Nature,* 367: 54-57.

Searle, D.J. and Woods, P.J. (1986). Detailed documentation of a Holocene sea-level record in the Perth Region, southern Western Australia. *Quaternary Research,* 26: 299-308.

Semeniuk, V. (1980). Quaternary stratigraphy of tidal flats, King Sound, Western Australia. *Journal of the Royal Society of Western Australia,* 63: 65-78.

Semeniuk, V. (1985). The age structure of a Holocene barrier dune system and its implication for sea level history reconstructions in southwestern Australia. *Marine Geology,* 67: 197-212.

Semeniuk, V. and Searle, D.J. (1986). Variability of Holocene sealevel history along the southwestern coast of Australia - evidence for the effect of significant local tectonism. *Marine Geology,* 72: 47-58.

Smart, J. (1976). Late Quaternary sea-level changes, Gulf of Carpentaria, Australia. *Geology,* 5: 755-759.

Stiros, S.C., Pirazzoli, P.A., Laborel, J. and Laborel-Deguen, F. (1994). The 1953 earthquake in Cephalonia (Western Hellenic Arc): coastal uplift and halatectonic faulting. *Geophysics Journal International,* 117: 834-849.

Thom, B.G. and Roy, P.S. (1983). Sea level change in New South Wales over the past 15 000 years. In Hopley, D., ed., *Australian Sea Levels in the Last 15,000 Years, a Review,* Department of Geography, James Cook University of North Queensland Monograph Series, Occasional Paper 3, pp. 64-84. Department of Geography, James Cook University of North Queensland, Townsville, Qld.

Thom, B.G. and Roy, P.S. (1985). Relative sea levels and coastal sedimentation in southeastern Australia in the Holocene. *Journal of Sedimentary Petrology,* 55: 257-264.

Wagner, C.A. and Cheney, R.E. (1992). Global sea level change from satellite altimetry. *Journal of Geophysical Research,* 97: 15,607-15,615.

Warrick, R.A., Le Provost, C., Meier, M.F., Oerlemans, J. and Woodworth, P.L. (1996). Changes in sea level. In Houghton, J.T., Meira Filho, L.G., Callander, B.A., Harris, N., Kattenberg, A. and Maskell, K. (eds), *Climate Change 1995: The Science of Climate Change,* Contribution of Working Group I to the Second Assessment Report of the Intergovernmental Panel on Climate Change, pp. 359-405. Published for the IPCC by Cambridge University Press, Cambridge.

Wigley, T.M.L. and Raper, S.C.B. (1987). Thermal expansion of seawater associated with global warming. *Nature,* 330: 127-131.

Woodroffe, C.D. (1995). Response of tide-dominated mangrove shorelines in northern Australia to anticipated sea-level rise. *Earth Surface Processes and Landforms,* 20: 65-85.

Woodroffe, C.D., Thom, B.G. and Chappell, J.M.A. (1985). Development of widespread mangrove swamps in mid-Holocene times in northern Australia. *Nature,* 317: 711-713.

Woodroffe, C.D., Chappell, J., Thom, B.G. and Wallensky, E. (1989). Depositional model of a macrotidal estuary and floodplain, South

Alligator River, Northern Australia. *Sedimentology,* 36: 737-756.

Woods, P.J. and Searle, D.J. (1983). Radiocarbon dating and Holocene history of the Beacher/Rockingham beach ridge plain, west coast, Western Australia. *Search,* 14: 44-46.

Wunsch, C. (1991). Global-scale sea surface variability from combined altimetric and tide gauge measurements. *Journal of Geophysical Research,* 96: 15,053-15,082.

Zerbini, S., Plag, H.P., Baker, T., Becker, M., Billiris, H., Bürki, B., Kahle, H.G., Marson, I., Pezzoli, L., Richter, B. Romagnoli, C., Sztobryn, M., Tomasi, P., Tsimplis, M., Veis, G. and Verrone, G. (1996). Sea level in the Mediterranean: a first step toward separating crustal movements and absolute sea-level variations. *Global and Planetary Change*, 14: 1-48.

Sea-Level Changes and Their Effects
B.J. Noye & M.P. Grzechnik (Editors)

Low Frequency Sea Level Variability in the Western Tropical Pacific 1992-1998

J-M. Verstraete
IRD*, Muséum, Paris, France

Abstract

Since 1992, the South Pacific Sea Level and Climate Monitoring project has run a network of eleven sea level stations in the western tropical Pacific ocean, maintained by the National Tidal Facility, to get estimates of the secular sea level trends at these locations. The project aims to monitor the spatial-time variability of the sea surface topography over large areas, namely the Pacific equatorial current system and the subtropical gyres, by a combination of permanent sea level observatories and altimetry technology. After a review of the seasonal mean sea level, heat content and steric height in the western tropical Pacific, the 1975-1994 and the 1992-98 sea level trends at each site are discussed. During both periods, the year to year variability was dominated by El Niño-Southern Oscillation (ENSO) episodes. The signature of the very strong 1997-98 El Niño appears clearly with negative trends at the sea level stations equatorward of 10° latitudes, whereas positive trends at the five stations south of 10°S give evidence of the warming of the south Pacific subtropical gyre over the period 1992-98, as compared with the 1975-1994 period. If both Pacific sutropical gyres were permanently warmer, the eastern edge of the warm pool could be shifted eastward of the date line.

Equatorial planetary waves, evidenced through the Topex/Poseidon observations, are studied on a four-year period, as they are of paramount importance in the leading ENSO theory. Sea level anomalies observed by Topex/Poseidon during the period October 1992 to October 1996 seem to favor wind forcing rather than reflections at the coastlines to generate equatorial Kelvin waves and planetary waves. The end of the 1993-94 El Niño was not due to upwelling RW reflecting at the western boundary as upwelling KW, but to upwelling KW starting from 170°E, generated by easterly wind anomalies initiated in January 1995. Similarly, repetitive downwelling RW reached the western boundary from March to December 1995, but none of them was the trigger of an El Niño event in 1996.

It is suggested that the lack of periodicity of ENSO is due in part to the seasonal forcing of the Australasian monsoon, through the concept that the "Australasian-Pacific Equatorial Climate System" (APECS) contributes to run the Indo-Pacific climate machine.

Key Words: tropical Pacific, heat content, steric sea level, sea level trend, sea level observatories, Topex/Poseidon (T/P) altimetry, sea level anomaly, ENSO (El Niño-Southern Oscillation), delayed oscillator, Kelvin wave (KW), Rossby wave (RW), climate change, TOGA (Tropical Ocean-Global Atmosphere), CLIVAR.

*Institut de recherche pour le développement

CONTENTS

1. Secular Trends, the South Pacific Project and T/P Satellite Altimetry

1.1 Secular trends and the South Pacific sea level project

In the debate on global warming, there is agreement that the twentieth century Earth's surface temperature has increased between 0.3° and 0.6 °C (Houghton et al., 1995). Sea surface temperature (SST) observations give evidence of a global mean warming trend of 0.4°C per century, although this warming is far from uniform. Then, it is not a surprise that most of the long tide gauge records indicate that, in stable tectonic areas, sea level has been rising during the past century at a mean rate of 1 to 3 mm per year, although this rise is not global and there is no evidence for any acceleration as a result of recent global warming (Woodworth, 1990). The secular sea level trend is embedded within the variability of the oceanic heat storage, which has received considerable attention in recent years because it is a major component of the Earth's climate system. The excess of heat received in equatorial regions is dispatched polewards, through the western boundary currents essentially, but there is a large interannual variability of the tropical ocean and atmosphere, leading to strong variations in the equatorial current system and subtropical gyres, generating large changes in sea level from seasonal to interannual time scales.

Actual climatic programmes, such as CLIVAR (1995-2010, Climate Variability and predictibility), monitor sea level variations by combining tide gauge networks, satellite altimetry (Topex / Poseidon, since August 1992 and Jason, scheduled in 2000) and long-term moorings, because in tropical areas sea level is a very good indicator of the heat storage. Estimates of the variability of this parameter are very difficult, due to the impossibility of maintaining large arrays of permanent deep sea moorings to observe continuously the temperature profile from surface to bottom.

However, sea level changes contain significant information about integrated quantities such as heat content, steric changes, dynamic height, (definitions given in chapter 3) and features of large-scale water density within the water column, parameters of great interest in climate variability studies. Moreover, in the tropical ocean, a close relationship exists between sea level and the depth of the thermocline. Sea level is therefore the key parameter providing much of the necessary empirical guidance to understand the magnitude of the oceanic heat storage transfer and variability within the oceans, on basin-wide scales and for periods from several days to years. In tectonically stable areas of the Earth, the secular sea level rise is an undisputable observational fact, although evidence appears only in very long sea level records. Unfortunately, very few sites satisfy both criteria of tectonic stability and duration. In France, only two sites are to be considered for these studies (Fig.1, annual mean sea levels compiled by the Permanent Service for Mean Sea Level, PSMSL, Bidston, GB): Brest (1807-1993), where the secular trend of 0.93 ± 0.05 mm/year, over 163 years of record since 1807, is comparable with the 1.18 ± 0.08 mm/yr trend observed since 1885 at Marseille, over 95 years of record (1885-1991). A 66 year series of sea levels recorded at Newlyn (1915-1981), Cornwall, in south-west England, where land movement is also negligible on this time-scale, were analysed by Cartwright (1983) with associated barometric data. The mean secular total rise of 2.0 mm/yr was reduced to 1.34 mm/yr, the increment of 0.66 mm/yr being due to the local positive trend in atmospheric pressure. All these secular trends are in agreement with estimates from comparable sea level records in the southern hemisphere, in areas of small tectonic activity, as for example the climatological time series of Sydney harbour, Australia, carried out since 1897 (Sydney, 1897-1983, positive trend of 0.7 ± 0.5 mm/yr, statistically consistent with the above mentioned European trends, PSMSL). In summary, all records of climatological significance and not affected by tectonic influences, give evidence of a positive trend and present estimates converge to a secular rate of sea level rise of about 1.2 mm/yr during the twentieth century.

The primary aim of the South Pacific Sea Level and Climate Monitoring Project (henceforth referred to the "South Pacific Project") is to give estimates of the average rates of the secular sea level trend at

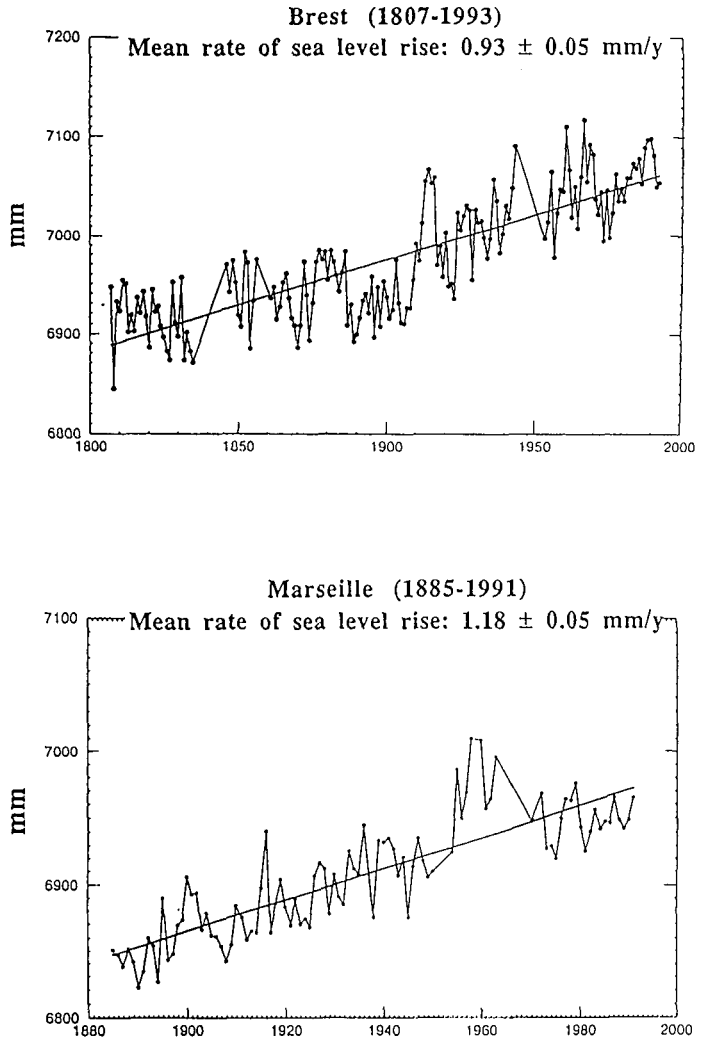

Figure 1

Mean rates of sea level rise at Brest (1807-1993) and Marseille (1885-1991), France. Data source: PSMSL (Permanent Service for Mean Sea Level, Bidston, GB). The reference level is the PSMSL "Revised Local Reference".

eleven sites of the western tropical Pacific. Curriculum modules dedicated to the Pacific Island peoples were incorporated within the project (Aung, Kaluwin and Lennon, 1998).

The aim of the South Pacific Project is difficult to reach because the Pacific is known to be the theatre of a permanent tectonic activity at geological time scales, generating numerous and unpredictable earthquakes. Furthermore, recent SST analyses indicate that the equatorial and tropical Pacific would be areas significantly different from the global mean warming trend. According to analysis of SST data from 1900 to 1991, there would be a warming in the equatorial Pacific west of the date line, and a cooling in the east (Cane et al., 1997), complicating further the natural variability at long time scales in this region. For all these reasons, it is very difficult to extract the secular sea level trend in the western tropical Pacific.

The present review focuses on the seasonal and interannual variations of sea level in the western tropical Pacific, within the framework of the Australian South Pacific Project. The sea level trend estimates for the period 1992-98 were compared with the 1975-1994 estimates. This study also presents a summary of the equatorial low-frequency long waves as evidenced through the Topex/Poseidon observations during the 4-year period October 1992 - October 1996, and an up-to-date of the current leading mechanism of the El Niño-Southern Oscillation (ENSO). The effectiveness of the delayed oscillator mechanism to trigger or stop an El Niño is questioned. In the conclusion, the significance of the 1992-98 heat content increase in the south Pacific subtropical gyre is discussed, in relation to the 1900-1991 SST warming in the western equatorial Pacific, and it is suggested that the equatorial climate machine is driven in part by the Australasian monsoon through the Indo-Pacific warm pool area.

1.2 The sea level observatories of the South Pacific project

Generally, on seasonal or larger time scales, sea level records in open areas, not contaminated by river discharges, are known to be negligibly biased by local effects and can be considered to be representative of the open ocean fluctuations. In the open ocean, a significant part of the seasonal and interannual variance in sea level is representative of the steric level, which is the effect of expansion and contraction of the water

column (Pattullo et al., 1955; Wunsch, 1972, Verstraete, 1987).

The South Pacific project has progressively implemented a network of eleven sea level stations employing equipment at the forefront of modern technology. The monitoring sites were deployed, on behalf of the South Pacific Forum countries, by the National Tidal Facility (NTF) at Flinders University, sponsored by the Australian Agency for International Development (AusAID, Canberra), starting in October 1992 (Fiji, Kiribati) to September 1994 (Solomon Islands and Papua New Guinea). The sea level monitoring stations use a very sensitive acoustic sensor within the SEAFRAME (Sea level Fine Resolution Acoustic Measuring Equipment) system, measuring sea level at six minutes intervals (from 181 one second samples over a period of 3 minutes) and meteorological data every hour: barometric pressure, wind speed, wind direction, maximum wind gusts, sea surface and air temperatures. Although the winds are very light in this area, some westerly wind bursts are very strong and cyclones may occur during the tropical cyclone season, and it makes sense to monitor these maximum wind speeds.

The expected error in sea level observed with mechanical tide gauges would be typically 10 mm, due to instrumental noise, and the accuracy of the monthly sea levels of the University of Hawaii Sea Level Center Pacific tide gauge network is estimated to be 3 to 10 mm (Wyrtki, 1973). The SEAFRAME equipment will improve this accuracy below the 3 mm threshold.

The SEAFRAME data are transmitted to Japan via the Japanese Geostationary Meteorological Satellite GMS, and to the NTF in Adelaide (over the internet from the Melbourne Meteorological Headquarters), where the data are downloaded, subjected to quality control, and archived in a secure data bank. The transmission interval from each station is one hour. The complete list of the South Pacific Project sea level stations and a map of the sites are given in the Appendix. The same equipment has also been installed around Australia.

1.3 The Topex/Poseidon global sea level monitoring system

It is clear that the ocean climatological signal is decoupled from the tectonics and must be studied per se. It is also known that the fastest tectonic motion in the world has been measured near the Samoan islands

and that a high seismic activity is present in the south-west Pacific region, related to the rapid subduction rate of the Pacific plate under the Australian plate (Nature, 374, 249, 1995). Although precise levellings are carried out regularly by the NTF to check the stability of the datum at each station, these techniques can identify land motion only in the near-vicinity of the tide gauge, but are unable to detect such large scale crustal motions, resorting to the spatial geodesy techniques. Actually, to separate the ocean climatological signal from large scale land motions, it is necessary to use another monitoring system. This system is available since August 1992, when the TOPEX/POSEIDON (T/P) satellite altimetry mission, the first entirely dedicated to Physical Oceanography, was launched. The initial major source of error in T/P altimetry was due to the aliasing of imperfectly removed semidiurnal and diurnal ocean tides with the T/P repeat period of 9.915625 days. Now the T/P data are corrected for ocean and earth tides with excellent tidal models and are free from aliasing problems, allowing the identification of low frequency phenomena. Due to the very high precision of its orbit, T/P has proved its capability to perform accurate sea level measurements, fully reproductible and without instrumentation drift (which is also properly corrected).

The actual measurements accuracies for the first four years of T/P's operations were 2.8 cm for its orbit and 3.2 cm for the distance between the satellite and the surface of the ocean (NASA, JPL, July 1997). Numerous calibrations and verifications have demonstrated that the TOPEX/POSEIDON (T/P) satellite altimetry, is able to measure global sea surface height with an accuracy better than 2 cm rms on time scales greater than 1 month (Cheney et al., 1994; Park and Gamberoni, 1995; Verstraete and Park, 1995; Park, Gamberoni and Verstraete, 1997). Due to geoid errors of about 25 cm for short wavelengths (100-200 km), and of about 10 cm for scales greater than 2000 km, only large-scale mean dynamic topography with wavelengths greater than 2000 km can be separated from the geoid error at a 10 cm level of uncertainty.

In summary, the tide gauge data are relative to a bench mark, whereas the reference of the T/P data is its orbit itself, so that the T/P data are free of land motion. The SEAFRAME sea level observatories and the T/P global sea level monitoring system are complementary and provide very

precise and accurate sea level measurements independently. The in-situ data check up on any possible drift of the satellite and in turn the satellite data check that the low frequency sea level changes at each sea level station are real ocean signals, not related with land motion.

2. The Tropical Pacific Sea Level: Background

2.1 The relationship between sea level and the thermocline

At seasonal and interannual time scales, changes in sea level are mainly due to variations of large-scale currents, temperature and salinity structures in the water column, due to changes in the atmospheric pressures and the wind field. Any abrupt change in the winds, any displacements of frontal areas separating fresh and warm waters from saline and cold waters are responsible for large changes in sea level as well. The interpretation of sea surface synoptic integrated fields such as the dynamic height given by hydrography, or the sea level as observed by tide gauges and altimetry, necessitate an understanding of the vertical structures which sustain them. For example, the sea surface upward slope of about 50 cm along the equator from central America towards Indonesia is the surface signature of a deepening of the tropical thermocline in the central-western equatorial Pacific. This westward deepening of the thermocline reflects large changes in the upper thermal and saline vertical structures due to the accumulation of warm waters in the "warm pool" area, west of the date line, in contrast to the prevailing upwelling "cool tongue" area in the central-eastern equatorial Pacific, leading to a sharp thermal zonal front at about 3°N.

In the tropical Pacific, a close relationship exists between sea level and the depth of the thermocline (the 20°C isotherm depth is an excellent indicator of the thermocline depth). Changes of sea level height h relate to changes of the thermocline depth D according to the relation $\Delta h = \Delta D \times \Delta\rho / \rho$ (1), where ρ is the density. For example, in the equatorial current system where $\Delta\rho / \rho = 5. 10^{-3}$ approximately (Wyrtki and Kendall, 1967), a change of ± 20 m of the thermocline depth results in a ± 10 cm change in sea level.

2.2 The atmosphere-ocean relationship

The western equatorial Pacific is a region of strong atmosphere-ocean interactions on annual and interannual time scales, although the mean

wind stress is comparatively small in relation to the seasonal variations. When the sea level atmospheric pressures are high (low) in the area Tahiti-Easter Island and low (high) over Darwin-Djakarta, the easterly trade winds prevail (weaken) over the tropical Pacific. To describe this basin wide atmospheric oscillation, an index was created, the "Southern Oscillation Index" (SOI), fairly representative of the sea level barometric pressure gradient over the South Pacific. This index allows us to monitor the difference of sea level barometric pressure between the high pressures referred to the Tahiti-Easter Island subtropical highs, and the low pressures straddling northern Australia (Darwin), Indonesia (Djakarta) and the warm pool. Positive (negative) SOI are related with stronger (weaker) than "normal" southeast trade winds and a well developed equatorial upwelling (weak or absent equatorial upwelling).

When the easterly trade winds prevail over the tropical Pacific, they may account for the accumulation of warm waters straddling the equator in the western Pacific, as well as for the downward slope of the thermocline from the American coast towards the west. Referring to these warm waters, a new term was coined for this vast oceanic area: the "warm pool". In the warm pool, SST are usually greater than 28°C and it is the largest heat storage in the tropical oceans. Huge amounts of heat and energy (each gram of water vapor extracted from the ocean, condensing into drops of water in the clouds, releases 2436 Joules) are injected from the ocean into the atmosphere over the warm pool through evaporation-condensation, convection and rainfalls (>3 m/yr in the area), all processes strongly linked with the high sea surface temperatures over the area.

As long as the trade winds blow steadily, warm waters move westwards and accumulate to the west of the basin. Sea surface temperatures (SST) in excess of 28-29°C are then observed all the year round to the west of the date line. At the same time, the thermocline is very shallow in the eastern equatorial Pacific, due to the divergence of the wind-driven upper waters, while it is very deep in the western equatorial Pacific where the winds are generally weak. In the warm pool area, the mean depth of the 20°C isotherm, representative of the thermocline (Fig. 2), deepens from 150 m at 0°-5°N to 200 m at 5°S, as compared with a mean depth of about 30 to

50 m at 90°W (5°N-5°S). Reflecting the thermal and salinity structures of the water column all along the equator, and in agreement with (1), the sea surface slopes upwards from central America towards Papua New-Guinea and Indonesia, the slope being essentially unaffected by the choice of the reference level (500, 1000, 2000,..., 4000 dbar). The mean sea surface dynamic heights computed with the historical 1°x1° hydrography data files (Levitus et al., 1994), either at 0°.30'N or at 0°.30'S, were nearly identical. Whatever the reference was, both equatorial sections at ± 0°30' give evidence of a sea surface higher by about 45 cm off Papua New-Guinea (130°E) than off central America (80°W), (Fig. 3). Note that west of the date line, the equatorial slope is near zero, although we do not observe a temperature front at 180°. Actually, a salinity front related to an oceanic zone of convergence situated on average at 180° (Picaut et al., 1997), separates rainfall-induced fresh water to the west of 180° from the more saline water to the east. Similar changes of sea level of about 60 cm were computed at 10° and 20° latitudes from the Philippines (10°-20°N) and Australia (10°-20°S) towards the Americas (Fig. 4 and Fig. 5). These changes in sea level are the signatures of the two subtropical gyres, where warm waters are accumulated through Ekman pumping, and are the "normal" topography of the tropical Pacific due to the so-called steadiness of the trade winds.

2.3 Interannual variability in the western tropical Pacific

The south-east trade winds do not blow steadily all the time, but weaken seasonally indeed. The western Pacific (130°E-180°) is a region of strong seasonal variation in the atmospheric forcing, due to the monsoon influence, clearly seen in the reversal of the winds twice a year: south-east trade winds (June-September), switch to northwesterly monsoon winds (December-April). Between July and January, the intertropical convergence zone (ITCZ) moves from about 15°N to about 15°S to the west of 160°E. The southeast trade winds weaken dramatically and westerly winds may appear to the west of the date line. During the Australasian monsoon (southern hemisphere summer, Dec-Jan-Feb), strong westerly wind bursts may occur at any time to the west of 180°, of paramount importance with respect to the early stages of a typical El Niño event (Rasmusson and Carpenter, 1982; Philander, 1990).

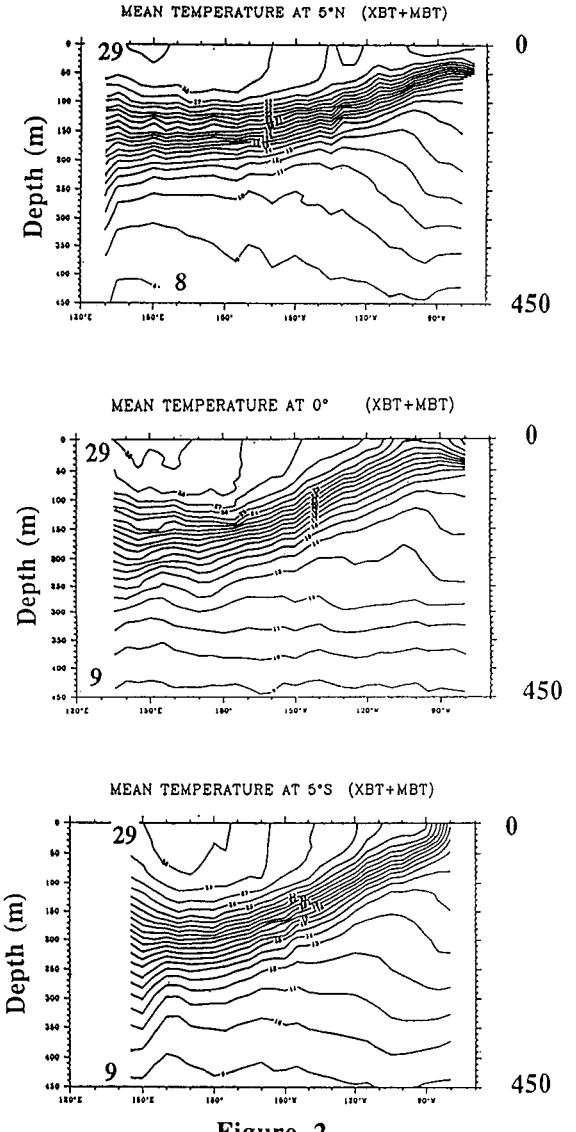

Figure 2

Mean Ocean temperature (in °C) 0-450 m, at 5°N, 0°N and 5°S; 130°E-80°W, (1970-1987). Contour interval: 1°C; ranges: 8-9°C to 29°C. From W. Kessler, NOAA technical memorandum PMEL-86, 1989.

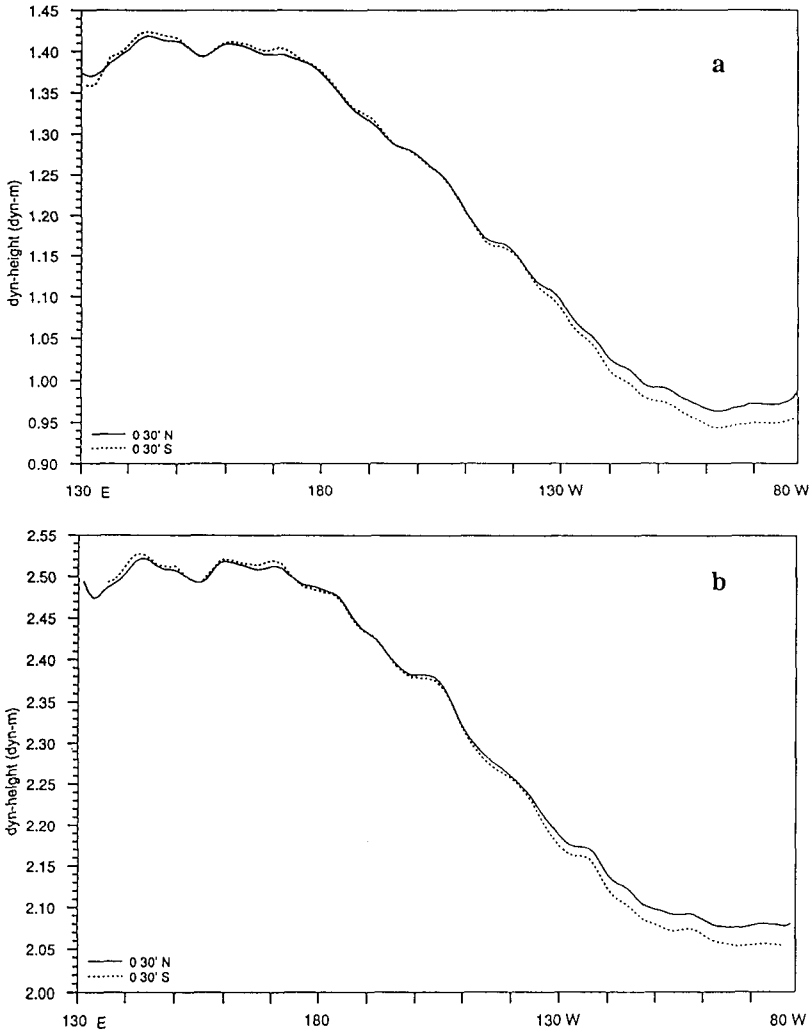

Figure 3

Sea surface topography along the equatorial Pacific. The sea surface dynamic heights along 0°.30'N and 0°.30'S are referred to a) 500 and b) 2000 dbar and computed every degree of longitude between 130°E and 80°W. Source of data: World Ocean Atlas, Levitus and col., 1994.

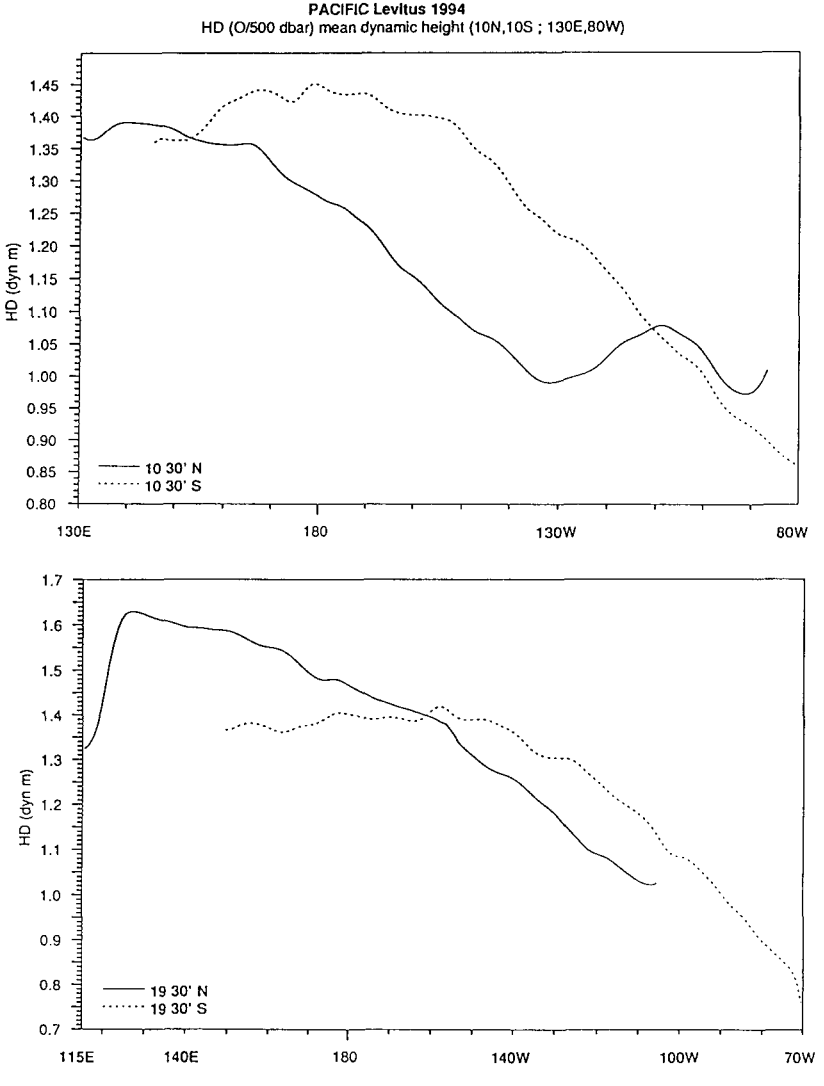

Figure 4

Sea surface topography at 10°N (S) and 20°N (S) from the Americas towards the Philippines (10°N-20°N) or Australia (10°S-20°S). Dynamic heights are referred to 500 dbar. Source of data: World Ocean Atlas, Levitus and col., 1994.

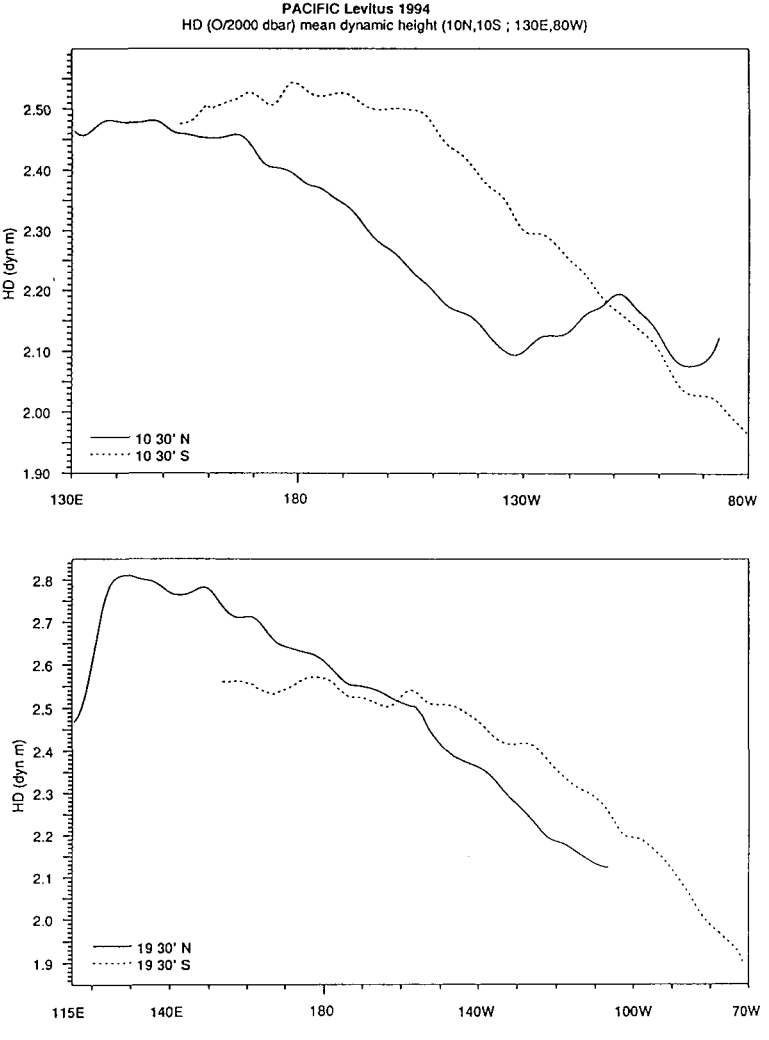

Figure 5

Same as figure 4, but sea surface dynamic heights are now referred to 2000 dbar.

Besides this strong monsoonal signal across the equator, the western tropical Pacific area is also known to be the theatre of the most significant Ocean-Atmosphere interannual interactions. Until the early sixties, it was thought that the invasion of warm waters off Equator and Peru was only a local event of small consequences. Peruvian fishermen had noticed in the past that this event occurred generally near Christmas and used the expression "Corriente d'El Niño", i.e., the current of the "Christ child". The relationship between the unusual sea surface temperature in the eastern equatorial Pacific and the unusual winds along the equator was discovered by Bjerkness (1966), who later demonstrated the link existing between the El Niño event and the Southern Oscillation (Bjerkness, 1969). Since then, the El Niño oceanic warm events are linked with the atmospheric Southern Oscillation (the ENSO events). El Niño is the result of the response of the equatorial Pacific ocean to the atmospheric forcing, and coincides with weaker trade winds and a decrease of the equatorial upwelling during the southern hemisphere summer. A warming in January-April would be a normal annual event as such, but in certain years this summer warming is excessively strong as in 1957-58; 1972-73; 1982-83; 1986-87 and 1997-98, or of excessive duration as in the repetitive warm events between 1991 and 1994. El Niño therefore seems to be first an amplification of the southern hemisphere summer warming with an unusual rise of temperature in the eastern Pacific, as large as 3°C in a 200 m thick layer, correlated with a rise of sea level of 15 cm.

In summary, the Southern Oscillation is the dominant mode of the interannual variability at time scales of about three-four years. Actually, the oscillation is so irregular that ENSO episodes may occur within a broad range of time scales, from two to ten years (Philander, 1990).

During ENSO events, the south east trade winds are unusually weak, and the sea level shrinks in the western Pacific by as much as 30-40 cm to the west of the date line, while it rises in the eastern Pacific. A complete ENSO episode may include, although not necessarily, the so-called "La Niña" phase, when the trade winds recover their full strength or are unusually strong, after an El Niño. During La Niña, the warm waters are pushed back to the west and the equatorial upwelling lifts back the thermocline in the central-eastern Pacific as well.

2.4 a The equatorial wave guide

The ocean response to the atmospheric forcing is known to be very rapid in the equatorial regions, and since Geosat (1986-89), satellite altimetry has tremendously increased our knowledge of the equatorial dynamics. Strong westerly (easterly) wind anomalies push downward (pull upward) the equatorial thermocline, and these impulses are very efficient to move up and down the thermocline and modify the equatorial current system. The warm waters (and low salinity waters in the western Pacific) "float" above the cold deep waters and, according to (1), the gravity in the upper layer is reduced to $g' = g \times \Delta\rho / \rho$, where $\Delta\rho / \rho = 5. 10^{-3}$. This explains why zonal wind bursts are able to move vertically in the equatorial thermocline so quickly. A change of ± 20-30 m of the thermocline depth results in a ± 10-15 cm change in sea level, easily detected by T/P as a ±10 to ±15 cm change of sea surface height. Positive (negative) sea level anomalies (SLAs) correspond to a downwelling (upwelling) of the thermocline and they move away from the initial impulse along the equator as free downwelling/upwelling Kelvin waves. Similarly, planetary waves are generated, moving westward as downwelling/upwelling Rossby waves.

These internal Kelvin and planetary waves alter the thermocline and current structure all the way over the basin (unless they are destroyed by opposed wind stress) until they collide with the coasts, where some of the incident energy is reflected as long waves radiating from the boundary. In the reflection process, they switch their father's names, but not their designation: an upwelling (downwelling) KW will reflect from the American coasts as an upwelling (downwelling) RW. Similarly, an upwelling (downwelling) RW impinging on the west Pacific coasts in the Papua New-Guinea area, will reflect back as an upwelling (downwelling) KW.

Wyrtki (1975) was the first to propose that El Niño was the dynamic response of the upper equatorial Pacific to a sudden weakening of the trade winds and presented a theory for the occurrence of El Niño, as follows: strong southeast trade winds in the central Pacific precede an El Niño for two years, strengthen the South Equatorial Current, building up warm waters in the western equatorial Pacific and increasing the normal

ascending slope of the sea level from east to west. Then, for some unknown reason, the trade winds in the central Pacific relax and the accumulated warm waters flow eastward, in the form of an internal downwelling equatorial Kelvin wave. This Kelvin wave leads to a deepening of the shallow thermocline and an excess of warm waters in the central-eastern equatorial Pacific, spreading later on off Ecuador and Peru, where a rise of sea level is observed at the coastal stations.

From this concept, it follows immediately that cold events (La Niña) will start due to upwelling Kelvin waves. Finally, one complete cycle of the oscillation, warm El Niño - cold La Niña, is conceivable as follows: westerly (easterly) wind anomalies in western-central (central-eastern) equatorial Pacific generate downwelling (upwelling) Kelvin waves, deepening (shallowing) the thermocline in the eastern Pacific and advecting eastward warm waters (eastward cold waters). If the response of the ocean was correctly described in this scheme, it was quickly recognized that the trigger of El Niño is not necessarily a matter of stronger than usual trade winds (TW) during one or two years preceding an event. For example, no El Niño occurred in 1975, although the TW were stronger than seasonal in 1973-74. Actually, the TW were stronger than usual for three consecutive years, in 1973, 74, 75, known to be La Niña years, although the 1976-77 El Niño was moderate (Rasmusson, 1984). On the contrary, the powerful El Niño of 1982-83 occurred without warning and was not at all preceded by stronger than usual TW. From these facts, it is clear that low-frequency fluctuations in the trade winds are secondary for El Niño. Empirical and theoretical studies point to changes in the zonal winds in the far western equatorial Pacific as an essential ingredient for launching an El Niño (Mc Creary, 1976).

2.4 b Recent theories

Coupled ocean-atmosphere ENSO theories recognize that the equatorial wave guide (Wyrtki, 1975; McCreary, 1976) as well as the off-equatorial subtropical dynamics (McCreary, 1983) play essential roles in the ENSO dynamics. According to these theories, the oscillatory nature of the ENSO is due to the reflections of long Rossby waves against the western boundary. Different authors have built further on this by considering the large scale wind stress curl associated with equatorial strong westerly (easterly) wind anomalies in the central equatorial Pacific. These wind

anomalies generate upwelling (downwelling) long off-equatorial Rossby waves that are reflected from the western boundary as upwelling (downwelling) Kelvin waves, acting as triggers for switching the ENSO from one mode to the opposite one. The "delayed oscillator" scheme (Batisti, 1988; Battisti and Hirst, 1989; Schopf and Suarez, 1988; Graham and White, 1988), was seriously questioned recently, because no observations had substantiated the reflection process on the western boundaries. However, since August 1992, the equatorial Pacific ocean has been monitored simultaneously by three operational observing systems, namely, two synoptic networks: the Pacific tide gauge network (including the Australian sea level stations) and the TAO (Tropical Atmosphere Ocean) moorings, in addition to the quasi-synoptic Topex/Poseidon altimetry network, delivering observations of unprecedented quality and sampling. Routine observations of the Pacific equatorial dynamics allow decisive investigations on fundamental questions about potentially important ENSO mechanisms, and among them, the "delayed action oscillator" theory which emerged as the most studied concept since the early 1990s.

2.5 The Southern Oscillation Index (1958-1999)

The intensity of the Pacific trade winds is modulated through variations in the intensity of the Walker circulation, which oscillates interannually between two opposite modes: either the trade winds are stronger than usual (periods known as "La Niña"), or they are weaker (such events are known as "El Niño"). The cycling between these two modes was first described by Sir Gilbert Walker in 1923-24 as the Southern Oscillation, and to-day the "Southern Oscillation Index" (SOI) reflects the state of the Walker circulation. The SOI is the mean monthly difference in sea-level barometric pressure between Tahiti and Darwin, so removing the seasonal cycle from the index and giving a clearer view of the interannual signal. The data are normalised relative to the data's standard deviation, so that the SOI is a dimensionless figure. Examination of the SOI between 1958 and 1999 gives evidence that the pressure gradient over the south Pacific was frequently not in a "normal" state during this 41 years period. The El Niño events (57-58, 63, 65, 72-73, 76-77, 82-83, 86-87, 91-92, 92-93, 93-94, and 97-98) clearly outnumbered the number of major La Niña

events (1964, 1971, 1974-75, 1988, 1999), and it is noteworthy that every El Niño was not followed by La Niña (Fig. 6). For example, the exceptionally strong El Niño observed in 1982-83 was followed by a weak La Niña in 1984-85, although the moderate 1986-87 El Niño was succeeded by a significant La Niña in 1988. A plot of the SOI for the period January 1958 to February 1999, gives evidence of a considerable weakening of the south Pacific sea surface pressure gradient during the last twenty years (Fig. 6).

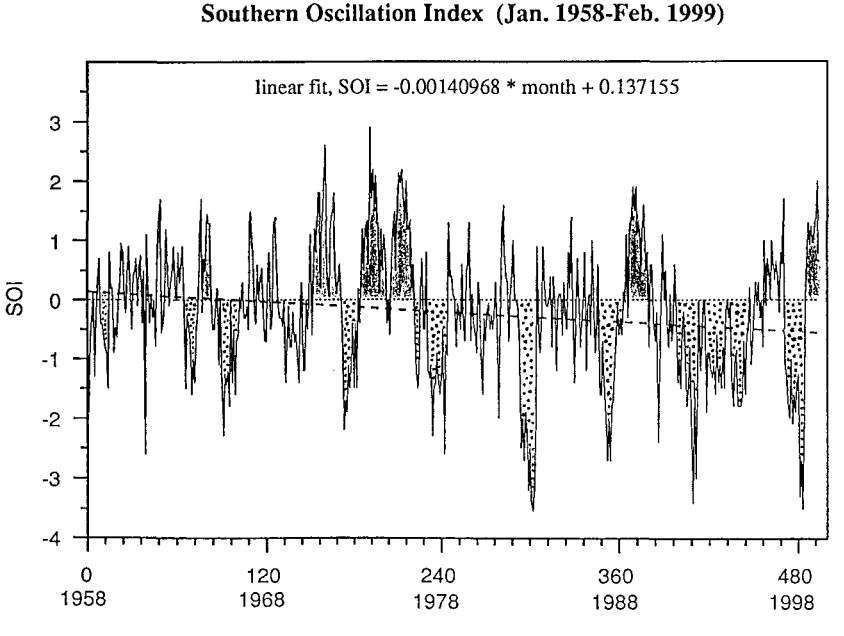

Figure 6

The Southern Oscillation Index (1958-1999). The negative slope (dashed line) of a linear fit computed from 494 monthly SOI values confirms the secular negative trend computed from 94 annual SOI values (1900-1993, not shown here). Continuously negative indexes for five consecutive years in 1991-95 are indicative of considerably weaker sea surface pressure gradients during the 1990s than during the three preceding decades. The 1997-98 El Niño event seems to be as strong as the 1982-83 El Niño. El Niño (La Niña) events are dotted (shaded).

The Southern Oscillation Index was nearly permanently negative for six consecutive years starting in 1990-91, and after a weak positive episode in 1996, it has been negative again from March 1997 to May 1998. In the 1990s, the pattern of positive atmospheric sea level pressure anomalies west of the date line and negative anomalies to the east has dominated the tropical Pacific for more than seven years, as of February 1999. If the 1982-83 El Niño was the strongest in intensity, the repetitive events of 1991-92, 1992-93 and 1993-94, the unusual warming of the western equatorial Pacific in 1995 and 1996, followed by the very strong 1997-1998 El Niño, all these facts give evidence that we have observed the most persistent ENSO events of the tropical Pacific in the twentieth century.

3. The Seasonal Cycle

3.1 The seasonal mean sea level

The 1992-1998 sea level and meteorological time series produced by the new tide gauge network since 1992 are too short to establish the seasonal cycle, particularly in repetitive El Niño years (1992, 93, 94, and 97-98). All the seasonal cycles in mean sea level adopted here were computed from the 1975 to 1994 Pacific monthly sea level deviations archived at the University of Hawaii Sea Level Center/Joint Archive for Sea Level (P. Caldwell and M. Merrifield, 1997). The reference of the sea level deviations at each Hawaiian site is the 1975 to 1986 mean sea level value, and it is noteworthy that this period includes two strong El Niño events in 1976-77 and 1982-83. The root-mean-square signal amplitudes (standard deviation) of the monthly mean sea levels for the period 1975 to 1994 were generally greater than 50 mm and smaller than 75 mm, associated with the climatic variability (Fig. 7).

Nine sites were selected in the Hawaiian data bank, corresponding to the closest SEAFRAME sites. The SEAFRAME sites of Port-Vila (17°.46'S, 168°.17'E, Vanuatu) and Nuku'alofa (21°.08'S, 175°.11'W, Tonga) have no equivalents in the Hawaiian data bank. The Hawaiian sites of Rabaul (4°.12'S, 152°.11'E, Papua-New-Guinea), Suva (18°.08'S, 178°.26'E, Fiji) and Pago-Pago (14°.17'S, 170°.41'W, American Samoa) were used as indicators for the SEAFRAME sites of Manus Island (2°.02'S, 147°.23'E, PNG), Lautoka (17°.36'S, 177°.26'E, Fiji) and Apia (13°.49'S, 171°.45'W, Western Samoa), respectively.

Oceanographic considerations lead to consider three groups of sea level stations as follows (see the mean sea surface topography on figure 14):

GROUP I: Majuro (7°.06'N, Marshall I.); Nauru (0°.32'S) and Tarawa (1°.22'N, Kiribati), figure 7 a.

In this group, two areas of the equatorial current system are to be distinguished: the sites of Nauru and Tarawa are situated, 6° of longitude apart, within the Equatorial Trough (Fig.14) and the South Equatorial Current (westward). The similarity of their seasonal cycle is evident, with low sea levels in the first half of the year and higher sea levels from July, typical of the tropical northern hemisphere.

The site of Majuro is close to the Countercurrent Ridge, situated generally at 3°N-9°N, and is usually within the North Equatorial Countercurrent (eastward). In contrast to the above equatorial stations, we observe a bi-annual cycle, with two maxima in March and October and two minima, in January and July. These bi-annual maxima and minima are associated with the latitudinal seasonal movement of the Countercurrent Ridge, cycling generally between 3°N and 9°N.

GROUP II: Honiara (9°.26'S, Solomon I.), Funafuti (8°.31'S, Tuvalu) and Rabaul (4°.12'S, PNG, the closest Hawaian site of interest in relation to the SEAFRAME station of Manus Is., 2°.02'S), figure 7 b.

The sites of Honiara, Funafuti and Rabaul are within the South Equatorial Current. Rabaul is situated on the northward rim of the south Pacific subtropical gyre, while Honiara and Funafuti are near the South Equatorial Ridge (Fig. 14). The annual cycle at the three sites is very similar, with high sea levels in March and low sea levels in July-August. These are typical cycles of the tropical Southern Hemisphere, due to the seasonal steric effect and the expansion (contraction) of the water column at the end of the southern summer (winter).

GROUP III: Rarotonga (21°.12'S, Cook I.), Suva (18°.08'S, Fiji) and Pago-Pago (14°.17'S, American Samoa). Suva and Pago-Pago are the closest Hawaiian sites of interest in relation to the SEAFRAME sites of Lautoka (17°.36'S, Fiji) and Apia (13°.49'S, Western Samoa), figure 7 c. The annual cycle at Pago-Pago is nearly flat, in contrast with the cycles at Rarotonga and Suva, two stations situated on the southward rim of the south Pacific subtropical gyre (Fig. 14).

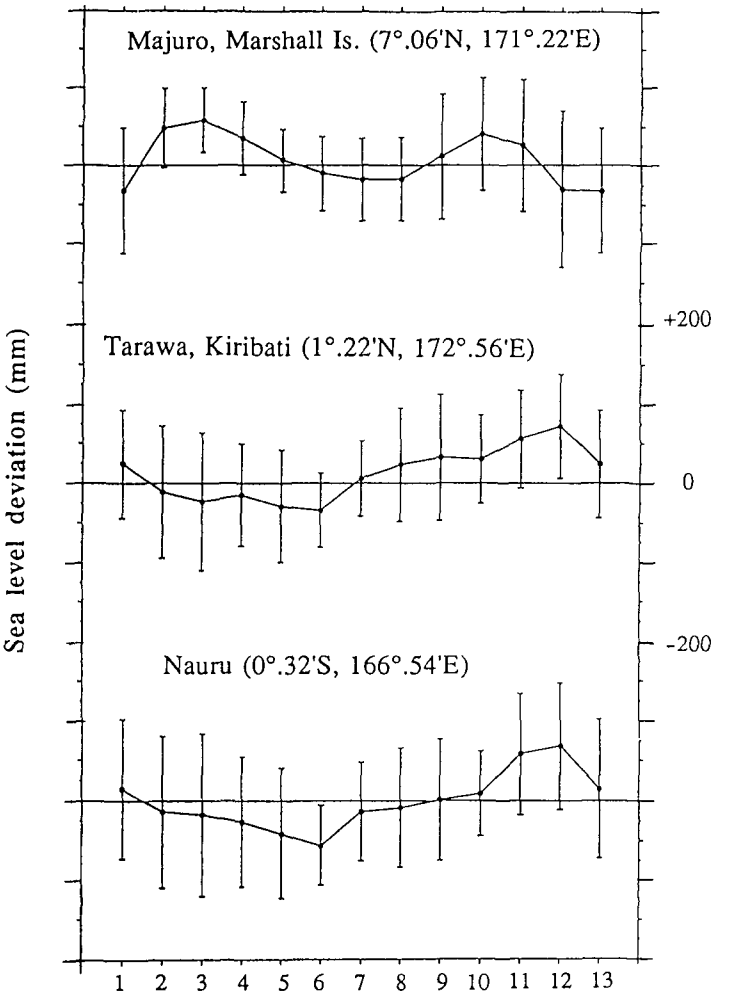

Figure 7 a

Seasonal sea level and standard deviations of the monthly mean sea levels for the period 1975-1994 at Nauru (0°.32'S), Tarawa (1°.22'N, Kiribati), Majuro (7°.06'N, Marshall Is.). Reference: MSL 1975-86. Data source: University of Hawaii Sea Level Center (UHSLC).

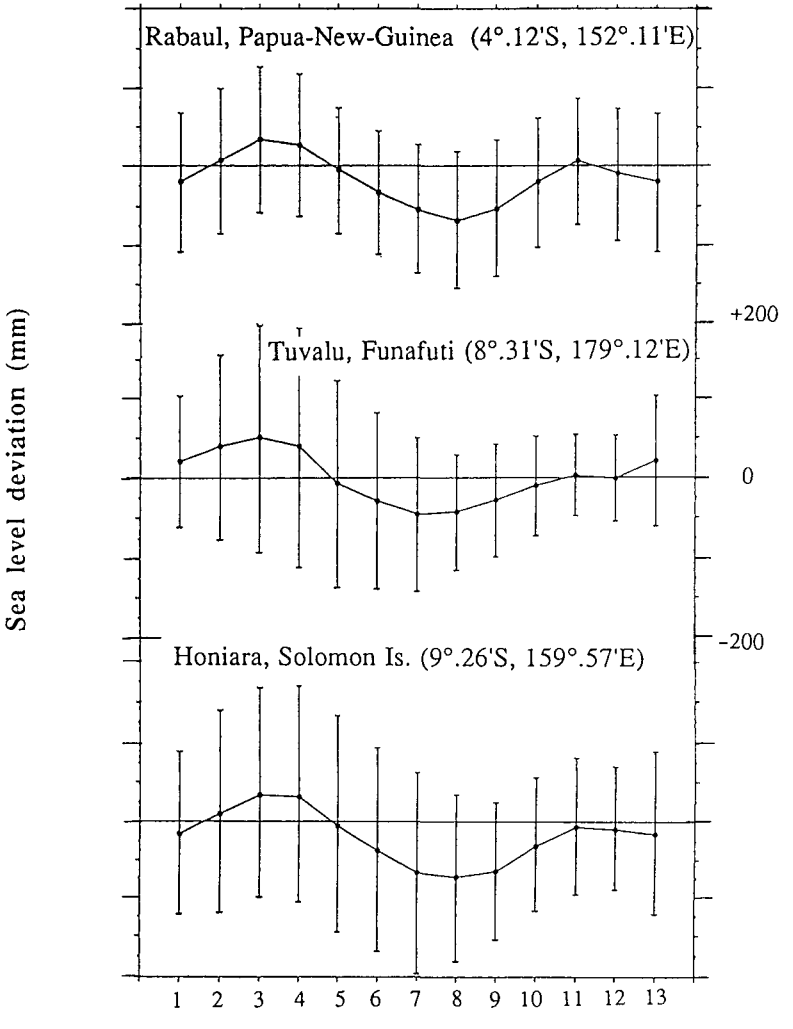

Figure 7 b

Seasonal sea level and standard deviations of the monthly mean sea levels for the period 1975-1994 at Honiara (9°.26'S, Solomon Is.), Funafuti (8°.30'S, Tuvalu) and Rabaul (4°.12'S, PNG). Reference: MSL 1975-86. Data source: UHSLC.

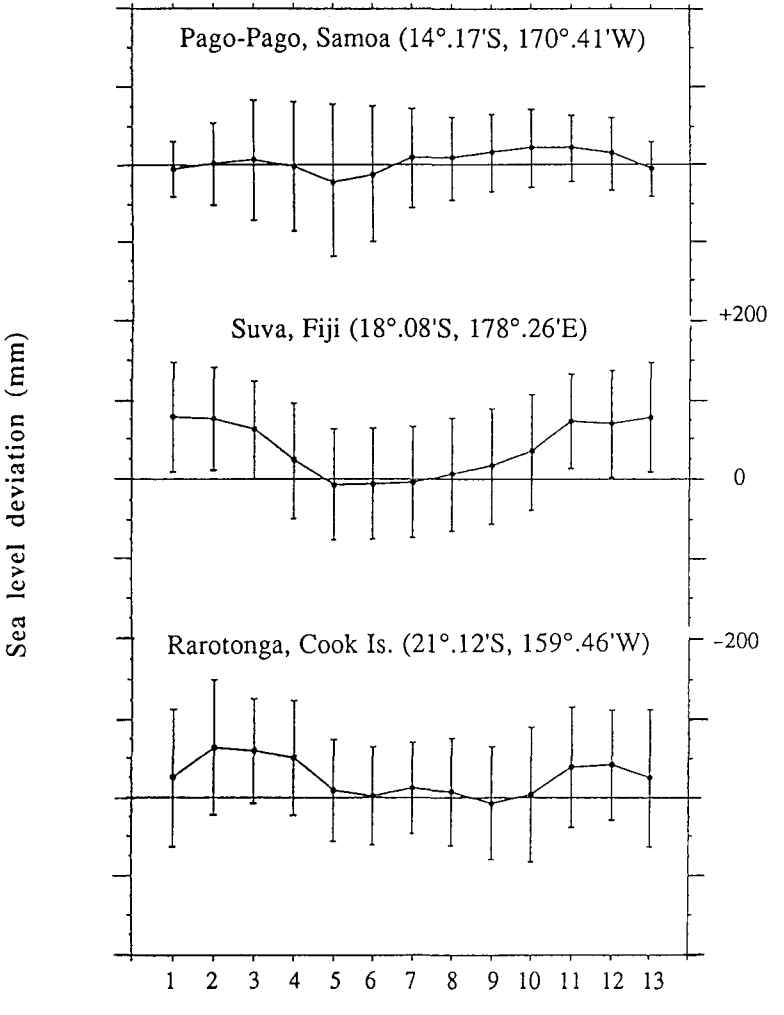

Figure 7 c

Seasonal sea level and standard deviations of the monthly mean sea levels for the period 1975-1994 at Rarotonga (21°.12'S, Cook Is.), Suva (18°.08'S, Fiji) and Pago-Pago (14°.17'S, American Samoa). Reference: MSL 1975-86. Data Source: UHSLC.

The monthly mean sea level deviations at Rarotonga and Suva for the period 1975-94 are similar and practically always positive. This is an artifact due to a too low reference level at both stations. Examination of the two series over the period 1975-1994 shows that after the period 1975-86 chosen as a reference, sea levels were significantly higher after 1986 (see below, section 4). We do not observe such a positive trend at Pago-Pago, close to the South Equatorial Ridge, lying at about 15°S. The trends observed at Suva and Rarotonga are not due to a southward move of the gyre after 1986, because such a move would have created a negative trend at Pago-Pago, not observed.

3.2 The seasonal cycle of the heat content, steric height and dynamic height in the western tropical Pacific

Relying upon the historical data of the 1994 World Ocean Atlas (NOAA Atlas, Levitus and col., 1994), a revised and expanded version of the 1982 Levitus' climatological atlas (Levitus, 1982), seasonal variations of the heat content, steric height and dynamic height, to the west of 160°W, were studied at each site, as close as possible to each Island where a SEAFRAME sea level station operates.

The 1994 World Ocean Atlas provides 0-1000 m monthly temperature and salinity profiles T(z) in °C and S(z) in psu (practical salinity unit) at standard levels, on a one degree latitude-longitude grid. The twelve 0-1000 m T(z) and S(z) monthly profiles in the vicinity of each island where a SEAFRAME sea level station is operated were extracted from the Atlas, plotted and corrected from obvious errors, when it was necessary and possible.

The **heat content H_c (Joules/m^2)** of a water column H is defined as:

$$H_c = \sum_{0}^{H} \rho . C_p . T . Dz \qquad (2)$$

where ρ (S,T,p) is the density (kg/m^3), C_p the specific heat (Joule. kilogram^{-1}.Kelvin^{-1}), p the pressure in Pa, T is the temperature in °C, and Dz is a 10 m thick slab of water.

After further verifications based upon T/S diagrams, T(z) and S(z) were linearly interpolated between the 19 standard depths (0, 10, 20, 30, 50, 75, 100, 125, 150, 200, 250, 300, 400, 500, ..., 1000 m) to get a regular 10 m vertical grid (101 levels after interpolations).

The equation of state of sea water ρ (S,T,p) and specific heat C_p (S,T,p) were computed along these 10 m vertical grids (formula in Siedlers Peters, Landolt-Bornstein New Series, V3, 247-248).

Errors in the seasonal heat content arise from errors in temperature (dT = 0.1°C) and depth (dD = 5 m) measurements (the errors in density and in specific heat are negligible by comparison). The estimated error in heat content of a 1000m deep water column is about 0.80 x 10^9 J/m^2.

Monthly **steric sea level anomalies (m)** were computed in various layers of the upper ocean, up to a depth of 1000 m. For example, the steric sea level in the upper 500 m of the ocean is given by :

$$\zeta_{steric} = -\frac{1}{\rho_0}\left(\int_{-500}^{0} \frac{d\rho}{dT} T' dz + \int_{-500}^{0} \frac{d\rho}{dS} S' dz\right) \qquad (3)$$

where T' and S' are the monthly temperature and salinity deviations in reference to their climatic annual mean values, ρ is the density and ρ_0 the sea surface density. The total steric changes ζ_{steric} arise from temperature (ζ_T) and salinity (ζ_S) variations, and $\zeta_{steric} = \zeta_T + \zeta_S$. The steric sea level change due to a temperature change T' (salinity change S'), in a slab of water Dz, depends on the thermal expansion coefficient α (salinity contraction coefficient β), according to:

$$\zeta_T = \alpha \, . \, T' \, . \, Dz \qquad (4a)$$
$$\zeta_S = -\beta \, . \, S' \, . \, Dz \qquad (4b)$$

Changes in the steric sea level represent the effect of expansion (4a) and contraction (4b) of the water column due to changes in density profiles, consequences of variations in temperature and salinity.

Errors in steric sea level arise from errors in the temperature and salinity measurements, estimated to 0.1°C in T and 0.02 practical salinity unit in S. The expected error in steric height of a 1000 m deep water

column would be about 2.5 cm. In addition, the coarse vertical resolution due to the grid of the standard depths below 100 m introduces about a 1.0 cm error in steric height. Finally, the choice of a 1000 m thick water column results in a loss of about 10% of the steric signal amplitude in the western equatorial Pacific. Adding all these errors results in a total error in the calculated steric sea level of about 3.5 cm. From (3), the seasonal variations of the steric sea level was computed for the upper 1000 m of the ocean in each area and have generally an amplitude of about 5 cm.

The **dynamic heights** (or geopotential thickness, unit $m^2.s^{-2}$) are simply the steric heights ζ_{steric} (3) scaled by the factor gravity g (g=9.8 $m.s^{-2}$).

The task of establishing the seasonal cycles of heat content, steric sea level and dynamic height was carried out in the eleven areas involved in the South Pacific Project, each area being representative of the large scale ocean structure near the corresponding SEAFRAME station (see the map of the locations of the SEAFRAME stations in the appendix and the T/P-derived mean sea surface topography on figure 14). For brevity, only four areas will be described here, fairly representative of the eleven areas. The four areas were selected as follows (below, in bold characters): (1) three areas situated within 10° of the equator and (2) one area in the south Pacific subtropical gyre.

Excepted in the areas of the Cook Is. and the Tongas, a salinity maximum always appears in the salinity profiles between 100m and 200m (Fig. 8b). This salinity maximum is within the equatorial thermocline, increasing from about 34.75 psu in the Marshall area to about 36.00 psu in the areas of Tuvalu and the Western Samoas. In all areas, except the Marshall Is. area, a salinity minimum appears clearly between 600m and 800 m, in relation to the Antarctic Intermediate Water, spreading into the Solomon and Bismarck Seas.

(1) Areas situated equatorward of 10° latitudes

Majuro (7°.07'N, 171°.22'E; Marshall Is.), on the southern edge of the north Pacific subtropical gyre; **Tarawa** (1°.22'N, 172°.56'E; Kiribati), in the equatorial trough, is representative of Nauru (0°.32'S, 166°.54'E) and

Manus Is. (2.02'S, 147°.23'E; Papua-New-Guinea). Situated near the ridge of the south Pacific subtropical gyre, **Funafuti** (8°.30'S, 179°.13'E; Tuvalu) will represent Honiara (9°.26'S, 159°.57'E; Solomon Is.).

Within 10° latitudes, the T (z) profiles (Fig. 8a) are characterized by high sea surface temperatures all the year round (28°-30°C) and a strong thermocline about 150 m thick, deepening from north (150m, area of Marshall Is.) to south (200m, area of Tuvalu).

(2) Areas situated poleward of 10°S

The main features of the seasonal cycles at **Nuku'alofa** (21°08'S, 175°11'W; Tonga) will be used to describe the cycles at Apia (13°.49'S, 171°.45'W; Western Samoa), Lautoka (17°.36'S, 177°.26'E; Fiji), Port Vila (17.46'S, 168°.17'E; Vanuatu) and Rarotonga (21°.12'S, 159°.47'W; Cook Is.), all sites situated within or close to the south western Pacific subtropical gyre (Fig. 14).

In the Cook Is. and Tonga areas, situated on the southern rim of the gyre, salinities are nearly constant in the upper 300 metres and the tropical thermocline is thicker than 500m all the year round. Within the south Pacific subtropical gyre, the thermocline is about 400m thick, between 100m and 500m, and the seasonal variations in the T(z) and S(z) profiles increase in the 0-100m layer from northern to southern areas.

Problems arise from significant errors in these T(z) and S(z) profiles (Fig. 8a and 8b), and in particular many errors were detected in the salinity files. It is obvious from these figures that the salinity profiles were more "noisy" than the temperature ones, with salinities often outside the ranges of 1-2 standard deviations from the mean in historical salinity profiles. Figure 8b gives evidence of a suspicious scattering in the 12 monthly salinity profiles, in contrast with the more homogeneous temperature profiles. For example, inspections by using the T/S diagrams confirm that the salinity profiles of April (Marshall) and October (Tuvalu) are certainly wrong, but there are no means to correct them. Consequently, the salinity part of the steric sea level is erroneous for these two particular profiles and were deleted. Other errors were unfortunately too numerous to be addressed, and the results are presented as preliminary results, as imperfect as they are.

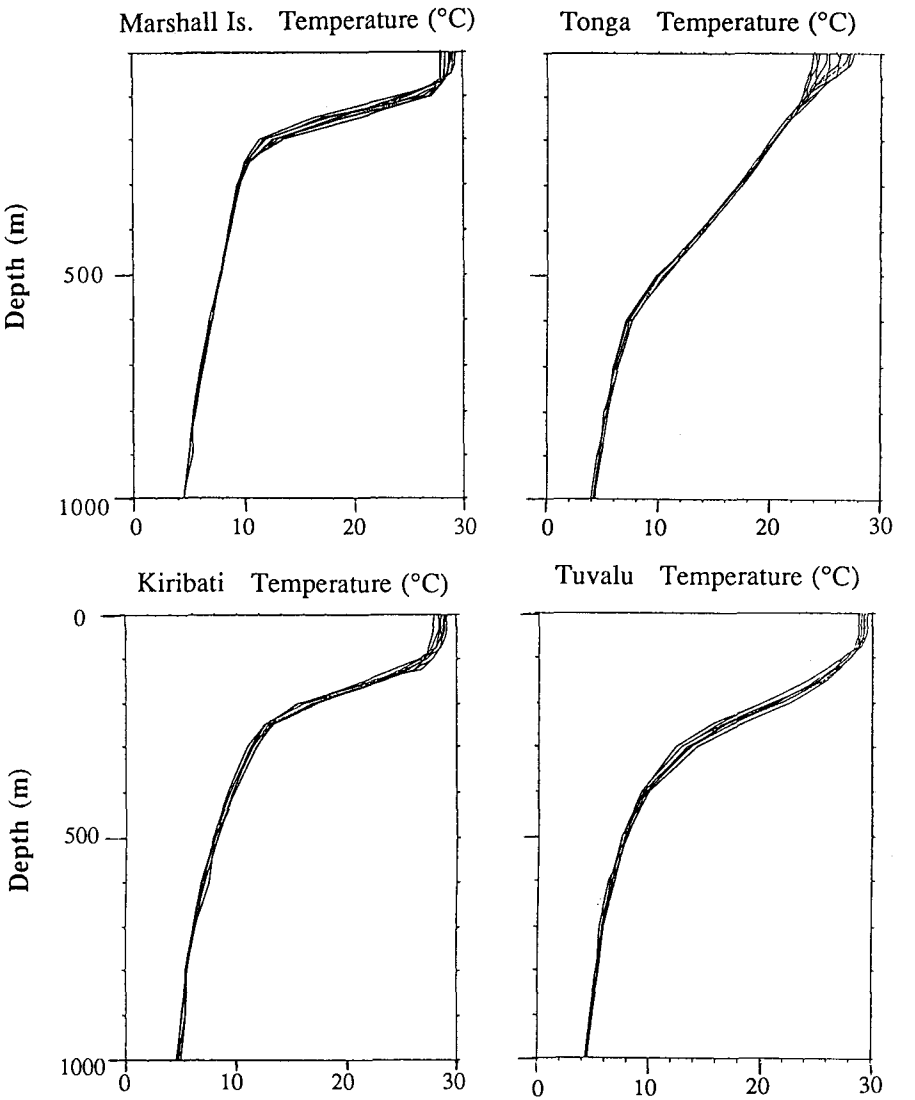

Figure 8 a

The twelve monthly T(z) profiles in the vicinity of Majuro (Marshall), Tarawa (Kiribati), Funafuti (Tuvalu) and Nuku'alofa (Tonga). Source of data: World Ocean Atlas, 1994.

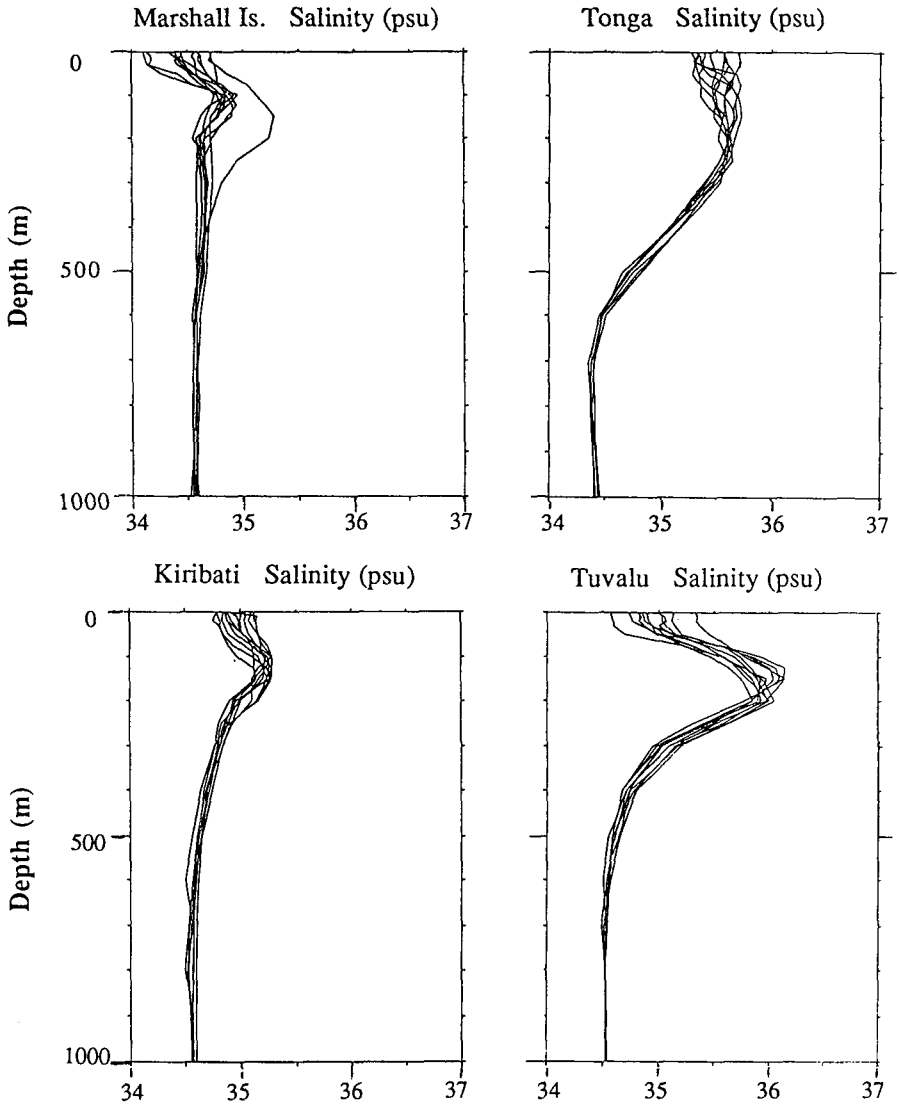

Figure 8 b

The twelve monthly S(z) profiles in the vicinity of Majuro (Marshall), Tarawa (Kiribati), Funafuti (Tuvalu) and Nuku'alofa (Tonga). Source of data: World Ocean Atlas, 1994.

Because the dynamic height (or geopotential thickness) seasonal cycles are nearly identical to the steric height cycles, they are not shown here. The monthly heat contents and steric sea level anomalies were computed for a 0-1000 m water column, and the annual ranges were found between 1 and 2 (10^9 Joules/m^2) and 7 and 12 cm, respectively, above the thresholds of their estimated errors ($0.8x10^9$ Joules/m^2 and 3.5 cm). Steric sea level annual ranges were as follows (all in cm): Majuro (12.3), Tarawa (8.8), Nauru (9.2), Manus Is. (10.3), Honiara (12.8), Tuvalu (15.9), Apia (7.0), Lautoka (7.2), Rarotonga (7.5), Port-Vila (12.2) and Nuku'alofa (8.8).

The seasonal cycles of the heat content Hc (Fig. 9) and steric sea level ζ_{steric} (Fig. 10) shown in the four selected areas have minima in July-September and maxima in January-April and again in October-November.

The ranges of the annual cycle of the mean sea levels at the nine "Hawaiian" tide gauges described in figure 7 were larger at the six stations within 10° latitudes of the equator (Majuro (9.0 cm), Tarawa (10.6 cm), Nauru (12.4 cm), Rabaul (10.2 cm), Honiara (10.7 cm) and Tuvalu (9.7 cm)) than at the three stations situated in the south Pacific subtropical gyre: Pago-Pago (4.3 cm), Suva (8.5 cm) and Rarotonga (7.1 cm). Majuro, Rabaul, Honiara and Tuvalu have maximum sea levels in March (end of the southern summer) and minima in July-August (southern winter). Tarawa and Nauru have maxima in December and minima in June. The annual cycle at Pago-Pago is barely perceptible, while the annual sea level cycles at Suva and Rarotonga are similar (maxima in February and November, and minima in May-September).

The hydrography-derived annual cycles are in reasonable agreement with the sea level annual cycles observed with tide gauges, although there are obvious discrepancies due to the above-mentioned problems (see for example Kiribati and Tuvalu). Those discrepancies with the observed sea level annual cycles shown in figure 7 are not surprising due to errors in the upper 1000m profiles and also considering the fact that the observed sea levels concern the total water column, about 4 km deep. Due to the actual state of the historical hydrography data, it is not appropriate to discuss further the intercomparisons, since such a process would require the scrutiny of individual temperature and salinity profiles in each area, a task not possible to complete in this format.

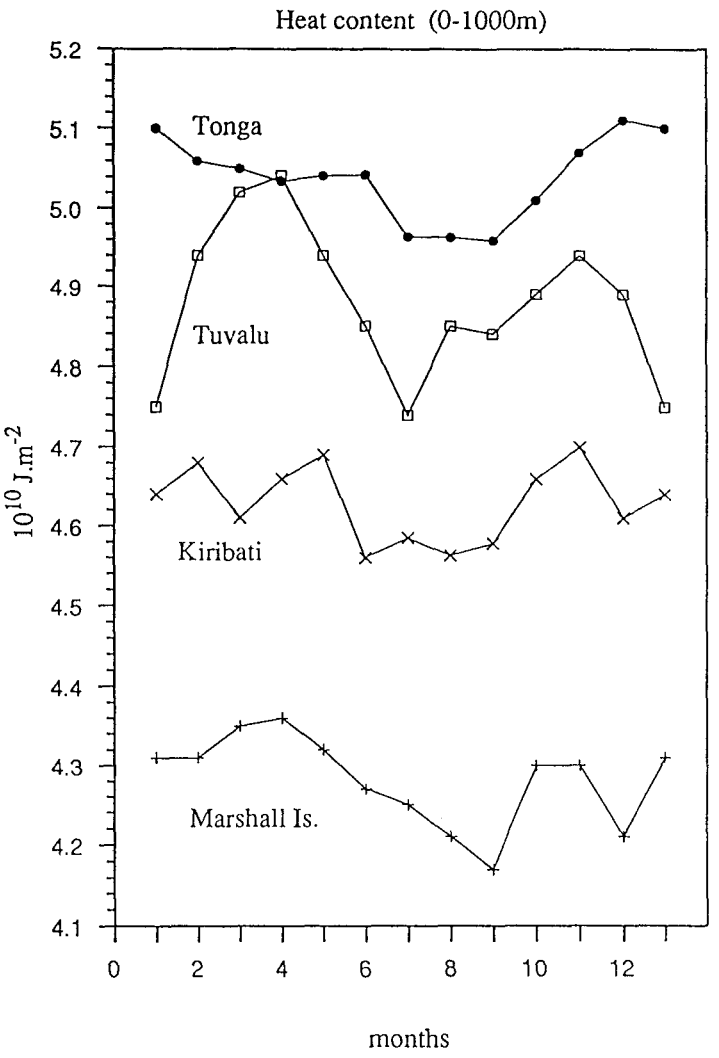

Figure 9

The heat content seasonal cycles in 10^{10} Joules/m^2 computed for the upper 1000 m of the ocean in the vicinity of Majuro (Marshall), Tarawa (Kiribati), Funafuti (Tuvalu) and Nuku'alofa (Tonga).

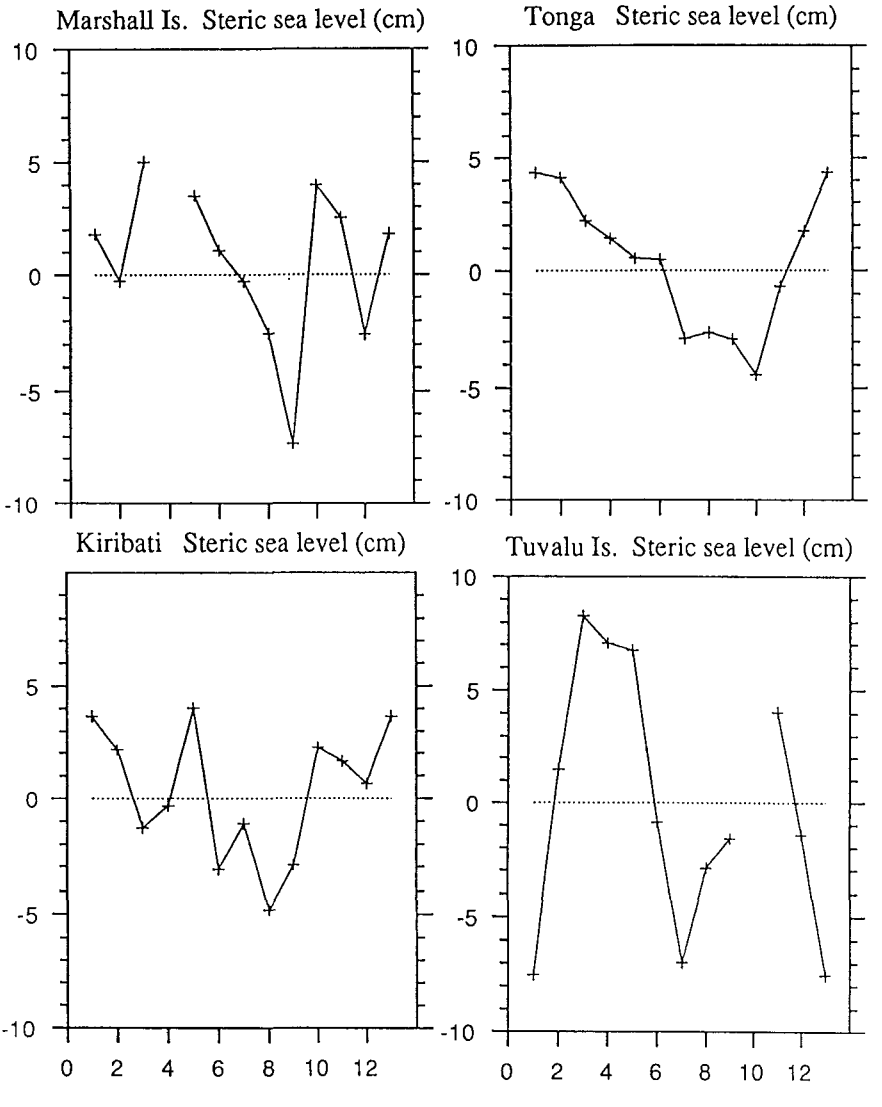

Figure 10

The seasonal cycles of the steric sea level in cm computed for the upper 1000 m of the ocean in the vicinity of Majuro (Marshall), Tarawa (Kiribati), Funafuti (Tuvalu) and Nuku'alofa (Tonga).

4. Interannual Sea Level Changes and Trends in 1975–1998

4.1 The historical time series 1975–94

The 1975-1994 monthly sea level deviations (in mm) provided by the Hawaiian Sea Level Center, relative to 1975-86, are presented in figure 11 for the nine closest sites of the correspondent SEAFRAME sites. The monthly values are calculated from the daily values with a simple average of all the daily sea levels in a month. Daily sea levels are obtained from detided hourly sea level data (Caldwell, 1998). During the twenty year period 1975-1994, five El Niño events occurred (Fig.6), in 1976-77, 1982-83, 1986-87, 1991-92 and 1992-93 (in figure 11, the El Niño years are underlined); three La Niña events were observed in 1975-76, 1978 (weak), and 1988-89. All the estimates of the secular trends at these stations are based on about twenty yearly averages.

GROUP I: Nauru (0°32'S), Tarawa (1°22'N, Kiribati); Majuro (7°07'N, Marshall I.), figure 11 a.

On the two records of Nauru and Majuro, the El Niño events appear as unusual low sea levels, as observed in 1976-77, and very unusual low sea levels in 1983 and 1992. But no such signal appeared in 1993. The low sea level (-11.8 cm) in June 1981 at Nauru seems to be part of the seasonal cycle, within one standard deviation, as shown in figure 7 a. The sea level deviation of -6.6 cm in June 1981 at Kapingamarangi (1° 06'N, 154° 47'E), the closest station, is normal and does not correspond to an El Niño signal as well (no data at Tarawa at this time, and no signal at Majuro). Although the Tarawa series suffer from many gaps, the synchrony of the three records at the seasonal and interannual time-scales is noteworthy.

Using the yearly mean sea level time series from 1975 to 1993 (19 years), the trends were negative at Nauru (-1.0 mm/y) and positive at Tarawa (+3.2 mm/y) and Majuro (+2.0 mm/y).

GROUP II: Honiara (9° 26'S, Solomon I.), Funafuti (8° 30'S, Tuvalu); Rabaul (4° 12'S, PNG), figure 11 b.

The three 19-year records (only 16 years at Funafuti) display a nearly perfect synchrony. Particularly evident are the unusual low sea levels in 1977, 1983, 1987, 1992 and 1993, corresponding to the five El Niño of 1976-77, 1982-83, 1986-87, 1991-92 and 1992-93. Superimposing the three records, nearly every high and low sea level at one station matches

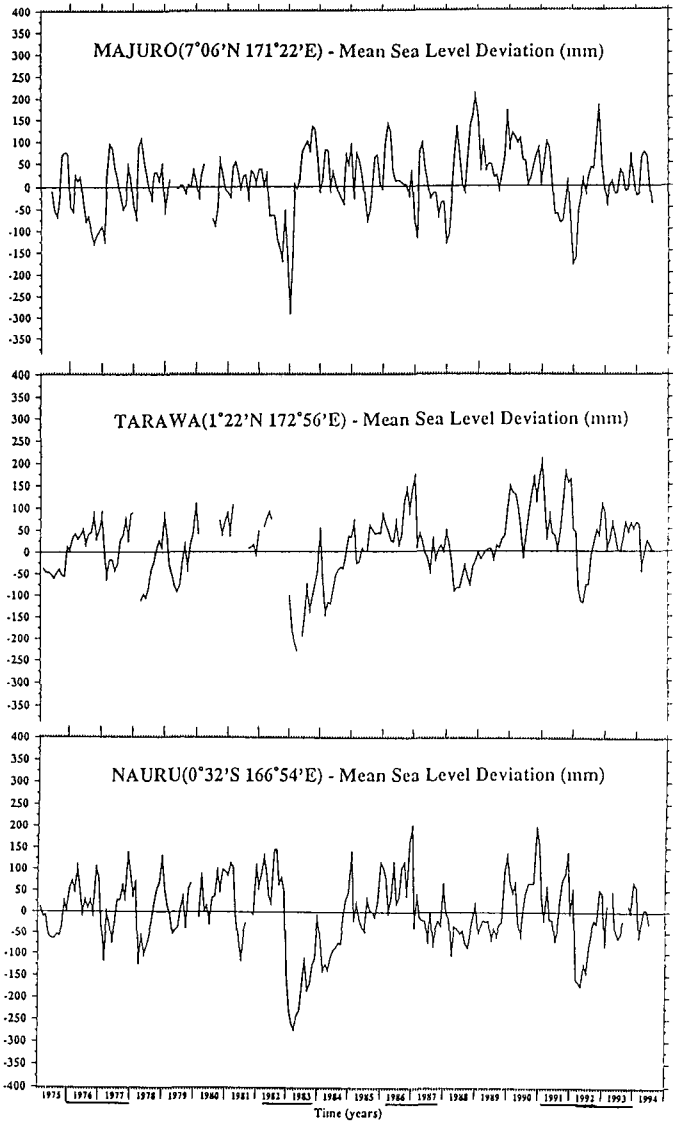

Figure 11a

The 1975-1994 sea level deviations, relative to 1975-86, at Nauru, Tarawa (Kiribati), Majuro (Marshall Is.). Data source: UHSLC.

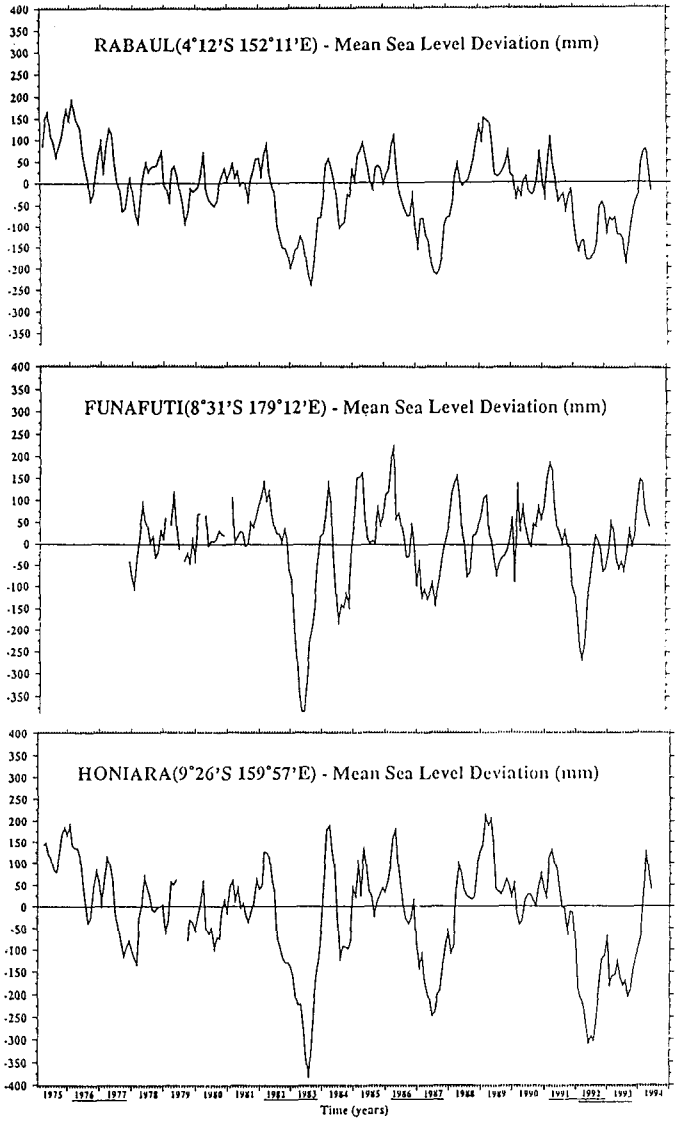

Figure 11b

Same as figure 11a, at Honiara (Solomon Is.), Funafuti (Tuvalu), Rabaul (PNG). Data source: UHSLC.

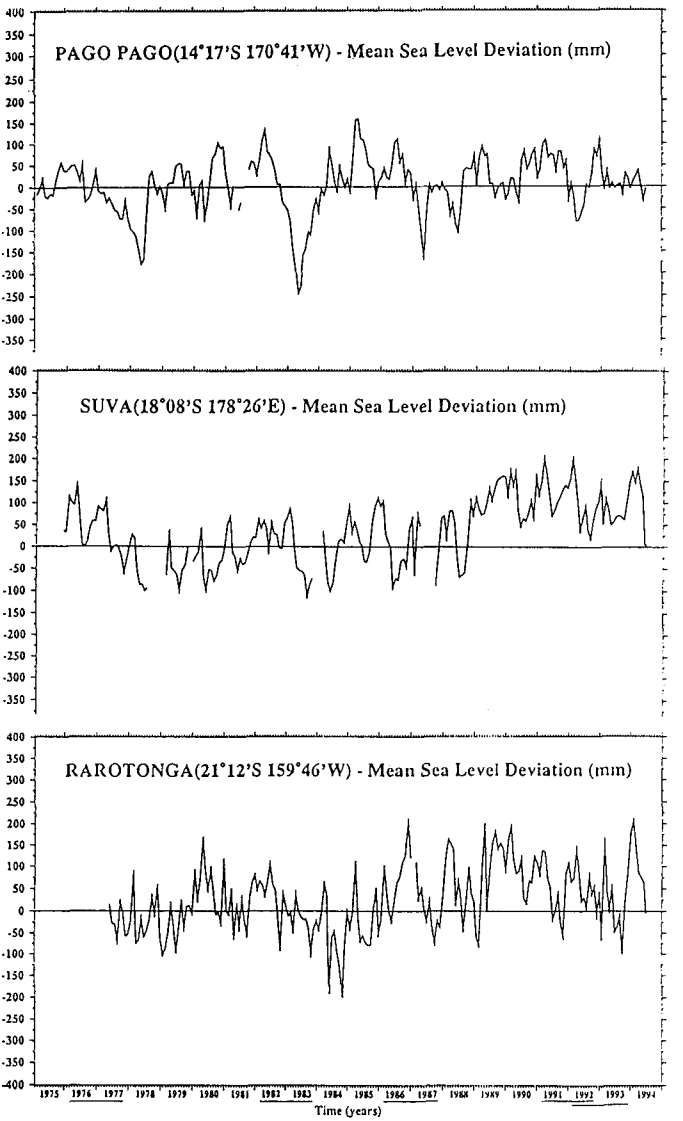

Figure 11c

Same as figure 11a at Rarotonga (Cook Is.), Suva (Fiji) and Pago-Pago (American Samoa). Data source: UHSLC.

the other two, throughout the whole period of observation. The maximum negative sea level deviations were observed in 1983 (-38 cm at Funafuti and Honiara in June and July, respectively; -24 cm in August, at Rabaul). A strong negative signal occurred simultaneously at the three stations in July 1984, within the range of the seasonal cycle (Fig. 7b), not related to an El Niño event.

The Honiara record (9°26'S, 159°57'E) is representative of the band 4°S-9°S west of the date line, and illustrates the strong negative deviations in the western Pacific during the above mentioned five El Niño events: -12 cm in 1977, nearly -38 cm in July 1983, -25 cm in June 1987, -30 cm in July-August 1992, surprisingly followed by a -20 cm deviation in August 1993. These changes give a measure of the sea level signature of El Niño. In the warm pool area as well as in the region of the South Pacific subtropical gyre, ENSO-related sea level changes may easily obscure any secular sea level rise, with sea level anomalies up to ±40 cm.

The sea level trends computed on the period 1975-93 are all negative, at Honiara (-6.5 mm/y), Funafuti (-1.0 mm/y) and Rabaul (-6.3 mm/y).

GROUP III: Rarotonga (21° 12'S, Cook I.), Suva (18° 08'S, Fiji) and Pago-Pago (14° 17'S, American Samoa), figure 11 c.

The 1975-94 deviations at Suva and Rarotonga are mostly positive after 1985, suggesting that the 1975-86 reference is too low. This bias appears in the seasonal cycles as described precedently. This impression is also supported by comparing the record at Suva with Pago-Pago.

No El Niño signal appears either at Suva or at Rarotonga. The 1975-94 deviations at Suva were positive first for 18 months, starting in November 1975, then after September 1988 for nearly 6 years. At Rarotonga, the observations started in May 1977, and sea levels were significantly higher during the 9-year period 1986-1994 than during the 9-year period 1977-1985. Therefore, both records of Suva and Rarotonga could give clues about a very low frequency climatic oscillation or a climatic trend. On the Pago-Pago record, unusual low sea level deviations were observed in May-June 1983 and May 87, probably related to the El Niño, but the minimum in March-April 1992 is within the seasonal range (Fig. 7c). The minimum in May-June 1978 and June 1988 appears as part of an enhanced seasonal cycle, during La Niña years.

Estimates of the sea level trends at Rarotonga (1977-93), Suva (1976-93) and Pago-Pago (1975-93) are all positive: +5.4 mm/y, +7.5 mm/y, and +2.1 mm/y, respectively.

In summary, during the 19-year period 1975-94, negative trends (all given in mm/yr) were observed at Nauru (-1.0), Rabaul (-6.3), Honiara (-6.5) and Funafuti (-1.0); and positive trends appeared at Tarawa (+3.2), Majuro (+2.0), Rarotonga (+5.4), Suva (+7.5) and Pago-Pago (+2.1).

4.2 The 1992-98 sea level trends at the SEAFRAME stations

The eleven SEAFRAME monthly mean sea level time series of the South Pacific sea level project were plotted (Fig. 12) from the start of each station (in 1992-93 for most of them) to January 1998 (locations and starting time of each station given in the appendix). Monthly mean sea level values are obtained from the detided hourly values, with a simple average of all the hourly values in a month (for example, the mean sea level in January is the average of 744 detided hourly values, etc.).

The sea level trend at each SEAFRAME station was computed for each continuous time series, without taking the liberty of filling the gaps when more than two months of data were missing consecutively (Fig. 12). The annual cycle was not discernible at the three stations situated within 2° of the equator (Manus Is., Nauru and Tarawa).

GROUP I: Manus (2°02'S, PNG), Nauru (0°32'S), Tarawa (1°22'N, Kiribati); Majuro (7°07'N, Marshall I.), figures 12 a, b, c, d.

A major sea level drop occurred at the four stations, starting in Feb-March 1997, due to strong westerlies (Fig. 13). At Manus Island (Fig. 12a), two opposite trends were observed, one positive (+130 mm/yr over 8 months) and one negative (-168 mm/yr, over 23 months). Only the 23 month time series from March 1996 to January 1998 is of significance (the first series of 8 months of data in 1994-95 is too short to give a reliable estimate) and the negative trend of -168 mm/y is essentially due to the decrease in sea level from February 1997 to January 1998. At Nauru (Fig. 12b), two series were studied, giving also totally different estimates: +75mm/y over 18 months (1993-94) and +5.5 mm/y over 33 months (May 1995-Jan 1998), opposite to the 1975-94 trend (-1.0 mm/y).

The two other stations (Majuro and Tarawa, Fig. 12c and 12d) indicate negative sea level trends of -6.6 and -18.7 mm/y, in contrast to the positive 1975-94 trends, essentially due to a strong decrease in sea level from March 1997 to January 1998. Examination of the monthly Pacific sea level maps delivered by the Sea Level Center (University of Hawaii) corroborates this drop of about 35-40 cm in the western equatorial Pacific, related to the very strong 1997-98 El Niño.

GROUP II: Honiara (9° 26'S, Solomon I.), Funafuti (8° 30'S, Tuvalu); figures 12 e, f.

The drop of about 20 cm observed at Honiara in August 1993 (see above Fig. 11b) is confirmed by a similar drop observed at Funafuti by the SEAFRAME station (Fig. 12f). Again, we observe a very significant drop in sea level from March 1997 to January 1998 at both stations, although the trends are opposite at the two stations: A negative trend of -17 mm/y over 43 months is detected at Honiara (Fig. 12e), whereas at Funafuti a very weak positive trend of +0.4 mm/y over 59 months is not significant.

GROUP III: Port-Vila (17°46'S, Vanuatu), Lautoka (17°36'S, Fiji), Nuku'alofa (21°08'S, Tonga), Apia (13°49'S, W. Samoa) and Rarotonga (21° 12'S, Cook I.), figures 12 g, h, i, j, k.

The sea level drop observed within the equatorial band ±10° in the western Pacific, and related to the very strong 1997-98 El Niño, was not the dominant feature in the areas situtated within the south Pacific subtropical gyre. In contrast to the "equatorial" stations, the annual cycle appeared more clearly at the five southern stations, although a strong year to year variability was superimposed on it. All the five stations, situated south of 10°S, gave evidence of positive sea level trends: 14.6; 15.9; 26.0; 15.9; 7.2 mm/y, respectively. Estimates of the historical trends at Rarotonga (1977-93), Suva (1976-93) and Pago-Pago (1975-93) were all positive: +5.4 mm/y, +7.5 mm/y, and +2.1 mm/y, respectively. However, the present estimated trends over the 1993- Jan 1998 five-year period were significantly greater than during the 1975-94 period, and one order of magnitude larger than the estimated secular sea level rise. This is related to the warming of the south Pacific subtropical gyre during the years 1990-1998, associated with repetitive El Niño events occurring during this 9-year period (only the year 1996 was nearly "normal").

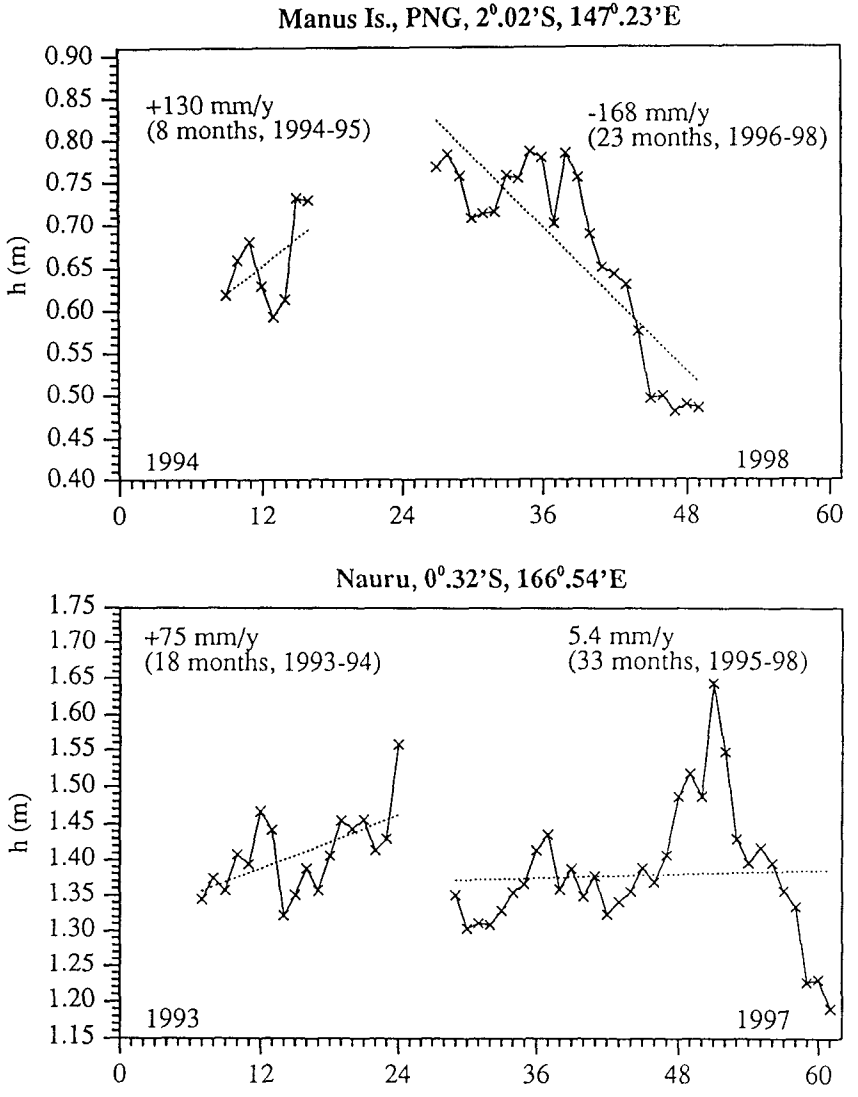

Figure 12

Estimates of the sea level trends at the SEAFRAME stations: **a)** Manus Is., PNG; **b)** Nauru. Data Source: National Tidal Facility, Australia.

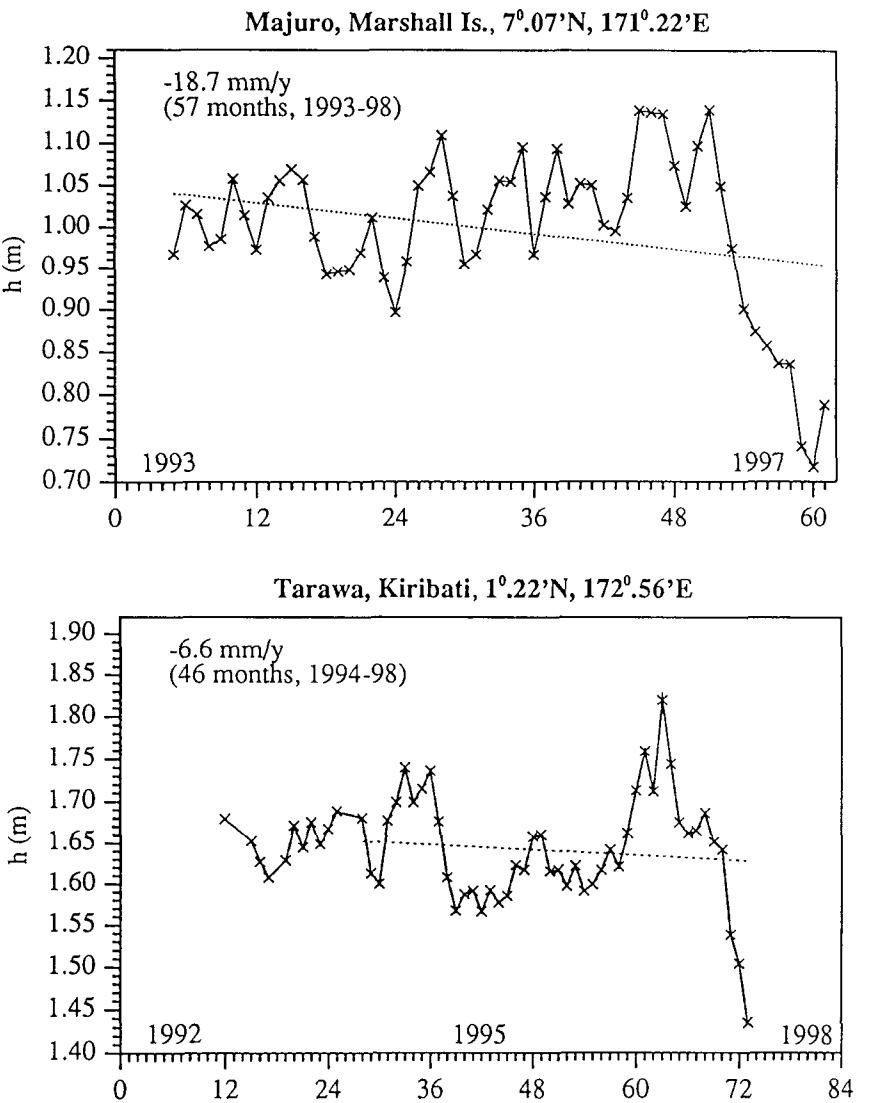

Figure 12

Estimates of the sea level trends at the SEAFRAME stations: **c)** Majuro, Marshall Is.; **d)** Tarawa, Kiribati. Data Source: NTF, Australia.

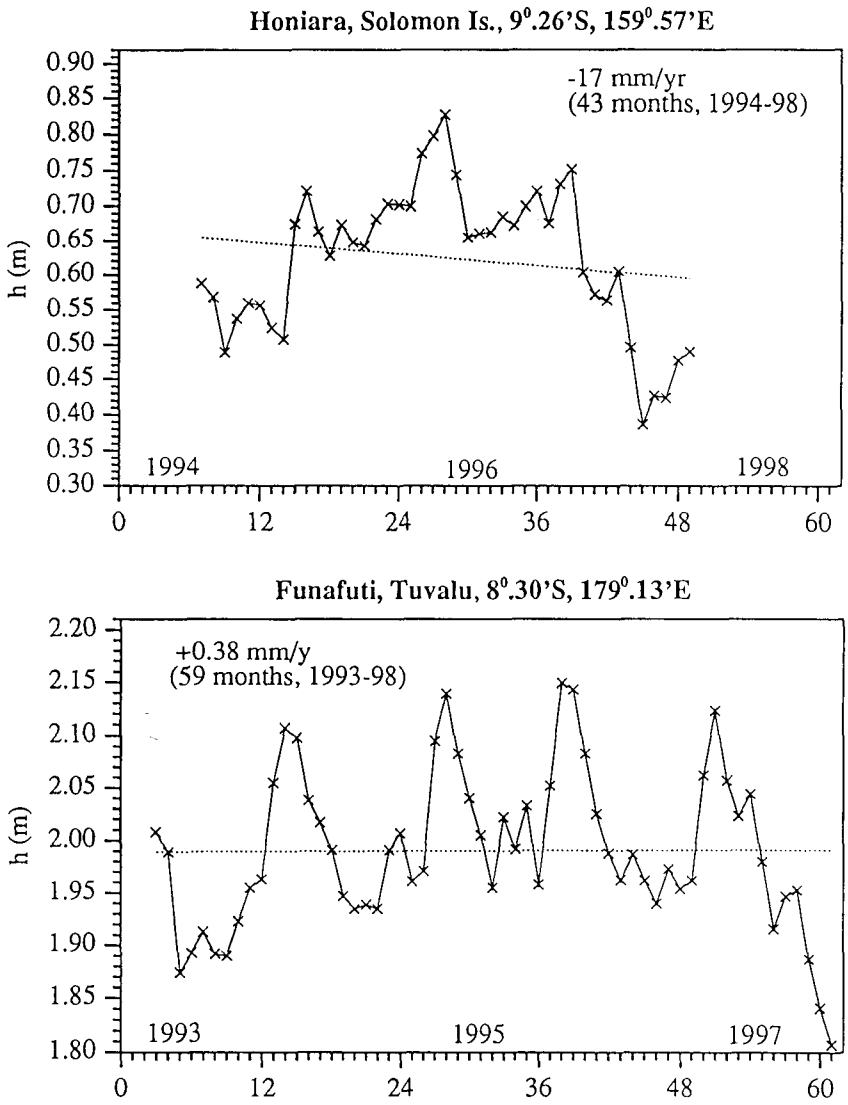

Figure 12

Estimates of the sea level trends at the SEAFRAME stations: e) Honiara, Solomon Is.; **f)** Funafuti, Tuvalu. Data Source: NTF, Australia.

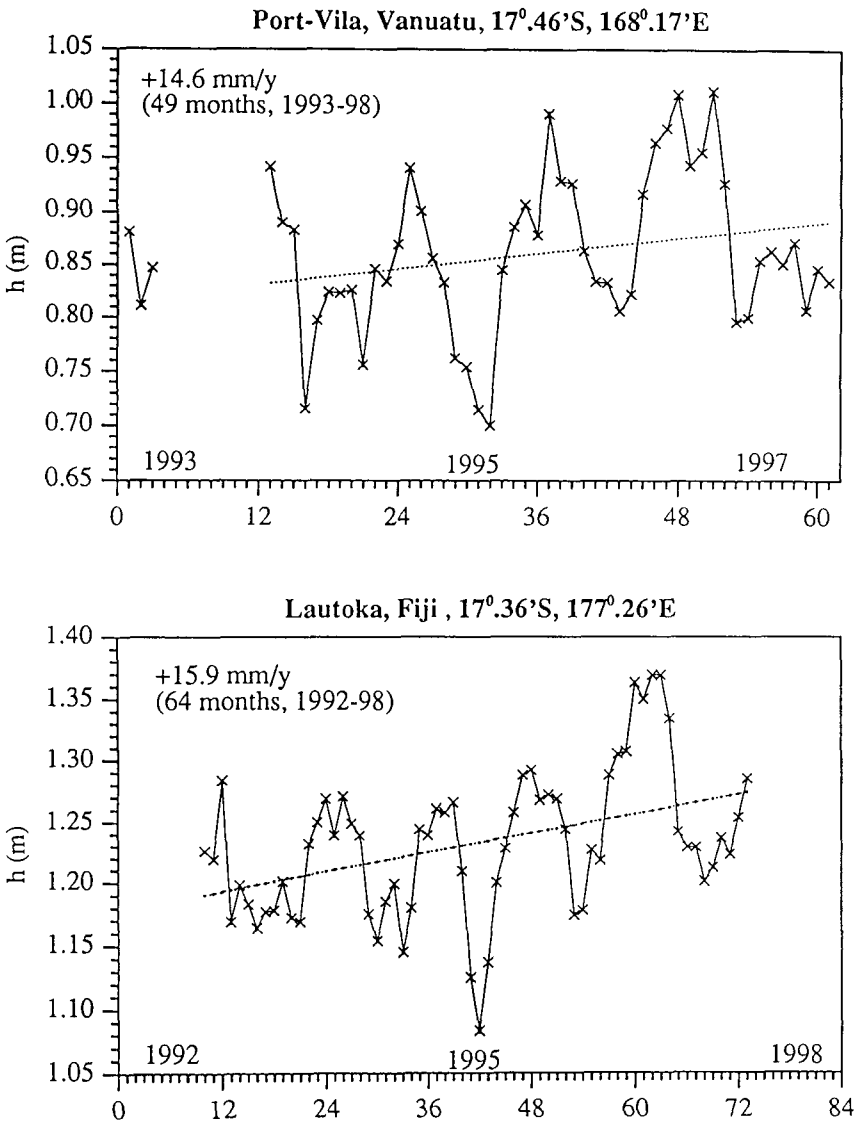

Figure 12

Estimates of the sea level trends at the SEAFRAME stations: **g**) Port-Vila, Vanuatu; **h**) Lautoka, Fiji. Data Source: NTF, Australia.

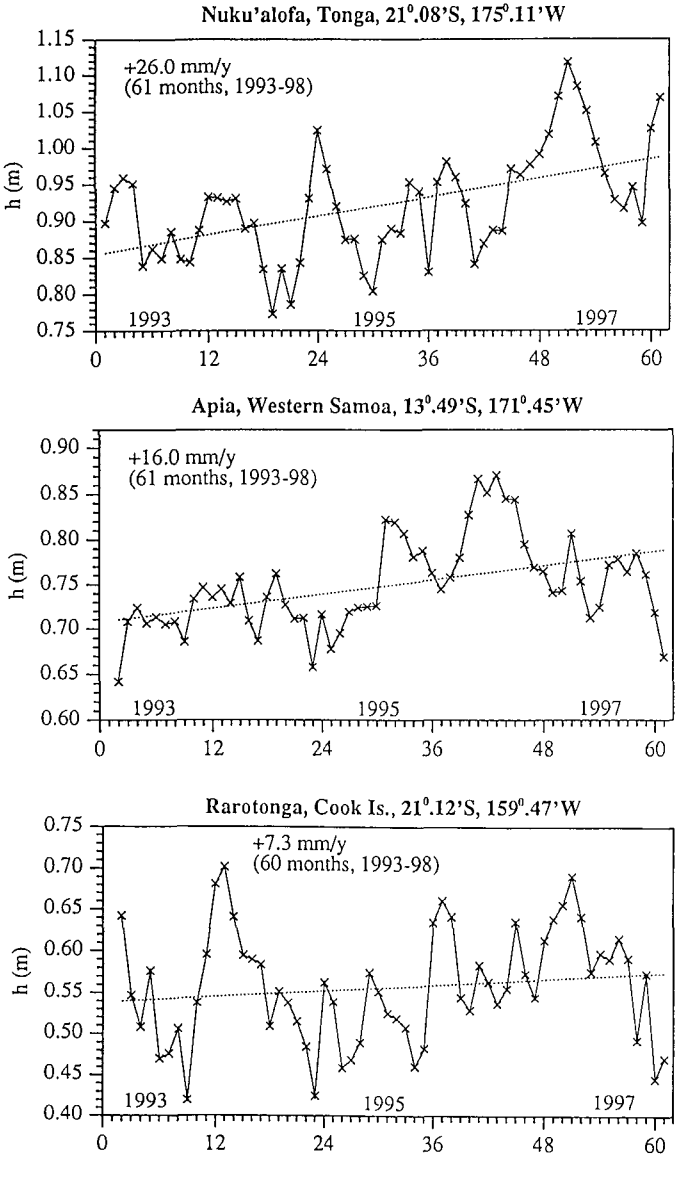

Figure 12
Estimates of the sea level trends at the SEAFRAME stations: **i)** Nuku'alofa, Tonga; **j)** Apia, W. Samoa; **k)** Rarotonga, Cook Is. Data Source: NTF, Australia.

5. The Pacific Sea Level Variability Observed by Topex/Poseidon

5.1 The zonal wind field observed by the TAO array (2°N-2°S)

Before presenting the T/P-derived maps of the sea surface topography and the analyses of the T/P ten-day sea level anomalies, it is necessary to give a brief overview of the zonal wind field in 1992-98, as observed between 2°N-2°S by the Tropical Atmosphere-Ocean (TAO) array (McPhaden, 1993; NOAA, Climate Diagnostic Bulletin).

In 1991, 1992, 1993 and 1994, the SOI was persistently negative (Fig. 6) and strong westerlies (wind and anomalies) were repeatedly observed in the western-central Pacific (McPhaden, 1993; in figure 13, the zonal wind field is shown for the period April 1993-Jan. 1999).

By August-September 1992 and again in November 1993-February 1994 the monthly SOI was near zero; however, the 1991-92, 1992-93 and 1993-94 El Niño were not over (Busalacchi et al., 1994). Until Jan-Feb 1995, the SOI was negative, but in March 1995 it became briefly positive, as well as in July-Aug-Sept 1995, and in November 95 again. With such vagaries of the atmospheric pressure gradient, the easterlies were weak and intermittent in 1995 (Fig. 13), and no La Niña occurred in 1995. Actually, during 22 months, from April 1995 to February 1997, the SOI began an irregular rise from negative to positive values, followed by a precipitous fall that was to last for four months (in Feb-June 1997), to reach finally record low values in March 1998 (-3.5). Then, within two months, the SOI switched to positive values in May 1998, reaching +2.0 in January 1999.

From April 1995 to February 1997, easterlies spred over the central-western equatorial Pacific (maxima larger than -6 m/s), and easterly wind anomalies greater than -2 m/s reached intermittently the far western equatorial Pacific (140°E) from July 1995 to October 1996 (Fig. 13). A weakening of the trade winds occurred in November 1996 and westerly wind anomalies greater than 2 m/s first appeared at 140°E-160°E in December 1996. Then, concomitant with the retreat of the trade winds in February 1997, westerlies and westerly wind anomalies strengthened at 135°E and migrated steadily eastward in 1997-98, reaching the far eastern equatorial Pacific (100°W) in April 1998.

The westerlies collapsed in December 1997 and weak easterlies prevailed until September 1998. Easterly wind anomalies first appeared in

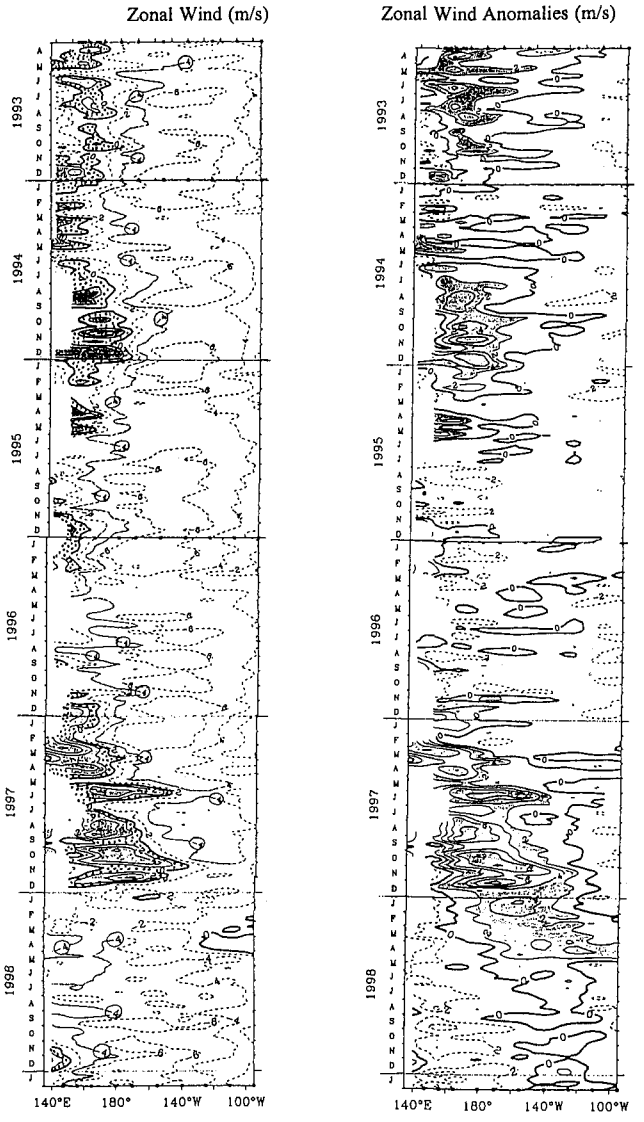

Figure 13. Time/longitude diagrams (April 1993-Jan. 1999) of surface zonal winds and their anomalies (both in m/s) from 5-day averages between 2°N-2°S of moored time series (Pacific TAO array). Squares indicate longitudes where the moorings operate. Dotted areas indicate eastward winds (westerlies), and dotted lines (-2, -4, -6 m/s) westward winds (easterlies). Zonal winds anomalies greater than +2 m/s are shaded. The thin continuous line joining the circles (-4 m/s) indicates the western limit of the trade winds. Adapted from the Climate Diagnostics Bulletin, McPhaden (NOAA/PMEL).

Nov-Dec. 1997 at 140°E and reached 160°W in December 1998 (Fig.13), switching the tropical Pacific climate system into a cold episode (La Niña) in July 1998. In summary, during the six-year period 1993-98, the trade winds reached 140°E only briefly in August 1996 and most of the year 1998. Westerlies were permanently observed at 140°E-160°E in 1993, 1994, most of the year 1995, and the whole year 1997.

5.2 The Topex/Poseidon sea surface topography

The T/P-derived mean sea surface topography showed on figure 14 for 1993-94-95 (Verstraete and Musiela, 1995; Musiela and Verstraete, 1996), is referenced to the Ohio State University OSU-91A geoid (Rapp et al., 1991). The T/P data were smoothed with a Gaussian filter with a radius of 1000km. The map gives evidence of a significant departure from the historic hydrography-derived Pacific sea surface topography (Wyrtki, 1974; Levitus, 1982; Kessler, 1989), both along the equator and at 10°-20° latitudes. According to the climatological zonal profiles obtained from the sea surface dynamic heights along the equator and at 10°-20° latitudes (Fig.3 and 5), the plateaux of maximum dynamic heights are to be observed to the west of 150°E (170°E) at 20°N (at 10°N), to the west of the date line at the equator, and to the west of 150°W both at 10°S and 20°S. Now, in the 1993-95 T/P-derived mean topography map, these plateaux were shifted by about 20°-30° to the east at 20°N, 10°N, 0°, and 20°S (Fig. 14). At 10°S, the T/P map shows a ridge from 150°E to 150°W, with two maxima at 160°E and 165°W. Also, the north and south Pacific tropical ridges, lying usually at 15°-17° latitudes at 180° (same references as above), were both shifted by about 5° northward. The south rim of the South Pacific subtropical gyre, which lies at about 25°S normally, was straddling 20°S (Fig. 14).

From the 1993-94-95 T/P-derived reference mean sea level, it is possible to compute sea level anomalies (SLAs or residuals), free of geoid errors (SLA= sea level X - mean sea level). The 1993 yearly residual map (not shown here) illustrated an El Niño situation, in relation to strong westerlies to the west of 180° (Fig. 13). Negative yearly sea level anomalies were observed in the western equatorial Pacific, greater than -4 cm to the east of PNG, consistent with the negative in situ sea level deviations at Rabaul, Funafuti and Honiara (see Fig. 11b and 12f).

In the central-eastern equatorial Pacific, the 1993 yearly sea surface topography anomaly was positive, with yearly anomalies greater than +2 cm as far as the Galapagos, and also consistent with the above mentioned eastward spreading of the south Pacific subtropical gyre.

The T/P yearly sea level anomaly for the year 1995 (T/P cycles 85-121, Fig.15 b) is in strong contrast with the monthly sea level anomaly for the period 13 January-12 February 1995 (T/P cycles 86-88, Fig.15 a), reflecting the occurrence of positive SOI values and stronger easterlies during the second half of 1995 (Fig. 6 and Fig.13). In Jan-Feb 1995, the sea level anomaly topography was typical of an El Niño situation, with lower (higher) anomalies than average to the west (east) of 180°. When the SOI became positive after July 1995, the equatorial sea level profile returned to its mean slope, with yearly positive anomalies to the west of 180° and yearly negative anomalies east of 180°.

The 1995 T/P-derived map of the yearly sea level anomalies gives evidence of positive anomalies distributed symetrically to the west of the date line with respect to the equator, at about 5°-10° latitudes, in contrast with the equatorially centered negative anomalies to the east of 180° (Fig.15 b). This distribution is in agreement with the meridional structure of symmetric Rossby waves and matches the annual harmonic of the wind stress curl structure, with two off-equatorial maxima to the west of 180°, at about 6° latitudes, and a uniform curl to the east. The annual phase of the wind stress curl is nearly uniform along the equator (Kessler, 1989).

Nota Bene:

Due to their format, and to facilitate their reading, the full legends of the figures 14, 15a and 15b are presented here in the text.

Figure 14

Topex/Poseidon-derived mean sea surface topography (cm) in 1993-94-95 (T/P cycles 11-121, 31 Dec. 1992 - 5 Jan. 1996). The reference is the Ohio State University "OSU91A" geoid. The positions of the South Pacific project sea level stations are indicated by black dots.

Figure 14 (continued)
The change in sea level along the equator, from the Galapagos (low sea levels) to 150°W (high sea levels) is about 60 cm. The sea surface elevation of both subtropical Pacific gyres (120 cm at 20°N, 160°E; 110 cm at 10°S,160°W) was about 60 cm higher than the sea surface along the Americas, between 20°N and 20°S. Note that along the equator as well as at 10°S-20°S, the slope is nearly zero from 150°W to 150°E. Data source: CNES-NASA.

Figure 15 a
The Topex/Poseidon monthly sea level anomaly (SLAs in cm) in January-February 1995 (T/P-cycles 86-87-88, period 13 January 1995 - 12 February 1995). Within 10° latitudes, note the large positive anomalies (+6 cm) in the central-eastern Pacific, and the strong negative anomalies (-6 cm) west of the date line, typical of an El Niño situation. Data source: CNES-NASA.

Figure 15 b
The 1995 T/P yearly sea level anomaly in cm (T/P-cycles 85-121, period 4 January 1995 - 5 January 1996). Positive SLAs, up to 5 cm, to the west of the date line, and negative SLAs east of the date line indicate a non-El Niño situation in 1995, from the El Niño situation observed in Jan-Feb 1995. Data source: CNES-NASA.

5.3 T/P equatorial ten-day sea level anomalies

T/P ten-day fields of sea level anomalies (SLAs) relative to the T/P-derived 1993-1995 mean sea level taken as a reference, were computed along the equator, at 5°N and 5°S, within one degree latitudinal bands, and between 140°E and and 80°W (Fig. 16, colour plates). The T/P data were smoothed with a Gaussian filter with a radius of 1000 km. Longitude-time plots of the SLAs from 3 October 1992 (T/P cycle 2) to 9 October 1996 (T/P cycle 149), show that the T/P altimeters captured very well the equatorial sea level planetary signals associated with the periods of westward and eastward zonal wind stress.

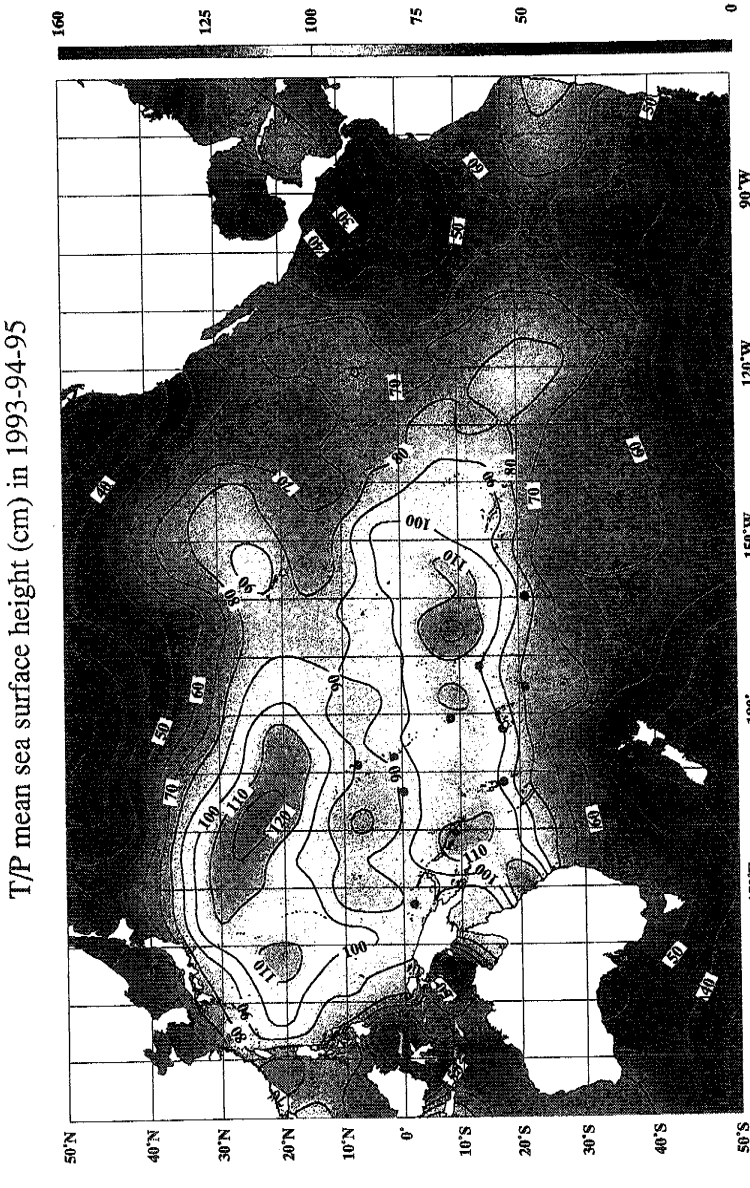

Figure 14

Figure 14 (see legend in the text)

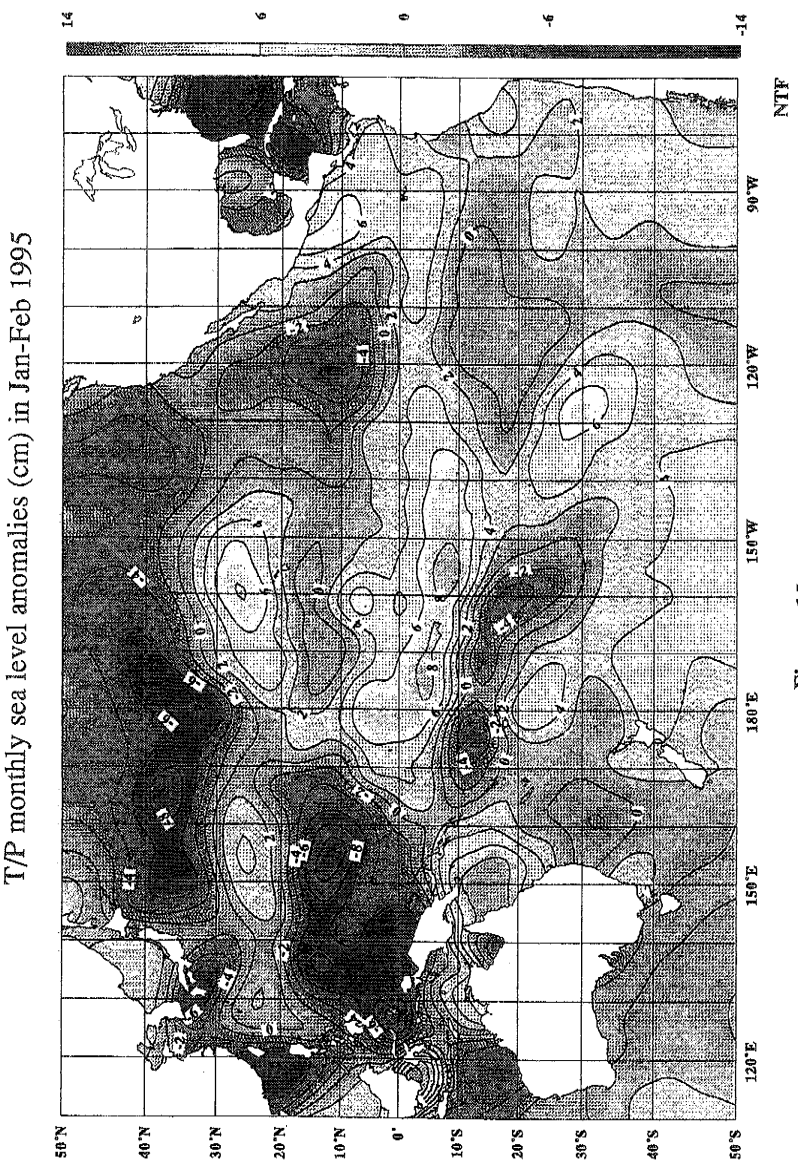

Figure 15a

Figure 15 a (see legend in the text)

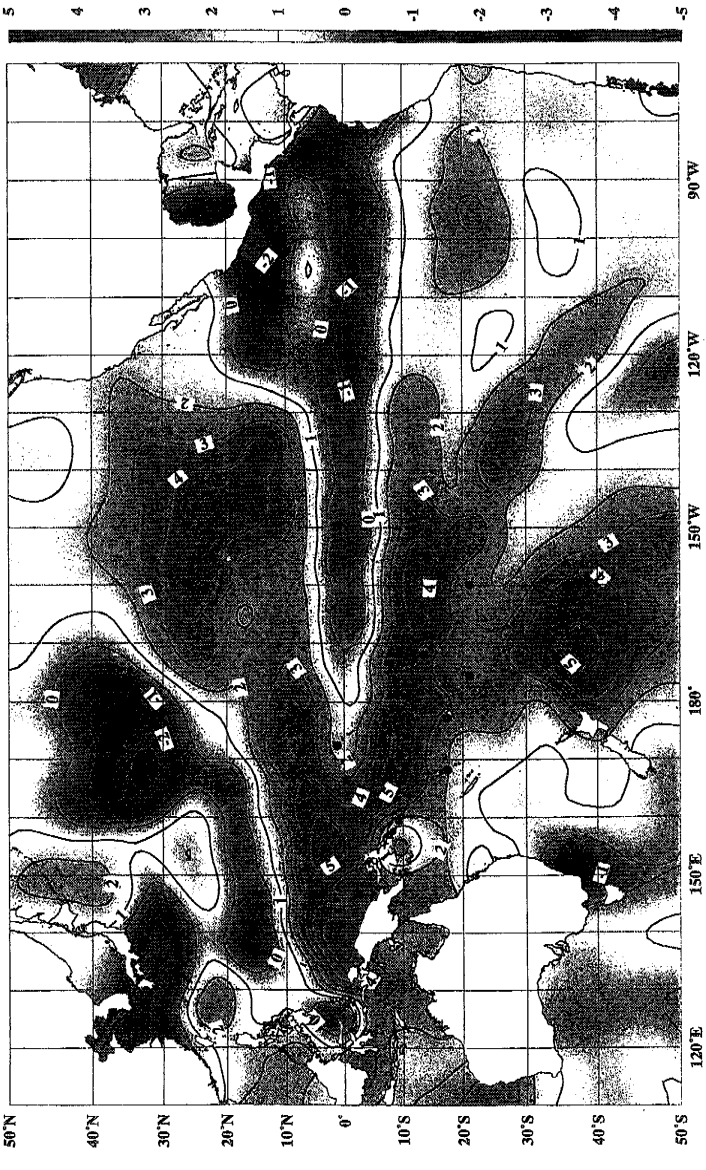

Figure 15b

Figure 15 b (see legend in the text)

The variations in the sea level topography observed by T/P during this four-year period indicate rapid propagations of positive and negative SLAs greater than 10 centimetres. These travelling "bumps" and "throughs" are the response of the equatorial Pacific to westerly and easterly wind anomalies, corresponding to negative and positive values of the Southern Oscillation Index (SOI) respectively. It may be useful to remark here that, when an upwelling KW (downwelling KW) starts its eastward voyage from say 180°, simultaneously, at 180°, a downwelling RW (upwelling RW) starts its westward voyage.

5.4 Equatorial Kelvin waves observed by T/P (Fig. 16a)

Fortuitously, the launch of TOPEX/POSEIDON occurred in the period of the very unusual 1990-1994 repetitive ENSO events. Due to westerly wind anomalies in Oct.1992-Jan.1993 (McPhaden, 1993), downwelling Kelvin waves (KW) started in late October 1992 from 140°E. In November 1992, positive SLAs greater than +9 cm moved eastward from 170°E to 235°E, without reaching the eastern boundary. Then, in late December 1992, a signal started from 175°E (SLAs greater than +12 cm), leading to SLAs of small amplitudes (+3 cm) at the eastern boundary in early February 1993.

In early April 1993, positive SLAs starting from 205°E reached the coast in April-May 1993, with amplitudes greater than +9 cm at 280°E. Weaker downwelling KW (+3 to +6 cm) started from 180° (240°E) in late-August 1993 (late Sept. 93), and weak signals (+3 cm) reached 280°E in late October 1993. Other positive signals at 180° and 160°E in Nov-Dec 1993 petered out eastward quickly. Weak easterlies at 140°E from December 1992 to October 1993 contributed to generate trains of upwelling KW starting from 140°E until mid-October 1993, reaching at most 220°E in June 1993.

In Jan-Feb 1994, strong easterlies distributed all over the equatorial Pacific (Fig. 13), generated strong upwelling KW starting from 170°E, that reached the eastern coast in Feb-March 1994. Between July and December 1994, strong westerly wind anomalies in the western-central Pacific (up to +7 m/s in Oct-Dec.1994) generated impressive trains of downwelling KW, starting from about 160°E-165°E. Most of them reached the American coast where positive SLAs up to +10 cm were observed from October 1994 through mid-January 1995.

In contrast, most of the downwelling KW starting from 140°E in May 1995 through September 1996, were stopped to the west of 180°.

A large time-space change of the wind regime was initiated in January 1995 (Fig. 13), when the equatorial zonal winds returned to normal intensity, switching from westerly anomalies dominating the western-central equatorial Pacific in 1994, to enhanced easterlies across the equatorial Pacific in the second half of 1995. Strong negative SLAs were observed in January 1995 at 140°E-165°E, distinctly not connected to those observed at 160°E in March 1995. Easterly winds prevailed from March 1995 until November 1996, and explain the regular succession of upwelling KW during the period March 1995-Oct 1996. The first ones started from 160°E in early March 95 and reached the eastern Pacific coast at 80°W (280°E) on late April 95 (Fig. 16a). The easterly wind anomalies at 95°W-120°W in Feb-March 1995 (Fig. 13) generated large negative SLAs at 270°E-280°E (90°W-80°W), not related to basin-wide KW.

During the period Aug 1995-Sept. 1996, downwelling KW appeared at 140°E but they did not propagate to the east of 180°, except in December 1995 (Fig. 16a). Due to the weakness of the westerlies in the area 140°E-160°E during this period, these downwelling KW could be due in part to the reflection of the strong downwelling RW observed at 5°N and 5°S, radiating from about 180° (see below). No basin-wide downwelling KW were observed in 1995 and 1996 as in the previous years since October 1992.

5.5 Equatorial Rossby waves observed by T/P (Fig. 16 b, c)

Along 5°N and 5°S, the T/P data from October 1992 to October 1996 give evidence of westward propagating non dispersive upwelling and downwelling Rossby waves (RW) with quasi-annual periodicities. Their amplitudes were larger in the central-western Pacific, up to ± 20 cm, as compared with amplitudes generally smaller than ± 6 cm in the eastern Pacific. Generally, the amplitudes of the planetary waves sharply increased westward of 100°W (260°E). Along 5°N most of the maxima were situated to the west of 110°W (250°E), and along 5°S they were generally to the west of 180° (Fig. 16b and Fig.16c). Both at 5°N and 5°S, most of the RW did not start from the eastern boundary, and very few RW were transpacific waves travelling from coast to coast.

N.B. In order to get the longitude-time diagrams of the sea level anomalies readable, the full legends of the three figures 16 (a,b,c) are presented here in the text. Only abridged legends are given at the bottom of each figure, and scales, smoothing, colour code and sea level reference are the same.

Figure 16 a. Longitude-time plot of sea level anomalies (cm) observed by Topex/Poseidon along the equatorial Pacific (0°.30'S-0°.30'N) for the period October 1992 through October 1996. Reference of the SLAs: T/P-derived mean sea surface topography computed for the 3-year period 1993-1995. The T/P data were smoothed with a Gaussian filter with a radius of 1000km. Longitudes are from 140°E to 280°E (80°W). The time scale is given in years and months, together with the corresponding T/P cycle numbers. Upwelling (cooling) and downwelling (warming) equatorial Kelvin waves appear as ±10 to ±15 cm changes of sea surface height (+ is for downwelling Kelvin waves, yellow to red colours; - is for upwelling Kelvin waves, green to purple colours).

Figure 16 b. Longitude-time plot of sea level anomalies (cm) observed by Topex/Poseidon in the equatorial Pacific along 5°N (4°.30'N-5°.30'N) for the period October 1992 through October 1996. Longitudes are from 140°E to 280°E (80°W). Upwelling (cooling) and downwelling (warming) equatorial Rossby waves appear as ±10 to ±20 cm changes of sea surface height (+ is for downwelling Rossby waves, yellow to red colours; - is for upwelling Rossby waves, green to purple colours).

During the 1992-96 four-year period, most of the nearly transpacific Rossby waves at 5°N radiated from about 260°E-270°E (100°W-90°W). Their amplitudes grew westward, being maximum in the central-western Pacific. SLAs larger than ± 10-15 cm were observed at 140°E frequently, while they were usually smaller than ± 3 cm at the eastern boundary. These observations give evidence that these equatorial planetary waves drew their energy first from the wind stress, rather than through a reflection process at the eastern boundary. Note the sea level build up (+9 cm to +12 cm) to the west of the date line in 1995 and 1996, indicative of an excessive heat content in the western Pacific and conditioning the ocean for the start of the very powerful 1997-98 El Niño in December 1996-January 1997.

Figure 16 c Longitude-time plot of sea level anomalies (cm) observed by Topex/Poseidon in the equatorial Pacific along 5°S (4°.30'S-5°.30'S) for the period October 1992 through October 1996. Longitudes are from 140°E to 280°E (80°W). Upwelling (cooling) and downwelling (warming) equatorial Rossby waves appear as ±10 to ±20 cm changes of sea surface height (+ is for downwelling Rossby waves, yellow to red colours; - is for upwelling Rossby waves, green to purple colours).

The annual transpacific Rossby waves along 5°S in the central-eastern equatorial Pacific were about 50% smaller at 5°S than at 5°N, while they were of comparable amplitudes to the west of the date line. Mimimum SLAs were observed at the eastern boundary during the 1992-96 four-year period. The sea level build up (+9 cm to +12 cm) to the west of the date line in 1995 and 1996 was similar to the sea level build up observed at 5°N.

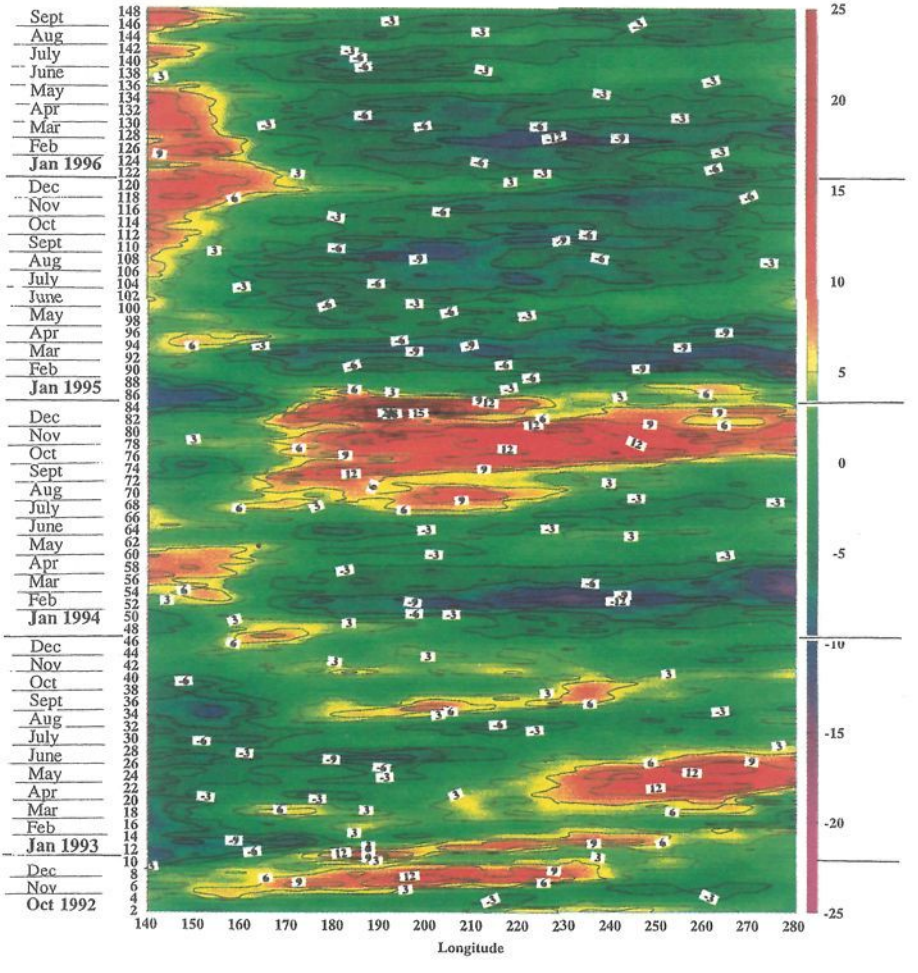

Figure 16 a. Sea level anomalies (cm) observed by Topex/Poseidon in the equatorial Pacific (1°S-1°N). + is for downwelling Kelvin waves (yellow to red colours); - is for upwelling Kelvin waves (green to purple colours). (Abridged legend, see the complete legend in the text).

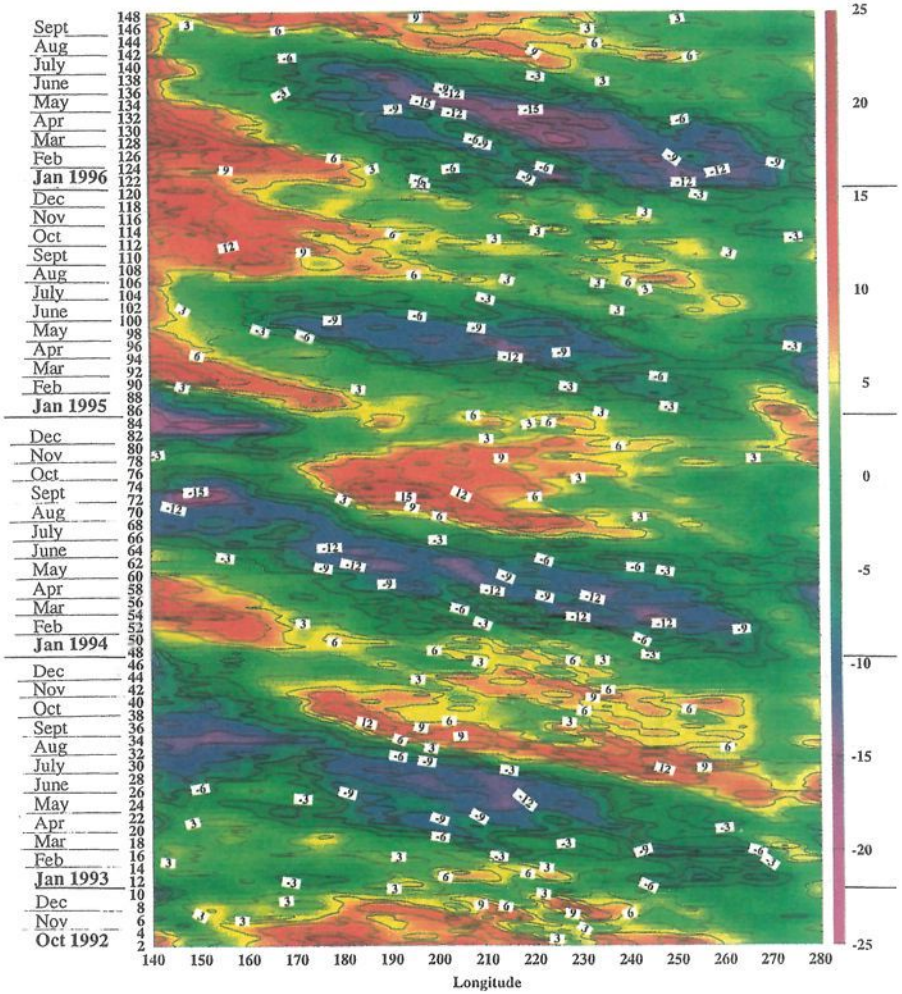

Figure 16 b. Sea level anomalies (cm) observed by Topex/Poseidon in the equatorial Pacific along 5°N (4°.30'N-5°.30'N). + is for downwelling Rossby waves (yellow to red colours); - is for upwelling Rossby waves (green to purple colours). (Abridged legend, see the complete legend in the text).

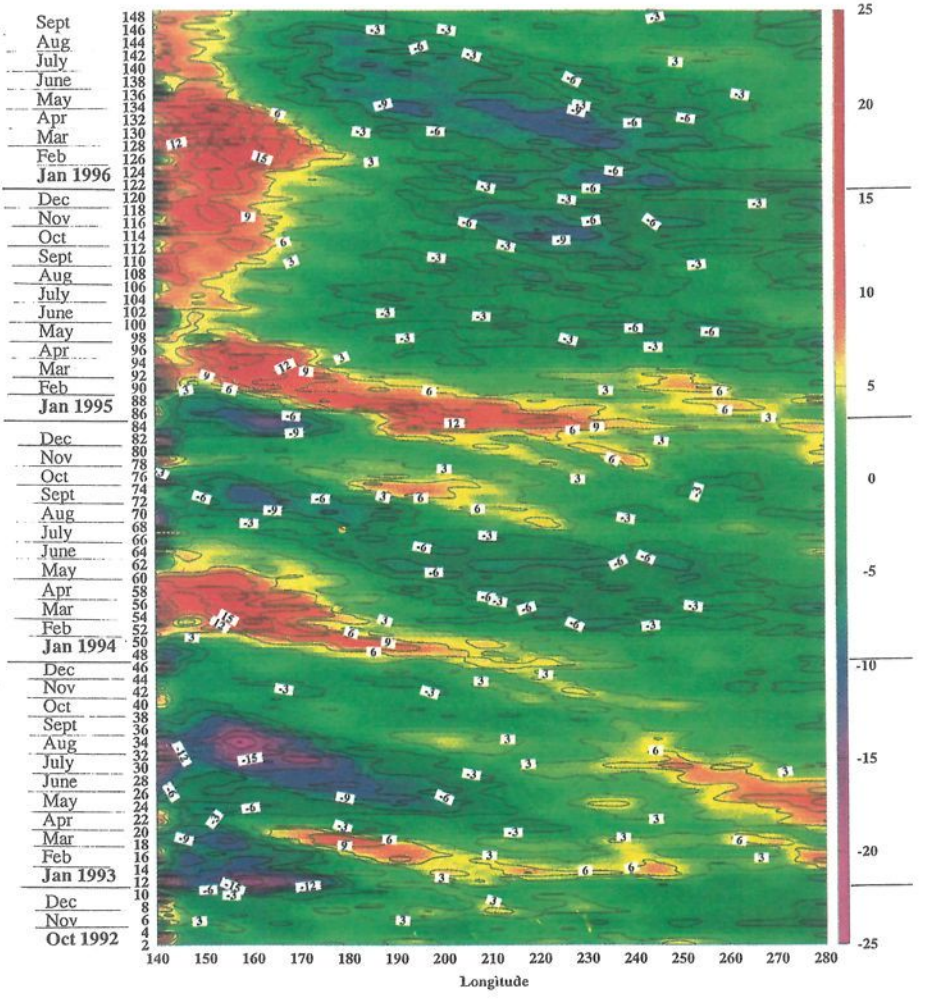

Figure 16 c. Sea level anomalies (cm) observed by Topex/Poseidon in the equatorial Pacific along 5°S (4°.30'S-5°.30'S). + is for downwelling Rossby waves (yellow to red colours); - is for upwelling Rossby waves (green to purple colours). (Abridged legend, see the complete legend in the text).

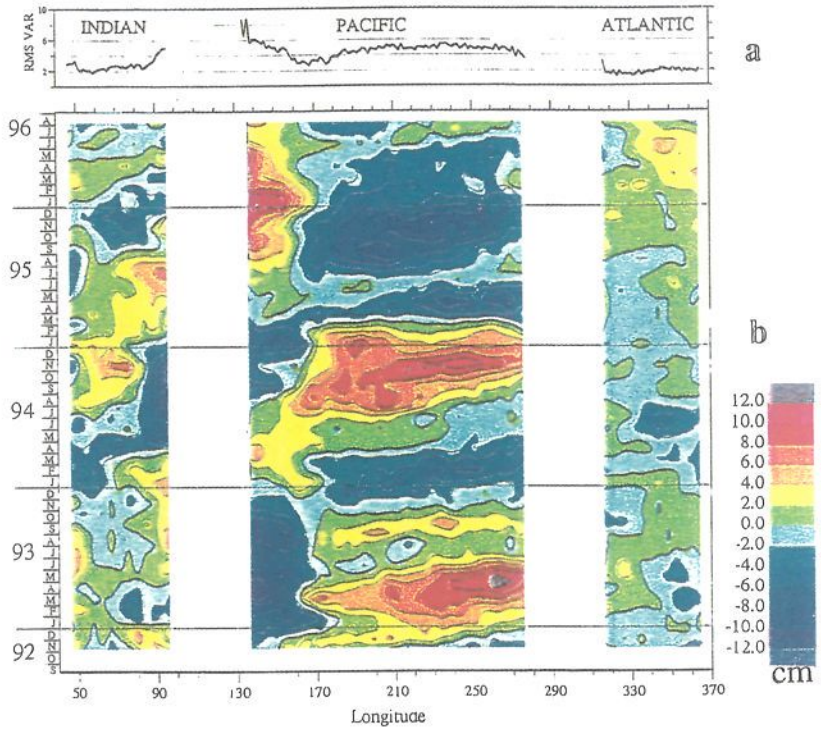

Figure 17

(Fig. 17a) Sea level interannual variability (sea level anomalies relative to the 4-year mean seasonal variations) in the equatorial Indian, Pacific and Atlantic oceans.

(Fig. 17b) Longitude/time diagrams of T/P interannual sea level anomalies along the equator of the Indian, Pacific and Atlantic oceans from November 1992 to August 1996. In the Pacific, to the east of 180°, the interannual SLAs propagated eastward at a mean speed of 2.1 m/s.

At 5°N-5°S, during the four-year period analysed here, upwelling and downwelling annual planetary wave trains propagated westward, with amplitudes significantly smaller at 5°S. The upwelling RW crossed the date line in June-July (on T/P cycles 30, 66, 100, and 139). The downwelling RW crossed 180° in October (on T/P cycles 2, 39, 75, 112, 148) and in March (on T/P cycles 19,54, 92-93, 129, although the signals were very weak at 5°S). In 1995 (except in January) and 1996, no upwelling RW reached 140°E, but only packets of downwelling RW emanating from about 180°. Most of the RW trains did not cross the Pacific from coast to coast and no significant downwelling RW reached the western boundary in 1993. Strong upwelling signals at the western boundary in July-Sept 1993 were not followed by transpacific upwelling KW emanating from 140°E. Again, large negative SLAs were observed at 140°E in July-Sept 1994, but no upwelling KW started from 140°E in Sept-Oct 1994 (Fig. 16a).

5.6 Sea level anomalies at the coastal boundaries

In relation to the delayed oscillator theory, it is necessary to scrutinize the SLAs at the western and eastern boundaries of the equatorial Pacific. Studying the time-longitude SLA diagrams (Fig. 16), isolated SLA areas of short duration and small longitudinal size were discarded. Planetary waves had large (small) amplitudes at the western (eastern) boundary, whereas KW had maximum amplitudes between 170°E and 270°E.

Eastern boundary (280°E or 80°W)

Along the equator (Fig. 16a), SLAs larger than 9 cm were observed at 280°E as follows: (1) April-May 1993: +9 cm, related to KW starting from 200°E; (2) Feb-March 1994: -12 cm, KW starting from 170°E; (3) Nov-Dec 1994: +10 cm, KW from 165°E; (4) March-April 1995: -10 cm, KW from 160°E; (5) March 1996: -9 cm, KW from 185°E.

At 5°N and 5°S (Fig. 16b and 16c), close examinations of the SLAs at 280°E gave evidence of the following signals: (1) May-June 1993: +9 cm; (2) Jan-Feb 1994: only -3 cm at 5°S, while the signal (-9 cm) at 5°N was at 265°E, not at the coast; (3) Dec 1994-Jan 1995: +9 cm at 5°N but no westward spreading beyond 265°E and +3 cm at 5°S; (4) March-May 1995: -6 to -12 cm at 5°N (no westward spreading beyond 265°E), -3 to -6 cm at 5°S; (5) January 1996: -6 cm at 5°N and -3 cm at 5°S.

Among these signals, only two occurrences of transpacific equatorial RW starting from 270°E-280°E and reaching 140°E were observed: (1) a downwelling RW starting in May-June 1993 (280°E), arriving at 140°E in March-April 1994 (noting that the signal was not continuous at 5°S); and (2) an upwelling RW, starting in Jan-Feb 1994 at 270°E-280°E and arriving at 140°E in Sept-Oct 1994. The large SLAs observed at 280°E (Fig. 16a) in Dec 1994-Jan 1995, March-May 1995 and in March 1996 did not generate transpacific RW.

Western boundary (140°E)

Turning our attention to the western boundary of the equatorial Pacific at 5° latitudes, it is obvious that the amplitudes of the SLAs were much larger than at the eastern boundary. It is also evident that most of the transpacific RW at 5° latitudes did not emanate from the eastern boundary situated at 277°E (83°W, 5°S) and 282°E (78°W, 5°N), but rather from about 265°E, very far away off the American coast.

SLAs greater than 12 cm were observed at 140°E as follows: (1) January 1993: -15 cm, only at 5°S; then at 5°N and 5°S, (2) August 1993: -15 cm; (3) March-April 1994: +15 cm; (4) Sept-Oct 1994: -12 cm; (5) Dec1994-Jan 1995: -15 cm; (6) March-April 1995: +15 cm; (7) Aug-Sept 1995: +15 cm; and (8), practically without interruption from September 1995 through October 1996, +12 to +15 cm. Among these signals, only (3) and (4) could be attributed to transpacific RW; the signals (2) and (6) could be linked to planetary waves starting from about 260°E, not from the eastern boundary. The signals (5, 7, 8) were linked to RW originating to the west of 180° and the signal (1) at 5°S was linked to negative SLAs at 140°E-180°, but without discernable propagation.

5.7 Origin of the equatorial Kelvin and Rossby waves

During the 4-year period studied, very few equatorial KW and RW were transpacific waves travelling from coast to coast. Most of the KW generated at 140°E did not progress beyond 180°, and most of the RW did not emanate from 280°E. Only one KW was transpacific, starting in late November 1992, and only two transpacific RW reached 140°E, in March-April 1994 and in Sept-Oct 1994. Although strong upwelling RW reached 140°E in Aug-Oct 1993 and 1994, and again in January 1995, none of them was efficiently reflected back as packets of transpacific KW signals.

Comparing the amplitudes of the sea level anomalies situated within the longitude-domain 140°E-180°, it is safe to conclude that most of the KW starting at 140°E could be generated either by the reflection of the Rossby waves arriving at 5° latitudes, or as well by the zonal wind anomalies at 140°E. At 280°E, amplitudes of the SLAs linked to RW matched those of the impinging KW, only in June 1993 and January 1996. The strong downwelling KW impinging on the east coast late Nov-early Dec 1994 could explain the positive SLAs observed at 280°E, 5°N and 5°S, in Dec1994-Jan1995, but no transpacific downwelling RW started from 280°E at that time.

In summary, only one downwelling KW emanating from 140°E late November 1992 crossed the entire Pacific basin during a four-year period (Oct. 1992-Oct. 1996, Fig. 16a). It is noteworthy that during this period, the equatorial SLAs reached maxima up to ± 20 cm in the central-eastern equatorial Pacific ocean (170°E-260°E) where the zonal wind stress was maximum, rather than at the boundaries (140°E or 280°E). Significant SLAs at the eastern boundary were not related to transpacific KW.

Kelvin waves radiated regularly from 140°E, but they usually did not propagate beyond the date line. Most of the Kelvin waves started their eastward travel at 160°E-170°E, not from 140°E, their amplitudes being maxima in the central part of the basin. These facts point to equatorial KW being generated in most cases in response to the zonal wind stress, rather than through the process of reflection of planetary waves at the western boundary.

Similarly, it is also very unlikely that the strong annual planetary waves observed at 5° latitudes during this four-year period were generated by the reflection of KW impinging on the American coasts. The weak amplitudes of the observed SLAs at 280°E dismiss the reflection process at the eastern boundary as the main contributor of transpacific equatorial RW. Actually, the amplitudes of the annual planetary waves closely matched the zonal wind annual distribution over the equatorial Pacific, their maxima being situated where the zonal wind stress and wind stress curl were maximum (170°E-250°E).

Some facts emerge from this analysis, summarized as follows:

(1) The annual cycle of the planetary waves at 5° latitudes and Kelvin waves at the equator is evident and well delineated in longitude-time diagrams. Upwelling RW (KW) were intertwinned with downwelling RW (KW), alternating every 6 months at the date line.

(2) In 1993, no upwelling Kelvin waves starting from 140°E were able to put an end to the 1992-93 El Niño, because they all were of small amplitude and most of them did not propagate beyond about 180°.

(3) In 1994, the strong downwelling KW arriving at 280°E in Nov-Dec 1994, did not reflect as strong transpacific downwelling RW in January 1995, and no El Niño occurred in 1995.

(4) In 1995 and 1996, no upwelling RW reached the western boundary for a period of 20 months, from March 1995 through October 1996.

So, neither the end of the 1993-94 ENSO, nor the small cold episode that occurred in 1996 were due to upwelling RW reflecting at the western boundary as upwelling KW. Both events were the consequence of many upwelling KW starting from 170°E, generated by easterly wind anomalies, initiated in January-March 1995, until October 1996.

(5) Although repetitive downwelling RW appeared omnipresent from March 1995 to October 1996 to the west of the date line, no transpacific downwelling KW was excited at the western boundary during this period.

(6) Repetitive downwelling RW from March 1995 to October 1996 to the west of the date line led to unusual positive SLAs along the western boundary, leading to a heat content build-up in the western equatorial Pacific at the end of 1996. But none of them reflected as significant downwelling KW acting to trigger the very strong 1997-98 El Niño.

(7) Actually, the 1997-98 El Niño was triggered in December 1996 by strong westerlies, not by the downwelling RW observed at 140°E in 1996.

In summary, a close examination of the 2°N-2°S zonal wind field (Fig. 13) observed by the TAO moorings and the sea level anomalies observed by Topex/Poseidon (Fig. 16) during the period Oct.1992-Oct.1996 favors annual wind forcing rather than reflections at the coastlines to generate equatorial Kelvin waves and planetary waves, in agreement with Delcroix et al. (1994) and Boulanger and Menkes (1995). The present analyses do not support the Pacific "delayed action oscillator" concept.

6. Discussion on ENSO Mechanisms

Equatorial planetary waves are certainly the flywheel carrying away the energy injected into the upper equatorial Pacific ocean by the zonal wind stress. Although the existence of planetary-gravity waves in the equatorial ocean had been predicted by Matsuno (1966), Moore (1968) and Lighthill (1969), due to their large phase speeds, evidence of these waves over the 15000 km of the equatorial Pacific was not possible without adequate systems of observations. Kessler (1989) analysed the 1970-87 bathythermograph observations, giving evidence that downwelling long Rossby waves commonly arrive at the western boundary at the Philippines coast, and Graham and White (1988) suggested that these waves could reflect as equatorial downwelling Kelvin waves and trigger subsequent El Niño.

However, only synoptic or quasi-synoptic data provided by permanent systems of observations could grasp the problem. Pioneer in this effort, Klauss Wyrtki (1974 and 1980), created the NORPAX tide gauge network and the TOGA Sea Level Center, the forerunner of the actual Sea Level Center at the University of Hawaii. Also, largely due to the efforts of the 1985-1994 TOGA programme, an array of about 70 deep-ocean moorings now monitors the equatorial Pacific between 8°N and 8°S (Tropical Atmosphere-Ocean (TAO) array).

But the breakthrough came from the satellite altimetry technology, first the Geodetic Satellite GEOSAT Exact Repeat Mission (1986-89), instrumental to assess the foundations of the equatorial linear wave guide theory (Delcroix et al., 1991; 1994), then since August 1992, the Topex/Poseidon (T/P) satellite altimetry mission, "The 2-cm solution" (Cheney et al., 1994). Actually, the basic mechanism of the "delayed action oscillator" (Battisti, 1988; Battisti and Hirst, 1989) relies entirely upon the equatorial linear wave guide theory and can be summarized as follows: a positive SST anomaly in the eastern equatorial Pacific produces westerly wind anomalies in the central equatorial Pacific, generating both equatorial downwelling Kelvin Waves and upwelling Rossby waves that propagate freely to the eastern and western boudaries, respectively. These RW reflect at the western boundary, sending upwelling equatorial KW back to the central basin, which stop instability growth and rapidly plunge the coupled system into a cold regime.

According to this scheme, the western boundary reflection is necessary for event termination. This raised the question of whether reflection of RW as equatorial KW from the western boundary is actually observed in nature. The western Pacific coast is far from continuous, with many islands in the Papua New-Guinea area. It was therefore crucial for the "delayed action oscillator" theory to see in nature if the reflection of the equatorial RW from these not north-south oriented broken coasts follows theoretical prediction.

According to Boulanger and Fu (1996), equatorial KW reflect quite well on the eastern boudary as equatorial RW, and according to Boulanger and Menkes (1999), RW are systematically reflected at the western boundary as KW. These analyses give evidence of reflections at both boundaries, the reflector efficiency (as compared with an infinite meridional wall) at the American coast and at the irregular western Pacific boundary being 75% and 50%, respectively.

However, other recent studies have suggested that the delayed action oscillator theory overestimated (underestimated) the importance of the reflection of RW (KW) at the western (eastern) Pacific coasts (Picaut et al., 1996). Also, other ocean mechanisms are not considered in the delayed action oscillator concept, such as the zonal advection of SST and the convergence of the zonal currents at the eastern edge of the warm pool. Considering that the positions of the simulated SST-wind stress field maxima were 30°-40° too far into the eastern equatorial Pacific, Picaut et al. (1996) proposed that the source of ENSO was located in the 28°-30°C SST area situated at the eastern edge of the warm pool, not in the eastern equatorial Pacific. Also, contrary to the delayed action oscillator, Picaut et al. (1997) argued that it is possible to get ENSO-like oscillations generated only by equatorial Kelvin waves reflecting on the eastern boundary, the reflections of Rossby waves at the western boundary being of secondary importance.

But, as effective as reflections at the coasts may be, debating about the reflector efficiency of each coast is not the central point of the problem. The present study questions the effectiveness of the delayed oscillator mechanism to initiate or terminate an ENSO event. Even if reflections were perfect, it is the delayed action oscillator itself that is questionable.

Its physics relies entirely upon the equatorial linear wave guide theory indeed, which is not able to explain the chaotic behavior of ENSO. If the upwelling and downwelling equatorial Kelvin and Rossby waves travelling back and forth across the Pacific were to pilot the ENSO cycle, then the mechanism would be invariant and ENSO would be more regular than observed. In summary, the delayed oscillator theory is detracted by the irregularity or the lack of periodicity of the ENSO cycles, contrary to the observed regularity of the annual equatorial planetary waves (see for example the figures 16b and 16c).

It must also be stressed that other analyses indicate that the propagation speeds along the equator of the SST, heat content and wind stress anomalies are rather slow. As early as 1984, Wyrtki (1984) had observed that during the 1982-1983 El Niño, the eastward wind stress anomalies moved eastward at about 30 cm/s, whereas the peak in sea level advanced eastward with a speed of about 90 cm/s (see his figure 5), much slower than the phase speed of the Kelvin waves. Tourre and White (1995) found propagation speeds along the equator of about 30 cm/s in the Pacific. The slow zonal back and forth advection of the eastern edge of the warm pool (Picaut et al., 1996) is the accumulated effect of many Kelvin and Rossby waves, slowly driving anomalous structures of temperature and currents, and finally responsible for the eastward (El Niño) and westward (La Niña) displacement of the eastern edge of the warm pool. Therefore, the location of the eastern edge of the warm pool may be considered as the integration of many advective processes along the equator, but not as the key parameter for triggering the basin wide ENSO episodes.

While the overwhelming significance of the equatorial dynamics in the ENSO cycle cannot be denied, these elements are symptoms rather than causes. In our quest to discover the elusive trigger of El Niño, many hypothesis have been made (volcanism, quasi biennal oscillation, pair of hurricanes, snow cover over Tibet, heat content anomalies in the Indian ocean...), but none of them is able to determine the basic pseudo periodicity of ENSO. What is the trigger to the onset of the aperiodic ENSO? How does the Pacific ocean-atmosphere climate machine switch from El Niño to La Niña?

These questions have not yet received an appropriate answer. Although there is general agreement that the equatorial ocean wave-guide contributes certainly to the evolution of each ENSO, it is not the trigger to the onset of the aperiodic ENSO cycles.

In an effort to discover a precursor outside of the Pacific ocean, the interannual variations of the T/P sea level anomalies along the equator of the Indian, Pacific and Atlantic oceans were analyzed from November 1992 to August 1996 (Park, Gambéroni and Verstraete, 1997). The raw T/P data were low-pass filtered at 30 days and subsampled at daily intervals. Mean seasonal variations were obtained by 4-year means of filtered daily values of the same Julian days, and interannual variations were defined as anomalies relative to these 4-year mean seasonal variations. The longitude/time diagrams (Fig. 17) were drawn with the data smoothed in time with a 30-day Gaussian filter and in space with a 250km-radius Gaussian filter, and gridded every 250 km along the equator. This processing allows to detect low-frequency variations with periods and wavelengths greater than 60 days and 1000 km, respectively.

The strongest interannual variability (Fig. 17a) was found in the western equatorial Pacific (8.5 cm rms). A strong interannual signal appeared in the eastern equatorial Indian ocean (5.0 cm rms), while the signal was weak and nearly flat all over the equatorial Atlantic (2 cm rms).

In the Pacific (Fig. 17b), to the east of 180°, the interannual SLAs propagated eastward at a mean speed of 2.1 m/s, significantly slower than the theoretical phase speed of the first baroclinic Kelvin wave in the equatorial Pacific (Philander, 1990; Delcroix et al., 1991). No evidence of Kelvin wave-like propagation was observed in the Indian as well as in the Atlantic equatorial oceans (Fig. 17b).

There is some evidence that interannual positive sea level anomalies along the equator in the eastern Indian Ocean led those in the western equatorial Pacific in 1992-96, suggesting a propagation of precursors of ENSO from the eastern Indian ocean to the western equatorial Pacific, in agreement with Diggs et al., (1996) and Barnett (1983). Exploring the interaction between the Indian monsoon system and the Pacific trade winds within 10° of the equator, Barnett (1983) had noted that the precursors to the large-scale changes of the Indo-Pacific convergence

system "seem to be in the zonal component of the wind". As early as 1983, Barnett pointed that the *u*- component wind disturbances move from the Indian ocean eastward into the Pacific, that they preceed El-Niño events and that they are phase-locked to the seasonal cycle. Barnett (1983) gave evidence that the largest variability in the zonal wind field over the Indian and the Pacific oceans occurred in the "maritime continent" between northern Australia and the northern hemisphere maritime continent, was symmetric about and had its maximum energy at the equator, and propagated from the Indian ocean to the western Pacific.

Numerous statistical and theoretical studies suggest that energetic episodes of westerly winds in the western equatorial Pacific may trigger El Niño events, launching the ENSO cycle. Evaluations of wind data taken from several islands in the western tropical Pacific (Harrison and Giese, 1991) have revealed that the strongest and the highest probability of occurrence of westerly winds were centred on and south of the equator, and that there is a strong seasonality. They have noted too the striking association of strong westerly wind events in the western Pacific, at or near the equator, with the months September to February during ENSO periods. These facts suggest to consider the interactions between the Pacific warm pool and the maritime continent, particularly during the northern hemisphere winter. The precursor of the 1997-98 ENSO was sought after in the Indian ocean, a step consistent with the strong interannual sea level signals observed in the eastern equatorial Indian ocean, east of 90°E, as well as in the western equatorial Pacific, west of 140°E, in 1992-1996 (Fig. 17).

At least* two atmospheric seasonal cycle forcings contribute to run the equatorial Indo-Pacific climate machine: (1) the Pacific trade winds, and (2) the Australasian monsoon, connected to the north-east Indian monsoon acting east of 65°E in the Indian ocean in boreal winter.

*The Indian summer monsoon and, in the eastern equatorial Indian ocean, a biennial oscillation (in Philander, 1990, ref. to Meehl, 1987) are not considered here.

Within 10° latitudes, the Australasian monsoon ($\omega_{Ausmonsoon}= 2\pi/1y$) generates westerlies at 95°E-110°E (Sumatra-Java) in November-December, that reach 130°E-160°E (Papua New-Guinea-Solomon Is) in December-March, and finally Guadalcanal (160°E), where maximum rains are observed in February.

In response to the annual trade wind forcing the equatorial Pacific oscillates but, due to its huge inertia, its natural adjustment time is estimated to about 14-15 months (Philander, 1990). The time it would take to establish equilibrium conditions after episodes of zonal winds is the adjustment time, and it is the natural period of oscillation of the Pacific equatorial basin. This period is simply the time it takes equatorial RW to propagate from the initial perturbation location to the western boundary plus the time it takes the reflected equatorial KW at the western (from incident RW) and eastern (reflected RW from the initial incident KW) boundaries to propagate back.

Let us consider the following coupled system (I): the equatorial Pacific basin and the Australasian monsoon. The frequencies of the two oscillators considered separately are very close ($\omega_{Ausmonsoon}= 2\pi/12$months, $\omega_{Pacificbasin} = 2\pi/14$-15months), leading the coupled system [equatorial Pacific basin -Australasian monsoon] to oscillate at the very low frequency:

$$\Omega_{\mathbf{coupled(I)}} = (1/2).\varepsilon_1.\omega_{\mathbf{Pacificbasin}} ,$$

where

$$\varepsilon_1 = \omega_{\mathbf{Ausmonsoon}} / \omega_{\mathbf{Pacificbasin}} - 1 \qquad (5)$$

However, a 10-14 year resonance has not been observed in the Pacific, dismissing this scheme to explain the pseudo-periodicity of ENSO.

Obviously, the equatorial Pacific basin and the Australasian monsoon interact necessarily, but not as simply as hypothezised above. Actually, in November-March, the Australasian monsoon is strongly forced not only by the warm waters of the Pacific warm pool (SST larger than 28°-29°C),

but also by the eastern Indian ocean warm pool and the Southeast Asian warm waters (Java, Flores, Banda, Arafura, Timor, Sulu and Celebes seas, a region also called the maritime continent), where SST larger than 28°-29°C are observed annually to the east of 90°E and south of 10°N (Wyrtki, 1961). Recent observations (A. Gordon and McClean, 1999) reveal SST larger than 29°-30°C in the Banda and Timor seas during the northwest monsoon of February 1994. These high SST are above the threshold of 28°C, leading to strong atmospheric convection and rains over the area. Winds converge towards this Pacific-Indian "super" warm pool area, and strong westerlies start to blow as early as November at 95°E-110°E. Consequently, during this period of the year, there are strong interactions between the eastern Indian ocean and the western Pacific ocean through the Australasian monsoon.

Now, in this new coupled system, what matters in the Pacific is not the whole equatorial basin, but only the Pacific warm pool area. Therefore, the coupled system (II) to be considered is as follows: the Pacific warm pool area and the eastern Indian warm pool area (including the "maritime continent"), and the Australasian monsoon, hereafter designated as the "Australasian-Pacific Equatorial Climate System" (APECS). Noting that the eastern Indian warm pool area located east of 90°E is less than half the size of the Pacific one, as a first guess, APECS will oscillate according to:

$$\Omega_{\mathbf{coupled(II)}} = (1/2).\varepsilon_2.\omega_{\mathbf{Pacwarmpool\text{-}area}} ,$$

where

$$\varepsilon_2 = \omega_{\mathbf{AusMonsoon}} / \omega_{\mathbf{Pacwarmpool\text{-}area}} - 1 \qquad (6)$$

The year to year Pacific warm pool area waxes and wanes around 180° according to the slow back and forth zonal displacement of its eastern edge (SST of 28°-29°C), thoroughly studied in the equatorial band 5°N-5°S by Picaut and Delcroix (1995) and Picaut et al., (1996). During the period 1950-1999, the eastern edge of the Pacific warm pool area within 5° latitudes oscillated 12 times, eastward (El Niño) and westward (La Niña) around 180°, with a mean periodicity of 4.0 years ($\omega_{\text{Pacwarmpool-area}} = 2\pi/4.0y$). According to (6), APECS oscillated in 1950-1999 at the pseudo-period 2.67 (8/3) years. Actually, the duration of each oscillation of the Pacific warmpool area varied from 1.6 years in 1964-65, to 7.0

years in 1957-63, leading the coupled system (II) to oscillate at pseudo-periods ranging from 2.3 years (corresponding to a 7.0 year period-like warm pool area oscillation) to 5.3 years (1.6 y).

However, more than the SST, which is nearly constant around 28°-29°C all the year round, it is the heat content of the warm pool, a quantity related to its volume, that is important because the response of the tropical atmosphere depends critically upon a redistribution of heat in the equatorial ocean (Gill and Rasmusson, 1983; Philander et al., 1984; Yamagata, 1985; McCreary and Anderson, 1991).

The heat content of the warm pool depends not only upon advective terms but also upon vertical mixing terms. A fundamental process of unstable air-sea interaction at the equator, relating linearly SST anomalies to the anomaly of thickness of the warm upper layer, appears appropriate in models of ENSO, because within the Indo-Pacific warm pool, the horizontal temperature gradients are so small that the advective terms are negligible in the equation of heat. In the core of the warm pool, vertical processes must dominate the heat budget. The volume of the warm pool is a robust indicator of the thermodynamics of the coupled system, because it integrates different complex processes leading to a delicate balance between unknown quantities (the net surface heat gain and the cooling by entrainment of heat to the deep ocean are not accurately quantified within the warm pool, Lukas, 1989; Lukas and Lindstrom, 1991; Webster and Lukas, 1992).

The relevant parameter to consider in the Australasian-Pacific Equatorial Climate System is therefore the Indo-Pacific warm pool volume. Observations of sea level allow a determination of the volume of warm water in the tropical ocean, but rather than the warm waters of the entire equatorial Pacific ocean between 15°N and 15°S (Wyrtki, 1985), it is here more appropriate to consider the Indo-Pacific warm pool region between Papua New-Guinea and Indonesia where the monsoon/trade winds interact. Long time sea level time series in the Indonesian area being not available, only the Pacific part of the Indo-Pacific warm pool was studied here.

The interannual variation of the Pacific warm pool volume ($\omega_{\text{Pacwarmpool-volume}}$) within 5° latitudes, (temperatures above 28°C within a layer about 80-100 m thick, Fig. 2), large at the beginning and

small at the end of each El Niño (Wyrtki, 1985), was studied for the period 1975-1994. Sea level deviations larger than ±5 cm are equivalent to a change of ±10m of the depth of the 28°C isothermal surface.

Using the 1975-94 series at Rabaul (Fig.11b), 13 cycles were evidenced, of which the durations ranged from 3/4 year to 34/12 years, the mean duration of one cycle being 1.47 years, close of the 1.3-year Wyrtki's estimate (1989).

The APECS system will now oscillate in mean at a 6.0 year pseudo-period, consistently slower than the previous estimates, and within a range of periodicities (3.1-6.0 y), close of the mean pseudo-period of the Southern Oscillation. Estimates obtained with other tide gauge data (Majuro, Nauru, etc...) within the equatorial band ±5° were very similar.

The fundamental result is that the Australasian monsoon is an external oscillator able to force the equatorial Pacific basin to oscillate at ENSO pseudo-periods, different of its natural mode of oscillation (at a period of about 15 months), leading the coupled system into a resonant mode.

7. Conclusions

The seasonal cycles of the mean sea level, steric sea level and heat content in the 0-1000 m water column were in reasonable agreement at the eleven sites studied here. However, significant errors in the T(z) and S(z) historical profiles, and in particular many errors in the salinity files, prevent to establish accurate correlations and the results are presented as preliminary results. Near the date line, the heat content for the upper 1000 m of the ocean (Fig. 9) increases of about 10^{10} Joule.m^{-2} from Majuro (Marshall Is., 7°N), to Nuku'alofa (Tonga, 21°S).

The mean rate of the secular sea level rise in stable tectonic areas is estimated now to about 1.2 mm/y. Using the historical 1975-1994 yearly mean sea level time series available at the University of Hawaii Sea level Center, negative trends (all in mm/y) were computed at Nauru (-1.0), Rabaul (-6.3), Honiara (-6.5) and Funafuti (-1.0); and positive trends appeared at Tarawa (+3.2), Majuro (+2.0), Rarotonga (+5.4), Suva (+7.5) and PagoPago (+2.1).

From monthly sea level data, estimates of the sea level trends were computed from the start of each SEAFRAME tide gauge station (in 1992-93 for most of them) to January 1998, without taking the liberty of filling the gaps when two consecutive months of data were missing.

At **Manus Island** (2°02'S, PNG), the 23 month time series from March 1996 to January 1998 gave evidence of a negative trend of **-168 mm/y**, essentially due to the decrease in sea level from February 1997 to January 1998. At **Nauru** (0°32'S), two series were studied, giving totally different estimates: +75mm/y over 18 months (1993-94) and **+5.5 mm/y** over 33 months (May 1995-January 1998), opposite to the 1975-1994 trend (-1.0). However, as of January 1998, these estimates at Manus Island and Nauru, computed on two different time periods and too short to be consistent with the other time series considered here, are only preliminary results.

The stations of **Tarawa** (1°22'N, Kiribati) and **Majuro** (7°07'N, Marshall I.) indicate negative sea level trends of **-6.6** and **-18.7 mm/y** over 46 and 57 months, respectively, opposite to the 1975-1994 trends (+3.2 and +2.0), and essentially due to a strong decrease in sea level from March 1997 to January 1998. A negative trend of **-17 mm/y** over 43 months is detected at **Honiara** (9° 26'S, Solomon I.), much larger than the 1975-1994 trend (-6.5), whereas at **Funafuti** (8° 30'S, Tuvalu) a very weak positive trend of **+0.4 mm/y** over 59 months is not significant. Again, the negative trend at Honiara is essentially due to the sea level drop that occurred within 11 months from March 1997 to January 1998. Examination of the monthly Pacific sea level maps (Sea Level Center, Hawaii) corroborates this drop of about 35-40 cm in the western equatorial Pacific, related with the 1997-98 strong El Niño.

In contrast with the above near equatorial stations, the five stations of **Port-Vila** (17°46'S, Vanuatu), **Lautoka** (17°36'S, Fiji), **Nuku'alofa** (21°08'S, Tonga), **Apia** (13°49'S, W. Samoa) and **Rarotonga** (21° 12'S, Cook I.), all situated south of 10°S, gave evidence of positive trends: **14.6; 15.9; 26.0; 15.9; 7.2 mm/y,** respectively. The 1975-1994 trends at Suva-Fiji (+7.5), Pago-Pago, American Samoa (+2.1) and Rarotonga (+5.4) were significantly smaller than the 1992-98 trends at Lautoka-Fiji (+15.9), Apia, Western Samoa (+15.9) and Rarotonga (+7.2).

Besides that, these five estimates over the five years 1993-1998 are one order of magnitude larger than the estimated secular sea level rise, and are clearly related with the repetitive El Niño events occurring during this period (only the year 1996 was nearly "normal").

The secular warming of the western equatorial Pacific is certainly related to the positive 1993-98 sea level trends observed during these five years at the five SEAFRAME sea level stations situated in the south Pacific subtropical gyre, while most of the low frequency sea level variability observed at the SEAFRAME sea level stations situated within 10° of the equator was due to the ocean dynamics of the equatorial wave guide. Kelvin and planetary Rossby waves, very well observed during the 1992-98 period, were studied here over a four-year period, from October 1992 to October 1996, through the T/P sea level data.

The 1992-98 positive sea level trends observed at the five South Pacific Project sea level stations situated south of 10°S are significant and indicate a sea level rise at a mean rate of about 15mm/yr, equivalent to a deepening of 15 m of the thermocline depth over five years. Since waters originating in the Pacific southern subtropical gyre are the dominant source (about 90% according to Peacock et al., 1999) of water to the Pacific equatorial thermocline, this result implies a warming of the Pacific equatorial warmpool in 1992-98.

These sea level estimates are confirmed independently by the 1992-98 T/P altimetry time series (Verstraete, Gambéroni and Park, 1999). The 1992-1998 sea level build-up of the south Pacific subtropical gyre between 160°W and 170°E is related to an unusual warming of the entire tropical Pacific ocean observed since the beginning of the 1990s, and characterised by repetitive El Niño events, very different from the El Niño/La Niña cycles observed in the 1980s.

The very strong 1997-98 ENSO led to different sea level signatures at each SEAFRAME station and demonstrates the fundamental importance of maintaining a permanent array of sea level observatories to evaluate safely the secular sea level trend in different areas of the western tropical Pacific.

The northern edge of the south Pacific subtropical gyre is partly responsible for the thermal structure and current system in the central

equatorial Pacific. A deepening of the thermocline in this gyre would increase the large scale barotropic equatorward subsurface pressure gradient. This would bring warmer thermocline waters to the equator, decreasing the equatorial upwelling and shifting eastward the eastern edge of the warm pool and the associated atmospheric equatorial convective system.

Although speculative, a long term scenario is conceivable in the central Pacific, very different from the present delayed oscillator theory, as follows: due to a warming of both Pacific subtropical gyres, warmer and deeper thermocline waters would be injected from both gyres into the equatorial thermocline through the large scale barotropic subsurface equatorward incremented pressure gradients. As a consequence, the equatorial thermocline waters would be warmer and thicker, and the cold waters deeper. If this were to occur, the equatorial upwelling generated by the large scale wind stress would be weakened in the central Pacific. Finally, the warm pool would extend into the central-eastern Pacific, because the upwelled waters in the central Pacific would be warmer than usual, leading to warmer sea surface temperatures. At decadal time scales, this scenario cannot be dismissed since five SEAFRAME tide gauge stations situated in the area 168°E-160°W, 15°S-20°S gave evidence of a significant positive sea level trend in a large area of the south Pacific subtropical gyre during five years (1993-January 1998), larger than the positive trend observed in the period 1975-1994 in the same area, and corroborating a 1900 to 1991 secular warming of the sea surface temperature in the equatorial Pacific west of the date line.

Linear fits calculated over the 1990-93 yearly Southern Oscillation Index series indicated a trend towards negative values during the twentieth century. This negative trend (see the figure 6 for the last forty years), implies increasing (decreasing) sea level pressures in the eastern equatorial Indian ocean (in the Tahiti-Easter Island anticyclone area) and increasing frequencies of westerlies in the eastern equatorial Indian ocean, and over the Australasian area (From Sumatra to New-Guinea).

In 1994, 95 and until October 1996, numerous downwelling KW started at 140°E, but none of them crossed the entire Pacific (Fig. 16a).

Equatorward of 10° latitudes, a sea level build-up occurred at 140°E-170°E in 1995-1996, very well observed by the SEAFRAME sea level stations (Fig. 12) and the Topex/Poseidon observations. This build-up was due to many equatorial downwelling planetary waves arriving at 140°E from March 1995 until at least October 1996 (Fig. 16b,c). However, none of them reflected as significant downwelling KW that could have triggered the 1997-98 El Niño (Fig. 16a). The heat content build-up in the western equatorial Pacific reached its maximum at the end of 1996.

The powerful 1997-98 El Niño was triggered in December 1996 by strong weather systems migrating into the western Pacific from the Indian ocean (NOAA, Climate Diagnostics Bulletin, December 1996, 850-hPa vector wind map), and there was a very clear relationship to the 1997-98 El Niño (McPhaden, 1998, and pers. com.). The strong westerlies observed in December 1996 in the eastern Indian ocean were related to the Australasian monsoon and penetrated into the western Pacific, triggering a transpacific downwelling KW that reached 280°E two months later (NOAA bulletin, Jan 1999), launching the 1997-98 powerful ENSO. Analyses by Barnett (1983), Tourre and White (1995), Diggs and al. (1996), Park, Gambéroni and Verstraete (1997), and by McPhaden (1998), among others, agree to consider the Indian ocean as a precursor of ENSO.

This study suggests that the eastern Indian ocean warm pool and the maritime continent interacts seasonally with the western equatorial Pacific, the link between the two oceans being the Australasian monsoon generating westerlies from 95°E to 160°E from November through March (period of the winter monsoon). These westerlies are crucial to trigger packets of downwelling equatorial Kelvin waves in the western equatorial Pacific, that travel towards the eastern equatorial Pacific, leading to the well known seasonal warming at the eastern boundary. Some years, due to more severe conditions over Asia (northern winter) and over Australia (southern summer), these gusts of westerlies are more persistent and stronger than usual in the western equatorial Pacific, generating more powerful and more numerous packets of downwelling Kelvin waves, that finally launch an El Niño.

The equatorial climate machine may be driven in part by the eastern Indian ocean-Australasian monsoon in November through March, interacting with the western Pacific warm pool climate machine.

However, the strength of the coupling depends upon the phase and strength of the Australasian monsoon which are not fixed. Year after year, the Australasian monsoon phase may vary by a few weeks up to one or two months, depending upon the climatic conditions over the continents and the SST in the eastern Indian ocean, and may be in phase or out of phase with the ENSO mode of the western Pacific equatorial warm pool. Hendon and Zhang (1997) have noted that there are large differences in the frequency of active and break periods of the Australasian monsoon from year to year.

The coupled system made of the Australasian monsoon and the Indo-Pacific warm pool, including the "maritime continent", is dominated by the huge inertia of the Pacific equatorial basin. However, the Australasian monsoon is able to modify the natural period of oscillation of the Pacific equatorial basin through non linear interaction, to some rational multiple of a year, typical of deterministic chaos, leading to the lack of regularity of ENSO.

In summary, the basic flaw of the delayed oscillator concept is to consider the equatorial Pacific basin as a self sufficient oscillator, able to drive the whole system. This is not so. In reality, the equatorial Pacific climate machine is coupled, via the Australasian monsoon, through the Indo-Pacific warm pool area.

Despite the importance of the Pacific equatorial wave guide, it does not explain all of the variance in climate variability. The heat source associated with the western Pacific warm pool is not the only region of intense atmospheric heating. During the boreal winter, there is a major region of convection extending across the Indian ocean, north Australia and the western Pacific ocean (Webster et al., 1998). From November to March, strong heating associated with the Australasian winter monsoon remains fairly close to the equator, bringing strong convection and precipitations from Indonesia, to north Australia and to Papua New-Guinea. In December through March, broad and strong westerlies extend from the central Indian ocean to the date line.

The westerly wind bursts in the western Pacific ocean correspond to the surges of the Australasian winter monsoon (Davidson et al., 1983; Mc Bride et al. 1995; Fasullo and Webster, 1998). Zhang et al.(1997) have examined the relationship of the East Asian winter monsoon (November through March) with ENSO. It is possible that the westerly wind burst phenomenon could be related to the Siberian high and cold surges through a cascade of interactions, because some of these surges propagate southward and affect the bulk of the maritime continent (100°E-130°E). According to Zhang et al.(1997), winter northerlies over the South China Sea are strong (weak) during La Niña years (El Niño year).

It is suggested that the lack of regularity of ENSO at the decadal time scale is due in part to the "Australasian-Pacific Equatorial Climate System", and to slowly changing background state, such as the slow increase of heat content as observed in the south western Pacific subtropical gyre in 1975-98.

Finally, do these vacillations in the tropical Pacific cause warm events in the Atlantic and in the Indian Ocean as well? Philander (1990) believes that upper-atmospheric changes associated with the increased convection in the eastern equatorial Pacific affects the trade winds over the Atlantic, leading to a strong interannual variability in the equatorial Atlantic.

Actually, some ENSO in the Pacific were followed by a "replica" in the equatorial Atlantic ocean, as it was the case in 1984 and in 1988, suggesting a link between the El Niño events and the Atlantic interannual warm events. For example, a very strong warm event was observed in the Atlantic after the 1982-83 ENSO, one of the most powerful of this century (Gill and Rasmusson, 1983; Philander, 1990). Numerical models (Zebiak, 1993) have confirmed that the 1982-83 positive SST anomalies in the eastern equatorial Pacific were able to remotely force wind anomalies in the tropical Atlantic, leading to the 1984 warm event in the equatorial Atlantic ocean with a time lag of about one year. According to Tourre and White (1995), the Atlantic ENSO is a passive response to a globally perturbed atmosphere, that lags by about one year to 18 months the Pacific ENSO.

Probably, this connection operated again in 1988 after the 1986-87 El Niño. In April 1995, positive SST anomalies (> 1°C) were found in large parts of the eastern Atlantic from the equator to 20°S, where anomalies greater than 4°C were observed along the African coast. However, at that time the 1993-94 El Niño situation was not over in the Pacific.

Contrary to the observed equatorial Pacific wind field, significant zonal wind stresses are observed only in the western-central (50°W-20°W) equatorial Atlantic, not in the Gulf of Guinea. In the former area there are no warm pool and no monsoon related to strong westerly wind bursts, as in the western equatorial Pacific. So, the seasonal impulses of the wind stress in April-May in the central-western equatorial Atlantic offered a wider spectrum of frequencies than in the Pacific. Also, the width of the Atlantic equatorial basin (6000 km) is about one third the size of the Pacific equatorial basin. Equatorial planetary waves (Kelvin waves) excited by impulses due to sudden zonal wind changes along the equator in the area 20°W-50°W will reflect quickly at the near Brazilian coast (at the African coast), leading to reflected equatorial KW (RW) that would stop rapidly the initial perturbations (Philander, 1990).

These multiple reflections at the coasts will destroy the individual signals in the interference processes. These theoretical reasons may explain why, although many analyses were carried out on the T/P SLAs since 1992 (Verstraete, 1997; Park, Gambéroni and Verstraete, 1997), it was impossible to give evidence of KW and RW propagating signals in the equatorial Atlantic as in the Pacific. However, it would be amazing that the same equatorial dynamics would not work in the Atlantic. When the trade winds collapsed over the whole equatorial Atlantic basin, from December 1983 through April 1984, an oceanic phenomenon similar to El Niño occurred in the Atlantic indeed: the equatorial thermocline was 50 m deeper than climatology in the Gulf of Guinea, and careful analyses gave also evidence than this deepening and the concomitant sea level rise of about +12 cm observed in the Gulf of Guinea were due to second mode baroclinic downwelling Kelvin waves in the equatorial Atlantic in 1983-84 (Verstraete and Vassie, 1990; Verstraete, 1992).

If some teleconnection between the tropical Pacific and the tropical Atlantic were demonstrated, we would get some skill in predicting, possibly one year ahead, the climate in the tropical Atlantic.

Other studies seem to demonstrate that the Indian Ocean also responds in its own way to El Niño events. Tourre and White (1995) concluded that there is an El Niño in the Indian Ocean, where the upper-ocean temperature anomalies propagate eastward into the Timor and Banda Seas, in phase with the Pacific El Niño. The Indian El Niño appears as a slow equatorial and eastward propagation in SST, heat storage of the upper 400 m and wind stress anomalies. The 10-15 cm/s propagation speeds of the temperature and wind stress anomalies are about half that observed in the Pacific Ocean.

Acknowledgements

This research was initiated in part in 1994-1995 during a contract fulfilled as Research Manager at the National Tidal Facility of Flinders University, Adelaide, contract sponsored by the Australian Agency for International Development (AusAID). I completed this work later at the Muséum-Paris. I am very grateful to Pr. Geoff Lennon who introduced me to the NTF and the South Pacific Sea Level and Climate Monitoring Project in 1993. I thank Maxence Revault D'Allonnes, Professor and Director of the Laboratoire d'Océanographie Physique at the Muséum for his steady and friendly support and for many stimulating informal talks. George Philander's book (1990), Klaus Wyrtki's works and NOAA monthly Climate Diagnostics Bulletins were a deep source of inspiration.

I acknowledge all my colleagues dedicated to the South Pacific Project since 1992: in Australia, at the AusAid headquarters (Canberra) and at the NTF; in Western Samoa, at the South Pacific Regional Environment Programme headquarters; and in France, at the Muséum-Paris. I am especially indebted to Young-Hyang Park and Lucien Gambéroni (Muséum-Paris) for their friendly collaboration and many instructive discussions. Very generously, Dr. Park provided his programs for processing the T/P data at the NTF.

Many discussions with Chalapan Kaluwin (SPREP) were of great help during the workshops. Bill Mitchell decisively helped for starting the T/P satellite altimetry at the NTF. I also thank all the staff of the NTF, particularly Greg Musiela, Souk Douangphoumy, Than Aung, the computer and technical staff, for their great work, both in the laboratory and in the field, to complete this splendid network of sea level observatories in the western tropical Pacific. I would like to ensure all the Islanders of the Forum Countries, who addressed themselves to the task during many workshops, of my deep appreciation for their untiring efforts and the high spirit of those meetings.

I am also indebted to Patrick Caldwell, Bernie Kilonsky and Mark Merrifield at the University of Hawaii Sea Level Center, who offered so many sea level time series, as well as the harmonic analysis software, generously; to Roger Lukas (JIMAR, Hawaii) for stimulating discussions; to Patrick Vincent and Frédérique Blanc of the AVISO team of CNES (France), attentive to help when we had problems to read the T/P CD-Roms at the NTF and to deliver very high quality Topex/Poseidon Geophysical Data Records.

Finally, I gratefully acknowledge the two anonymous Reviewers and the Editor for their very constructive comments and careful corrections, improving an earlier version of the manuscript considerably.

Research supported by IRD (Institut de Recherche pour le Développement) and Muséum-Paris, under the umbrella of the French national CLIVAR programmes. The South Pacific Project and the tide gauge array are funded and supported by AusAID, Canberra.

References

Anonymous, Climate Diagnostics Bulletin, Climate Prediction Center, National Oceanic and Atmospheric Administration, Washington D.C., 1992-1999.

Aung, T., C. Kaluwin, and G. Lennon, Climate change and sea level, Part one: Physical Science, National Tidal Facility, the Flinders University of South Australia, pp 106, 1998.

Barnett, T.P., Interaction of the Monsoon and Pacific Trade Wind System at interannual time scales. Part I: the equatorial zone, Monthly Weather Review, 111, 756-773, 1983.

Battisti, D.S., Dynamics and thermodynamics of a warming event in a coupled tropical atmosphere-ocean model, J. Atmos. Sc., 45, 2889-2919, 1988.

Battisti, D. S., and A. C. Hirst, Interannual variability in a tropical atmosphere-ocean model: influence of the basic state, ocean geometry and non-linearity,.J. Atmos. Sci., 46, 1687-1712, 1989.

Bjerkness, J., A possible response of the atmospheric Hadley circulation to equatorial anomalies of ocean temperature, Tellus, 18, 820-829, 1966.

Bjerkness, J., Atmospheric teleconnections from the equatorial Pacific, Mon. Weather Rev., 97, 163-172, 1969.

Boulanger J-P., and C. Menkes, Propagation and reflection of long equatorial waves in the Pacific ocean during the 1992-1993 El Niño, J Geophys. Res., 100, 25041- 25065, 1995.

Boulanger J-P., and L.-L. Fu, Evidence of boundary reflection of Kelvin and first-mode Rossby waves from TOPEX/POSEIDON sea level data, J Geophys. Res., 101, 16361-16371, 1996.

Boulanger J-P., and C. Menkes, Long equatorial wave reflection in the Pacific ocean from Topex/Poseidon data during the 1992-1998 period, Climate Dynamics, (in press, 1999).

Busalacchi, A.J., M.J. McPhaden, and J. Picaut, Variability in equatorial Pacific sea surface topography during the verification phase of the T/P misssion, J. Geophys. Res., 99, 24 725-24 738, 1994.

Caldwell, P., Sea level data processing, JIMAR contribution N° 98-319, 72 pp., December 1998.

Caldwell, P., and M. Merrifield, Research quality data holdings of the University of Hawaii sea level Center: August 1997, Jimar contribution N0 96-312, Data report N° 15, 1997.

Cane, M. A., A. C. Clement, A. Kaplan, Y. Kushnir, D. Pozdnyakov, R. Seager, S. E. Zebiak, and R. Murtugudde, Twentieth-Century Sea Surface temperature Trends, Science, 275, 957-960, 1997.

Cartwright, D.E., On the smoothing of climatological time series, sea-level at Newlyn, Geophys, J. R. Astr. Soc., 75, 639-658, 1983.

Cheney, R.E., L. Miller, R. Agreen, N. Doyle, and J. Lillibridge TOPEX-POSEIDON: The 2-cm solution, J Geophys. Res., 99, 24555-24564, 1994.

Davidson, N., J.L. McBride, and B.J. McAveney, The onset of the Australian summer monsoon during winter MONEX: synoptic aspects, Mon. Weather Rev., 111, 496-516, 1983.

Delcroix, T., J. Picaut, and G. Eldin, Equatorial Kelvin and Rossby waves evidenced in the Pacific Ocean through GEOSAT sea level and surface current anomalies, J Geophys. Res., 96 suppl., 3249-3262, 1991.

Delcroix, T., J-P. Boulanger, F. Masia, and C. Menkes, GEOSAT-derived sea level and surface current anomalies in the equatorial Pacific, during the 1986-1989 El Niño and La Niña, J Geophys. Res., 99, 25,093-25,107, 1994.

Diggs, S., N. Hall, and W. White, Joint Environmental Data Analysis Center Contributions to WOCE, International WOCE Newsletter, 22, 15-17, 1996, (Unpublished manuscript).

Fasullo, J., and P.J. Webster, Structure of the ocean-atmosphere system in the tropical western Pacific during strong westerly wind bursts, Q.J.R.Meteorol. Soc., in press, 1998.

Gill, A.E., and E. Rasmusson, The 1982-83 climate anomaly in the equatorial Pacific, Nature, 306, 229-234, 1983.

Gordon, A., and J. McClean, Thermohaline stratification of the Indonesian seas: Model and observations, J. Phys. Oceanogr., 198-216, 1999.

Graham, N. E., and W. B. White, The El-Nino cycle: a natural oscillator of the Pacific ocean-atmosphere system, Science, 240, 1293-1302, 1988.

Harrison, D.E., and B.S. Giese, Episodes of surface westerly winds as obsrved from islands in the western tropical Pacific, J. Geophys. Res., 96, 3221-3237, 1991.

Hendon, H., and C. Zhang, Propagating and standing components of the Intraseasonnal oscillation in tropical convection, J. Atmos. Sci., 54, 741-752, 1997.

Houghton, J. T. et al., Eds., Climate Change 1995-The Science of Climate Change, Cambridge Univ. Press, Cambridge, 1995.

Kessler, W. S., Observations of long Rossby waves in the northern tropical Pacific, NOAA technical memorandum ERL PMEL-86, 1989.

Levitus, S., Climatological atlas of the world ocean. NOAA Professional paper 13, US Gov., 173 pp, 17 microfiches, 1982.

Levitus, S., R. Burget, and T.P. Boyer, World Ocean Atlas 1994, Vol. 3 and 4 Salinity and Temperature, NOAA Atlas NESDIS 3 and 4, Washington D.C., 1994.

Lighthill, M. J., Dynamic response of the Indian Ocean to onset of the southwest monsoon, Phil. Trans. Roy. Soc., 265, 45-92, 1969.

Lukas, R., Observations of air-sea interactions in the western Pacific warm pool during WEPOCS, in Proceedings of the Western Pacific International Meeting and Worshop on TOGA-COARE, edited by J. Picaut, R.Lukas and T. Delcroix, pp. 599-610, Orstom, Noumea, New Caledonia, 1989.

Lukas, R., and E. Lindstrom, The mixed layer of the western equatorial Pacific ocean, J. Geophys. Res., 96, 3343-3357, 1991.

Meehl, G.A., The annual cycle and interannual variability in the tropical Pacific and Indian ocean regions, Mon. Weather Rev., 115, 27-50, 1987.

Mc Bride, J.L., N.E. Davidson, K.Puri, and G.C. Tyrell, The flow during TOGA COARE as diagnosed by the BMRC tropical analysis and prediction scheme, Mon. Weather Rev., 123, 717-736, 1995.

McCreary, J., Eastern tropical ocean response to changing wind systems with application to El Niño, J. Phys. Oceanogr. 6, 632-645, 1976.

McCreary, J., A model of tropical ocean-atmosphere interaction, Mon. Weather Rev., 111, 370-389, 1983.

McCreary, J., and D.L.T. Anderson, An overview of coupled ocean-atmosphere models of El Niño and the southern oscillation, J. Geophys. Res., 96, 3125-3150, 1991.

McPhaden, M.J., TOGA-TAO and the 1991-93 El Niño-Southern Oscillation event, Oceanography, 6, 2, 36-44, 1993.

McPhaden, M.J. et al., The Tropical Ocean-Global Atmosphere observing system:a decade of progress, J. Geophys. Res., 103, 14,169-14,240, 1998.

Matsuno, T., Quasi-geostrophic motions in the equatorial area, J. Meteorol. Soc. Jap., 44, 25-42, 1966.

Moore, D., Planetary-gravity waves in an equatorial ocean, Ph. D. Thesis, 207 pp, Harvard Univ., Cambridge, Mass., 1968.

Musiela, G., and J-M. Verstraete, Topex/Poseidon Altimetry data management at the National Tidal Facility in 1996, Proceedings of the T/P meeting, Southampton, 1996.

Park, Y-H., and L. Gambéroni, large scale circulation and its variability in the south Indian Ocean from TOPEX-POSEIDON altimetry, J. Geophys. Res., 100, 24,911-24,929, 1995.

Park, Y-H., L. Gambéroni, and J-M. Verstraete, Variabilité interannuelle dans l'Océan austral et le long de l'équateur, Actes des colloques du meeting Topex/Poseidon, Biarritz, Octobre 1997.

Patullo, J., W. Munk, R. Revelle and E. Strong, The seasonal oscillation in sea level, J. Mar. Res., 14, 88-155, 1955.

Peacock, S., W., Jenkins, R., Key, and W. Broecker, Assessing the importance of subtropical waters in ventilating the equatorial Pacific thermocline: a combined transient-tracer approach, International WOCE Newsletter, 35, 18-24, 1999, (Unpublished manuscript).

Philander, S.G.H., El Niño, La Niña, and the Southern Oscillation, Academic press, International Geophysics Series, 293pp, 1990.

Philander, S.G.H., T. Yamagata, and R.C. Pacanowski, Unstable air-sea interactions in the tropics, J. Atmos. Sci., 41, 604-613,1984.

Picaut, J., and T. Delcroix, Equatorial wave sequence associated with warm pool displacements during the 1986-1989 El Niño - La Niña, J Geophys. Res., 100, C9, 18393-18408, 1995.

Picaut J., M. Ioualalen, C. Menkes, T. Delcroix, and M. J. McPhaden, Mechanism of the zonal displacements of the Pacific warm pool: Implications for ENSO, Science, 274, 1486-1489, 1996.

Picaut J., F. Masia, and Y. du Penhoat, An advective-reflective conceptual model for the Oscillatory nature of the ENSO, Science, 277, 663-666, 1997.

Rapp, R. H., Y. M. Wang, and N. K. Pavlis, The Ohio state 1991 geopotential and sea surface topography harmonic coefficient models, report, 91pp; Dep. of Geod. Sci., Ohio State Univ., Columbus, 1991.

Rasmusson, E. M., El Niño: The Ocean/Atmosphere connection, Oceanus, 27, 5-12, 1984.

Rasmusson, E.M., and T.H. Carpenter, Variations in tropical sea surface temperature and surface wind fields associated with the Southern Oscillation/ El Niño, Month. Weather Rev., 110, 354-384, 1982.

Schopf, P. S., and M. J. Suarez, Vacillations in a coupled ocean-atmosphere model, J. Atmos. Sci., 45, 549, 1988.

Tourre, Y.M., and W.B. White, ENSO signals in global upper-ocean temperature, J. Phys. Oceanogr., 25, 1317-1332, 1995.

Verstraete, J-M., Seasonal heat content in the eastern tropical Atlantic, Oceanologica Acta, Proceedings International Symposium on equatorial vertical motions, Paris, 6-10 May 1985, 85-90, 1987.

Verstraete, J-M., The seasonal upwellings in the Gulf of Guinea. Progress in Oceanography, 29, 1, 1-60, 1992.

Verstraete, J-M., Comparison of the Pacific and Atlantic equatorial Dynamics as evidenced through tides gauges and Topex/Poseidon altimetry, Jimar Seminar, University of Hawaii, 22 July 1997.

Verstraete, J-M., and J. Vassie, The vertical structure of the zonal and meridional pressure gradients in the equatorial Atlantic during 1983 and 1984, Deep Sea Res., 37, 1-26, 1990.

Verstraete, J-M., and G. Musiela, Maps of the Topex/Poseidon-derived sea surface topography and anomalies (colour plates 3, 4, and 5), 1994 National Tidal Facility Report, 1995.

Verstraete, J-M., and Y-H. Park, Comparison of TOPEX-POSEIDON altimetry and in situ sea level data at Sao Tomé Island, Gulf of Guinea, J. Geophys. Res., 100, 25,129-25,134, 1995.

Verstraete, J-M., L. Gambéroni, and Y-H. Park, Estimates of the secular sea level trend from an array of eleven sea level stations operated in the western tropical Pacific Ocean in 1992-1998, Proceedings of the Oceanology International 99 Pacific Rim Conference, 1999.

Webster, P.J., and R. Lukas, TOGA-COARE: The coupled Ocean-Atmosphere Response Experiment, Bull. American Meteorol. Soc., 73, 9, 1377-1416, 1992.

Webster P.J., V.O. Magaña, T.N. Palmer, J. Shukla, R.A. Tomas, M. Yanai, and T. Yasunari, Monsoons: Processes, predictability, and the prospects for prediction, J. Geophys. Res., 103, C7, 14,451-14,510, 1998.

Woodworth, P.L., A search for accelerations in records of European mean sea level, Intern. Journ. of Climatology, 10, 129-143, 1990.

Wunsch, C., Bermuda sea level in relation to tides, weather and baroclinic fluctuations, Rev. Geophys. Space Phys., 10, 1-49, 1972.

Wyrtki, K., Physical oceanography of the Southeast Asian Waters, NAGA report 2, University of California, 195pp, 1961.

Wyrtki, K., sea level and seasonal fluctuations of the equatorial currents in the western Pacific Ocean, J. Phys. Oceanogr., 4, 91-103, 1973.

Wyrtki, K., The dynamic topography of the Pacific Ocean and its fluctuations, Rep. HIG-74-5, 19 pp., 37 figs., Hawaii Inst. of Geophys., Honolulu, 1974.

Wyrtki, K., El Niño - The dynamic response of the equatorial Pacific Ocean to atmospheric forcing, J. Phys. Oceanogr. 5, 572-584, 1975.

Wyrtki, K., The Pacific NORPAX Sea level network, TOAN Newsletter, 1, 3-5, 1980.

Wyrtki, K., The slope of sea level along the equator during the 1982/83 El Niño, J. Geophys. Res., 89, 10419-10424, 1984.

Wyrtki, K., Water displacements in the Pacific and the genesis of El Niño cycles, J. Geophys. Res., 90, C4, 7129-7132, 1985.

Wyrtki, K., Some thoughts about the west Pacific warm pool. Western Pacific International Meeting and Workshop on TOGA COARE, J. Picaut, R.Lukas and T.Delcroix Eds., Nouméa, 1989.

Wyrtki, K. and R. Kendall, Transports of the Pacific Equatorial Contercurrent, J. Geophys. Res., 72, 8, 2073-2076, 1967.

Yamagata, T., Stability of a simple air-sea coupled model in the tropics, in Coupled Ocean-Atmosphere Models, edited by J.C.J. Nihoul, 637-658, Elsevier, New-York, 1985.

Zebiak, S., Air-sea interaction in the equatorial Atlantic regions. J. Climate, 6, 1567-1586, 1993.

Zhang, Y., K.R. Sperber, and J.S. Boyle, Climatology and interannual variation of the East Asian winter monsoon: Results from the 1979-95 NCEP/NCAR reanalysis, Monthly Weather Rev., 125, 10, 2605-2619, 1997.

Appendix

South Pacific Project

SEAFRAME (SEA level Fine Resolution Acoustic Measuring Equipment)

Lautoka, Fiji		
17° 36' S, 177° 26' E	Start of observations	23 October 1992
Tarawa, Kiribati		
1° 22' N, 172° 56' E		4 December 1992
Port Vila, Vanuatu		
17° 46' S, 168° 17' E		15 January 1993
Nuku' alofa, Tonga		
21° 08' S, 175° 11' W		21 January 1993
Rarotonga, Cook Is.		
21° 12' S, 159° 47' W		20 February 1993
Apia, W. Samoa		
13° 49' S, 171° 45' W		February 1993
Funafuti, Tuvalu		
8° 30' S, 179° 13' E		March 1993
Majuro, Marshall Is.		
7° 07'N, 171° 22' E		May 1993
Nauru		
0° 32' S, 166° 54' E		8 July 1993
Honiara, Solomon Is		
9° 26' S, 159° 57' E		July 1994
Lombrum, Manus Is., Papua New-Guinea		
2° 02'S, 147° 23' E		28 September 1994; March 1996

N.B. The tide gauge in Lombrum was dismantled 3 May 1995, due to some major repairs to be done on the wharf where it was operating. In operation again since 8 March 1996.

National Tidal Facility

Monitoring sites of the South Pacific Project

Sea level Observatories

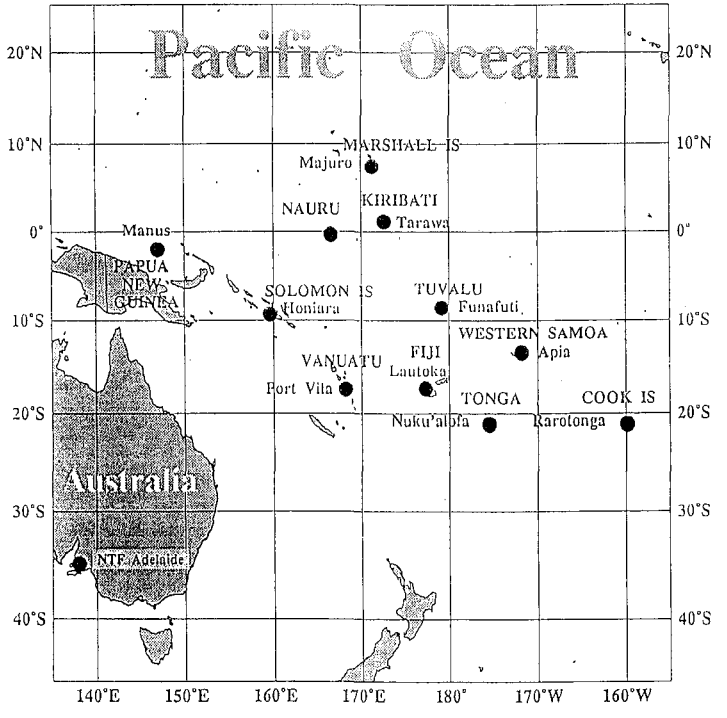

The "Sea level Fine Resolution Acoustic Measuring Equipment" (SEAFRAME) measures sea level at six minutes intervals (from 181 one second samples over a period of 3 minutes) and meteorological data every hour: barometric pressure, wind speed, wind direction, maximum wind gust, sea surface and air temperatures. The accuracy of the monthly sea levels of the NTF SEAFRAME Pacific tide gauge network is estimated to be better than 3 mm.

The SEAFRAME data are transmitted to Japan via the Japanese Geostationary Meteorological Satellite GMS, and to the NTF Adelaide, Australia (over the internet from the Melbourne Meteorological Headquarters). The transmission interval from each station is one hour.

Sea-Level Changes and Their Effects
B.J. Noye & M.P. Grzechnik (Editors)

An Analysis of Variance in Pacific Tide Gauge Data

J. L. Luick
National Tidal Facility, Flinders University, GPO Box 2100, Adelaide SA, Australia.

ABSTRACT: A network of acoustic tide gauges was installed in 1992/93 to monitor long term relative sea level change and contribute to understanding of the tropical Pacific oceanography at shorter time scales. This study analyses the tide gauge data in conjunction with other sources of sea level information, weather and other oceanographic phenomena, over a range of time scales. For simplicity, the study is divided into two Parts. In Part 1, the data from the new network is verified by comparison with data from pre-existing, conventional tide gauges at seven sites where older technology had previously been installed. The accuracy of the acoustic data is found to improve on that of the pre-existing tide gauges, but an error analysis shows that the reduction in random error is not sufficient to reduce the time required to establish a linear trend by more than about one half year. In Part 2 attention is turned to observations of seasonal cycles and planetary waves. Two sites are selected for analysis: Rarotonga and Nuku'alofa. The tide gauge results are compared to sea levels from satellite altimeter and numerical model output. However, the intent is simply to present a preliminary statistical description as a basis for more exhaustive analyses which will be justified as more data comes available.

KEY WORDS: sea level, tide gauge, Rossby waves.

CONTENTS

1. Comparison of Collocated Gauges

1.1 Introduction

Beginning in 1992, the National Tidal Facility (NTF) began installing a network of eleven tide gauges on Pacific island sites (Figure 1). Of the eleven NTF gauges, seven were more or less collocated with pre-existing gauges, which were designed and located either for port operations or to study oceanographic variability at time scales of a few hours to a few years. The NTF network had an additional purpose: to provide the peoples of the Pacific islands accurate information concerning longer term sea level trends in as timely a manner possible. The NTF gauges therefore required a higher resolution than their predecessors, which was achieved by installing gauges based on acoustic technology. Acoustic gauges had previously been installed at a large number of North American sites and have been shown to have higher resolution and improved statistics. The NTF gauges are carefully maintained and first order levelled to coastal benchmarks at 18 month intervals.

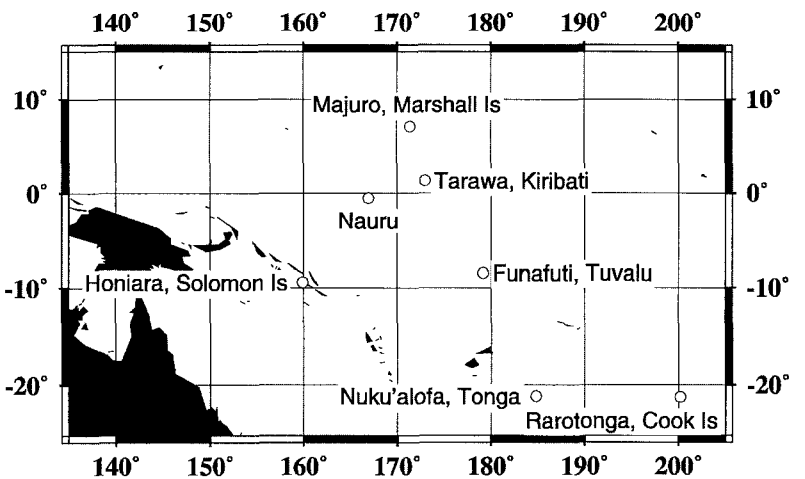

FIGURE 1. Location of study sites.

The NTF gauges are essentially the same as the "Next Generation Water Level Measuring System" (NGWLMS) used by NOAA in its new North American network. However, the NTF has adopted the acronym SEAFRAME (SEA-level Fine Resolution Acoustic Measuring Equipment), as being more descriptive, and this is the term I will use in this report. The SEAFRAME stations contain a pressure-type backup system for water levels but the data used here is entirely from the primary (acoustic) sensor. For simplicity I will refer to the pre-existing gauges, which are of a variety of designs based on conventional bubbler, float- or pressure-driven devices, as "conventional" gauges.

1.2 Sea level data

The SEAFRAME instrument is based on the return travel time of an acoustic pulse. A pulse is sent down a 13 mm (i.d.) ABS tube every second for three minutes, with the time required for each return trip being stored in a buffer. Every six minutes the standard deviation of the three minute data cycle is computed, and an average taken over all values within two standard deviations of the mean. This average, and the standard deviation, is recorded along with the time at the centre of the data cycle. The 13.2 mm tube runs down the centre of a six inch ABS "environmental tube" that also protects the inner tube. A cone at the bottom of the environmental tube reduces the diameter from six to two inches; thus, it has a 3:1 orifice ratio, as compares to a 10:1 ratio typical for the conventional gauges, meaning that the SEAFRAME relies more heavily on digital electronic filtering.

1.3 Comparison with pre-existing gauges

The seven SEAFRAME gauges collocated with pre-existing gauges are on sites ranging from the same wharf on the inside of an atoll to separate wharves on neighbouring boat harbours. The geometry must be understood when comparing the data as the effects of wind set-up,

radiation stress, and river inflow (buoyancy effects) are highly localised.

The seven collocated pairs are shown in Figure 2. The gauges at Tarawa, Nauru, and Honiara are in extremely close proximity, separated by less than twenty metres. Differences in the sea level record are virtually assured to be of instrumental origin. Although the Nauru site is a small boat harbour, westerly winds can cause large amplitude oscillations of period less than one minute. The "conventional" gauge at Honiara was inside a building over 100 metres from the shoreline, connected to the water by an underground pipeline. The Majuro gauges are about two km apart, on the inside of and at the narrow eastern end of an elongated atoll. At Rarotonga, the gauges are about one km from each other, in separate boat harbours, on an

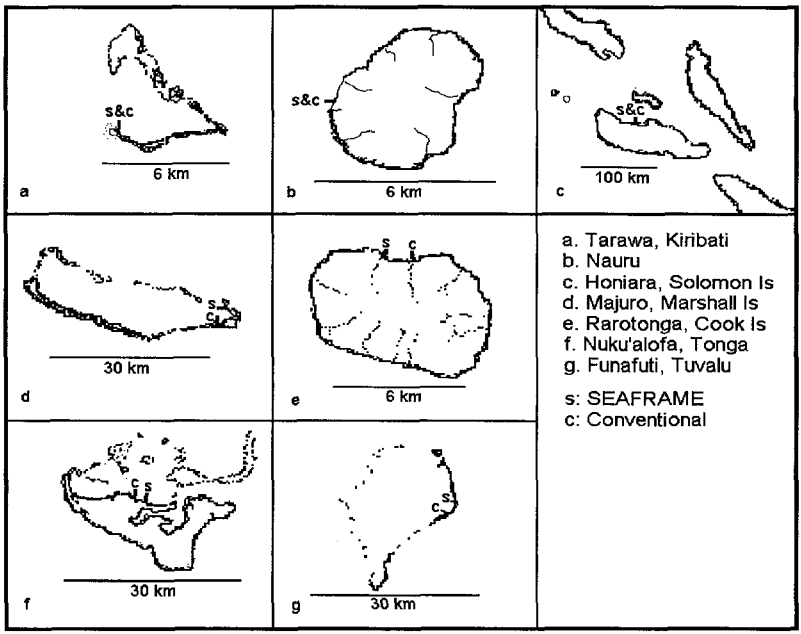

FIGURE 2. Island maps showing locations of SEAFRAME and conventional gauges.

exposed coast. The Nuku'alofa and Funafuti gauges are similarly removed, but are in more protected waters.

Analysis began by subtracting tidal predictions, followed by averaging at hourly and daily intervals. Most of the highest frequency (surface wind wave) portion of the sea level spectrum has already been removed mechanically (by the stilling well) and electronically (six minute averaging) in the case of the SEAFRAME. Variance not thus removed effectively biases the next lower frequency range, i.e., the daily sea levels. The degree to which the daily SEAFRAME values are contaminated by higher-frequency noise can be assessed by comparing them with those from neighbouring conventional gauges (Parke and Gill, 1995).

The sea levels from the pre-existing gauges were reduced from hourly to daily by the University of Hawaii (Mitchum 1987). Because the SEAFRAME records at six-minute intervals, the data was first reduced to hourly (2.5hr lowpass filtered and subsampled), after which a process identical to Mitchum's was used to reduce to daily values. Finally, the mean was removed from each series.

A single time series of *differences* between the daily averages of the sea levels recorded by the SEAFRAME and conventional gauges was formed. These are plotted in Figure 3. The rms differences ranged between 0.4 cm at Tarawa, Honiara, and Funafuti, to 2.0 cm at Tonga.

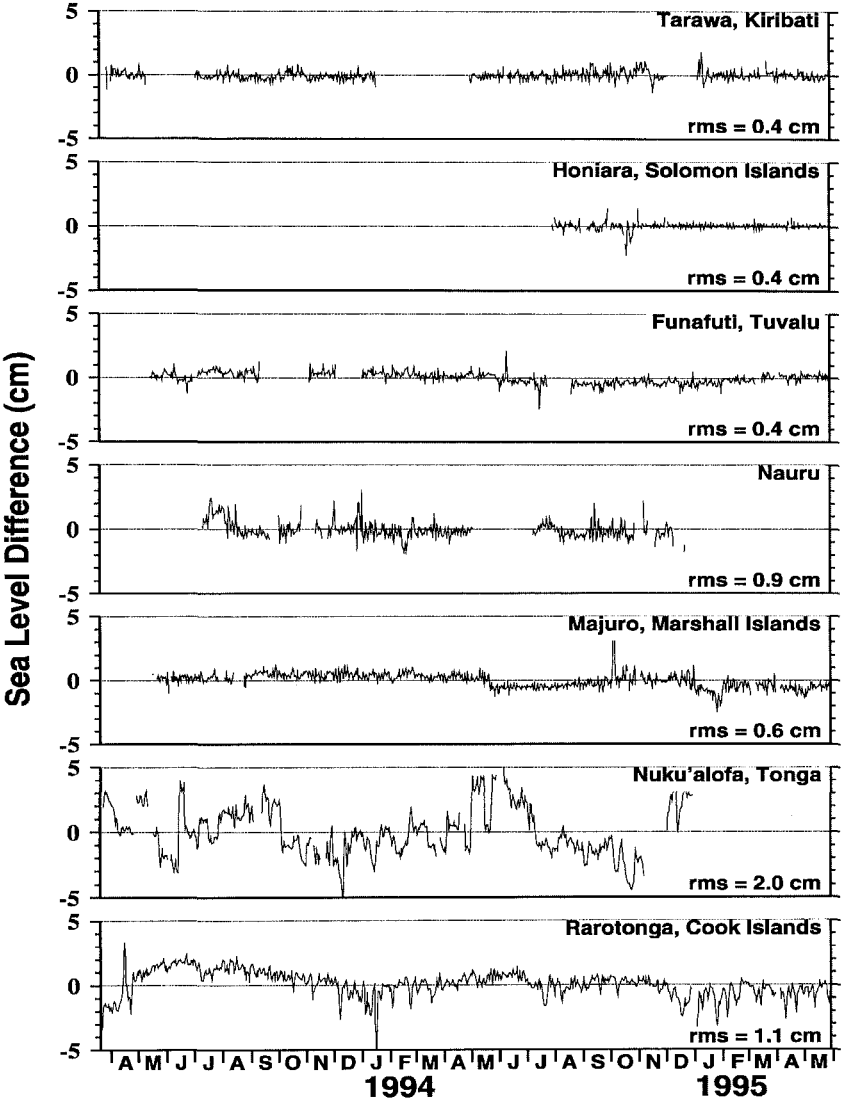

FIGURE 3. Sea level difference time series (SEAFRAME - Conventional).

The smallest rms differences were found at Tarawa, Honiara, and Funafuti. Tarawa and Honiara were two of the three sites whose

gauges were twenty metres or less apart, implying that the geographical separation at the other sites, though only a few kilometres or less, causes significant local differences. The small rms value for Honiara is also significant in that it confirms the accuracy of the sea level record from the long-established conventional gauge.

The third close-proximity site, Nauru, produced a comparatively high rms value (0.9 cm). Possible explanations include degradation of the conventional gauge, which was eventually abandoned following a storm in early 1995, and inability of the stilling well of either or both gauges to damp the oscillations in the small boat harbour in which they are located.

For much of the record at Majuro Atoll, the difference was less than 1 cm. Several exceptional episodes were examined in an unsuccessful effort to identify a systematic cause. These occurred in May 1994 (negative shift of 2 cm), October, 1994 (positive "spike" lasting one week), and December 1994 (negative trend over the course of a month). As none of these anomalies were accompanied by unusual weather patterns, the cause is likely to be at least partly instrumental (eg temporary biological fouling). However, the individual time series of the May 1994 episode (Figure 4) reveal that both gauges recorded a decrease in daily average level. While the SEAFRAME gauge fell by about 12 cm over the course of two weeks, the conventional gauge fell

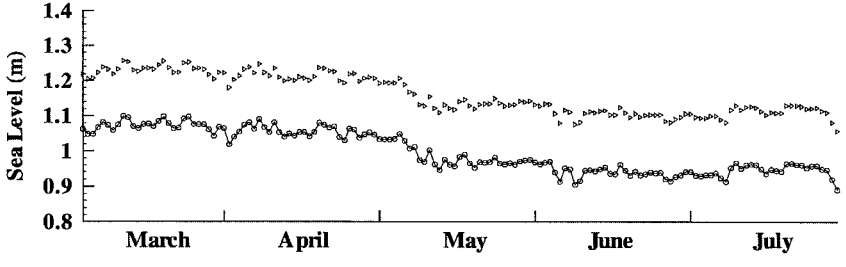

FIGURE 4. Time series of conventional (upper curve) and SEAFRAME sea levels at Majuro.

by only 10 cm. The sea level presumably fell because of the arrival or departure of a mesoscale oceanographic feature; the different response is instrumental.

The conventional gauge at Tonga was in operation a relatively short period (several years) and experienced a history of difficulties. Comparisons with SEAFRAME data revealed numerous short-term datum shifts (a typical example, in March 1994, was left in the figure for the purpose of illustration).

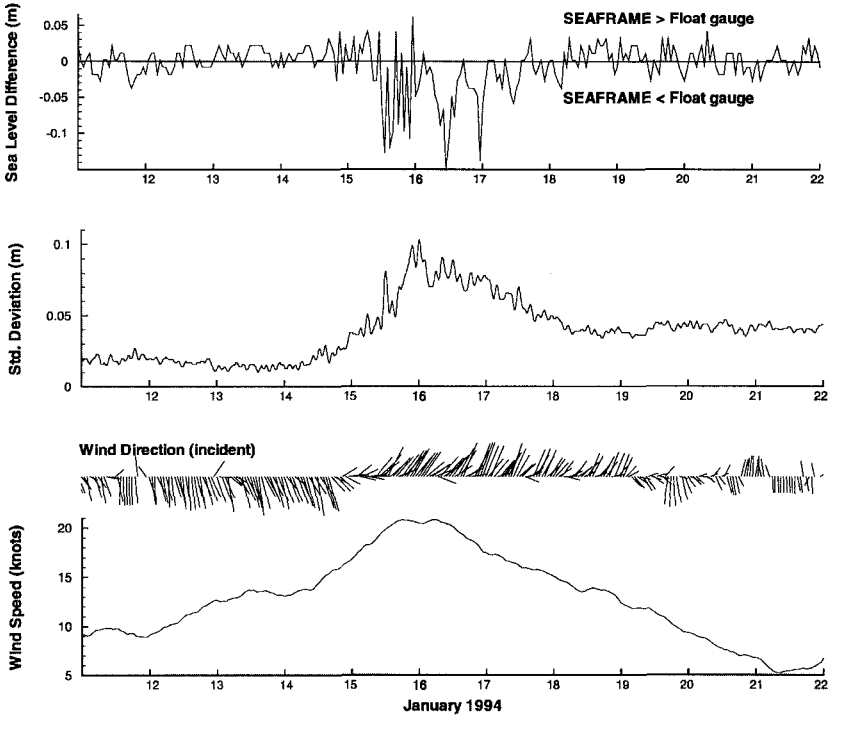

FIGURE 5. Sea level difference (SEAFRAME-Conventional), standard deviation of three-minute SEAFRAME data cycles, incident wind direction, and wind speed at Rarotonga, Cook Islands.

At Rarotonga, Cook Islands, differences as large as 5 cm persist for several months. Apart from the Tonga case, the rms difference was largest for this pair. The cause for this was investigated by focusing on the large episode in January, 1994. The time series of the difference between the hourly averaged sea level records from the two gauges at Rarotonga is presented in Figure 5, along with the standard deviation (σ), wind direction, and wind speed. During the episode, the sea levels recorded by the conventional gauge were further above average than those of the SEAFRAME.

$H_{1/3}$, the mean of the highest one-third of wave crests, can be estimated in accordance with Parke and Gill (1995) as 6.46σ, where σ is the standard deviation of the three minute data cycle described above. Until midday on the 15th, the sea levels recorded by the two gauges differed by less than 5 cm. There followed a sharp increase in σ accompanied by a relative increase in the conventional gauge sea level over that of the SEAFRAME. Over the succeeding two days, σ varied between 0.07 m and 0.1 m, corresponding to an $H_{1/3}$ of between 45 cm and 65 cm.

Prior to the event, winds were light and southerly (offshore). As it developed, the winds increased in strength while swinging around through easterly to northerly (onshore). During the event the hourly averaged wind speeds exceeded twenty knots.

The conventional gauges in this comparison, although heavily "stilled", are not immune to wave pumping, and record an instantaneous, rather than an average value. This may explain the apparently artificially high values in the records from the conventional gauge at the Cook Islands. The SEAFRAME gauges employ a very different design principle. The 3:1 orifice ratio of the SEAFRAME gauge was designed to eliminate resonances within the environmental tube, rather than damp normal wind waves. Wind waves of periods greater than 3 seconds are effectively eliminated by digital filtering of the 3-minute sample bursts (Gill et al., 1995).

1.4 Discussion of Part 1 results

RMS differences between daily sea level derived from SEAFRAME and conventional gauges were found to vary between 0.4 cm and 2.0 cm. The 2.0 cm value was due to a faulty gauge. The next highest rms value was 1.0 cm, and the average rms difference of the six pairs was 0.6 cm, but some of this appears to be due to the small (approx 2 km), but significant, separation between the sites. I estimate that 0.5 cm is a typical rms difference in the daily sea levels.

Close inspection of the effect a minor storm had on sea levels recorded at Rarotonga indicated that the conventional gauge recorded artificially high values. This accords with the more rigorous evaluation by Parke and Gill (1995). Since the rms difference between the two data sets is 1.1 cm, a first estimate of the maximum reduction in standard deviation gained by the SEAFRAME system is on the order of one centimetre. This may be put in terms of the conventional estimate of the time required to establish a trend within prescribed confidence limits. For example, at Rarotonga, the standard deviation about the trend in daily sea levels over the past 2.25 years, is about 7.7cm (based on SEAFRAME data). To compute a trend of ±0.9mm/year (half the global average), with 95% confidence limits, given σ=7.7cm, requires nearly ten years of daily sea level data. In order to cut that interval in half, to five years, σ would have to be reduced to 2.7 cm. Although these estimates are very preliminary, they are in agreement with the view that the *precision* gained by the new acoustic and digital technology can not be expected to remove the requirement for long (> 2 decades) sea level time series for trend estimates.

Tarawa, Kiribati	Honiara, Solomon Is	Funafuti, Tuvalu	Nauru	Majuro, Marshall Is	Nuku'alofa, Tonga	Rarotonga, Cook Is
6.0 (643)	5.6 (302)	6.9 (632)	7.2 (443)	5.9 (719)	6.7 (697)	7.7 (821)

TABLE 1. Standard deviation (cm) about the trend in daily sea levels, based on SEAFRAME data. The numbers in parentheses are the number of days of data analysed.

The above arguments assume that the measurement error follows a random gaussian distribution, which is not the case for errors caused by datum shifts or instrument problems. In order to meaningfully expedite trend detection, we have to look beyond the reduction in random error to other sources of uncertainty. At most sites σ can be reduced by careful filtering of oceanographic "noise" such as inverse barometer response and Rossby waves. This will be especially true of sites such as Rarotonga with large values of σ. More important, perhaps, are rigorous schedules of instrument maintenance and vertical datum control.

Finally, the difference time series at the Majuro site suggests that collocated gauges may also be of aid in datum control. The difference series (719 days) shows a trend of -1.3mm/yr (the SEAFRAME sinking relative to the conventional gauge). Further investigation is required to determine the cause.

2. Low Frequency Variability at Rarotonga and Nuku'alofa

2.1 Introduction

In Part 1, it was suggested that elimination of low frequency oceanographic noise from sea level time series might significantly narrow the error bars on estimates of statistical parameters such as trend. Part 2 takes the logical next step, ie, to identify large spatial scale signals in the satellite altimeter data in the vicinity of the sites, in order to design appropriate filters.

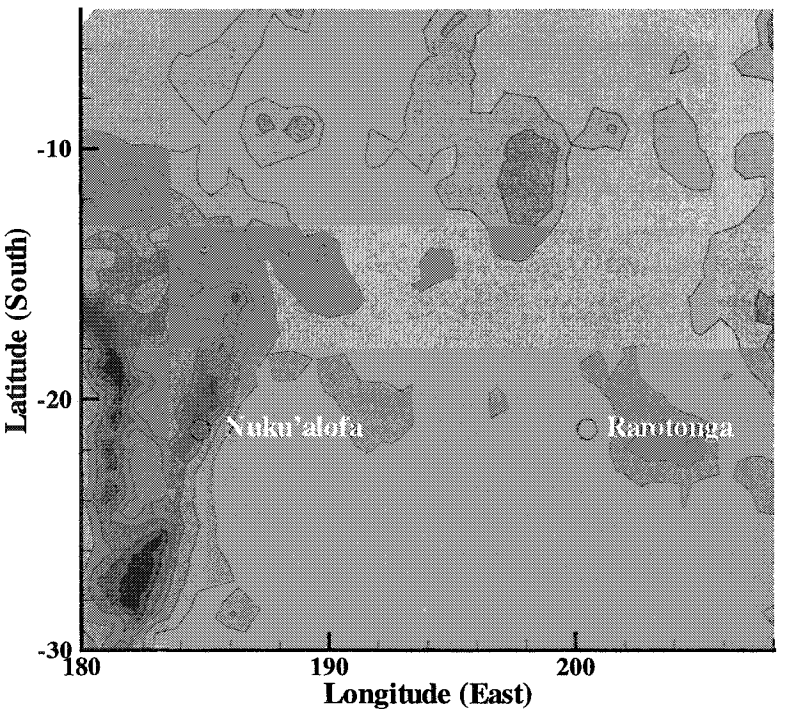

FIGURE 6. Bathymetric map of region with tide gauge sites. Note the Tonga Ridge, which trends northeastward through Nuku'alofa.

With less than two years of data avilable, the two sites were chosen because they are *not* heavily influenced by El Niño (ie, interannual) variability, but *are* affected by Rossby waves. Rarotonga, Cook Islands sea levels were shown by Mitchum (1994) to contain signals of free, westward-propagating, non-dispersive, baroclinic Rossby waves. Nuku'alofa, Tonga, is located on a north-south oriented topographic ridge. The ridge parallels the Tonga Trench, which runs along the eastern side of the ridge. Evidence presented below indicates that free Rossby waves are scattered by the trench/ridge into topographic modes. The two sites are shown on the bathymetric map (Figure 6).

2.2 Sea-level data

The tide gauge data was lowpass filtered twice; first, with a cosine filter with a 2.5 day cutoff period, and then again with a one-dimensional inverse square weighted scheme (Chelton and Schlax, 1993) with an effective 25 day cutoff period. The filters were designed to remove first tidal and then meteorological variability. The series was then subsampled at weekly intervals.

Topex/Poseidon satellite altimetric data (T/P) was obtained from NOAA. Details of the atmospheric and other corrections, and the collinear difference method, can be found in Cheney (1998). As received, data have been averaged along-track and binned at 0.2° intervals of latitude. Afterwards, it was interpolated to a common weekly time base with the tide gauge data, and the mean was removed. The same scheme used for the tides was used for the time interpolation within each bin. Lastly, following common practice in altimeter/tide gauge comparisons, the T/P sea level was spatially interpolated to the location of the tide gauge. A two-dimensional version of the inverse square scheme was used for this, with a search radius of 2°.

Results (sea surface pressure) of a numerical model of the tropical Pacific were obtained from NOAA. The model, known as the Ocean Analysis System (OAS), is driven primarily by assimilation of temperature (XBT) and wind data (Ji *et al.*, 1995). Sea levels are reconstructed "diagnostically" by integration of the steric difference in the model upper layer. At 20°S, the meridional grid spacing is 1° while the zonal spacing is 1½°. The "Weekly Analysis" or WA2 (as opposed to the "re-analysis") was chosen for the following comparisons. A process similar to that used for T/P data was used to interpolate the OAS data to the tide gauge location.

The three resultant time series at each of the two sites are plotted in Figure 7.

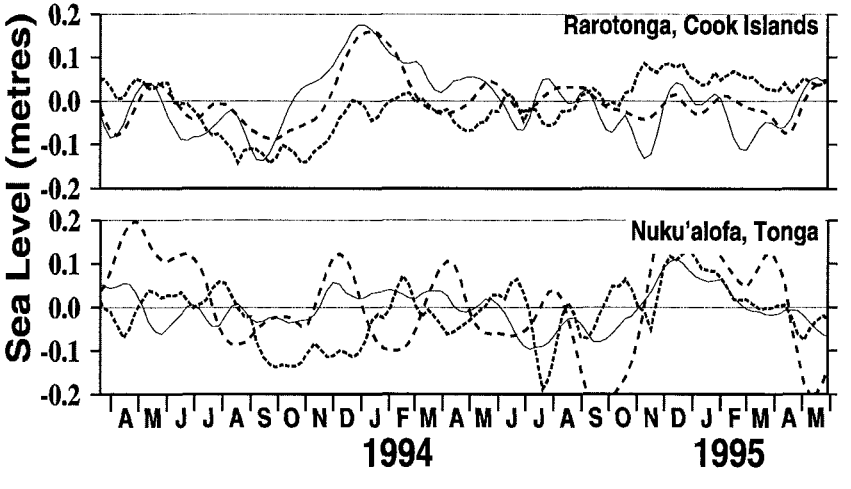

FIGURE 7. Three representations of sea level at the two sites. Solid lines: tide gauge data. Long dashed lines: Topex/Poseidon. Short dashed lines: OAS model.

2.3 Semi-annual and annual cycles

With less than two years of data, estimates of semi-annual or annual cycles (S_{sa} and S_a) can hardly be considered definitive. It is difficult to pick these frequencies visually at either site in Figure 7. The most visible fluctuations, which have an amplitude of 0.1-0.2 m, have shorter periods. Analyses of the tide gauge and T/P series for S_a and S_{sa} are presented in Table 2. Phase is adjusted so that zero phase corresponds to 1 January (and also 1 July for S_{sa}).

	Tide Gauge	T/P	Tide Gauge	T/P	Tide Gauge	T/P	Tide Gauge	T/P
	Sa Amp	Sa Amp	Sa Phase	Sa Phase	Ssa Amp	Ssa Amp	Ssa Phase	Ssa Phase
CI	3.9	1.7	31.8	64	3.0	2.5	9.6	32
TG	5.6	3.2	8.8	28	0.5	1.0	132.6	215

TABLE 2. Amplitudes (cm) and phases (degrees) of annual (Sa) and semi-annual (Ssa) tides at Cook Islands (CI) and Tonga (TG).

Because of the poor agreement between the tide gauge and T/P estimates, it was decided not to remove S_a and S_{sa} from the data prior to analysing the T/P data for Rossby waves.

2.4 Topex/Poseidon ground tracks

The T/P satellite follows exact-repeat tracks. Those nearest Tonga and the Cook Islands are shown in Figure 8. During processing certain sections of the tracks were eliminated, but remaining sections were binned along the track at the points given in the figures.

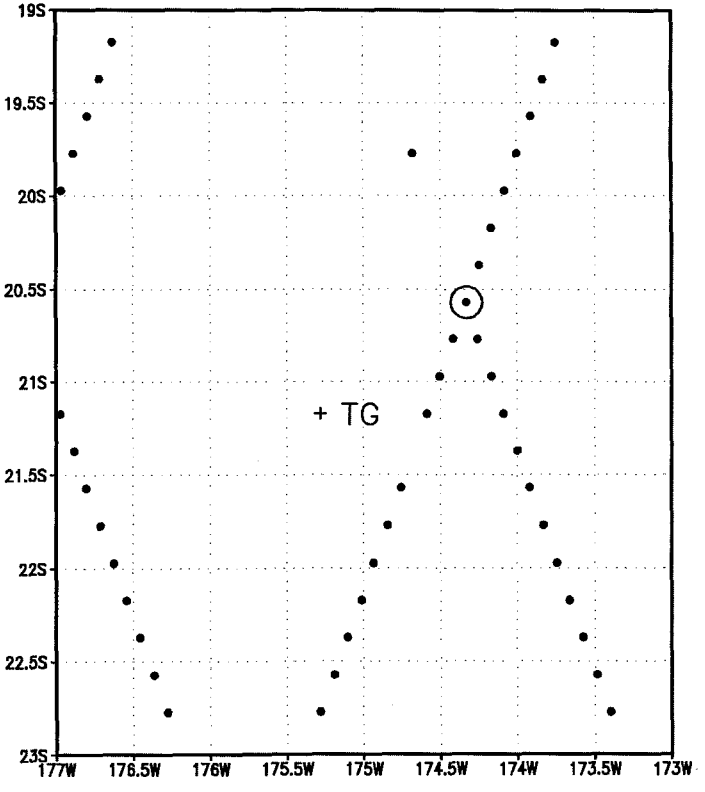

FIGURE 8a. Ground tracks of Topex/Poseidon satellite altimeter in the vicinity of Tonga (TG). The circled point is the "crossover point". Ascending tracks are southwest-to-northeast; descending tracks are northwest-to-southeast.

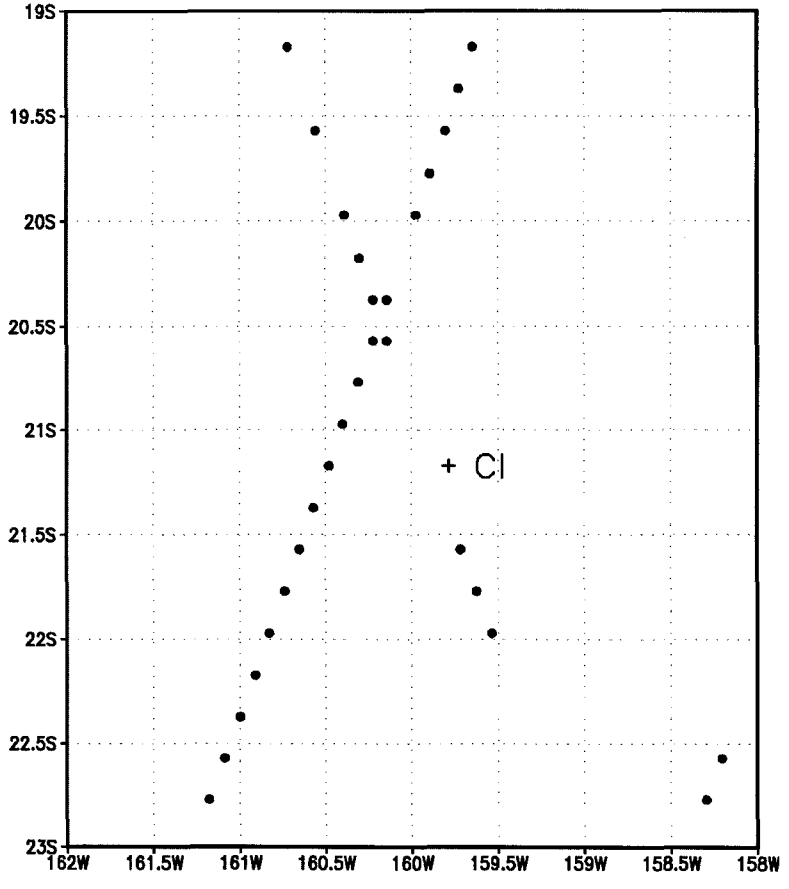

FIGURE 8b. Ground tracks of Topex/Poseidon satellite altimeter in the vicinity of Rarotonga, Cook Islands (CI). Ascending tracks are southwest-to-northeast; descending tracks are northwest-to-southeast.

2.5 Rossby Waves in Cook Island sea levels

In January, 1994, the sea level recorded at the Rarotonga tide gauge was nearly twenty centimetres above normal (Figure 7). To the west, the nearest T/P ground point is located 0.66°, or 70 km, from Rarotonga. At the nearest grid point on the OAS model grid, approximately 0.8° to the south (at 21.5°S, 159.75°W) the model sea levels also rose, by about half the extent observed at the tide gauge. The sea level recorded by T/P at this point was of similar magnitude to the tide gauge, but delayed by approximately 1½ weeks. Mitchum (1994) pointed out that a nondispersive Rossby wave of the correct wavenumber and speed could produce such a delay, ie, when sea levels were delayed or shifted forward in time by the period required for wave propagation, correlations between the tide gauge and T/P sea levels improved. Scatterplots of the tide gauge and T/P data confirm that for the January 1994 event, such is indeed the case (Figure 9). The right hand panel differs from the first only in that the theoretical phase lag (twelve days) for a first-mode, baroclinic, westward-travelling long Rossby wave (wave speed 0.065 m/s at 20°S, for a typical density profile), was applied to the altimeter data at each point prior to the spatial interpolation. The January event is recognisable in the scatterplot because the sea levels were greatest then (points >.1m for T/P). When propagation was accounted for, the relationship became nearly linear for those points greater than 0.1 m, and the rms fit for all points goes from 0.05m to 0.04m, an improvement of 20%. The best fit straight line is obviously improved in that the slope became closer to unity:

propagation ignored (top panel):

$$\text{sealevel}_{(T/P)} = 0.79\text{x}10^{-4} + 0.73 * \text{sealevel}_{(\text{tide gauge})};$$

propagation accounted for (bottom panel):

$$\text{sealevel}_{(T/P)} = 2.8\text{x}10^{-4} + 0.80 * \text{sealevel}_{(\text{tide gauge})}.$$

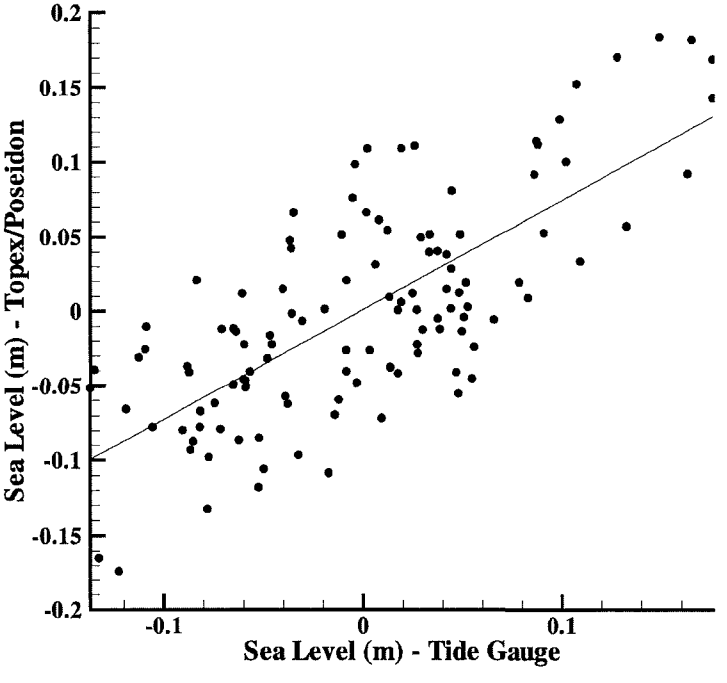

FIGURE 9a. Scatterplots of Rarotonga tide gauge (21.2°S, 159.78°W) vs T/P sea level data at 21.2°S, 160.45°W. In this plot no account is taken for Rossby wave propagation.

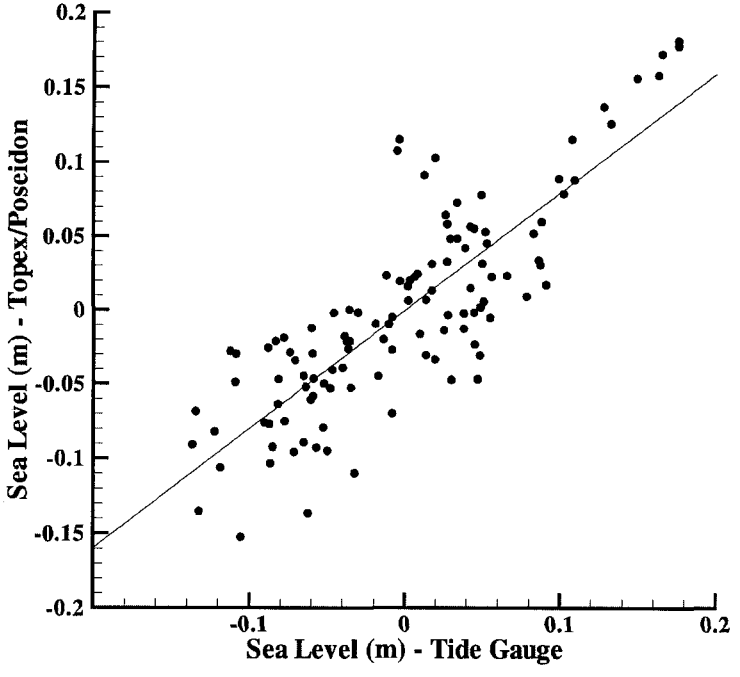

FIGURE 9b. Scatterplots of Rarotonga tide gauge (21.2°S, 159.78°W) vs T/P sea level data at 21.2°S, 160.45°W. In this plot sea levels are delayed in time by an amount equal to the time required for a Rossby wave to travel from the tide gauge to the T/P ground point.

2.6 Topographic Rossby waves near Tonga Ridge

Visual comparison of the Nuku'alofa time series in Figure 7 shows that, compared to the Rarotonga case, poor correlation exists between the T/P and tide gauge data. For example, beginning in September, 1994, T/P records an event which saw the sea level rise from at least 20 cm below normal to more than 20 cm above normal. This event lasted for approximately one half year. Unlike the Rarotonga event, in this case the OAS model sea levels are close to those of the tide gauge, and both show less than half the amplitude of deviation recorded by T/P.

Between October 1993 and August 1994 T/P recorded two positive events with peak to peak amplitudes of about 20 cm. The tide gauge was almost completely unaffected. Again, the T/P time series in Figure 7 is an interpolation over a 2° radius. In order to discriminate specific signals, the individual T/P series were separated into two groups of five time series, with one, the crossover point in Figure 8, in common. The first group included the crossover point and the four nearest ground points along the track running towards the southwest. The second group was similiarly constructed, except that it included ground points from the track leading to the south*east*. Thus (referring also to Figure 6), the first group was comprised of points along a track parallel to the Tonga Ridge, and the second group was from a track leading *across* the Tonga Ridge at an angle of about 45°.

These will be referred to as the "along-shelf group" and the "cross-shelf group".

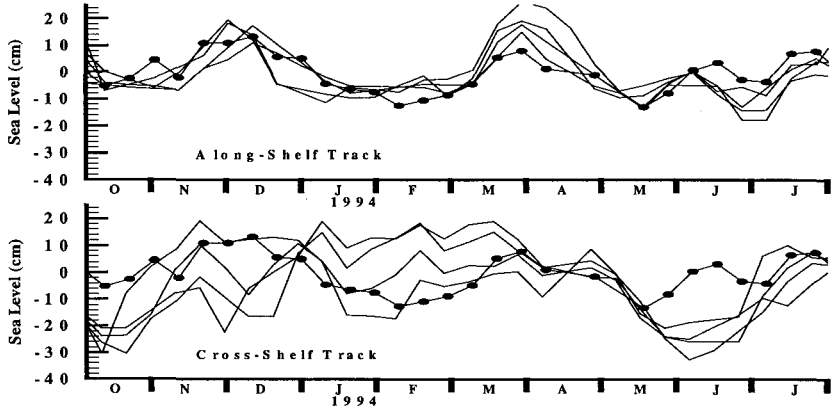

FIGURE 10. Individual time series of sea level from the alongshelf (upper panel) and cross-shelf (lower panel) tracks leading southwards away from the crossover point (dotted in both panels).

The individual time series of the two T/P groups, during the period October 1993 - August 1994, are given in Figure 10. The upper panel series (the alongshelf group) are highly coherent in comparison to the cross-shelf group. In the latter, even the point nearest the crossover point is out of phase with it over most of the interval, showing that the cross-shelf scales of sea level variability are very narrow (tens of kilometres) and also explaining why the signals are not observed at the tide gauge. The fluctuations have periods of about two months.

2.7 Discussion of Part 2 results

Sea levels at two Pacific islands sites were analysed for the presence of large scale planetary waves known as "Rossby waves". In the first instance, the time lag between the occurence of maximum sea level at the Rarotonga tide gauge and at a satellite altimeter ground point to the west led to the conclusion that the sea level maxima were caused by westward-travelling free Rossby waves. In the second case, coherence between sea levels along a satellite track parallel to Tonga Ridge (and incoherence along a track crossing the ridge) led to the conclusion that topographic Rossby waves were present in the data from the along-shelf track. In this case, the tide gauge recorded little or no effect. Sea levels derived from a general circulation model were also affected. At these spatial and temporal scales, such effects are normally associated with changes in the upper layer depth (consistent with the Rossby wave interpretation).

A basic aim of the tide gauge network is to provide estimates of sea level trends. As such, it is important to eliminate oceanographic "noise". The size of the reduction in rms noise achieved by accounting for Rossby wave propagation is about one centimetre. This is on the order of the improvement achieved by installing high precision acoustic instruments rather than conventional gauges (Part 1). It is likely that similar values could be achieved at other sites also affected by planetary waves, such as equatorial Kelvin waves.

At the theoretical wave speed, the Rossby wave observed at Rarotonga at the beginning of 1994 would take somewhat less than a year to reach Nuku'alofa, which is situated due west, on the Tonga Ridge. It is not unlikely that the sea level maximum seen in late December 1995 (Figure 7) was caused by the same wave, despite the fact that the wave amplitude (in T/P sea level) has increased with time. This type of wave is non-dispersive. The amplitude at the Nuku'alofa tide gauge is about half that recorded by T/P. (Although the T/P value is a weighted interpolation over a 2° radius, its amplitude is almost completely determined by its value at the nearest groundpoints to the east). The coherence of sea levels along a track parallel to the Tonga Ridge, combined with the apparent arrival of a free Rossby wave suggests strong trapping along the Tongan Ridge/Trench. The observations are in agreement with a conceptual model in which the wave is generated (presumably by trade winds) to the east of Rarotonga, thereafter propagating westward and increasing in strength as far as the Tongan Ridge/Trench system, at which point about half of its energy is scattered into topographic modes. Conclusive evidence for this model, however, is outside the scope of this article.

The above reconstruction is consistent with the baroclinic model of Wang and Koblinsky (1994), and earlier observations in Geosat data (Okkonen, 1993), but it is speculative and by no means unique. The important point is that the T/P sea levels in the vicinity of Nuku'alofa contain considerable variance, probably due to topographic Rossby waves, which, because it does not appreciably affect the Nuku'alofa sea levels, will degrade any comparison of Nuku'alofa tide gauge data with altimeter data.

2.8 Acknowledgements

The tide data from the pre-existing gauges was produced by the University of Hawaii Sea Level Center. The T/P and OAS data was provided by Robert Cheney of US National Oceanographic and Atmospheric Administration (NOAA), and Ants Leetma and Ming Ji at

the US National Meteorological Center, respectively. Thanks also to RF Henry, Geof Lennon, and an anonymous reviewer for helpful remarks.

3. REFERENCES

Chelton, D.B., and M.G. Schlax (1993) Satellite altimetry: an attempt to progress beyond studies of the statistics of mesoscale variability. *Proceedings of the Aha Huliko'a Hawaii Winter Winter Conference, Univ. of Hawaii,* p.55-101. Eds.: Peter Müller and Diane Henderson, 525 pages.

Cheney, R.E. (1998) Operational altimeter data processing and Assimilation for El Niño forecasts. *Symposium Proceedings, "Monitoring the Oceans in the 2000's", Biarritz, France,* October 1997.

Gill, S.K., R.F. Edwing, D.F. Jones, T.N. Mero, M.K. Moss, M. Samant, H.H. Shih, and W.M. Stoney (1995) NOAA/National Ocean Service Platform Harvest Instrumentation. *Marine Geodesy,* **18**, 49-67.

Ji, M., A. Leetma, and J. Derber.(1995) An Ocean Analysis System for climate studies. Mon. *Weather Rev.*, **123**, 460-481.

Luick, J.L. (1998) An analysis of variance in Pacific tide gauge data. Part 1: Comparison of collocated gauges. *Ocean Atmosphere Pacific* (this volume).

Mitchum, G. (1987) Computation of daily sea level values at the TOGA Sea Level Center. *(Unpublished manuscript) TOGA Centre, Honolulu, Hawaii.*

Mitchum, G. (1994) Comparison of TOPEX sea surface heights and tide gauge sea levels. *J. Geophys. Res.*, **C12**, 24541-24554.

Okkonen, S.R. (1993) Observations of topographic planetary waves in the Bering Slope Current using GEOSAT altimeter. *J. Geophys. Res.*, 98, C12, 22603-22613.

Parke, M.E., and Gill, S. K., (1995) On the sea state dependence of sea level measurements at Platform Harvest. *Marine Geodesy*, **18**, 105-116.

Wang, L., and C.J. Koblinsky (1994) Influence of mid-ocean ridges on Rossby waves. *J. Geophys. Res.*, 99, C12, 25143-25153.

This page is intentionally left blank

Sea-Level Changes and Their Effects
B.J. Noye & M.P. Grzechnik (Editors)

Hindcast Modelling of Recent Tsunamis in the Australian Region

W.M.Mitchell, J.B.Chittleborough and B.J.Noye
National Tidal Facility, GPO Box 2100, Adelaide S.A., 5001, Australia

ABSTRACT: Propagation across the open ocean onto the continental shelf of Australia of tsunami waveforms generated by submarine earthquakes has been modelled using a coarse-grid depth-averaged hydrodynamic-numeric model. The initial conditions require the specification of the seafloor displacement field, which is determined analytically using the seismic parameters of the fault which generated the tsunami.

Focussing mechanisms are evident as the waveform propagation responds to bathymetric features. Near the land boundary, emphasis is upon the envelope of tsunami amplitudes and arrival times, which are compared with tide gauge data where available.

This model has been developed with a view to identify the areas of the Australian coast most vulnerable to tsunami damage due to seismic activity in the Indonesian region and large earthquakes south of Australia. The next phase of this project involves linking this model to a fine-grid coastal-sea model to simulate runup and inundation.

KEY WORDS: tsunami, hindcast, hydrodynamic-numeric, seismic, waveforms, Northwest Shelf.

CONTENTS

1. Introduction

Tsunamis are long gravity waves produced in oceans and coastal seas mainly due to earthquakes, such as the 1993 Hokkaido Nansei-Oki tsunami (Satake and Tanioka, 1995), due to landslides, for example the 1994 Skagway tsunami in Alaska (Nottingham, 1997) or due to volcanic eruption, such as the 1883 Krakatau tsunamis (Latter, 1981). These long ocean waves travel freely from their source with a speed which is proportional to the square root of the water depth - over the deep ocean this can be as great as 700 km/hr. While over the deep ocean their maximum elevation above ambient sea level may only be up to 1 m, they can magnify up to 20 times due to the nature of the coastal topography and may cause much damage to coastal structures and loss of life (Bernstein, 1954).

Tsunamis are commonly observed every few years along the Australian coastline. They are usually small, inflict little damage and can only be detected from tide gauge records. However, the arrival on the northwest coast of Australia of several recent tsunamis which were generated from the seismically active Sunda Arc in the Indian Ocean to the north, has shown they have the potential for great damage.

An earthquake of seismic surface wave magnitude Ms 7.2 off East Java on June 2, 1994 (see Fig.1) generated a tsunami which reportedly inundated some of the Australian coast near North West Cape (AGSO,1998). The height of the tsunami waves which arrived upon this coast were estimated to have reached 4m. On August 19, 1977 a larger earthquake of magnitude Ms 7.9 south of Sumbawa (Fig. 1) also generated a sizeable tsunami, whose arrival upon the northwest Australian coast produced a reported runup of 6m at Cape Leveque, the largest ever reported in Australia (Gregson et al., 1979).

Whilst the seismic activity and relative proximity of the Sunda Arc makes the northwest the most vulnerable section of the Australian coastline to tsunami damage, tsunamis generated from other seismic source regions also reach Australia, such as those due to the 1883 Krakatau volcanic eruption, the 1868 and 1960 Chilean earthquakes, the 1964 Alaskan earthquake and the 1989 Macquarie Island earthquake (AGSO, 1998). More recently, on March 25, 1998, a large earthquake of magnitude Ms 7.9 which occurred south of Australia near the Balleny Islands (Fig. 1) generated a tsunami which produced

oscillations up to 20 cm range on some tide gauges in Australia and New Zealand.

As coastal communities and infrastructure expand, so also does the potential risk of tsunami damage. In order to implement a prediction scheme for tsunamis in the Australian region, a coarse grid hydrodynamic-numeric computer model has been developed for numerical simulation of tsunami generation and waveform propagation from distant seismic sources to the shallow waters of the continental shelf of Australia. The qualitative effects of some such tsunamis have been published. For example, Gregson et al. (1979) have documented the effects of the August 1977 Sumbawa tsunamigenic event, Foley (1994) has described the effect of the tsunami waves which were produced by the June 1994 East Java earthquake and Gregson and Van Reeken (1998) have collected observations of the four major tsunamis in Western Australia since 1880, namely those in 1883, 1885, 1977 and 1994 respectively. Results of a preliminary application of an early version of this computer model to the propagation of the 1994 East Java tsunami to the Northwest Shelf of Australia, is briefly described in Mitchell (1998).

A detailed description of an improved coarse grid deep ocean model and the results obtained for simulation of the East Java, Sumbawa and Balleny Islands tsunami events described above, follows. A nested fine grid model will next be added to permit accurate calculation of runup and inundation in the shallower coastal regions. This is necessary because of the sensitivity of the tsunami-induced flow to rapid changes in coastal topography, as illustrated by both Mader et al. (1988) and Liu et al. (1998). The latter showed the sensitivity to changes in coastal topography of the inundation of Hilo Bay, Hawaii, using both physical and hydrodynamic-numeric models, of the 1960 Chilean tsunami.

The application of the complete model will be of benefit to port authorities, the offshore mining industry, coastal developers and emergency services, as well as serve as a tool for a comprehensive tsunami risk assessment.

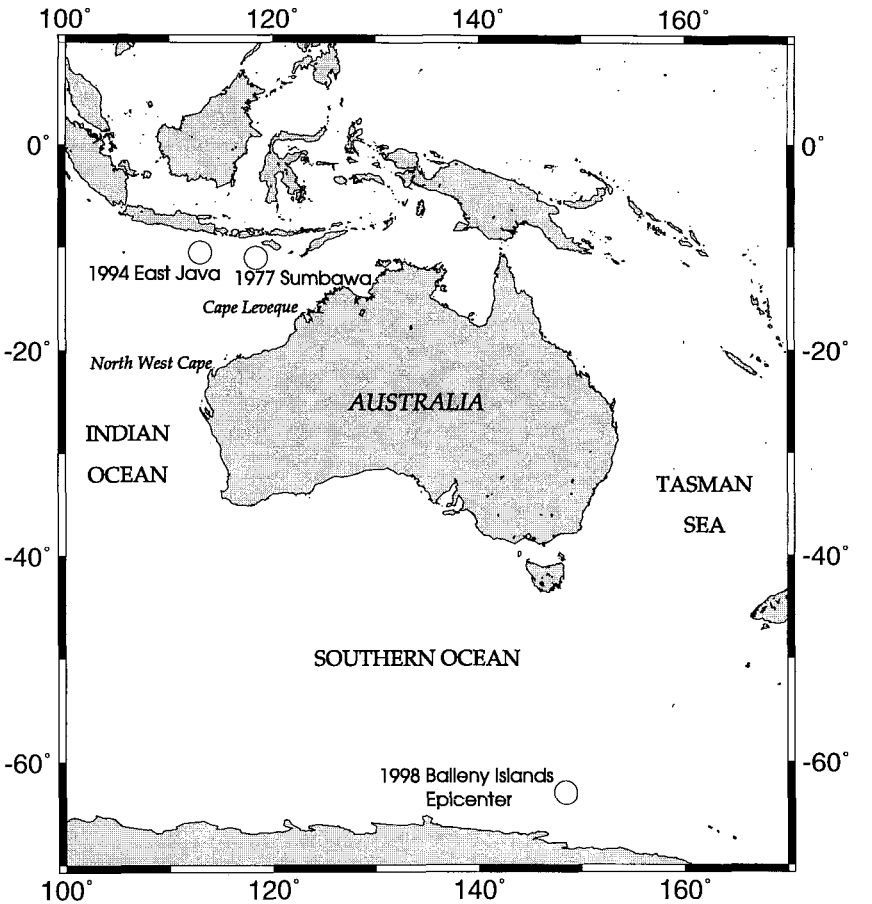

Figure 1. Location of the epicenters (shown by circles) of the modelled tsunamigenic earthquakes. Longitude (see horizontal axis) is in degrees East, latitude (see vertical axis) in degrees North.

2. The Tsunami Source Model

The initial conditions for the hydrodynamic-numeric model are specified by the tsunami source model which is based on the analytical solution of Okada (1985) for the surface deformation due to shear and tensile faults in a half space. This very comprehensive article provides a list of misprints in 11 publications from 1968-1983, of formulae for seismic surface deformation fields.

Whilst Okada's solution allows for an instantaneous seafloor deformation to the steady state solution, in practice allowance must be made for the time taken for the steady state solution to be reached. Therefore the initial results at the seismic source are best obtained by time varying the Okada solution so that it is ramped over a small duration (see, for example, Sinolakis et al.,1995).

The seismic parameters required for the tsunami source model include the strike, dip and slip of the fault measured in degrees, the depth of the hypocenter given in km, the duration of the earthquake given in seconds (s) and the latitude and longitude of the epicenter. Each of these quantities may be obtained from the Harvard University Centroid-Moment Tensor (CMT) solutions, which are produced on a routine basis for events with moment magnitudes greater than 5.5 and published quarterly in *Physics of the Earth and Planetary Interiors*.

The tsunami source model also requires specification of the length and width, given in km, of the seafloor displacement field. Due to the difficulties in acquiring survey data at abyssal depths, this field may be estimated from the spatial distribution of epicenters of the aftershocks. Additionally, a gain factor for the solution may be specified so that the magnitude of modelled sea level disturbances may be scaled to be of the same order of magnitude as observational data.

The parameters used for the source models of the three tsunamigenic events considered are listed in Table 1. A purely thrust type faulting mechanism (dip-slip faulting), where slip is set at 90 degrees, was used to generate a smooth solution. The corresponding spatial distribution of maximum seafloor displacements, $\eta(t)$ at time t, measured in metres, positive upwards, are shown in Figures 2, 3 and 4.

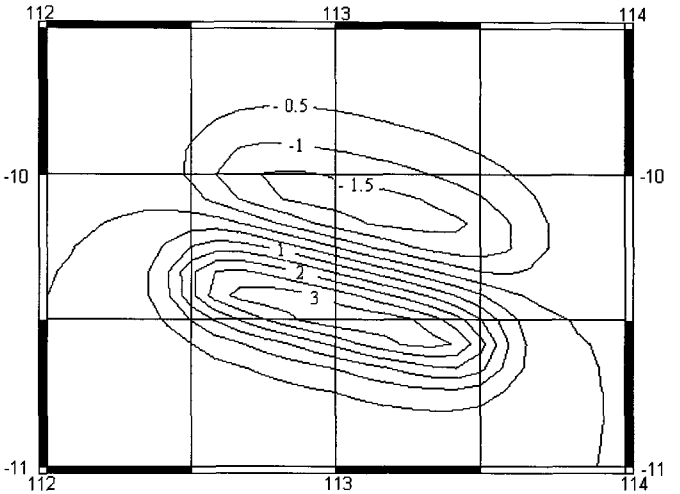

Figure2. Seafloor elevation (metres) from the tsunami source model for the 1994 East Java earthquake.

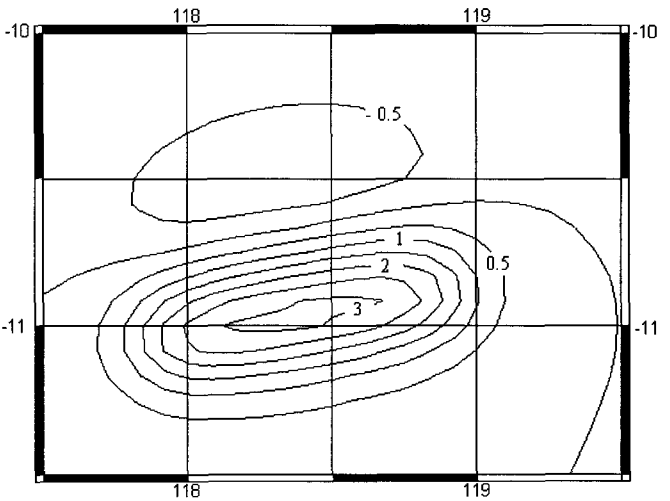

Figure 3. Seafloor elevation (metres) from the tsunami source model for the 1977 Sumbawa Earthquake.

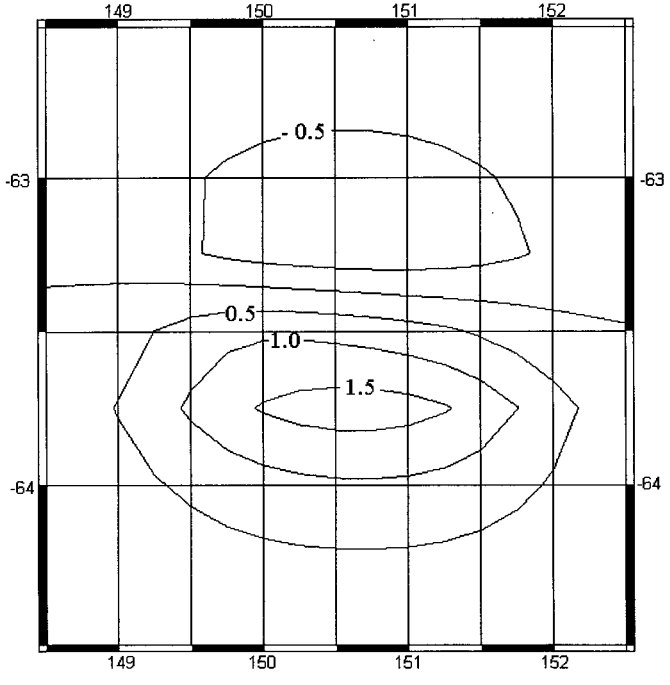

Figure 4. Seafloor elevation (metres) from the tsunami source model for the 1998 Balleny Islands earthquake.

Earthquake	1994 East Java	1977 Sumbawa	1998 Balleny Islands
Magnitude (Ms)	7.2	7.9	7.9
Latitude (deg)	-10.5	-11.0	-63.5
Longitude (deg)	113.0	118.4	150.6
Depth (km)	15	23	35
Length (km)	120	120	120
Width (km)	40	40	40
Strike (deg)	284	260	94
Dip (deg)	12	24	76
Slip (deg)	90	90	90
Duration (secs)	23	60	60

Table 1. Seismic fault parameters used in the tsunami source models.

3. The Hydrodynamic-Numeric Model

The numerical model of the tsunami wave propagation is a finite difference discretisation of the two-dimensional depth-integrated equations for the conservation of mass and momentum in spherical polar coordinates. Assuming that the seas are well mixed in the vertical and that there is negligible non-linear interaction between tides, winds, atmospheric pressure and the tsunami propagation, the equations may be written as follows:

Conservation of mass:

$$\frac{\partial \zeta}{\partial t} - \frac{\partial \eta}{\partial t} + \frac{1}{R\cos\varphi}\frac{\partial U}{\partial \lambda} + \frac{1}{R}\frac{\partial V}{\partial \varphi} - \frac{V\tan\varphi}{R} = 0$$

Conservation of momentum:

$$\frac{\partial U}{\partial t} + \frac{1}{R\cos\varphi}\frac{\partial}{\partial \lambda}\left(\frac{U^2}{H}\right) + \frac{1}{R}\frac{\partial}{\partial \varphi}\left(\frac{UV}{H}\right) - \frac{2UV\tan\varphi}{HR} - fV$$

$$= \frac{N_\lambda}{\rho R^2\cos^2\varphi}\frac{\partial^2 U}{\partial \lambda^2} + \frac{N_\varphi}{\rho R^2}\frac{\partial^2 U}{\partial \varphi^2} - \frac{gH}{\rho R\cos\varphi}\frac{\partial \zeta}{\partial \lambda} - \frac{\tau_{b\lambda}}{\rho}$$

$$\frac{\partial V}{\partial t} + \frac{1}{R\cos\varphi}\frac{\partial}{\partial \lambda}\left(\frac{UV}{H}\right) + \frac{1}{R}\frac{\partial}{\partial \varphi}\left(\frac{V^2}{H}\right) + \left(U^2 - V^2\right)\frac{\tan\varphi}{HR} + fU$$

$$= \frac{N_\lambda}{\rho R^2\cos^2\varphi}\frac{\partial^2 V}{\partial \lambda^2} + \frac{N_\varphi}{\rho R^2}\frac{\partial^2 V}{\partial \varphi^2} - \frac{gH}{\rho R}\frac{\partial \zeta}{\partial \varphi} - \frac{\tau_{b\varphi}}{\rho}$$

in which

t is the time (s),

λ is the longitude, taken as positive in the eastern hemisphere,

φ is the latitude, taken as positive in the northern hemisphere,

$\zeta = \zeta(\lambda, \varphi; t)$ is the sea surface disturbance in metres (m) above mean sea level (M.S.L.) due to the seismic disturbance,

$h = h(\lambda, \varphi)$ is the depth (m) of the sea bed below M.S.L.,

$\eta = \eta(\lambda, \varphi; t)$ is the sea bed elevation (m) due to the seismic event,

$H = H(\lambda, \varphi; t) = h(\lambda, \varphi) + \zeta(\lambda, \varphi; t) - \eta(\lambda, \varphi; t)$ is the total depth (m),

$U = U(\lambda, \varphi; t)$ is the depth-integrated horizontal velocity component ($m^2 s^{-1}$) in the positive λ direction,
$V = V(\lambda, \varphi; t)$ is the depth-integrated horizontal velocity component ($m^2 s^{-1}$) in the positive φ direction,
$f = f(\varphi)$ is the Coriolis parameter in units of s^{-1},
R is the mean radius (6.371315×10^6 m) of the Earth,
ρ is the mean ocean density (1027 kg m^{-3}),
N_λ, N_φ are the mean horizontal eddy viscosity coefficients ($kgm^{-1}s^{-1}$),
g is the acceleration due to gravity (9.81 ms^{-2}),
$\tau_{b\lambda}, \tau_{b\varphi}$ represent bottom friction ($kgm^{-1}s^{-2}$) in the λ, φ directions.

The Coriolis parameter f has the form $2\Omega \sin\varphi$ where Ω is the angular velocity of rotation of the Earth (7.2722×10^{-5} s^{-1}) and the latitude φ is negative in the southern hemisphere. The horizontal eddy viscosity coefficients are given in the Schwiderski (1980) manner, namely

$$N_\lambda = AR\Delta\lambda H(1 + \gamma \cos\varphi)/2$$

$$N_\varphi = AR\Delta\varphi H(1 + \gamma \cos\varphi)/2$$

where $\Delta\lambda$, $\Delta\varphi$ are the uniform numerical grid spacings in the λ, φ directions respectively, A (s^{-1}) is the reduced eddy viscosity coefficient, and γ is a dimensionless longitudinal grading parameter given by $\lambda = 1$ for $-60° < \varphi < 60°$. The value of A was chosen to be 0.0055 s^{-1}, based on Bills (1991).

The quadratic friction formulation is used at the sea floor, namely

$$\tau_{b\lambda} = \rho C_b U\sqrt{U^2+V^2}/H^2$$

$$\tau_{b\varphi} = \rho C_b V\sqrt{U^2+V^2}/H^2$$

where C_b is a dimensionless bottom drag coefficient. A typical value, if C_b taken to be globally constant, is $C_b = 0.0025$ (see Bills, 1991).

The coastal boundary condition is that the velocity component normal to the coast is set to zero, namely $U = 0$ across line segments approximating the coast in the φ direction, and $V = 0$ along line segments approximating the coast in the λ direction.

Along the open boundary the Sommerfeld (1949) formulation of the radiation condition is used in conjunction with a specification of no tide. The Sommerfeld-type formulation of the open boundary condition is along lines of fixed latitude φ = constant,

$$\frac{\partial \zeta}{\partial t} \pm \frac{C}{R\cos\varphi} \frac{\partial \zeta}{\partial \lambda} = 0 \qquad \text{in the } \pm \lambda \text{ direction (respectively),}$$

and along lines of fixed longitude λ = constant,

$$\frac{\partial \zeta}{\partial t} \pm \frac{C}{R} \frac{\partial \zeta}{\partial \varphi} = 0 \qquad \text{in the } \pm \varphi \text{ direction (respectively),}$$

where

$$C = \sqrt{gH}$$

is the phase speed of a free progressive wave in shallow water of depth H.

It was found that this formulation allows the tsunami waves to propagate out of the open boundary of the model with practically no reflection back into the modelled region. This contrasts with the Orlanski (1976) type of calculation of the phase speed, namely, at a given point

$$C = -l_n \frac{\partial \zeta}{\partial t} \Big/ \frac{\partial \zeta}{\partial n}$$

which is computed at a nearby point within the modelled region. Here, l_n is the spherical Lamé parameter in the direction of the outward normal n to the open boundary. This causes most of the incident tsunami wave to be reflected back from the open boundary into the modelled region, as is clearly seen in the following test.

A hypothetical seismic event was located in the deep ocean south of Australia, with epicentre at 134°E, -36°N (see centre of circle, Figure 5). The fault was assumed to be of dimension 120 km x 40 km at a depth of 15 km, with a transient seismic duration of 23 s. ETOPO5 (1988) topography was used in the hydrodynamic-numeric model with 5 minute resolution in latitude and longitude, and a timestep of Δt=12 s. Although the ETOPO5 data resolved the South Australian coastline very poorly (see Figure 5), this was irrelevant to the test being carried out on the open boundaries.

Figure 5(a) shows the tsunami wave after 50 minutes using the Orlanski (1976) formulation for C in the Sommerfeld (1949) radiation boundary condition. The reflection of the waveform from the western and southern open boundaries is very clear. Figure 5(b) shows the waveform at the same time using the classical value of $C = \sqrt{gH}$ in the Sommerfeld formula; the tsunami has passed out through the open boundaries with negligible reflection.

This is more clearly seen in Figure 6, which shows the tsunami profile through the epicentre along the line of longitude 134°E, at 10 minute intervals from 10 to 40 minutes after its generation, for both types of open boundary radiation condition. At 10 min and 20 min, before the first tsunami wave has reached the southern boundary at -40°N, the waveforms appear identical. At 30 min and 40 min an undesired reflection of the south travelling wave by the southern open boundary is clearly seen in the Orlanski (left) sequence of diagrams. This contrasts with the almost complete radiation through the southernmost boundary for the classical scheme (see right sequence of waveforms).

It is worthy to note that the slowing down and amplification of the waveform between -36°N and -34°N occurs over the continental slope, and that 40 minutes after its generation the tsunami has not propagated onto the continental shelf which lies between -34°N and -33°N.

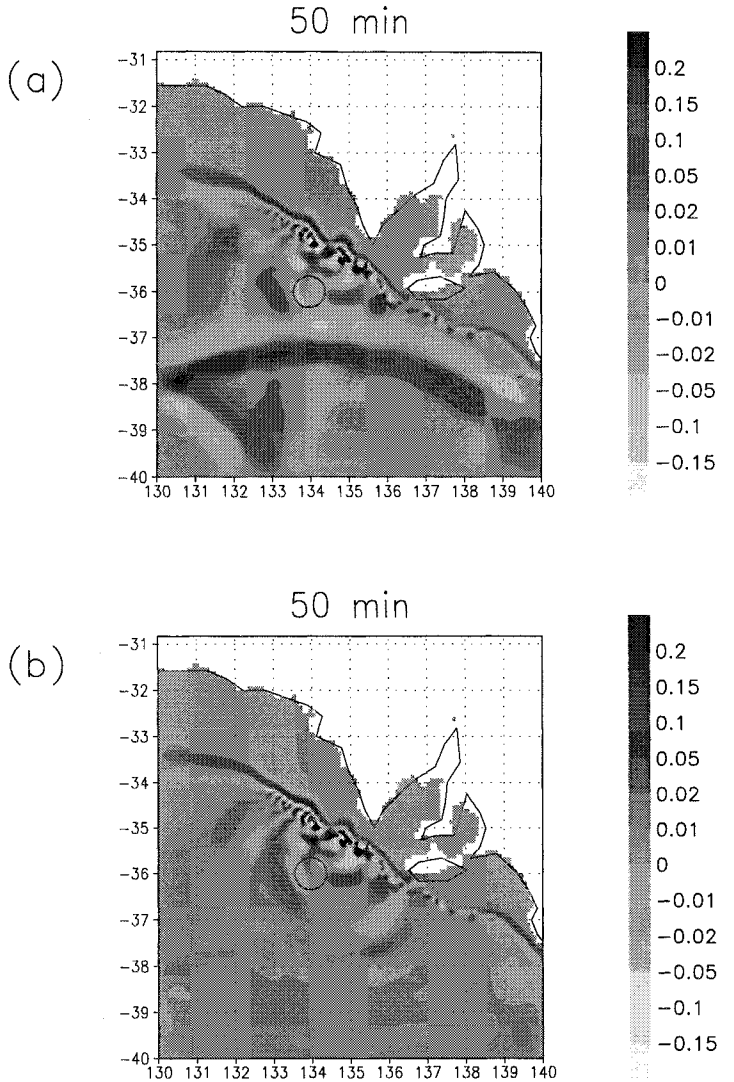

Figure 5. The region modelled for the testing of the two types of radiation boundary conditions tested: 5(a) Orlanski type, 5(b) classical type. The modelled tsunami waveforms (m) are shown 50 minutes after their generation. The ETOPO5 bathymetric data covered the shaded region.

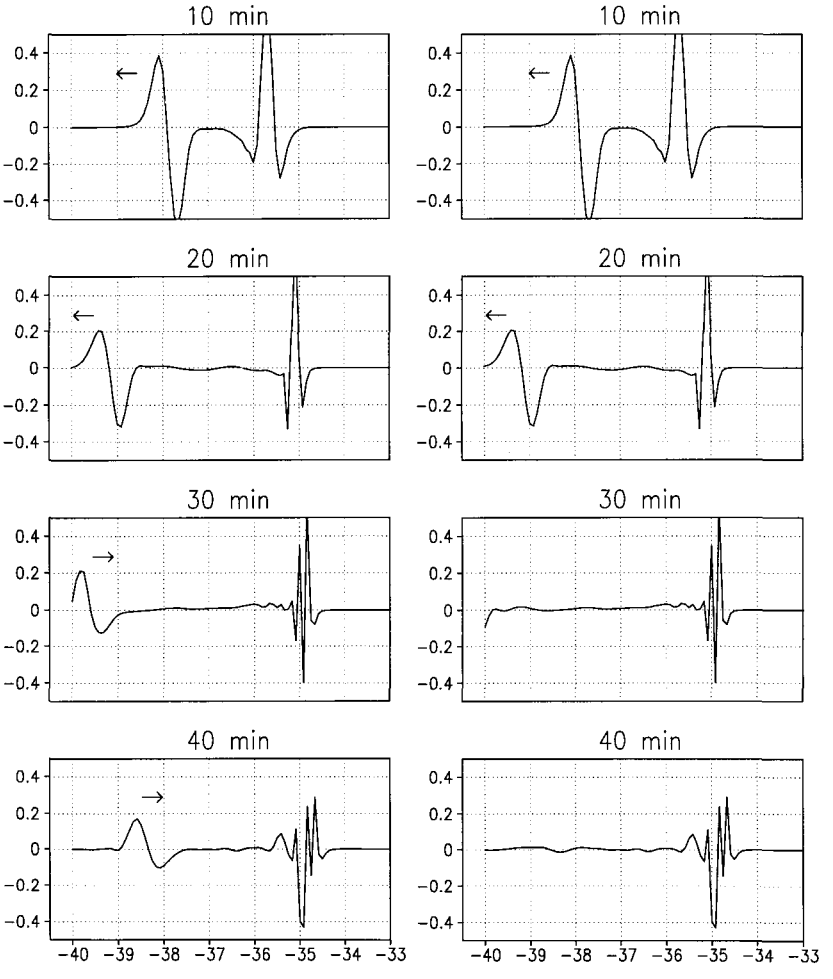

Figure 6. Comparison of the tsunami profile along the line of longitude 134°E between the Orlanski (left) and classical $C = \sqrt{gH}$ (right) methods of calculating the phase speed used in the Sommerfeld-type formulation of the open-boundary condition. The time shown is that which has elapsed from the instant of generation of the tsunami at (134°E, -36°N), as described in the text. The height (m) of the tsunami is shown on the vertical axis, and the latitude (°N) is shown on the horizontal axis.

The grid size used was 5 minutes by 5 minutes latitude and longitude in the Indian Ocean for the Sunda Arc tsunamis. For the Balleny Islands tsunami simulation the grid size used in the Southern Ocean was 15 minutes by 15 minutes. The Arakawa "C'' space-staggered grid system was used for the discretisation, as described in Arakawa and Lamb (1977). The bathymetry was derived from the ETOPO5 (1988) dataset with corrections made for the areas around Darwin, Sumba Island and Timor Island. The model time step, primarily determined by the deepest water and the grid size in the modelled regions, was 12 seconds for the Sunda Arc tsunamis and 30 seconds for the Balleny Islands tsunami. These values were obtained by applying the Courant-Friedrichs-Lewy condition (Courant et al., 1952) which yields the stability criterion for the timestep Δt to be

$$\Delta t \leq \min\{R\,\Delta\varphi,\ R\cos\varphi\,\Delta\lambda\} \Big/ \sqrt{2gh_{\max}}$$

where $h_{\max}$ is the maximum depth below M.S.L.

Initial conditions of zero velocities and zero sea surface elevations were used. Then sea surface elevations provided by the seafloor displacement field, calculated using the tsunami source model based on Okada's (1985) instantaneous deformation solution, were applied in a ramped-up manner over a small interval of time to simulate the transient stage of the deformation.

4. Modelled Indian Ocean Tsunamis

The propagation of the tsunami is determined by the time history of the sea-surface displacements computed by the depth-integrated hydrodynamic-numeric model, using the initial conditions provided by the tsunami source model. Since tsunamis are characteristically very long waves, the physics of their propagation obeys shallow water wave theory in which phase speed is given by $C = \sqrt{gH}$. This dependence of tsunami phase speed on depth is clearly seen by focussing and other features as the waveform propagation responds to changes in depth caused by bathymetric features. The bathymetry of the Indian Ocean off the northwest coast of Australia is shown in Figure 7.

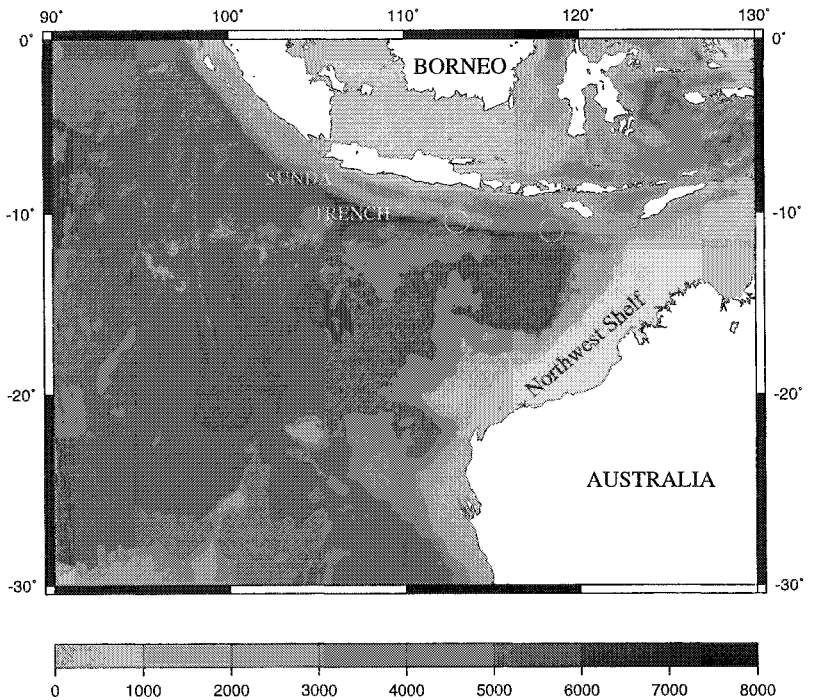

Fig 7. Contoured ETOPO5 bathymetry data (depth in metres) used for modelling the East Java and Sumbawa earthquake tsunamis, epicentres shown by circles.

The location of important bathymetric features such as the Sunda Trench and Exmouth Plateau, and locations on the Australian coast, such as North West Cape and Cape Leveque, are shown in Figure 8.

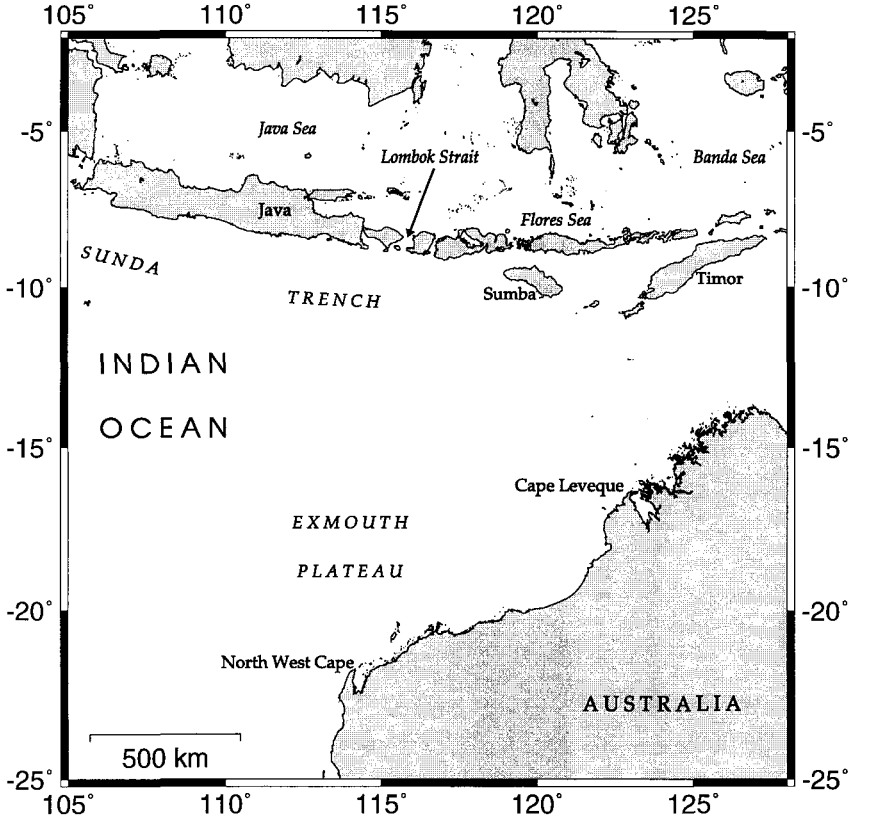

Figure 8. Map locating features mentioned in the text.

4.1 Tsunami Waveform Propagation

1994 East Java Earthquake Tsunami Waveform

The propagation of the East Java tsunami waveform is shown in Figures 9(a)-(f). After 30 minutes from the initiation of the seismic event (Fig.9(b)) the leading waves have made landfall on the southeast coast of Java. After 60 minutes (Fig.9(c)) landfall has extended to West Java and Sumba Island to the east, whilst some wave energy has propagated into the Indonesian Archipelago through Lombok Strait. The effects of shallowing bathymetry off the northwest coast of Australia is evident as the southbound primary wave slows down as it passes over the Exmouth Plateau. After 90 minutes (Fig.9(d)), waveform refraction processes over the Exmouth Plateau are clearly evident, while to the east the shallow continental shelf has slowed the incident tsunami waves. The effects of the wide continental shelf upon the tsunami is clearly seen in the 120 and 180 minute "snapshots" (Fig.9(e)-(f)) as wavelength and phase speed are dramatically reduced compared to the tsunami waves propagating rapidly into the deep waters of the Indian Ocean. The waveform refraction over the Exmouth Plateau appears to focus the tsunami as it makes landfall toward the North West Cape, relatively unhindered by the narrow continental shelf on this section of the coast. The presence of underwater features to the west are highlighted by the waveform propagating into the Indian Ocean.

1977 Sumbawa Earthquake Tsunami Waveform

The propagation of the Sumbawa tsunami waveform is shown in Figures 10(a)-(f). After 10 minutes (Fig.10(a)) the leading wave is about to make landfall on Sumba Island. After 60 minutes (Fig.10(b)) landfall has occurred from East Java to Timor, and the tsunami has begun to penetrate into the Indonesian Seas. Closer to Australia, the leading wave has reached the shallow continental shelf and has slowed down, a junction in the wavefront highlighting its refraction at the edge of the continental shelf. From 90 to 120 minutes (Fig.10(c)-(d)) the tsunami waves have advanced over the continental shelf toward the Australian coastline with reduced phase speed and wavelength. Refraction around the Exmouth Plateau again acts to focus the tsunami prior to its landfall upon the coastline in the vicinity of the North West Cape. By comparison, the tsunami is seen to propagate rapidly into the Indian Ocean, with two underwater features off the west coast producing perturbations in the wavefront.

(a) Elapsed time 10 mins

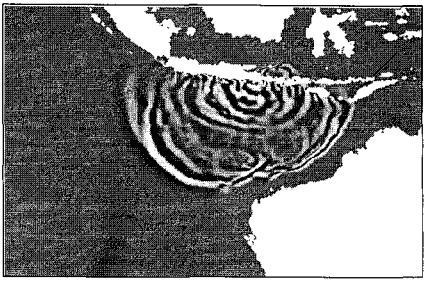

(d) Elapsed time 90 mins

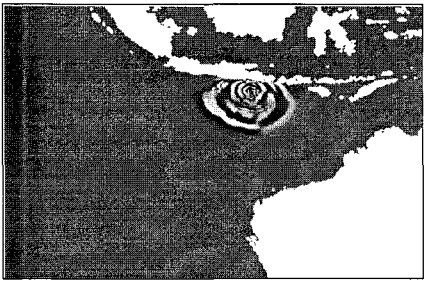

(b) Elapsed time 30 mins

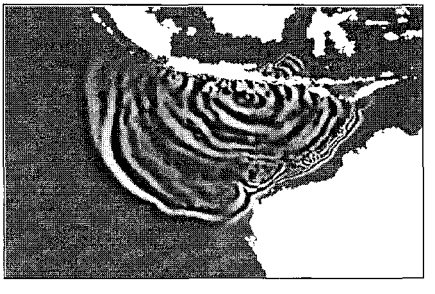

(e) Elapsed time 120 mins

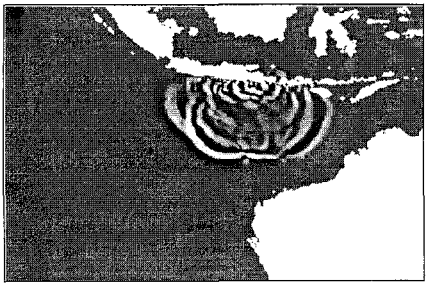

(c) Elapsed time 60 mins

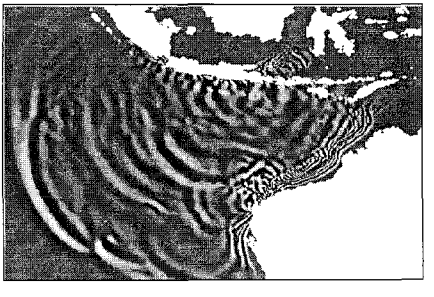

(f) Elapsed time 180 mins

Figure 9. The modelled 2 June 1994 East Java tsunami propagation.

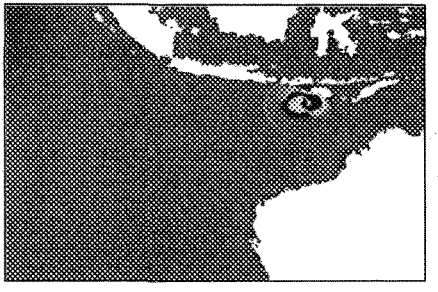

(a) Elapsed time 10 mins

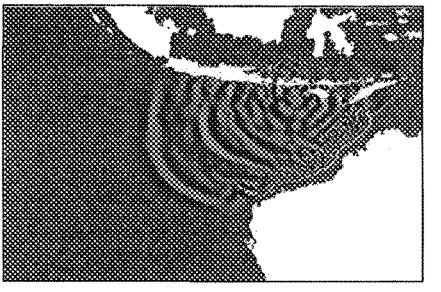

(d) Elapsed time 120 mins

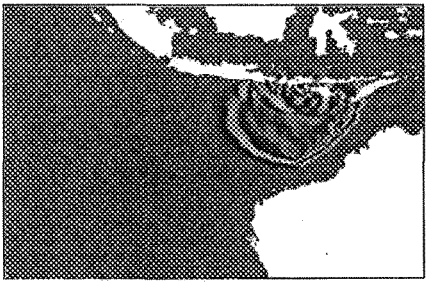

(b) Elapsed time 60 mins

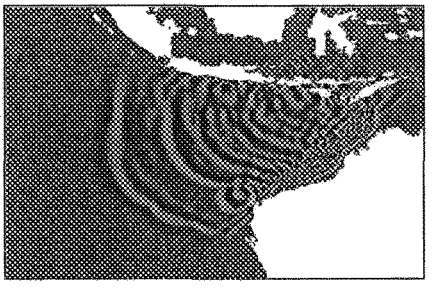

(e) Elapsed time 150 mins

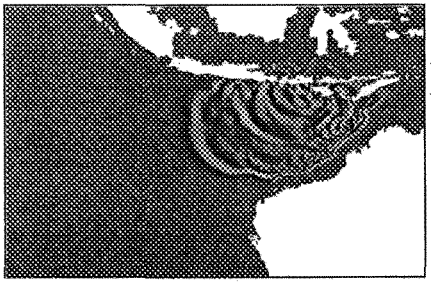

(c) Elapsed time 90 mins

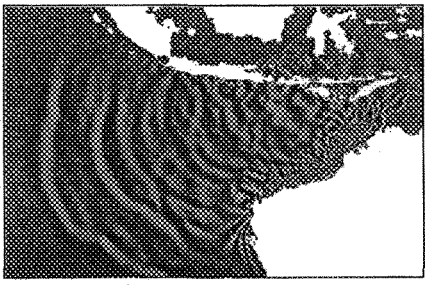

(f) Elapsed time 200 mins

Figure 10. The modelled 15 August 1977 Sumbawa tsunami propagation.

4.2 Arrival at the Australian Coast

1994 East Java Tsunami

Figure 11 identifies locations in Australia which are vulnerable to sea-level changes caused by tsunamis generated in the East Java region. The largest modelled sea-level changes and earliest arrival (Fig.11(a)) were at the extreme northwest tip of Australia where the continental shelf width is at its minimum. The envelope of tsunami disturbance is clearly centred about this section of the coast, where inundation of the Ningaloo National Park led to reports of four metre high tsunami waves. This is shown more clearly in Figure 11(b), which illustrates the relative range of the East Java tsunami waveform at certain places along the northwest coast. For a given location this range is defined as the distance between the maximum and minimum modelled sea level, which is then divided by the largest range which occurred for all locations considered to give the *normalised maximum range*.

1977 Sumbawa Tsunami

The modelled sea levels along the northwest Australian coast for the 1977 Sumbawa tsunami are shown in Figure 12. Tsunami arrival times (Fig.12(a)) are again centred about the extreme northwest tip where the shelf width is at its minimum. Despite a local maximum in sea-level perturbations here, a significant tsunami range is also found on parts of the coast where the continental shelf is wider. Unlike the East Java tsunami, the largest modelled tsunami range for the 1977 Sumbawa tsunami (Fig.12(b)) was found at Cape Leveque, north of Broome, which is in agreement with the observed tsunami of 6m at this location, the largest ever reported in Australia (AGSO, 1998). Modelling of the 1977 and 1994 Sunda Trench earthquake tsunamis has identified an area of high tsunami risk towards the northwest tip of the Australian coastline. Waveform refraction processes over the Exmouth Plateau effectively focus tsunami waves upon this section of the coast, which is characterised by a narrow continental shelf and exposed coastline. Elsewhere along the northwest Australian coast, the arrival and height of tsunamis appears sensitive to the location and orientation of the fault.

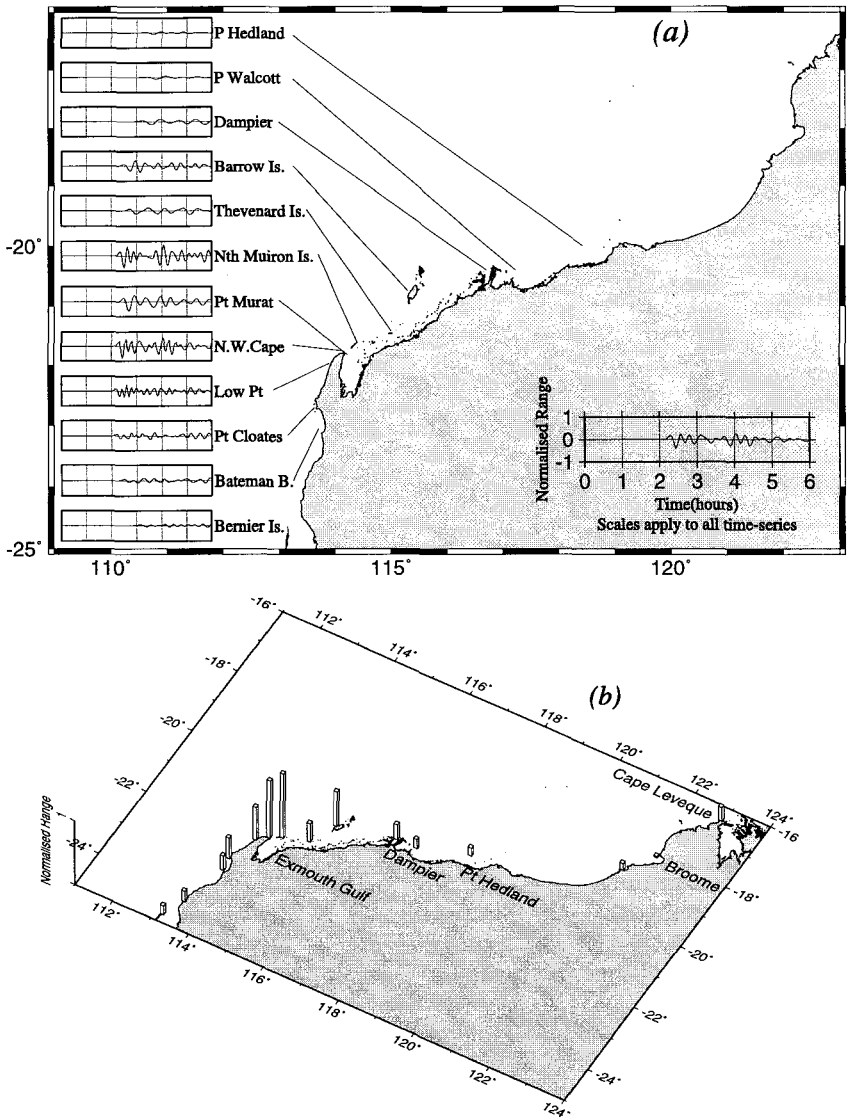

Figure 11. Features of the East Java tsunami upon arrival on the northwest coast of Australia. 11(a) (top): The modelled sea-level time series at selected locations. 11(b) (bottom): Normalised modelled maximum tsunami ranges.

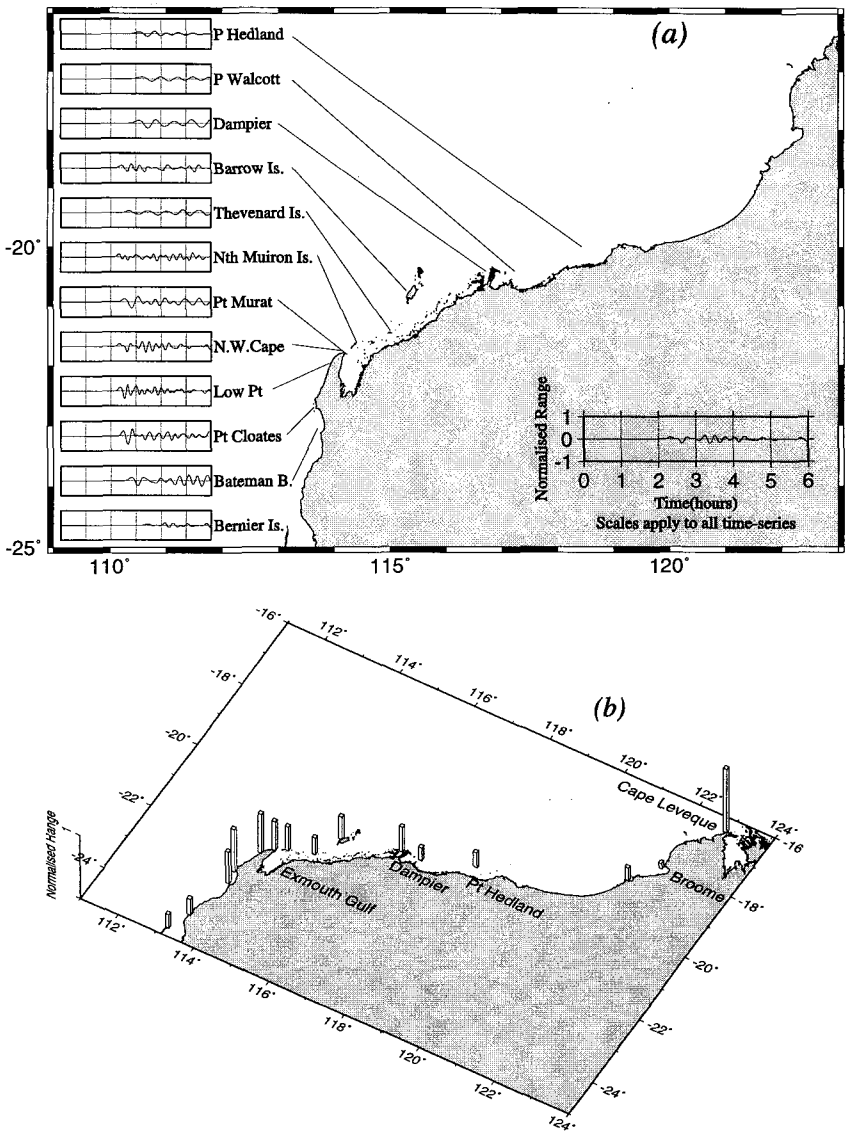

Figure 12. Features of the Sumbawa tsunami upon arrival on the northwest coast of Australia. 12(a) (top): The modelled sea-level time series at selected locations. 12(b) (bottom): Normalised modelled maximum tsunami ranges.

5. Modelled Southern Ocean Tsunami

The bathymetry of the Southern Ocean south of Australia is shown in Figure 13 while the location of the important features are shown in Figure 14. Features which influence the propagation of long waves in the Southern Ocean include the Southeast Indian Ridge, with depths as small as 200m in parts, which separates the South Indian Basin, with depths as large as 4850m, from the South Australian Basin which has a maximum depth of 5950m. Somewhat similar features may be seen each side of the Pacific-Antarctic Ridge south of New Zealand.

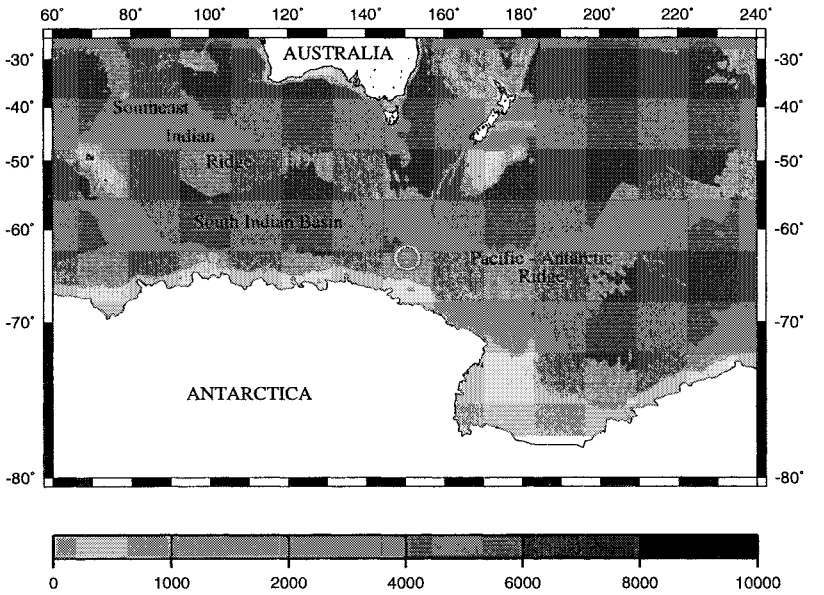

Figure 13. Contoured ETOPO5 bathymetry data (depth in metres) used for modelling the Balleny Islands earthquake tsunami. The circle shows the location of the epicentre of the Balleny Islands tsunamigenic earthquake.

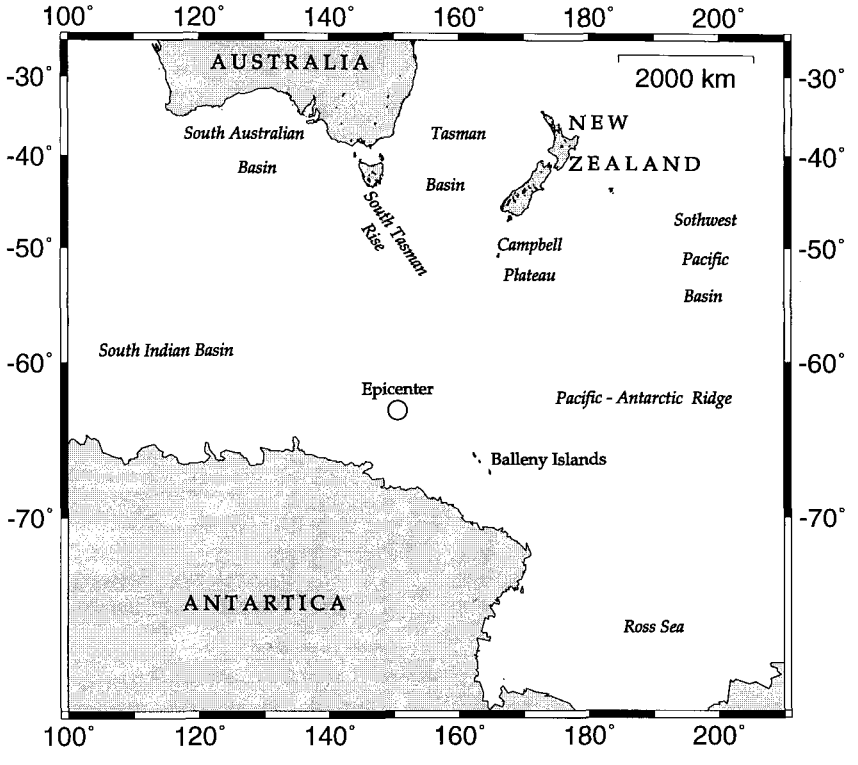

Figure 14. Map of the Southern Ocean south of Australia showing features mentioned in the text.

5.1 Tsunami Waveform Propagation

The propagation of the Balleny Islands tsunami waveform is shown in Figure 15(a)-(f). After 60 minutes (Fig.15(b)) the tsunami waveform has made landfall and is subsequently reflected from the Antarctic coastline. From 120 to 180 minutes after its generation (Fig.15(c)-(d)) the waveform has responded to the shallowing bathymetry of the Campbell Plateau south of New Zealand, as well as that of the South Tasman Rise south of Tasmania. As time progresses (Fig.15(e)-(f)) a sizeable tsunami continues to propagate eastwards into the South West Pacific Basin and the Ross Sea of Antarctica, slowing over the Pacific-Antarctic Ridge.

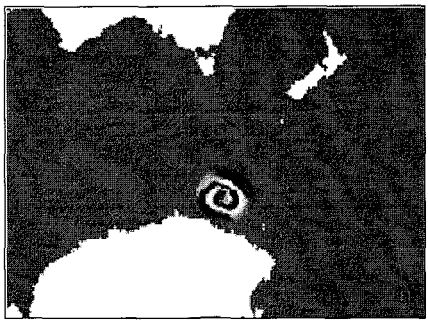

(a) Elapsed time 20 mins

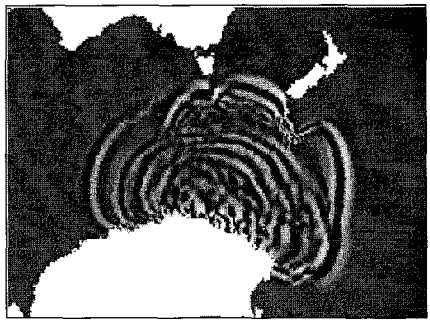

(d) Elapsed time 180 mins

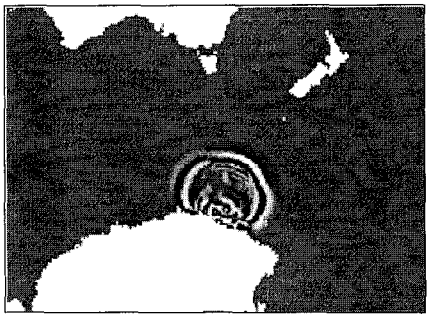

(b) Elapsed time 60 mins

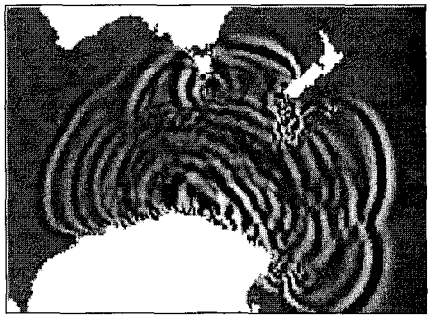

(e) Elapsed time 240 mins

(c) Elapsed time 120 mins

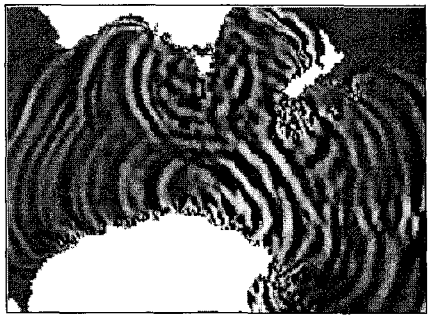

(f) Elapsed time 320 mins

Figure 15. The modelled 25 March 1998 Balleny Islands tsunami.

The deep Tasman Basin allows the tsunami to rapidly propagate up the east coast of Australia and west coast of New Zealand, without much loss of amplitude, while the east coast of New Zealand appears protected by the shallow Campbell Plateau (see Figs.13 and 14). Refraction around the South Tasman Rise propagates waves into the South Australian Basin, which are seen to reach the Great Australia Bight after 320 minutes.

5.2 Comparison with Tide Gauge Data

The locations of the tide gauges against which the Balleny Islands tsunami simulation is compared are shown in Figure 16. The size of the finite difference grid used for this model (15 x 15 minutes) restricts its ability to resolve the effects of coastal topography.

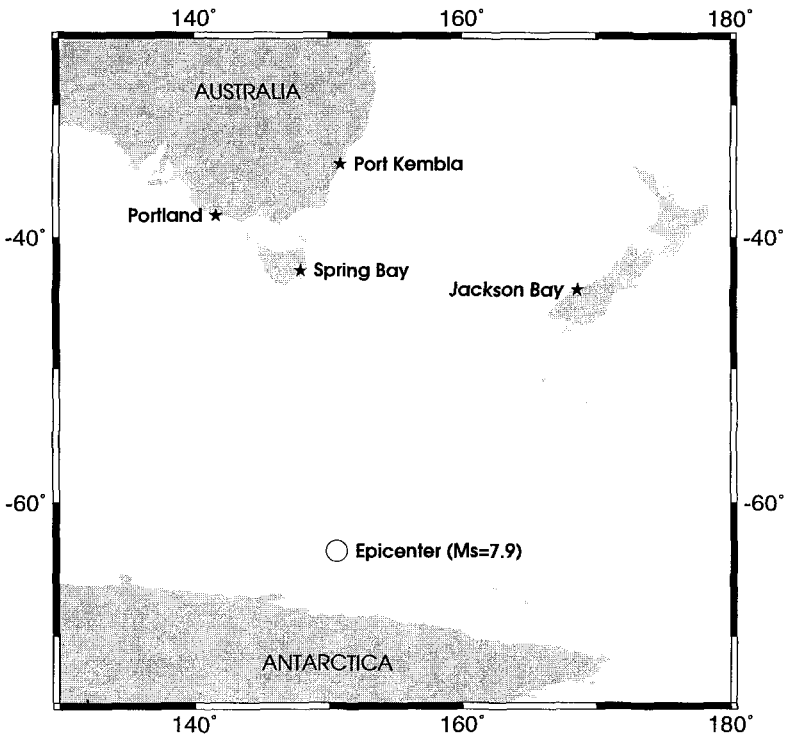

Figure 16. Location of tsunami source and tide gauges where a tsunami signal was recorded for the 1998 Balleny Islands earthquake tsunami.

This is seen in Figure 17, which shows the coastline, location of the tidegauge and the corresponding model element used for the comparison. The effect of a relatively coarse grid is that sub-grid scale tsunami resonance within small coastal basins, which are seen on tide gauge records, are not resolved by the model. This problem will be overcome when fine-grid sub-models are incorporated in the system.

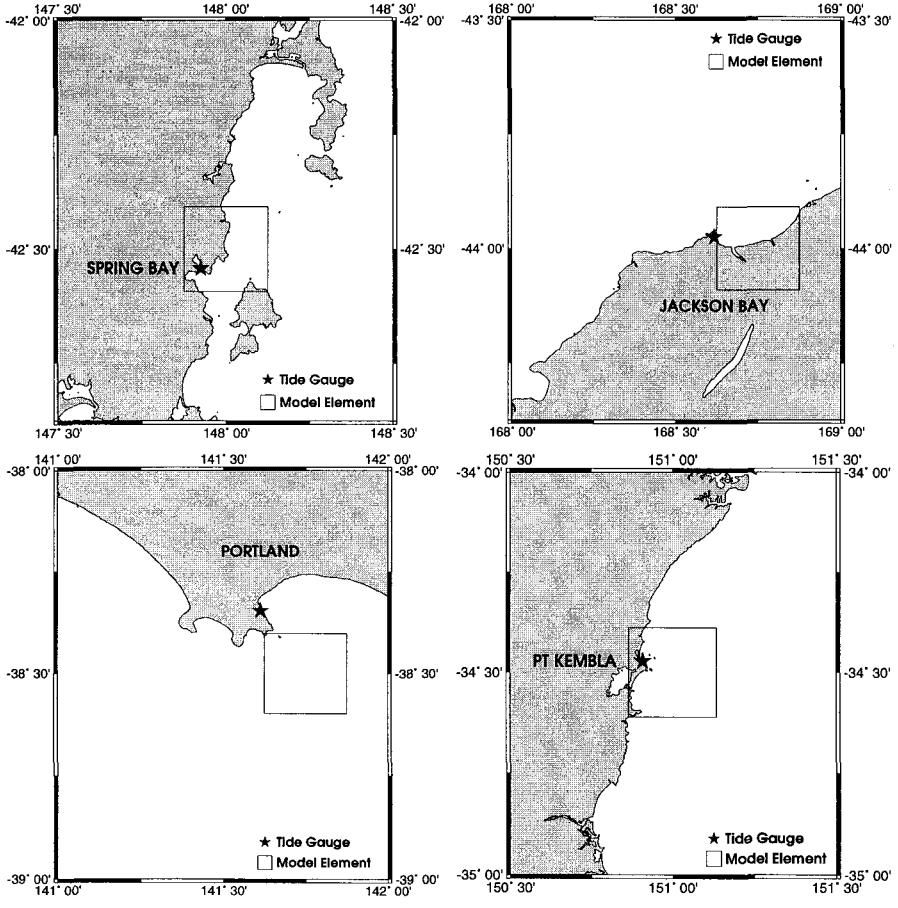

Figure 17. Coastline detail (land is shown shaded), tide-gauge location and nearest model element used for the comparison of predicted and observed tsunami signals.

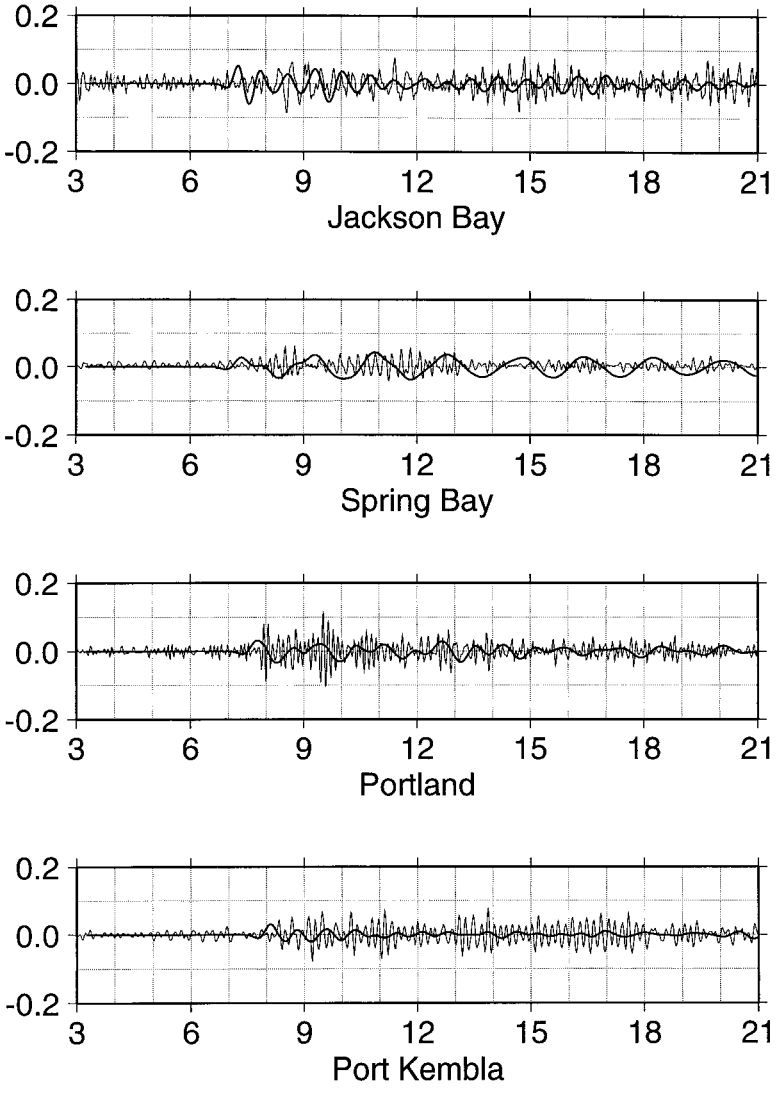

Figure 18. Comparison of observed (faint line) and modelled (bold line) tsunamis for the 1998 Balleny Islands earthquake. Horizontal axes denote Greenwich Mean Time (hours) on 25/3/98. Vertical scales denote amplitude (metres).

However, a comparison between observed and predicted tsunami arrival times (or relative amplitudes) enables an assessment of the model in terms of regional dynamics. Comparison between observed and modelled sea-level data at the chosen locations are shown in Figure 18. The observational records consist of data at one minute time intervals which has been band pass filtered for periods between 5 to 25 minutes. The exclusion of lower frequencies removes the influence of tides, while the exclusion of higher frequencies removes excessive residual noise and some harbour oscillations, leaving a space and time averaged tsunami signal which has undergone little attenuation due to filtering.

Even though the modelled data and filtered observations are somewhat different, the arrival time of the modelled tsunami waveform is in reasonable agreement with that of the observed arrival time of the tsunami signal. In this respect, the capability of this finite-difference tsunami model in simulation of transoceanic waveform propagation appears to be as good as the finite element model of Myers and Baptiste (1995), which used a very fine grid near the coast - whereas this model used a very coarse grid near the recording station.

The observed signal shows harbour waves excited by the tsunami, these resonant oscillations being at a much higher frequency and smaller spatial scale than can be resolved by the present deep sea propagation model. The observations clearly show the arrival time at each location. In all four cases the tsunami arrived a little later than the modelled version, because lack of resolution of the model did not include the slowing of the tsunami in very shallow coastal waters. Modelling of small scale features, such as resonant harbour waves, requires the use of sub-models featuring smaller grid sizes.

6. Conclusion

The use of a coarse-grid depth-integrated hydrodynamic-numeric tsunami model for hindcasting tsunami events in the Australian region has been presented. General agreement between model results and observations, particularly in the prediction of arrival times and relative tsunami amplitude distribution along the coastline, indicates that the model seems to perform well in simulating tsunami generation and regional propagation. The model seems well suited to identify tsunami risk areas as has been demonstrated by the hindcast results for the northwest coast of Australia.

Further studies will concentrate on the modelling of coastal effects using finer-grid hydrodynamic-numeric sub-models to provide information such as tsunami runup, inundation or harbour resonance at localities identified as being at risk.

References

AGSO (1998) Australian Geological Survey Organisation: Personal Communication.

Arakawa, A. and Lamb V.R. (1977) Computational design of the basic dynamical processes of the UCLA General Circulation Model. *Methods of Computational Physics,* 16: 173-263.

Bernstein, J. (1954) Tsunamis. *Scientific American*, August, 1954: 56-59.

Bills, P.J. (1991) *Barotropic depth-averaged and three-dimensional tidal programs for shallow seas.* Ph.D. thesis, University of Adelaide.

Courant, R., Isaacson, E. and Rees, M. (1952) On the solution of non-linear hyperbolic differential equations by finite differences. *Communications on Pure and Applied Mathematics*, 5: 243-255.

ETOPO5 (1988) *Digital Relief of the Surface of the Earth.* Data Announcement 88-MGG-02, NOAA, National Geophysical Data Center, Boulder, Colorado.

Foley, G. (1994) The tsunami event along the northwest Australian coast on 3 June 1994. *National Tsunami Workshop, 1994.* Bureau of Meteorology, Australia: 25-31.

Gregson, P.J., Paull, E.P. and Gaull, A. (1979) The effects in Western Australia of a major earthquake in Indonesia on 19 August, 1977. *B.M.R. Journal of Australian Geology and Geophysics,* 4: 135-140.

Gregson, P.J. and Van Reeken, L.A. (1998) Tsunami observations in Western Australia. *Maritime Natural Hazards in the Indian Ocean Region.* (Ed. By Woodroffe, C.D.) University of Wollongong, Australia: 131-145.

Latter, J.H. (1981) Tsunamis of volcanic origin: summary of causes, with particular reference to Krakatau, 1883. *Bulletin of Volcanology,* 44(3): 467-490.

Liu, P.L.F., Cho, Y.S., Yoon, S.B. and Seo, S.N. (1995) Numerical simulations of the 1960 Chilean tsunami propagation and inundation at Hilo, Hawaii. *Tsunami: Progress in Prediction, Disaster Prevention and Warning.* (Ed. By Tsuchiya, Y. and Shuto, N.) Kluwer Academic Publishers, Netherlands: 99-115.

Mader, C.L., Vitousek, M. and Lukas, S. (1988) Numerical modelling of atoll reef harbors. *Natural and Man-Made Hazards.* (Ed. By El-Sabh, M.I. and Murty, T.S.) D. Reidel Publishing Co., Dordrecht: 215-225.

Mitchell, W.M. (1998) Modelling of tsunamis on the Northwest coast of Australia. *Maritime Natural Hazards in the Indian Ocean Region.* (Ed. By Woodroffe, C.D.) University of Wollongong, Australia: 147-153

Myers, E.P. and Baptista, A.M. (1995) Finite element modelling of the July 12, 1993 Hokkaido Nansei-Oki tsunami. *Tsunamis:1992-1994; Their generation, Dynamics and Hazard.* (Ed. by Satake,K. and Imamura,F.) Birkhauser: 769-801.

Nottingham, D. (1997) The 1994 Skagway tsunami tide gauge record. *Science of Tsunami Hazards,* 15(2): 81-89.

Okada,Y. (1985) Surface deformation due to shear and tensile faults in a half space. *Bulletin of the Seismological Society of America,* 75 (4): 1135-1154.

Orlanski, I. (1976) A simple boundary condition for unbounded hyperbolic flows. *Journal of Computational Physics,* 21: 251-269.

Satake, K. and Tanioka, Y. (1995) Tsunami generation of the 1993 Hokkaido Nansei-Oki earthquake. *Tsunamis:1992-1994; Their generation, Dynamics and Hazard.* (Ed. by Satake,K. and Imamura,F.) Birkhauser: 803-822.

Schwiderski, E.W. (1980) On charting global ocean tides. *Reviews of Geophysics and Space Physics,* 18 (1): 243-268.

Sinolakis, C., Imamura, F., Tsuji,Y., Matsutomi, H., Tinti, S., Cook, B., Chandra, Y.P. and Usmann, M. (1995). Damage, conditions of East Java tsunami of 1994 analysed. *EOS, Transactions of American Geophysical Union,* 76(26): 257-262.

Sommerfeld, A. (1949). *Partial Differential Equations.* Academic Press, New York.

Sea-Level Changes and Their Effects
B.J. Noye & M.P. Grzechnik (Editors)

Adaptation Policies – Addressing Climate Change Impacts in the Pacific Region

C. Kaluwin
South Pacific Regional Environment Programme, P.O. Box 240, Apia, Samoa

ABSTRACT: In 1990, scientists agreed that increasing atmospheric concentrations of greenhouse gases (GHG) will enhance the earth's average temperature in the coming decades. Later, the same group from Intergovernmental Panel on Climate Change (IPCC) 1995 reported that there is now a discernible effect of human activity. There continues to be substantial scientific uncertainty as to the magnitude of this impact on population, economic, environment and other sectors of the ecosystems, at global, regional and national levels. These uncertainties do not mean that GHG emissions can be safely ignored, rather they call for urgent response strategies to be developed.

This paper discusses the outputs from a number of scientific monitoring and research activities currently being implemented in the Pacific region, including the "South Pacific Sea Level and Climate Monitoring Project" in the Forum Island countries. These aim to reduce the uncertainties in order to formulate national response strategies to mitigate or reduce the impacts of climate change and sea level rise in the region.

The response options developed in the Pacific region will be discussed, emphasising especially the development of adaptation option-Integrated Coastal Management (ICM) and Planning.

KEY WORDS: climate change, Pacific, sea level, adaptation

CONTENTS

1. Introduction

The South Pacific Regional Environment Programme (SPREP) region (see Figure 1) consists of tens of thousands of islands scattered over 30 million square kilometres. The most serious challenges to achieving sustainable development that exist in the 22 developing oceanic nations and territories stem from environmental and socio-economic factors. With a combined population of a little more than six million people, the tiny developing nations of the Pacific face global environmental changes, including climate changes coupled with sea level rise.

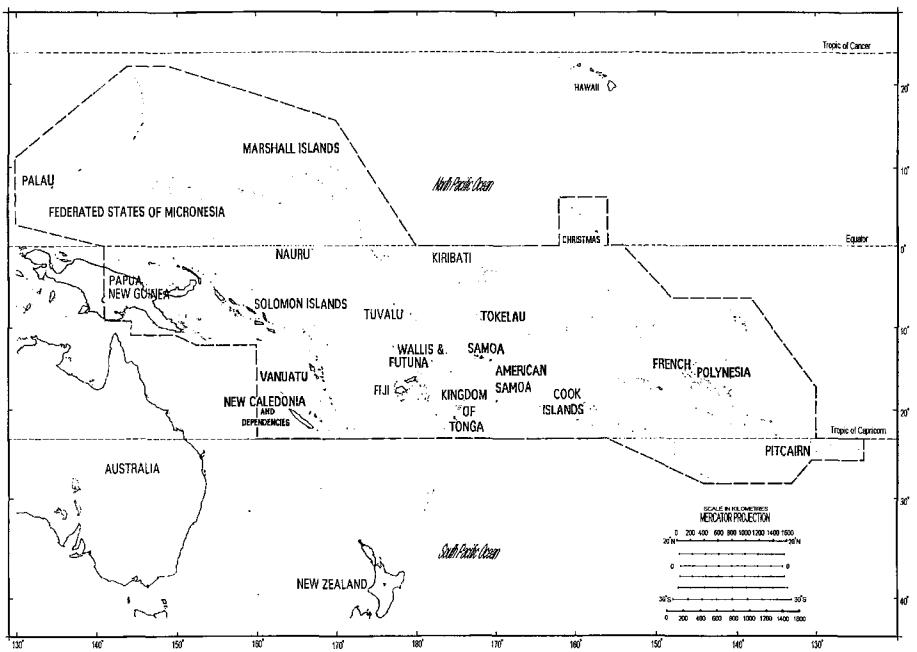

Figure 1: The South Pacific Regional Environment Programme (SPREP) region, illustrated by the black broken line. This should not be interpreted as showing international boundaries.

National capabilities to deal with these problems while stimulating economic development are limited by traditional land management systems, unique population dynamics, the complexity and fragility of islands' ecosystems, limited natural resources bases, heavy reliance on foreign aid and geographic isolation. The Forum Island Countries have agreed that sea level rise and climate change is one of the priority issues affecting the coastal areas and atoll nations of the region. While scientists (Intergovernmental Panel on Climate Change - IPCC) continue to reduce or minimise the uncertainties in differentiating between the greenhouse energy signals and natural climate variability, the magnitudes of the potential impacts of sea level rise and climate change are serious, and action must be taken today (even if all the facts are not ready) in order to manage the risks. The term "adaptation option" would mean developing a programme to reduce the risk of climate change and sea level rise, even in the absence of climate change, which will have positive implications for cultural, traditional, social, environmental and economic development in a sustainable manner. For example, establishing "sinks" for atmospheric carbon dioxide through reforestation programmes will provide employment, supplies of timber, fuelwood, stabilise soil, improve water catchments and enhance agricultural productivity (see below).

2. Understanding the Impacts of Climate Change

The IPCC Second Assessment Report (1995), in a major change from its 1990 Report, stated that it is unlikely that the heating is entirely natural. But how much the earth will warm and how much sea level will rise in the future depends on many factors. By 2100 the temperature is expected to increase by 1.0–3.5°C (2.0°C middle scenario) and global sea level by 15–95cm (50cm middle scenario). Unfortunately, at present, little can be said with any certainty about regional scale changes, especially in the Pacific.

A recent SPREP report in 1997 (16) contains reviews and evaluations of scientific information and understanding in the Pacific regarding Climate Change and Sea Level Rise, and draws on information from a range of sources such as oceanographic, meteorological, vulnerability and adaptation assessment studies, and programmes and activities implemented at national and regional levels. Results show that temperatures have been increasing by 0.1°C per decade in the region and sea levels by 2mm/yr. There is also evidence that climate phenomena such as El Nino-Southern Oscillation (ENSO) will have a

major influence. It is also recognised that the Pacific region plays an important role in understanding global climate change.

Modeling, scenario development and vulnerability assessments will play key roles in helping the Pacific respond to climate change, variability and sea level rise. Models currently suggest that a doubling of $C0_2$ concentration will increase sea-surface temperatures by 1°C and increase rainfall intensity in the central equatorial Pacific. Although the second assessment of the IPCC did not reveal a consensus regarding tropical cyclones in a changed climate regime, recent research has indicated possible intensity increase of 10-20% with a doubling of $C0_2$. Vulnerability assessments have shown Pacific Islands Countries (PICs) to be highly vulnerable to climate change and sea level rise but with a low capacity to respond. This response capability needs to be strengthened through regional and international cooperation and education, training and awareness raising. Countries also need to be encouraged to perform integrated impact assessments in addition to sectoral ones.

The National Tidal Facility, established by Australia at The Flinders University of South Australia in 1989, as a service to Australia and the South Pacific Forum Countries, manages eleven sea level monitoring sites in the South Pacific. In its five years of operation the data has provided useful information on sea level changes during cyclones and tsunamis as well as for modeling tidal information. Over the short term, sea-level changes have been heavily influenced by El Nino events showing positive and negative anomalies. The findings have been validated by satellite data.

The New Zealand Meteorological Service has supported a number of PIC meteorological services since around 1940. Analysed data show that since 1920 temperature has risen 0.6–0.7°C in Noumea (New Caledonia), and Rarotonga (Cook Is); much greater than average worldwide increases. Data is from 34 stations throughout the Pacific from about 160° East and mostly south of the equator. Research shows that surface air temperatures have increased by 0.3–0.8°C this century, with the greatest increase in the zone south-west of the South Pacific Convergence Zone (SPCZ). This is well in excess of global rates of warming. The records also indicate that rainfall had increased in the north-east and decreased in the south-west of the Pacific. Interannual variations in temperature and rainfall were found to be associated with the Southern

Oscillation Index (SOI) and the research also found an eastward movement of the SPCZ. The changes observed in the twentieth century may be considered to be consistent with anthropogenic activity for this region.

A great deal of international effort has enabled the identification of seasonal and interannual trends in oceanic conditions, but scientists are not yet in a position to identify long term trends in temperature and salinity. More oceanographic observational work is needed to achieve understanding of the mechanisms that govern climate in the region.

According to the statistics of tropical cyclones (TCs) between 1940 and 1994, the average number of TCs per year is seven. Although the general TC season is between October and May, most TCs occur between January and March each year. Changes in frequency, area of occurrence, time of occurrence, mean intensity and the maximum intensity of the TC cannot be predicted by present numerical models. Based on the present records, no two TCs are the same. However, TCs usually take place between latitudes 8°S and 20°S and longitude 145°E and 125°W. Probability of occurrence is maximised near 8°S and decreases with increasing latitude. During ENSO a TC has more than a 40% chance of being a severe one.

Climate change and its impact on human health is a new area of research. One of the problems is that we do not know enough about what might happen in the future. This highlights the importance of integrated assessment models (IAM) for assessing the climate change impacts on human health. At present there are significant amounts of health related disasters in the developing world. There is a threat posed by infectious and vector-borne diseases such as malaria and cholera. Cholera incidence is on the rise and there have been reports of malaria incidence in areas which previously did not have malaria - for example, in the highlands of Papua New Guinea. Future studies would include;

(i) identification of vulnerable population to health risks;
(ii) development of indicator species of vectors, and response strategies and;
(iii) establishment of early warning systems such as ENSO.

This work is particularly relevant for PICs. Regional, national and international communities should focus on adapting to present natural variability and prepare for extreme events. The National Oceanic and Atmospheric Administration (NOAA) and the Pacific Community (PC) are in the process of collaborating on work related to health indicators and ENSO related extreme events.

The impacts of climate oscillation on tuna fisheries in the Pacific Ocean have been studied by the South Pacific Commission (SPC). Tuna activities have expanded considerably and some 70% of tuna catches come from the Pacific Ocean. The catch is mostly skipjack and yellow fin tuna, with the majority coming from the western equatorial Pacific. The tuna resource is very closely linked to the position of warm pool, an area of low primary productivity. This is surprising as tuna need to consume 10% of their body weight each day. The convergence zone along the eastern boundary of warm pool may provide a possible mechanism for replenishing productivity in the warm pool. Hence, research is being conducted into the presence of the convergence zone and the presence of tuna. Results from a 1988–95 study show a large interannual variation and high spatial variability. Conclusions based on simulation studies indicate that secondary production (up-welling) enables the concentration of tuna in otherwise 'poor' productivity areas as a result of convergence zones. The impact of ENSO is clearly established: zonal movements include east-west movement of primary production and tuna levels.

The IPCC assessment of the social and economic dimensions of climate change has little reference to Pacific Island Countries but focuses on mitigation. All islands are treated as if they are the same. The IPCC report uses models which are mainly for developed economies.

For the world as a whole the IPCC estimates a net loss for doubling carbon dioxide of about 1.5–2.0% of global Gross National Product (GNP). Developing countries are estimated to have net loss of 2–9% GNP.

The social and economic dimensions of Global Climate Change have a number of implications for the Pacific region such as:
(a) PICs make a small or negligible contribution to GHG
(b) They are among the countries which are most impacted, and
(c) Knowledge of relevant parameters is very low.

Thus, Pacific Island Countries should take precautionary approaches given the lack of scientific data and information about their countries and region. They should acquire more understanding and knowledge about the causes than effects, and more about migration than adaptation. Understanding effects and adaptation is essential in the political arena and thus public awareness is important to the Pacific region.

Most Pacific Island governments are aware of climate change, but they wish to know what they have to do to address the problem. The cultural dimension involves the environmental influence on both people and culture. For example, the larger islands with more resources would influence class structure and culture of communities living in them. Traditional knowledge has governed activities and survival of people in the region, both in the past and present. The socio-economic dimension has indicated a change from subsistence to dual economy. Issues that need to be addressed include population concentration and location infrastructure, food security, culture and activities. The response options that have existed and will continue to exist in the region include migration, resettlement and decentralisation. All of these need planning as they have policy implications. Thus the future direction will have to be researched so that some response strategies will be well planned and recommended for the future adaptations.

3. Review of Vulnerability and Adaptation Studies

IPCC predictions (1,7) suggest that if Greenhouse Gases (GHG) can be reduced significantly or stabilised by the year 2050, a potential lag time could still cause ocean levels to rise. The IPCC 'Business-As-Usual' (BAU) scenario estimates that by 2100, global sea level rise would be 65cm, or 41cm should 'atmospheric stabilisation' occur.

Whilst research and monitoring within the South Pacific regional institutions continues to address the issue of sea level rise regionally, it could be advisable to use the IPCC BAU estimates to plan for policy development to address the climate change and sea level rise impacts. For the purpose of this paper, the regional vulnerability studies coordinated by SPREP have adopted the scenarios of 39–100cm for sea level rise impact on the six indicated countries of the Pacific Ocean, and planning for the development of response strategies by the year 2100.

Global warming and 50–100cm rise in sea level could impact in the following ways for the majority of the Pacific islands:

- Severe and frequent storm damage and flooding;
- Erosion, inundation and loss of barrier beaches and shorelines;
- Destruction of coral reefs and atolls;
- Disappearance of wetlands and lowlands;
- Increased salinity of rivers, bays and aquifers;
- Reduction of biodiversity;
- Loss of beaches and low islands;
- Loss of coastal structures, both natural and man-made; and
- Changes of biophysical and biochemical properties of the coastal areas.

The impact of global warming will vary among coastal regions, and assessing a nation's vulnerability to sea level and climate change has become of paramount importance. Many nations already suffer from severe erosion, coastal storms, salt water intrusion and loss of wetlands, even under current conditions. As population and development activities grow in the fragile coastal environments, sea level rise, climate change and climate variability will exacerbate threats to life, property and natural resources.

There is an urgent need for vulnerable coastal nations to begin the process of adapting to sea level rise. Even though sea level rise is predicted to be a relatively gradual response, adaptive strategies may require lead times of 20–50 years to tailor them to consider the unique island coastal resources and areas. It is appropriate to begin planning now to avoid actions that could increase vulnerability to the impacts of sea level rise and climate change.

In the midst of these national vulnerability assessments, the importance of considering sea level rise from the regional and international approach has become evident. New partnerships and joint collaborations to share information and mutually benefit have resulted from these case studies in the SPREP region.

Global:

IPCC Working Groups II and III (1,7,14), responsible for formulating appropriate response strategies for management of climate change, were tasked to develop adaptation options. In 1991, the Coastal Zone Management Sub-group (CZMS)

coordinated a global survey with regards to the impacts of sea level rise on 37 countries; approximately 90% of the reports indicated that their coastal areas will be vulnerable to sea level rise coupled with climate change.

A Coastal Zone Management Sub-group (CZMS) had the specific task:

- to provide information and recommendation to national and international policy centres enabling decision making on: (i) coastal zone management strategies for next 20–50 years; and (ii) long-term polices dealing with adaptation with respect to sea level rise and climate change.

To determine costs of basic coastal protection measures to defend a 20–100cm rise in sea level globally, the CZMS group devised a common methodology to be tested before being accepted by all.

Regional:

Global environmental changes (especially climate change) combined with a range of extreme climatic events, including tropical cyclones, sea surges, floods and droughts, have adversely affected the islands and coastal areas of the Pacific islands region (see section 2). A seven step approach was formulated (1,7,14) for assessing vulnerability to sea level rise globally and tested in the SPREP region. SPREP coordinated and implemented six case studies, for Tonga (6), Kiribati (9), Fiji (3,5), Samoa (2,4), Tuvalu (13) and Marshall Islands (8) in an attempt to test the IPCC Common Methodology and, where appropriate, modify it to account for the unique cultures, traditions, environment and economic practices of these countries. Below is a summary of the coastal vulnerabilities and resilience to sea level and climate changes in the region with a focus on those six countries.

3.1 Current vulnerability

These islands were adversely affected by climate change and sea level rise, including extreme climatic events such as tropical cyclones, sea surges, floods and droughts. These events, particularly cyclones, produced abnormally high waves and storm surges, considerably impacting the different sectors. Soil erosion and landslides are important secondary factors related to periods of high rainfall, particularly associated with cyclones and El Nino. Soil erosion, and consequently high levels of sediment in rivers and inshore marine areas, can have adverse effects on coastal resources.

3.2 Vulnerability of environmental sectors

Agriculture.
The occurrence of climate change and extreme events has a significant negative impact on agricultural productivity. Heavy rainfall, high winds and huge waves associated with cyclones have caused damage and destruction to both trees and ground crops. In addition, these result in the waterlogging of soil and consequent washing out or rotting of crops. Droughts have been experienced with serious impacts on agriculture due to insufficient soil moisture leading to cessation of crop growth and thus reduced productivity.

Forests.
Forests provide a range of resources, including fuel wood and timber, which are harvested at both a subsistence and commercial level and as a carbon dioxide sink. Forests are vulnerable to climate change and cyclones as high winds and temperatures cause damage and loss of foliage and branches, and in some circumstances result in uprooting. In addition, periods of low rainfall increase the vulnerability of forests to fire damage.

Water.
The most serious effects of climate change on water resources occur following prolonged dry spells which have resulted in a shortage of water supplies on some islands. In addition, contamination of water resources can be attributed to sea level rises, abnormally huge waves from cyclones, and the *El Nino* effect. Such effects tend to be confined to the drier parts of the larger islands or coastal areas and smaller, outer islands which are still inhabited.

Fisheries.
Fish and other marine resources are important protein resources for the majority of the islanders. Fisheries may be adversely affected by increased UV radiation, high temperatures, high volume of sedimentation due to soil erosion. Also, increased frequencies of cyclones in the region have resulted in fish kills and damage to coral reefs as fish habitat.

Mangroves.
Mangroves act as a buffer zone between land and sea and play a significant role in protecting both the coastal areas and coral reefs. Mangroves are also

important habitat for fish and other marine species, and provide a range of resources used by the islanders. Impacts of climate change, sea-level changes, large storm surges associated with cyclones, and flooding resulting in high levels of sediments, have greatly affected the mangroves.

Coral Reefs.
Coral reefs provide physical protection to the shoreline and are an important habitat for fish and other marine organisms. Corals have been observed to be stressed or even killed due to high UV radiation, sudden increased temperature changes, increased concentrations of sediments and flooding (from freshwater). In addition, increased cyclone frequencies in the region have killed or injured corals.

3.3 Vulnerability of socio-economic sectors

Population.
Approximately 90% of the population sustain their lives in the coastal areas within 1km of the sea. This means that the majority of the population are more at risk from the impacts of climate change and sea level rise coupled with natural climate variability. In addition, infrastructure, agriculture and other activities are located in the coastal areas. High frequencies of cyclones observed in the islands associated with huge sea surges, high winds and rainfall means the coastal areas are vulnerable. Similarly, on some of the islands, people or activities along the rivers are most at risk from flooding, for example in Fiji (3,5).

Health.
The impacts of climate change, including abrupt changes in temperatures and rainfall, are many (14). Heavy rainfall and flooding have resulted in outbreaks of diarrhea and other water-borne diseases, and at times vector-borne diseases such as dengue. Shortage and contamination of water due to long spells of dry weather and sea level rise have lead to outbreaks of diarrhea, eye and skin infections and a decline in general health. Many of the problems were identified in rural areas, urban squatter settlements, and remote islands.

Well-being.
In all the study cases, the poorest people were noted as being the most vulnerable members of society, and more often affected by climate change and extreme climatic events. Part of this vulnerability stems from the generally poor structure and low quality of housing, which are often unable to withstand the impacts of climate change, cyclones, flooding, high winds and storm surges. Furthermore, the poor are financially less able to cope with the losses and costs of repair associated with these events.

The majority of the people of the islands retain strong links to the land and environment through their subsistence or small-scale commercial farming and fishing activities. Small-scale commercial activities for income-generation are particularly vulnerable to the adverse effects of climate change and climatic extremes because they place heavy reliance on a single crop and have very few options for either income or food supply. In contrast, the majority of subsistence farmers grow a wide range of crops and are, generally, more resilient to the impacts of climate change and natural variability.

Economy.
Climate change and the associated sea level rise and cyclones have altered the vulnerability of the majority of the islands environment, society and economy. The majority of island export trade and overall economy is heavily dependent on the production of a small number of principally unprocessed products, particularly seafood, sugar, taro, wood and wood products. This means that the negative effects of climate change and climatic extremes on primary resources are important at both local and national levels. Tourism also makes a significant contribution to the national economies. Although impacts of cyclones on industries are short-lived, the economic recovery is generally long term and expensive.

4. Coastal Vulnerability Due to Sea Level Rise in the Pacific

The IPCC Common Methodology was employed in assessing the coastal vulnerability to sea level rise and climate change for Tonga, Marshall Islands, Kiribati, Fiji, Tuvalu and Samoa. It is recognised that the Common Methodology did not account for the importance of the following issues for these countries or the region:

- subsistence economy;
- close ties of the people to land through customary land tenure;
- gift giving and remittance as a mechanism for extended family economic resilience;
- lack of urban land use planning or building codes;
- importance of the proximity to roads in rural area;
- ineffective linkages between national (parliamentary) and village (customary) decision making;
- decision making powers of village communities;
- strength of religious beliefs; and
- human resources, technical and data limitations.

As a result of these concerns and other work internationally (11), four main issues can be derived from the methodology:

(a) applicability of economic-based assessment techniques within primarily subsistence economies;

(b) utility of the Common Methodology for aiding coastal planners in formulating sea level rise impact assessment policies;

(c) lack of time dependency in the Common Methodology does not allow realistic assessment of potential sea level rise impacts on highly dynamic coastal systems, including socio-economic and cultural systems; and,

(d) narrow geographic concept of the "coastal zone" does not take into account important interactions with the adjoining land and marine system.

4.1 A new approach to sea level rise impact assessment

The four fundamental concerns with the Common Methodology meant a new approach to the assessment of potential future impacts of sea level rise and climate change had to be developed for the region and the respective countries.

In terms of environment-economic sustainability for these island nations and the region it was important that the new approach did not limit itself to analyses of the effects of sea level rise and climate change, but it covered a wider range of external stresses. A flexible framework was therefore adopted which assesses the vulnerability, resilience and sensitivity of coastal systems to external stresses such as waves, tropical cyclones, global economic markets, tourists, sea level rise and climate change. In addition, internal system stresses, such as population pressure,

natural resource depletion, pollution and cultural changes, are considered in the decision support framework. The detailed new approach is documented and tested for Fiji, Samoa and Tuvalu (2–5,13).

5. Future Methodology

The new approach (2–5) and its flexible concept of addressing the external and internal stresses allows Pacific island countries to focus on response policies in establishing appropriate adaptive strategies to global warming, sea level rise and climate change. The South Pacific Regional Environment Programme has been promoting Integrated Coastal Management (ICM) taking into account future threats as discussed in the new methodology.
In 1994, IPCC Working Group II (1) released a report, "IPCC Technical Guidelines for Assessing Climate Change Impacts and Adaptation", which reviews methods of climate impacts and adaptation. The report was further tested and refined (14). It outlines a basic framework for the study of climate-environment-society interactions, with particular emphasis on assessing the impacts of climate coupled with the enhanced greenhouse effect.

By combining the new approach (2–5) and the IPCC (1) methods, it is anticipated that a better understanding of the effects of past and present climate variability is useful to assess the impacts induced by future climate change and sea level rise from the present to the year 2050. These methodologies are developed by SPREP for Fiji and Tuvalu Islands (13) and the results are primarily useful for planning for sea level and extreme events in the island situations.

6. Adaptation Strategies for the Pacific Islands

The potential impacts of climate and sea-level change in the Pacific region are sufficiently serious to take immediate action, even when all of the facts are not yet available in order to manage this risk. Many of the strategies that can be undertaken to reduce the risk of climate change, have positive implications for social and economic development are justified even in the absence of climate change and sea level rise issue.

The current development of these methodologies (1–5, 13) will assist Pacific island nations to assess the impacts of global environmental changes, including climate

change and sea level rise. The facilitation and implementation of adaptation options and the benefits that they can provide are discussed here, and include:

(i) *Energy conservation and renewable energy use.*

Development of energy strategies could cover improvement of the efficiency in providing energy services and expanded use of renewable and non-carbon-based fuels. The SOPAC Secretariat in Fiji (regional policies) recommendation to disseminate technologies with higher energy-efficiencies can help in the implementation of these strategies. Energy conservation reduces the use of fossil fuels and electricity, which for the majority of the Pacific island countries reduces bills for imports of fuels and electricity generation equipment. These strategies also provide the potential to use indigenous resources — sunlight (Solar power in Kiribati and Tuvalu) and wind power (Cook Islands) for example in the place of imported fuels — to reduce pollution from fuel combustion equipment by improving combustion efficiencies.

(ii) Improved Forest Management.

Better forest management can halt deforestation and enhance forest sinks of carbon dioxide, especially for countries in regions like Papua New Guinea, Fiji, Solomon Islands and Vanuatu. Forest management typically provides other national benefits as well, including stabilisation of soils and watershed management of the forest base for enhanced production of food, fuel, fibre and employment. Other benefits include agro-forest opportunities for rural populations and securing habitat for economically and environmentally important plant and animal species.

(iii) Use of agricultural systems to minimise GHG emissions

This strategy includes using animal breeds that utilise feed more efficiently and rice cultivation and fertiliser application techniques that reduce methane emissions, as well as improving methods of agricultural waste management. These methods of mitigating greenhouse gas emissions can use agricultural inputs more efficiently, and can reduce local pollution problems such as odours and surface water pollution from livestock waste disposal. In the case of some waste treatment methods (biogas production), energy and additional agricultural products (eg. animal bedding and soil amendments) can be produced and methane emission will be abated.

(iv) Improving methods of management of municipal wastes

The strategy includes management of sewage and solid wastes in ways that typically, while reducing methane emission, can also assist in recycling materials and nutrients, reduce the amount of land required for refuse disposal, improve public health, and serve as a source of renewable energy fuels.

(v) Integrated Coastal Management (ICM)
For the Pacific countries or small island nations, perhaps the best strategy for sustaining environment-economic development while taking into account the global environmental changes including (or no) climate and sea-level changes, would be the development and implementation of an Integrated Coastal Management (ICM) framework/approach at national and regional levels (discussed in section 7).
The output from the current modifications (2–5) to the Common Methodology for assessing Coastal Vulnerability to Climate Change and sea level rise and the "IPCC Technical Guidelines for Assessing Climate Change Impact and Adaptation (1)" would provide the solid foundation for the development of a regional ICM concept/framework to test in countries of the SPREP region.

These adaptation strategies provide ways for policy makers to implement responses to climate and sea-level changes today, even while our scientific understanding of the issues continues to remain in flux. The Climate Change and sea level rise issue for the island governments/regions can serve policymakers as a lever to obtain international and bilateral support for strategies, financial assistance, and technology transfers that enhance the process of development while reducing the risks of (or increasing preparedness for) climate change and its potential impacts.

7. Climate Change Impacts on Coastal Management

In conclusion, potentially the most effective and realistic adaptation strategy for sea level rise, coupled with climate change and natural variability, for the small island states of the Pacific region is Integrated Coastal Management (ICM). Even if there are no climate and sea-level changes, the development and implementation of national level ICM programmes appropriate to the circumstances of the Pacific islands will provide the means to address both the short and long term issues identified in the vulnerability assessment studies, as well as other issues affecting coastal areas.

The ICM will involve the comprehensive assessment, setting of objectives, planning and management of coastal systems and resources, while taking into account traditional, cultural and historical concerns and conflicting interest and uses. It is an iterative and dynamic process, which includes adapting to the impacts of climate and sea-level changes, developing and implementing a

continuous management capability that can respond to the economic-environmental changes. However, those seriously interested in the development of an ICM framework can consult the outline of what ICM is, and how it needs to be developed and implemented in the Pacific islands' context in Fuavao (10), Ashe and Griffith (11), World Bank Report (12) and IPCC Working Group Report (14).

References

1. Carter, T. R., Parry, M. L., Harasawa, H. and Nishioka, S. (1994). IPCC Technical Guidelines for Assessing Climate Change Impacts and Adaptation.

2. Nunn, P. D., Balogh, E., Ravuvu, A. D., Mimura, N. and Yamada, K. (1994). Assessment of Coastal Vulnerability and Resilience to Sea-Level Rise and Climate Change; Case Study: Savai'i Island, Western Samoa. Phase II: Development of Methodology, 1994. South Pacific Regional Environment Programme (SPREP).

3. Nunn, P. D., Aalbersberg, W., Ravuvu, A. D., Mimura, N. and Yamada, K. (1994). Assessment of Coastal Vulnerability and Resilience to Sea-Level Rise and Climate Change; Case Study: Yasawa Islands, Fiji. Phase II: Development of Methodology, 1994. South Pacific Regional Environment Programme (SPREP).

4. Kay, R. C., Cole, A., Elisara, F. M. and Yamada, K. (1993). Assessment of Coastal Vulnerability and Resilience to Sea Level Rise and Climate Change; Case Study : Upolu Island, Western Samoa. Phase I: Concepts and Approach, South Pacific Regional Environment Programme, SPREP.

5. Nunn, P., Kay, R. C., Ravuvu, A. and Yamada, K. (1993). Assessment of Coastal Vulnerability and Resilience to Sea Level Rise and Climate Change: Case Study: Viti Levu Island, Fiji. Phase I: Concepts and Approach, South Pacific Regional Environment Programme, SPREP.

6. Fifita, N. P., Mimura , N. and Suzuki, K. (1993). Assessment of the Vulnerability to Sea Level Rise for the Kingdom of Tonga: Tongan Case Study, 1993. Report submitted to Tongan Government

7. Carey, J. J. and Mieremet, B. (1992). Reducing Vulnerability to Sea Level Rise: International Initiatives. Ocean & Coastal Management **18**:161-177.

8. Holthus, P., Crawford, C., Makroro, C. and Sullivan, S. (1992). Case Study: Majuro Atoll, Republic of Marshall Islands, SPREP Reports and Studies Series No.60.

9. Woodroffe, C. D. and McLean, R. F. (1992). Kiribati Vulnerability to Accelerated Sea Level Rise: A Preliminary Study, Department of Environment, Sports and Territories, Canberra.

10. Fuavao, V. A. (1995). Coastal management in small island developing states. In: Small Islands, Big Issues: Crucial Issues in the Sustainable Development of Small Developing Islands. World Development Studies 1, pp 84-111. World Institute for Development Economics Research, The United Nations University, Helsinki, Finland. Paper prepared by: Andrew Smith, Roger Cornforth, Gerald Miles, Vili Fuavao and Chalapan Kaluwin.

11. Griffith, M. D. and Ashe, J. (1993). Sustainable development of coastal and marine areas in small island developing states: A basis for integrated coastal management. Ocean & Coastal Management, **21**:269-284.

12. World Bank (1993). Noordwijk Guidelines for Integrated Coastal Zone Management. Land, Water and Natural Habitats Division, Environment Department, The World Bank, International Conference on Coastal Zone Management, Noordwijk, The Netherlands.

13. Sem G., Hay, J., Campbell J., Yamada, K., Mimura, N. and Onno, K. (1996). Tuvalu Vulnerability Studies. South Pacific Regional Environment Programme Report, 1996.

14. Watson, R. T., Zinyowera, M. C. and Moss R. H. (editors, 1996). IPCC Working Group II. Impacts, adaptation and mitigation of climate change: Scientific- Technical Analyses

15. Houghton J. T., Meria Filho, L. G., Callander, N. H., Kattenberg, A. and Maskell, K. (editors, 1995). The Science of Climate Change, IPCC WGI (1995); Cambridge University Press. pp 4-5.

16. Kaluwin, C. and Hay, J. (editors, 1999). The Proceedings of the 3rd Climate Change and Sea Level Rise Conference 1997 in New Caledonia. SPREP Report. pp 299-303.

This page is intentionally left blank

Index

D

E

F

G

H

I

J

K

L

M

N

O

P

Q

R

S

T

U

V

W

Y

This book contains updated, reviewed versions of some selected papers on "Sea-Level Changes and their Effects" presented at the International Ocean and Atmosphere Pacific Conference (OAP 95), held in Adelaide, South Australia, 23–27 October 1995. In addition several reviewed articles on important topics not covered by the papers presented at OAP 95 were invited. The articles in this volume will find an audience among coastal developers, marine biologists and environmentalists. They cover a range of topics including the efforts of long-term sea-level rise on coastal flows and its impact on mangrove communities, the determination of long-term sea-level change relative to the vertical motion of the land, to the numerical modelling of short term sea-level changes due to tides, tsunamis and the weather.

World Scientific
www.worldscientific.com
3919 hc

ISBN 981-02-3618-2
9 789810 236182